BIOASSAY GUIDED PHYTOCHEMICAL STUDIES ON RESINS OF SOME *COMMIPHORA* SPECIES

BY

WORKU DINKU AYANA

OFFICE OF GRADUATE STUDIES

ADAMA SCIENCE AND TECHNOLOGY UNIVERSITY

NOVEMBER 2020

ADAMA, ETHIOPIA

BIOASSAY GUIDED PHYTOCHEMICAL STUDIES ON RESINS OF SOME *COMMIPHORA* SPECIES

BY

Worku Dinku Ayana

Advisor: Aman Dekebo (Professor)

A Dissertation Submitted to the Department of Applied Chemistry

School of Applied Natural Sciences

Office of Graduate Studies

Adama Science and Technology University

November, 2020

Adama, Ethiopia

APPROVAL SHEET

Adama Science and Technology University

School of Applied Natural Sciences

Department of Applied Chemistry

This is to certify that the thesis prepared by Worku Dinku Ayana, entitled: Bioassay Guided Phytochemical Studies on Resins of Some *Commiphora* Species, submitted in full fulfillment of the requirement of the degree of Doctor of Philosophy in Chemistry (Medicinal Chemistry stream) complies with the regulation of the University and meets the accepted standards with respect to originality and quality.

Approved by the examining committee:

Name	Signature	Date
_____	_____	_____
Name of Student		
_____	_____	_____
Advisor		
_____	_____	_____
External examiner 1		
_____	_____	_____
External examiner 2		
_____	_____	_____
Internal examiner		
_____	_____	_____
Chair Person		
_____	_____	_____
Head of Department		
_____	_____	_____
School Dean		
_____	_____	_____
Post graduate Dean		

DECLARATION

I hereby, declare that the dissertation submitted for the degree of Doctor of Philosophy (PhD) in Medicinl Chemistry at Adama Science and Technology University, School of Applied Natural sciences. It is my own original work, and has not been submitted previously to any institution or higher education. All sources of materials used in this work have been accordingly, acknowledged.

This work was done from March 2014 to June 2020 at the Department of Applied Chemistry, School of Applied Natural Science, Adama Science and Technology University and Korean Research Institute of Chemical and Technology, under the supervision of professor Aman Dekebo.

TABLE OF CONTENTS

LIST OF FIGURES

LIST OF TABLES

LIST OF ACRONYMS AND ABBREVIATIONS

A-2780	human ovarian cancer cell line
A-549	human non-small cell lung cancer
ATCC	American Type Culture Collection
ATF	Activating Transcription Factor
BuOH	n-Butanol
CC_{50}	Cytotoxicity concentration at 50%
COSY	Correlation Spectroscopy
DCM	Dichloromethane
DEPT	Distortionless enhancement by polarization transfer
DENV	Dengue virus
DF	Dengue fever
DHF	Dengue hemorrhagic fever syndrome
DSS	Dengue shock syndrome
EC_{50}	Effective concentration at 50%
EI-MS	Electron Impact Mass Spectrometry
EO	Essential oil
ERK1/2	Extracellular signal regulated kinase
ESI-MS	Electrospray Ionization Mass Spectrometry
EtOAc	Ethyl acetate
FCC	Flash Column Chromatography
FT-IR	Fourier Transform Infrared
GC-MS	Gas Chromatography Mass Spectrometry
HMBC	Heteronuclear Multiple Bond Correlation
HPLC	High performance liquid chromatography
HR-ESI-MS	High resolution electrospray ionization mass spectrometry

HSQC	Heteronuclear Single Quantum Coherence
iNOS	Induced nitric oxide synthase
IR	Infra-red
IC_{50}	Inhibitory concentration at 50%
LCMS	Liquid Chromatography Mass Spectrometry
MeOH	Methanol
MIA-pac-2	human pancreatic cancer cell line
NF-κB	Nuclear Factor kappa b
NIST	National Institute of Standards and Technology
NMR	Nuclear Magnetic Resonance
RI	Retention Index
SNU638	Human stomach cancer cell line
ROESY	Rotating Frame Overhausser Enhancement Spectroscopy
ROS	Reactive Oxygen Species
SRB	sulforhodamine B
TIC	Total Ion Chromatogram
TLC	Thin Layer Chromatography
VCD	Vibrational circular dichromism
UV	Ultraviolet

Papers Published and Presented from This Thesis

This research work has contributed the following to the body of scientific knowledge:

Publication 1

- Worku Dinku, Sang Un Choi, Sang-Ho Lee, Young-Sik Jung, Zae Sung No and Aman Dekebo, Antiproliferative Effect of Sterols from Resin of *Commiphora habessinica.* Journal of Pharmacy and Nutrition Sciences, 2019, Vol. 9, No. 2. 71-80.

Publication 2

- Worku Dinku, Johan Isaksson, Fredrik Garnås Rylandsholm, Petr Bouř, Eva Brichtová, Sang Un Choi, Sang-Ho Lee, Young-Sik Jung, Zae Sung No, John Sigurd Mjøen Svendsen, Arne Jørgen Aasen, and Aman Dekebo. Antiproliferative activity of a novel tricyclic triterpenoid acid from *Commiphora africana* resin against four human cancer cell lines. The Korean Society for Applied Biological Chemistry, 2020, Vol 63, No 16. 1-11.

Publication 3

- Worku Dinku, Aman Dekebo, and Young-Sik Jung. Chemical constituents and anti-proliferative activity of resin of *C. sphaerocarpa* against four human cancer cell lines. Ethiopian Journal of Science and Sustainable Development, 2020, Vol 7, No.2. 21-28

Manuscript under review

Publication 4

- Worku Dinku, Su Bin Park, Jin Boo Jeong, ChuleuiJung and Aman Dekebo. Chemical Composition and anti-inflammatory effect of Essential Oils from four resins of *Commiphora* species. Molecular Medicine Reports. Under review.

ACKNOWLEDGEMENTS

It is with immense pleasure that I express my deep sense of gratitude to my research advisor professor Aman Dekebo, Department of Applied Chemistry, Adama Science and Technology University for suggesting the research topic, for his invaluable guidance, support and endless kindness throughout my study. I am indebted to pass my sincere gratitude to the following people without whom this work could have not been a success.

I have a special thanks to Dr. Young-Sik Jung**,** Organic Synthesis, Principal Research Scientist Korea Research Institute of Chemical Technology (KRICT), Daejeon, Korean Republic, for granting me the opportunity to use his laboratory to undertake extraction, fractionation, and isolation of compounds, running NMR, ESI-MS, HR-ESI-MS of the isolated compounds. All bioactivity screening was carried out under his financial support by Virus Research and Testing Center (KRICT). I would like to thank him for his immediate and invaluable response without hesitation for all our questions. I would like to express my gratitude to Professor Johan, Department of Chemistry, UiT the Arctic University of Tromsø, for recording the NMR spectra, VCD and computation of the novel compound "commafric A".

I wish to thank Dr. Su Bin Park, Jin Boo Jeong, Department of Medicinal Plant Resources, Andong National University, Rebublic of Korea, Chuleui Jung Agricultural Science and Technology Research Institute Andong National University, Republic of Korea for their support on running GC-MS of the essential oils and anti-inflammatory test.

I wish to thank former and present Deans of Applied Natural science, Department of Applied Chemistry, Heads for their support and encouragement. I express my sincere thanks to all other staffs of Applied Chemistry Department for their friendly care, encouragement and moral support to accomplish my study. I would like to express my gratitude to all the members of administrative, academic programme and technical staff of Adama Science and Technology University. I express my gratitude aslo to Mr Shambel Alemu a taxonomist, Addis Ababa Univestiy, for identifying the plants. I am deeply indebted to my family at large for their patience, love, encouragement and support.

Above all I praise and thank 'Almighty God' for everything.

Worku Dinku

Bio-assay Guided Phytochemical studies on Resins of Some *Commiphora* Species

By: Worku Dinku
Advisor: Professor Aman Dekebo

ABSTRACT

Resins of *Commiphora* species are known for their medicinal properties either alone or in combination with other medicinal plants to treat various ailments in Ethiopia. The bioassay guided antiproliferative screening showed that chloroform fraction of the resin of *C. habessinica,* n-hexane and chloroform fraction of *C. africana* exhibited potency against A549, A2780, MIA-PaCa-2, and SNU-638 cancer cells, which prompted their chemical investigation. Predominantly, the cytotoxicity of chloroform fraction against all cancer cell lines was the highest and attributed to further investigation such as isolation, characterization and screening of compounds.

In this study, two groups of compounds were isolated and characterized by IR, MS, 1D and 2D NMR. Cholestane type phytosterols: cholesterol (**48**) and lathosterol (**112**) and a mixture from *C. habessinica* and two novel tricyclic triterpenes (3*S*,4*S*,14S,7*E*,17*E*,21*Z*)-3,30 dihydroxypodioda-7,17,21-trien-4-carboxylic acid (**113**), (3*S*,4*S*,14S,7*E*,17*E*,21*Z*)-3-hydroxypodioda-7,17,21-trien-4-carboxylic acid (**114**) along with a known compound α-amyrin (**56**) a pentacyclic triterpene from resin of *C. africana*. In the cytotoxicity assay, the A549 (NSCLC) cell line was the most sensitive to the *Commiphora* species. The anti-proliferative effect of commafric A against A549 (NSCLC) cells with IC_{50} values of 4.52 μg/ml was the highest among the isolated compounds and a mixture of cholesterol (**48**) and lathosterol (**112**) showed more cytotoxicity with IC_{50} 13.77 μg/ml due to synergism.

Compared to the other resin essential oils, *C. sphaerocarpa* resin EO demonstrated significant dose response inhibition LPS-mediated NO production by 26.76% at 10 μg/ml and 62.26% at 20 μg/ml in RAW264.7 cells. The anti-inflammatory effect attributed to the presence of oxygenated and hydrocarbon sesquiterpenes (94.19%), mainly β-caryophyllene (**83**) (28.025%) and β-caryophyllene oxide (**99**) (13.891%) where both possess significant anticancer activities. EO of *C. sphaerocarpa* resin inhibited LPS-mediated iNOS overexpression, phosphorylation of ERK1/2, p38, ATF2, Nrf2 nuclear accumulation and HO-1 expression, ROS regulation.

The *n*-BuOH fraction of *C. schimperi* showed the most desirable antiviral profile for flu A virus with high S.I. values (> 5.2 for PR8 and > 13.2 for HK), to ribavirin (RBV) (> 4.3 for PR8 and > 4.5 for HK) the positive control. Towards DENV-2 serotype the *n*-BuOH fraction of *C. habessinica* was the highest with 100% and 44% inhibition at 100 and 20 μg/ml. The presence of various bioactive compounds and fractions provide more opportunities for the discovery of new bioactive principles from the genus.

CHAPTER ONE

INTRODUCTION

Medicinal plants are groups of plants with vital roles in alleviating human suffering and provided an endless source of medicine, and are still used as a primary source of medical treatment in developing countries [1]. In addition to traditional medicinal purposes, medicinal plants have served as a common link between the traditional and modern medicinal sciences as modern drugs contain bioactive plant derived constituents [2]. The plants are of most interest to researchers because of isolation and identification of bioactive compounds as lead compounds in the development and production of new drugs with efficacy and safety. In modern medicine, drugs developed from natural products have been used to treat infectious diseases such as cancer, hypertension, and inflammation [3]. Secondary metabolites exhibit a wide range of biological functions, including anti-cancer, analgesic, anti-inflammation, and anti-microbial activities [1]. Plants have generated about 25% of clinically used modern drugs [4]. About 80 % of the African population have been reported to use traditional medicines to meet their health care needs due to economic and geographical constraints [5].

In Ethiopia, plants have been reported to have a number of medicinal values, for thousands of years and traditional Ethiopian medicine have been the primary means for maintaining health as well as preventing and treating human diseases. According to Endashaw (2007) [6], there are 6500 species of higher plants in Ethiopia making the country one of the most diverse floristic regions in the world. There are large numbers of moderate to high value medicinal plants, spices existing in the wild in the country. The bulk of the plant matter used for medicinal purposes is collected from natural vegetation stocks [6]. However, of the existing medicinal plants only small percentage have been subjected to chemical and pharmacological investigation. The principle of traditional Ethiopian medicinal therapeutics is the synergism, that is, often multiple components in traditional medicine play a synergistic role which is greater than that of the individual drug. As a result, the active extracts and effective compounds responsible for the biological effects are often unknown [7]. Now a day, scientists including phytochemists and pharmacologists continue to study the chemical components of medicinal plants hoping to find new compounds with biological activities which can be used as lead compounds and further

developed them into therapeutic agents. Overall, drugs derived from natural products obtained from natural products have played and still playing a dominant role in pharmaceutical care. Some successful examples include discovering antitumor and cancer chemo-protective agents such as paclitaxel (**1**), camptothecin (**2**), vinblastine (**3**), magnolol (**4**), and resveratrol (**5**) (Figure 1.1),which proved to be effective in the treatment and management of cancer [8-10].

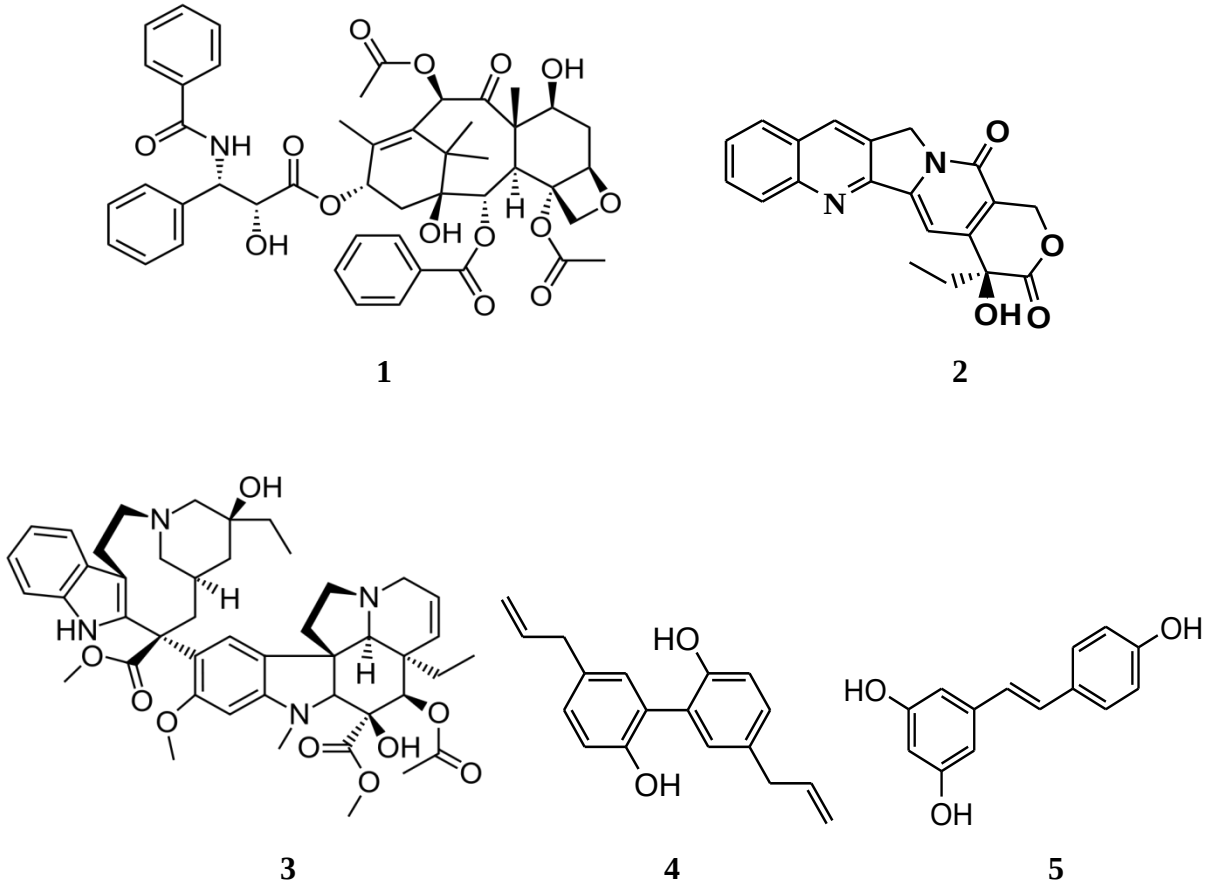

Figure 1. 1 Examples of drugs for treatment of cancer obtained from medicinal plants

Many of these plant-derived anticancer agents have been discovered through large-scale screening programs [11]. The most efficient method of discovering drugs such as these were done by bioactivity-guided fractionation, isolation and characterization [12].

The genus *Commiphora* Jacq., comprising more than 200 species, is one of the 20 genera belonging to the Burseraceae family, of which more than 52 *Commiphora* species exists in

Ethiopia [13]. Indigenous communities have for a long time incorporated the use of traditional medicines, mainly from plant source in the cure or lessening of impact of common ailments. In Ethiopia, some of the plants used in folkloric medicine have been identified and application of their crude extracts documented and *Commiphora* species are one of them [14]. Even though *Commiphora* species have a lot of traditional uses there is insufficient studies on chemical and biological activities studies on the plant resins of Ethiopian origin. The chemical and biological investigation of some of the *Commiphora* species native to Ethiopia resulted in the isolation of different secondary metabolites that include terpenes, lignans etc [15, 16].

1.1 Statement of the research problem

Even though identification of phytochemicals and traditional medicinal claims of most *Commiphora* plants resin documented, the chemistry and pharmacological activity of resins of these plant resins of Ethiopian origin is not yet fully known due to lack of screening to active principles. This encouraged us to undertake extraction, fractionation and isolation of compounds on the selected *Commiphora* species. This might help to proof whether there is a correlation between traditional use in combination with other medicinal plants or alone. Bioassay guided isolation is the foundation for the isolation and identification of natural products for new biological active compound that serve as a lead compound and drug candidates.

1.2 Significance of the Study

Natural products serve as a rich source of lead compounds for the development and production of modern chemotherapeutic agents. Resins of *C. africana, C. habessinica, C. schimperi and C. sphaerocarpa* from the family of Burseraceae have been used alone or in combination with other medicinal plants to treat various ailments in the area of collection. The resinous exudates of the genus *Commiphora* are commonly used as perfume, incense, or embalming ointment and their medicinal values have been gradually recognized by humankind [17]. The resin is also used to treat various ailments such as wound, pain, fracture, calming nerves, inflammation, stomach disorders and antiseptic. Due to the absence of modern scientific studies, the indigenous knowledge related to *Commiphora* resins has not been realized and not well documented. Thus, this study intended to answer some of the major questions in some *Commiphora* species Ethiopian origin including pharmacological activity and structural identifications of compounds

to ascertain credibility of their traditional medicinal uses. The results (findings) of the study would

- used to establish base line information on composition of *Commiphora* resins indigenous to Ethiopia
- lay the foundation for identification of bioactive solvent fractions and compounds.
- benefit market providers which generate their income by supplying resins of *Commiphora* for domestic consumption and internationally

1.3 Scope of the research

In this study, the methanol extract and related solvent fractions from *C. africana, C. habessinica, C. sphaerocarpa,* and *C. schimperi* were screened on four human cancer cell lines, three viral strains and a dengue virus serotype 2 (DENV-2). The fraction with the highest cytotoxicity was subjected to chromatographic separation and spectroscopic analysis. Cytotoxic effects of the isolated compounds were tested on the four human cancer cell lines. Structure of the isolated compounds were elucidated using different spectroscopic techniques to provide further insight and understanding on the structural features that could influence the activity of a compound. In addition, constituents of hydrodistillate of resin essential oils were identified using GC-MS technique and anti-inflammatory effect were studied. Comparison with literature reported data was made on the major constituents of the essential oils to justify for its/their anti-inflammatory effect.

1.4 Objective of the study

1.4.1 General objective

This investigation was designed to conduct bioassay-guided identification of compounds from some resins of *Commiphora* species native to Ethiopia for biological principles.

1.4.2 Specific objectives

- To estabilish the profile of the composition of the essential oils of *C. habessinica*, *C. africana*, *C. sphaerocarpa* and *C. schimperi* using GC-MS, and evaluate its anti-inflammatory activities.
- Investigate *in vitro* cytotoxicity, anti-viral and anti-dengue activity of the crude extracts and solvent fractions of different polarity using SRB (sulformaide B), CPE (cytopatheic effect) and IFA (immunofluorescence assay).
- To Isolate and characterize compounds from the most cytotoxic fractions using flash column chromatography (FCC) and column chromatography (CC) and spectroscopic techniques, such as IR, MS, 1D and 2D NMR and computational analysis.
- Evaluate cytotoxicity of isolated compounds against human tumor cell lines, namely the A549 (non-small Cell Lung Cancer), A2780 (Ovarian cancer), MIA-PaCa-2 (Pancreatic cancer) and SNU638 (Stomach Cancer) using SRB assay.
- Determine antiviral potentials of crude extract and solvent fractions on influenza viral strains of PR8, A/Puerto Rico/8/34 (H1N1); HK, A/Hong Kong/8/68 (H3N2); Lee, B/Lee/40against by *in vitro* assays.
- Determine S.I a ratio of CC_{50} (cytotoxicity) and EC_{50} (effective concentration) of selected solvent fractions that showed potential antiviral activity

CHAPTER TWO

LITERATURE REVIEW

2.1 Biological activity

Traditionally in different parts of the world *Commiphora* species used to treat various ailments to heal wound, pain, arthritis, fractures, obesity, parasitic infection, amenorrhea, tumour and gastrointestinal diseases [18]. Pharmacological studies revealed, antiproliferative, anti-inflammatory, antimicrobial, hypolipidemic and anesthetic properties of the purified metabolites and crude extracts of some *Commiphora* species have been investigated [19]

2.1.1 Inflammation

Inflammation is a physiological immune response process by various immune cells including macrophages for the protection against the harmful stimuli such as virus and bacteria [20]. Macrophages play an important role in inflammatory response by producing inflammatory mediators such as nitric oxide (NO) [21, 22]. Overproduction of inflammatory mediators-induced chronic inflammation is considered to be a cause of numerous human diseases including cancer, atherosclerosis, arthritis and septic shock [23-25]. Among inflammatory mediators NO, an important molecule produced in the process of oxidative stress, is synthesized by the enzyme inducible NO synthase (iNOS) and results in many disease processes such as carcinogenesis, obesity and diabetes [26, 27]. Therefore, iNOS-mediated NO is a common mediator of a wide range of inflammatory conditions and reflects degree of inflammation, thus providing a marker (measure) of the inflammatory process [28]. It has been reported that development of cancer is associated with inflammation [28, 29].

2.1.2 Cancer

Cancer is a major public health problem worldwide and is the second leading cause of death in the United States [30]. Cancer, a cellular malignancy that results in the loss of normal cell-cycle control, such as unregulated growth and the lack of differentiation, can develop in any tissue of any organ at any time and unlimited proliferation which can result in death [31]. Unlike normal cells, cancerous cells lose their ability to respond to death signals that initiate apoptosis (programmed cell death). Despite the therapeutic advances made in understanding the processes

involved in carcinogenesis, cancer has become one of the most serious medical problems today. It is the second leading cause of mortality around the world with an incident rate of more than 2.6 million cases per year [32, 33]. Literature report indicated that most cancers are caused by a dysfunction of many genes coding for proteins such as growth factors, growth factor receptors, antiapoptotic proteins, transcription factors, and tumor suppressors, all of which constitute a target for cancer treatment [34, 35]. The increase in the incidence of cancer along with the undesirable side effects observed with chemotherapy urges the discovery of new agents from natural sources. In fact, the concept of chemoprevention by naturally derived compounds has gained increasing attention especially that prevailing cancer treatments have shown limited therapeutic success [36]. By their original locations cancers are classified into various types of cancer, such as lung, colon, breast, or prostate cancer.

Cancers of the lung, with two broad histological subtypes of lung cancer i,e., small-cell lung cancer (SCLC), which is the cause of 15% of cases, and non-small-cell lung cancer (NSCLC), which accounts for 85% of cases is one of the top three cancer types in terms of incidence, and is ranked the first in terms of mortality. Ovarian cancer (A2780) is the seventh-most common cancer among women and the eighth-most common cause of death from cancer. Pancreatic cancer (MIA-Paca-2) is the seventh highest and responsible for 6% of cancer deaths each year [30]. Globally, stomach cancer (SNU-638) is the fifth commonly diagnosed cancer and the third leading cause of death from cancer making up 7% of cases and 9% of deaths. Up to now, numerous clinical trials have investigated potential cures for cancer via radiation, chemotherapy, antibody treatment, and immunotherapy [37]. Radiation and chemotherapy have severe side effects due to their cytotoxicity to normal cells. Additionally, many types of cancer tend to relapse and acquire resistance after treatment. Currently, combination therapies involving several drugs or therapies are being used to attempt to overcome the limitations and the drawbacks of individual therapies [37]. Nowadays, dueto advancement of technology localized tumors can be removed by surgery or irradiation with high survival rates [37].

More than 60% of drugs with anti-cancer activity originated from plants [38]. Plant-derived metabolites are good sources of new anti-cancer drugs with reduced cytotoxicity and increased activity [39]. Additionally, the combination of phytochemicals with existing anti-cancer drugs or

other chemical compounds represent alternative approaches to natural-product-based drug development. Several secondary metabolites have been discovered to have inhibitory activity against cancer. For instance, Epigallocatechin gallate (EGCG), a major component of green tea from *Camellia sinensis*, has been reported to have preventive effects on carcinogenesis [40].

A study of cancer incidence on a population-based cancer registry data revealed that in Ethiopia cancer has become the second leading cause of death in the adult population [41]. The most common adult cancers reported so far are: cancers of the breast and cervix, colorectal cancer, non-Hodgkin lymphoma, leukemia, and cancers of the prostate, thyroid, lung, stomach and liver. The most common cancer in men age ≥ 15 years was colorectal cancer (CRC), followed by non-Hodgkin lymphoma (NHL), prostate cancer (CaP), leukemia, and lung cancer. In females 15 years and older, the most common cancer has been found to be breast cancer (BC), followed by cervical cancer (CC), ovarian cancer, CRC, and leukemia [41].

2.1.3 Influenza virus

Influenza virus remains to pose a direct threat to human beings and society for causing severe epidemics of respiratory illness. This highlights an urgent need for new anti-influenza drugs. The influenza virus is one of the major pathogens leading to seasonal outbreaks and even pandemics and annual influenza epidemics such as avian H5N1 and pandemic H1N1 (swan flu). Influenza outbreaks result in morbidity and mortality in human population and commonly occur during winter, or the rainy season in tropical countries [42, 43]. Due to its high mutation rate, currently available drugs like Tamiflu and Amantadine have already resulted in drug resistance virus. Therefore, there is an urge to develop novel and effective antivirals for influenza virus associated infections. The lack of effective therapies and/or vaccines for several viral infections, and the rapid emergence of new drug-resistant viruses have necessitated the need for developing new and effective antiviral agents.

2.1.4 Dengue virus

Dengue is a viral disease caused by Flavivirus and belongs to family Flaviviridae, are the causative agents of dengue fever and its associated complications, dengue haemorrhagic fever

(DHF) and dengue shock syndrome (DSS) [44]. There are four distinct serotypes DENV-1, DENV-2, DENV-3, and DENV-4 [45-47]. DENV-2 is known to be more lethal than other serotypes [48]. Dengue fever, regardless of its serotypes, is transmitted from person to person by *Aedes aegypti* and *Aedes albopictus* mosquitoes in the domestic environment [49]. In the recent decade, dengue has re-emerged and with it being endemic in more than 110 countries. It has been the most prevalent arthropod-borne viral diseases in terms of morbidity and mortality [50]. Two fifths of the world populations are at risk, estimating around 100 million of dengue fever infections, 2.1 million cases of dengue hemorrhagic fever and 200 thousand deaths worldwide are caused by dengue every year. Despite extremely high rates of dengue for decades, Southeast Asia region still recorded an increase of 67% from 1985- 1989 to 2002-2006 [51]. Similarly, a total of 4.6-fold increase in dengue cases has also been reported in America over the three decades [51]. There is currently no treatment or vaccine available for dengue infection [52]. Therefore, the development of a plant-based antiviral preparation promises a more potential alternative in combating dengue disease.

2.2 The family Burseraceae

The family Burseraceae, with twenty genera and over 500 species, is widespread in tropical and subtropical regions, and is often a dominant constituent of the vegetation in dry lowland areas of Eastern Africa [53]. The *Acacia-Commiphora* woodlands of Northern Kenya, Southern Ethiopia and Somalia, particularly are dominated by species of the genera *Acacia* (Leguminosae). The species produce gum resins, such as frankincence and *Commiphora* have been used as incense in religious and cultural ceremonies since the beginning of written history [54].

Indeed, frankincense and myrrh were described in Bible: “When they saw the star, they rejoiced with exceeding great joy. And when they were come into the house, they saw the young child with Mary his mother, and fell down, and worshipped him: and when they had opened their treasures, they presented unto him gifts; gold, and frankincense, and myrrh.” (The Gospel According to St. Matthew 2: 10-11). They were also the most prized aromatic gums of the ancient world and a significant source of wealth in southern Arabia [54]. Their common medicinal properties are recognized in the treatment of inflammatory conditions, some cancerous

diseases, and wound healing in the traditional medicines of India, China, Rome, Greece, Babylon and elsewhere [54].

The genera *Commiphora* produce resins, which have considerable commercial, medicinal and cultural uses. Most of these species were little known until recently because of poor botanical descriptions which were based on insufficient materials [55]. In Ethiopia there are only 2 genera, namely, *Boswellia* and *Commiphora* that belong to the family Burseraceae [56]. These genera produce resins, which have considerable commercial, medicinal and cultural uses. Although the history of resins from the Burseraceae family dates as far back as the times of the pharaohs of ancient Egypt, it is quite surprising to note that the chemistry and pharmacological activity of these resins is not yet fully known.

2.2.1 The genus *Commiphora*

The name *Commiphora* originates from the Greek words *kommi* (means 'gum') and *phero* (means 'to bear'). The majority of the species yield a fragrant oleogum-resin following damage to the bark either naturally or intentionally. These trees or shrubs are characterized by an outer bark often papery and peeling, an inner bark usually greenish, containing ducts which form large interconnecting cavities from which the gum-resin, usually aromatic, flows freely on wounding or from natural fissures. Many species are leafless most of the year and usually set flower and fruit when leafless, making the collection of fertile botanical specimens difficult [13]. According to Soromessa (2013), South east lowland of Ethiopia is characterized by its high diversity of *Acacia* and *Commiphora* species [57]. The report indicated that out of total species in the genus *Commiphora* about half of them are endemic to the small area of southeastern Ethiopia, north eastern Kenya and Somalia [57]. Over 50 *Commiphora* species are known to occur in Ethiopia, several of which 14 (25%) of the species are endemic [56]. *C. myrrha* (Nees) Engl. is the most well-known member of the genus *Commiphora*, yielding one of the most important resins of all times, commonly known as myrrh. Myrrh, a culturally and commercially important resin product, is derived from *C. myrrha* (Nees) Engl, a tree found in abundance in the dry and arid regions of Ethiopia and Somalia and to some extent in Northern Kenya [13]. The chief *Commiphora* gum of highly economic importance is myrrh, produced by *C. myrrha* (Nees) Engl. (synonum *C. molmol*). This is an important commodity of commerce in Southern and South Eastern Ethiopia [56]. Myrrh has also been used in the Ayurvedic medical system due to its therapeutic effects for

treatment of inflammatory diseases, some cancerous diseases, coronary artery diseases, gynecological disease, obesity, etc [58]. Other oleo-gum resins resembling myrrh are produced by various species of *Commiphora* such as *C. africana* (A. Rich) Engl., *C. habessinica* (Berg) Engl., *C. kua (*J.F Royal) Vollesen, *C. schimperi* (Berg) Engl., *C. sphaerocarpa*. These resins are sometimes found in true myrrh as adulterants. In this genus, species of *C. myrrha, C. mukul, C. molmol, C. erlangarina, C. kua* and *C. confusa* are the ones that have received more phytochemical and bioactivity attention [19] .

Previous studies on the genus have showed the prescence of a series of metabolites including terpenoids, steroids, flavonoids, lignans, carbohydrates, and long chain aliphatic alcohol derivatives [59, 60]. These secondary metabolites and crude extracts of the *Commiphora* species exhibited diverse biological activities, such as cytotoxic, anesthetic, antiinflammatory, and antimicrobial effects, and so on [19, 61].

2.2.2 Ethnobotany of *Commiphora* species

Ethnobotany is concerned with the use of plants within traditional medical systems [62, 63]. The gum-resins of *Commiphora* are heavily used in international trade but, a few of the species are known to produce gum-resins [56, 64]. Ethnobotanical information was gathered by interviewing the local people and through observation. The *Commiphora* plant is widely grown in Borena lowlands, southern Oromia, Ethiopia. The gum-resins of *C. africana* and *C. habessinica* (Berg) Engl. are used by Borana people of Southern Ethiopia to heal burn (in human beings), wound, and to eradicate cattle ticks [65]. In addition to the above mentioned uses, the gum-resins from *Commiphora* are also used by followers of both the Orthodox Christian (in church and at home) and Muslem religions during their prayers, essentially to 'calm and collect' their nerves. It is also used as incense during coffee ceremonies at home. In Eeastern Ethiopia, the gums are also chewed to ease "tooth ache". The leaves and roots are used in the treatment of lymphadenopathy [66]. In different parts of the world, *Commiphora* species are used in indigenous medicines for the treatment of wound, pain, arthritis, fractures, obesity, parasitic infection and gastrointestinal diseases [18, 67].

Myrrh has many medicinal powers and has been used to treat various diseases, such as amenorrhea, ache, dysmenorhhea, tumors, fever, stomach complaints (for example, for

stimulating the appetite and the flow of digestive juices), diseases of gall bladder, chest ailments, snake and scorpion bites, and skin infections in India, China, Rome, Greece and Babylon [60, 68]. Traditionally, *C. africana* is used to treat measles, hyperlipidemia and cardiovascular disorders [69, 70]. Additionally, the leaves are used as sedative and soporific [69] the resin is used to prepare antiseptic washes and baths for skin infections, sores and leprosy [71]. Antiproliferative, anti-inflammatory, antimicrobial, hepatoprotective and cardiovascular properties of the purified metabolites and the crude extracts of the plant have been also recorded [19, 60].

Table 2. 1 List of some common *Commiphora* resin bearing species and their traditional medicinal uses

No	Name of *Commiphora species*	Resin traditional uses	Reference
1	*C. myrrha* (Nees) Engl.	used as incense, snake and fly repellent, as remedy for joint problems and against stomachache.astringent, antiseptic, emmenagogue, carminative, expectorant and stimulant	[72, 73]
2	*C. molmol*	Used as antimicrobial agent, remedy for sore throats, canker sores, gingivitis	[68]
3	*C. mukul*	Anti-obesity, anti-inflammatory, antibacterial, anticoagulant, anti-arthrosclerotic, reduce symptoms of osteoarthritis	[74, 75]
4	*C. africana* (A. Rich.) Engl.	Hedge plant, root edible; stem to make utensils and gum chewed to ease "tooth ache". Bark, resin and leaf to treat tumour, stomach ache, expelling tapeworms	[76, 77]
5	*C. habessinica* (Berg) Engl.	As soap substitute and for cleansing (disinfectant) new born baby. To treat eye infection	[78]
6	*C. boranensis* Vollesen	heal burn and wound and to eradicate cattle ticks	
7	*C. guidottii* Chiov.	used against stomach complaints in particular diarrhea, and to facilitate withdrawal of placenta.	
8	*C. schimperi* (Berg) Engl.	for smoothening of skin.	[79]
9	*C. sphaerocarpa*	Against cough, diarrhea and headache, against ticks of cattle.	
10	*C. erythraea* (Ehrenb) Engl.	As incense, repels insects	[80]
11	*C. kua* (R. Br. Ex. Royle) Vollesen	as incense, for healing wounds, to reduce the swelling of udder; stomach disorders, Stem: to make home utensils.	[15, 81]
12	*C. rostrata*	fluid resin: to treat eye diseases, perfume; branches: tooth stick; resin: poisonous, incense to repel mosquitoes and flies.	[15]
13	*C. tenuis* Vollesen	to treat itching, wound	[82]

2.3 Chemical constituents and pharmacological activity of some *Commiphora* species

Many plants belonging to the *Commiphora* species (family Burseraceae), have a history of medicinal use in systems of traditional medicine. Best known *Commiphora* species, such as *C.*

myrrha, C. mukul and *C. molmol* have been the subject of substantial phytochemical, pharmacological and clinical investigations over the last four decades [19], but many lesser known species are also used, mostly in East Arica (Ethiopia, Kenya, Somalia and Sudan), where the majority are native [53].

2.3.1 *Commiphora myrrha*

C. myrrha (Nees) Engl. is the most well known member of the genus *Commiphora*, it is found in the dry and arid regions of Ethiopia and Somalia (the largest producers and exporters of myrrh) and to some extent in northern Kenya [83] yielding one of the most important resins of all times, commonly known as myrrh. These plants yield economically important gum exudates that have been collected for centuries as medicinal and perfumery substances [84]. It comprises 3-8% essential oil, 30-60% water soluble and 25-40% alcohol soluble components [85]. Internally, myrrh is used as cure for indigestion, ulcers and bronchial congestion [86]. Based on the theory of Chinese traditional medicine, myrrh possesses variety of curative effects, and was primarily applied for the treatment of blood stagnation and inflammatory diseases, as well as for relief from swelling and pain. The alcoholic solution, when concentrated after filtration, yields the so-called "absolute" while the hexane extract yields a "resinoid". Other oleo-gum resins resembling myrrh are produced by various species of *Commiphora* such as *C. africana* (A.Rich.) Engl., *C. habessinica* (Berg) Engl., *C. kua (*J.F Royal) Vollesen, *C. schimperi* (Berg) Engl., etc. These resins are sometimes found in true myrrh as adulterants. A study by Zhu, (2003) from the ethyl acetate extract of *C. myrrha* subjected to column chromatography over silica gel eluted with chloroform-methanol mixture with increasing methanol content, furanogermacra-1*E*,10(15)-dien-6-one (**6**), 2-methoxyfuranogermacra-1(10),4-diene (**7**), 3α-eudesm-4(15)-ene-1β,6a-diol (**8**) and Tcadinol (**9**), (Figure 2.1) some new compounds have been isolated [87].

Moreover, a bioassay guided fractionation and isolation of a peteroleum ether fraction fo the *C. myrrha* afforeded compounds belonging to the class of sesquiterpene and diterpene acid type of compounds; **10, 11, 12, 13** and **15** [88]. It has been reported that a cytotoxicity study based on bioassay-guided showed the petroleum ether fraction of *C. myrrha* was active in the cytotoxicity

assays against human gynecologic cancer cells, ovarian cancer cell lines A2780, SK-OV-3, cervical carcinoma cell line SiHa, and endometrial carcinoma cell line Shikawa using MTT assay. Among the compounds isolated from petroleum ether, 2 - methoxy - 5 - acetoxy - furanogermacr - 1(10) - en - 6 – one (**11**), abietic acid (**14**), dehydroabietic acid (**15**) and sandaracopimaric acid (**16**) (Figure 2.1) antiproliferative activity has been studied. Results indicated that dehydroabietic acid (**14**) (Figure 2.1) inhibited SK-VO-3 cell growth with IC_{50} of 26.93 μM, while the abietic acid (**14**) significantly inhibited A2780 cell growth with IC_{50} of 46.89 μM [88].

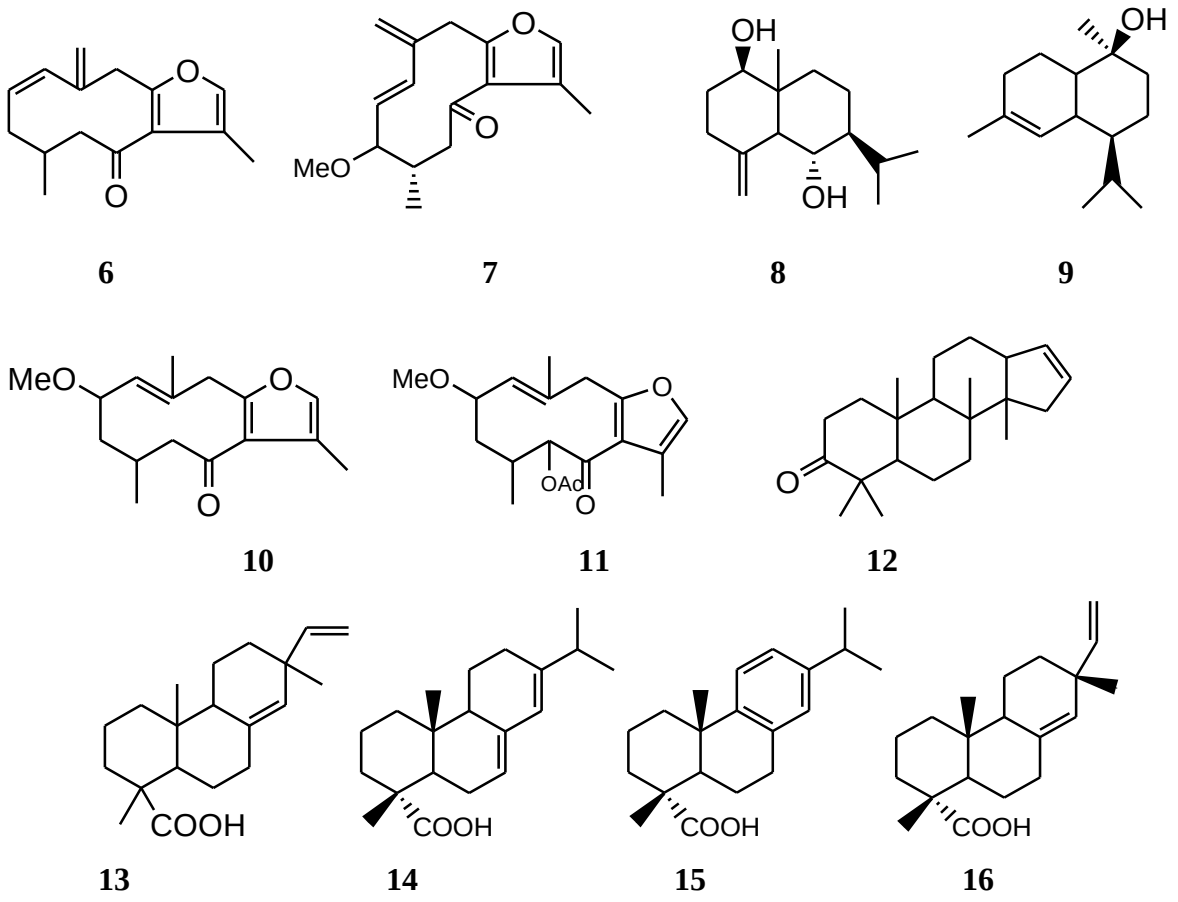

Figure 2. 1 The chemical structures of compounds (**1-16**) isolated from *C. myrrha*.

In Indian traditional system of medicine "Ayureda", guggulu and plant extract of *C. mukul* has been used for thousands of years in the treatment of arthritis, inflammation, gout, rheumatism, obesity, and disorders of lipids metabolism [89]. *C. mukul*, because of its wider application against different ailments in India Ayruvedic traditional medicine, is the most

well-known gum resin and highly investigated by different scholars. The bioactive constituents are mainly steroids with the most prominent being 4,17(20)-(*trans*)-pregnadiene-3,16-dione (Z- guggulusterones) (**17**), 4,17(20)-(*cis*)-pregnadiene-3,16-dione (E-guggulsterones) (**18**), guggulsterol-I (**19**), guggulsterol-II (**20**), guggulsterol-III (**21**) [89], 20α-hydroxy-4-pregnen-3-one (**22**), 20β-hydroxy-4-pregnen-3-one (**23**), 16β-hydroxy-4,17(20)*Z*-pregnadien-3-one (**24**) and 16α-hydroxy-4-pregnen-3-one (**25**) [90]. The diterpenoids cembrene-A (**26**) and mukulol (**27**) also occur in *guggulu* [89] (Figure 2.2)**.** The chemical structures of compounds (1-16) obtained from *C. myrrha*. Two new polypodane-type triterpenes, myrrhanol A (**28**) and myrrhanone A (**29**), were isolated from the 50 % aqueous methanolic extract of guggul-gum resin [91].

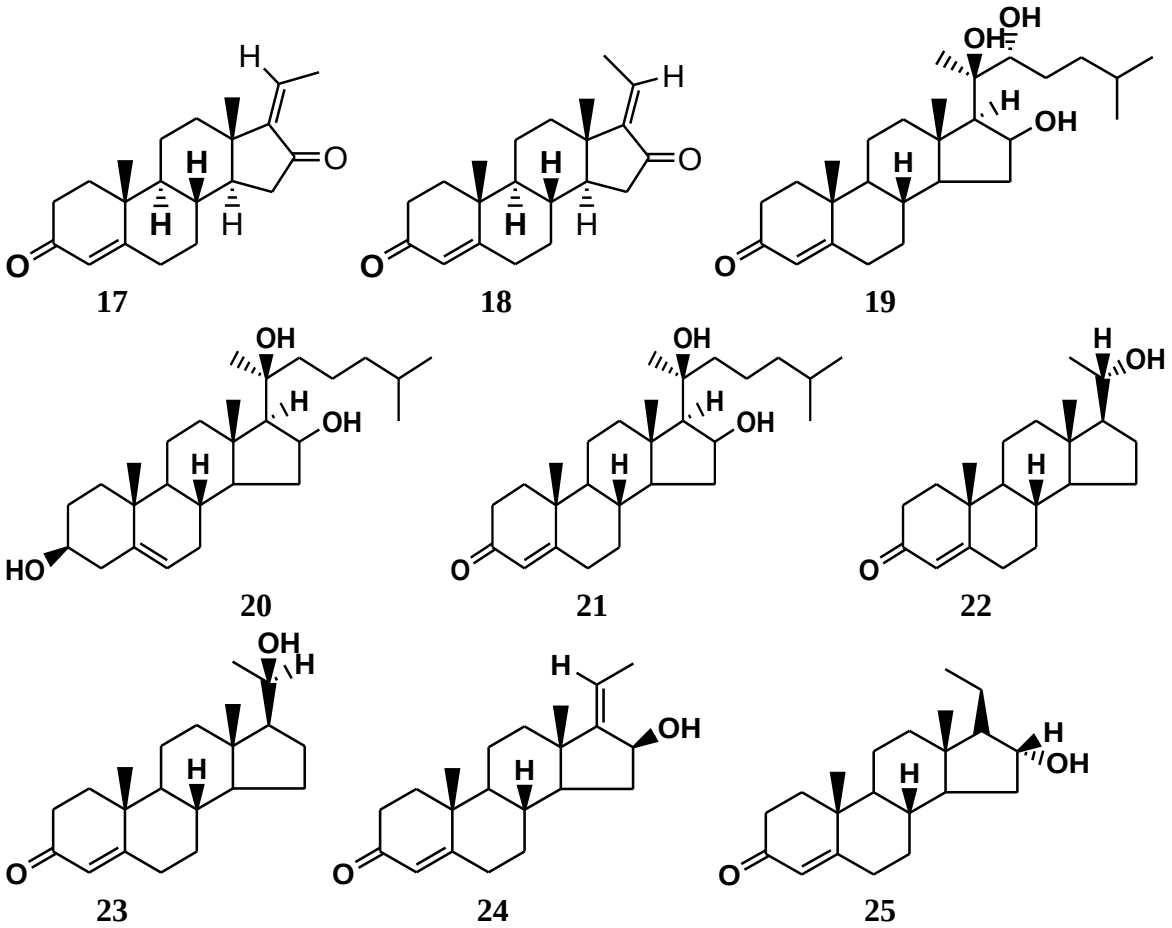

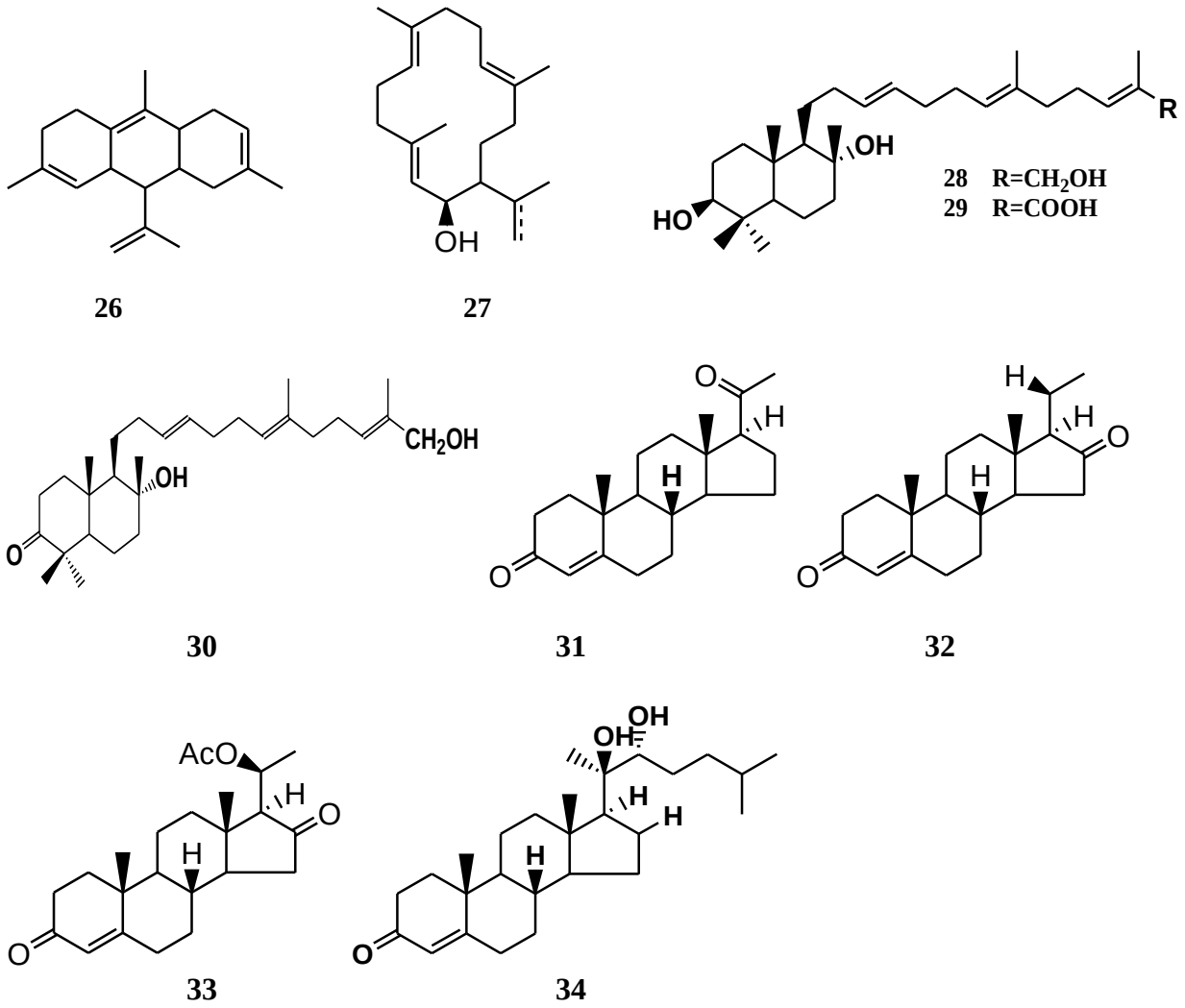

Figure 2. 2 The chemical structures of compounds (**17-34**) obtained from *C. mukul*

The steroids, *Z*- guggulsterone (**17**) and *E*-guggulsterone (**18**) induces apoptosis using PC-3 human prostate cancer cells. The viability of these cells was significantly reduced upon treatment with guggulsterones, in a concentration-dependent manner [92]. Among the bioactive molecules of *Commiphora mukul* bicyclic triterpenes such as myrrhanol A (**28**) and myrrhanol B (**29**), myrrhanone A (**30**), (Figure 2.2) were reported to exhibit significant anti-inflammatory and anticancer activities [93, 94].

A study by Matsuda [93, 95] showed that the methanol extract of *C. mukul* was found to inhibit NO production in LPS activated mouse peritoneal macrophages with IC_{50} value of about 15 μg/mL. On the other hand, the isolates from the gum resin of *C. mukul*, two pregnane type

steroids, *Z*- and *E*-guggulsterones (**17** and **18**), three polypodane type tritrpenes, myrrhanol A (**28**), myrrhanol B (**29**) and myrrhanone A (**30**) were found to prevent NO production with IC_{50} values of 1.1, 3.3, 25, 61 and 35 μM, respectively [95]. A pregnane type sterols, progesterone (**31**), 4-pregnene-3,16-dione (**32**), 20*S*-acetyloxy-4-pregnene-3,16-dione (**33**) showed anti-inflammatory effect with IC_{50} 11, 40, and 56 μM respectively. Other compounds isolated from *C. mukul*, like a cholestane-type steroid, 20*R*, 22*R*-dihydroxycholest-4-en-3-one (**34**) and cembrane-type diterpene, mukulol (**20**) resulted an IC_{50} 20 μM and a 24 μM respectively. Thus, these compounds were found to prevent overproductions of NO and inhibited the induction of inducible nitricoxide synthase (*i*NOS) in LPS-activated mouse peritoneal macrophages in a concentration dependent manner [75, 93]. Furthermore, Z- guggulsterone (**17**) and E-guggulsterone (**18**) steroids (Figure 2.2) have been found to exert their anti-inflammatory properties by suppressing activation of NF-kB and expression of NF-kB-regulated gene products [96, 97] that indicate their potency towards inflammation. Besides these, other signal path ways such as ROS, TNF-a, PGE2, and MAPK have been verified as potential anti-inflammatory targets.

2.3.3 *Commiphora erlangeriana*

The resin of *C. erlangeriana* [Syn: Dhunkal in Ethiopia and Somalia] was known to be poisonous to humans and animals and had traditionally been used as an arrow poison. Phytochemical studies by Dekebo et.al 2002 on this plant material identified four polygamain-type lignans named erlangerin A (**35**) and erlangerin B (**36**), and erlangerin C (**37**) and erlangerin D (**38**) related to podophyllotoxin (**39**) (Figure 2.3) from the resin of *C. erlangeriana* from the MeOH-EtOAc (1:1) extract of the resin of *C. erlangeriana*, a plant occurring in Ethiopia and Somalia. [98].

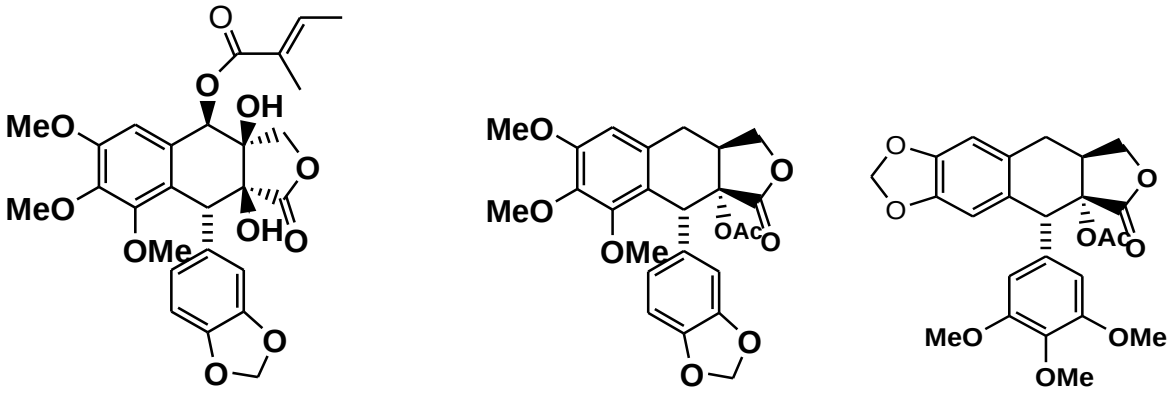

35 **36** **37**

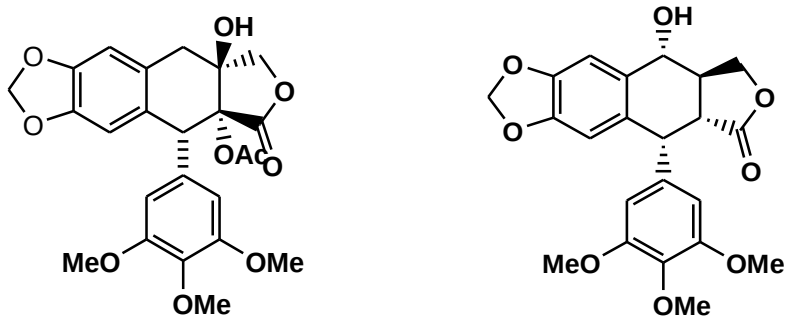

38 **39**

Figure 2. 3 The chemical structures of compounds (**35-39**) obtained from *C. erlangarina*

The effects of erlangerin C (**37**) and D (**38**) were reported to be closely related to the activity profile of podophylotoxin (**39**): they induced a concentration-dependent cytotoxicity in the murine macrophage cells (RAW 264.7) and a cytostatic effect in HeLa, EAhy926 and L929 cells. On the other hand, erlangerins A (**35**) and B (**36**) suppressed cell viability at relatively higher concentrations (EC_{50} values higher than 3 μM as compared with nM concentration range for erlangerins C (**37**) and D (**38**) and podophyllotoxin (**39**) (Figure 2.3) and their activity appears to be consistent with a cytotoxic mode of action in all cell lines studied [99].

2.3.4 *Commiphora kua*

Chromatographic separation of the resin of *C. kua* afforded mansumbinone (**40)**, mansumbinoic acid (**41)** and picro-polygamain (**42)** [100] (Figure 2.4), mansumbinol (**43)**, and (16S, 20R)-dihydroxydammar-24-en-3-one (**44)** and two new octanordammarane triterpenes, namely 15α-

hydroxymansumbinone (**45)** and 28-acetoxy-15α-hydroxymansumbinone (**46)** (Figure 2.4) [15]. Among the isolated compunds from the gum resin of *C. kua*, mansumbinol (**43**) (Figure 2.4) was found to inhibit the overproduction of NO stimulated by LPS in macrophages with strong anti-inflammatory activity with 74 μM concentration [58].

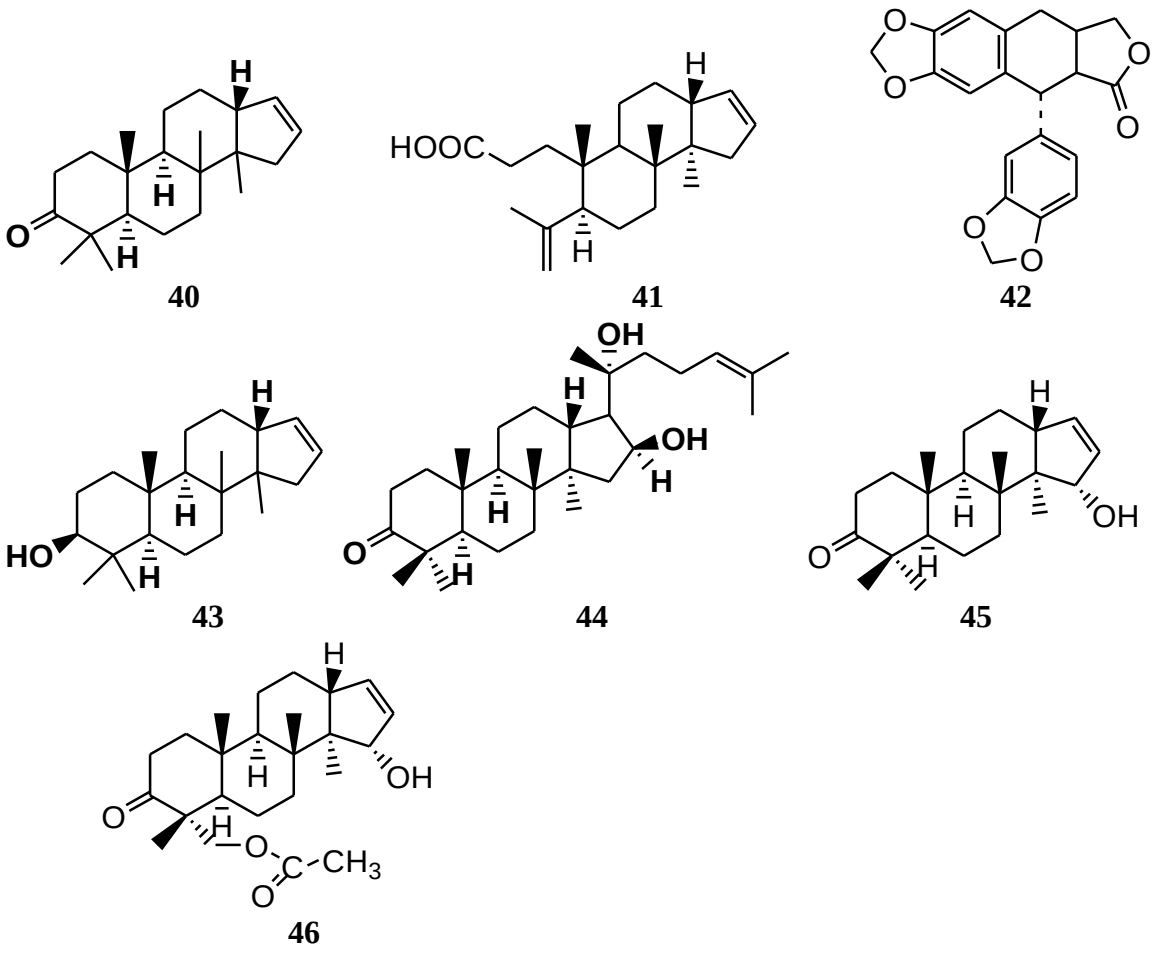

Figure 2. 4 The chemical structures of compounds (**40-46**) obtained from *C. kua*

2.3.5 *Commiphora africana and C. habessinica*

The resin of *C. africana* was observed to contains betulin (**47**), [101] which showed an antitumor activity, especially in combination with cholesterol (**48**) [102]. Betullinic acid (**49**) derivatives were found to be inhibitors of HIV-1 [103]. Bioassay-guided fractionation of a crude extract from *Commiphora africana* led to the isolation of the dihydroflavonol glucoside, phellamurin (**50)** [104]. The resin obtained from *C. habessinica* was reported to contain 6.5% of steroids.

Further fractionation by column chromatography followed by mass spectrum analysis revealed the presence of cholest-5-en-3β-ol (**48**), Δ5-campestan-3β-ol (**51**) and β-sitosterol (**52**) (Figure 2.5) [105].

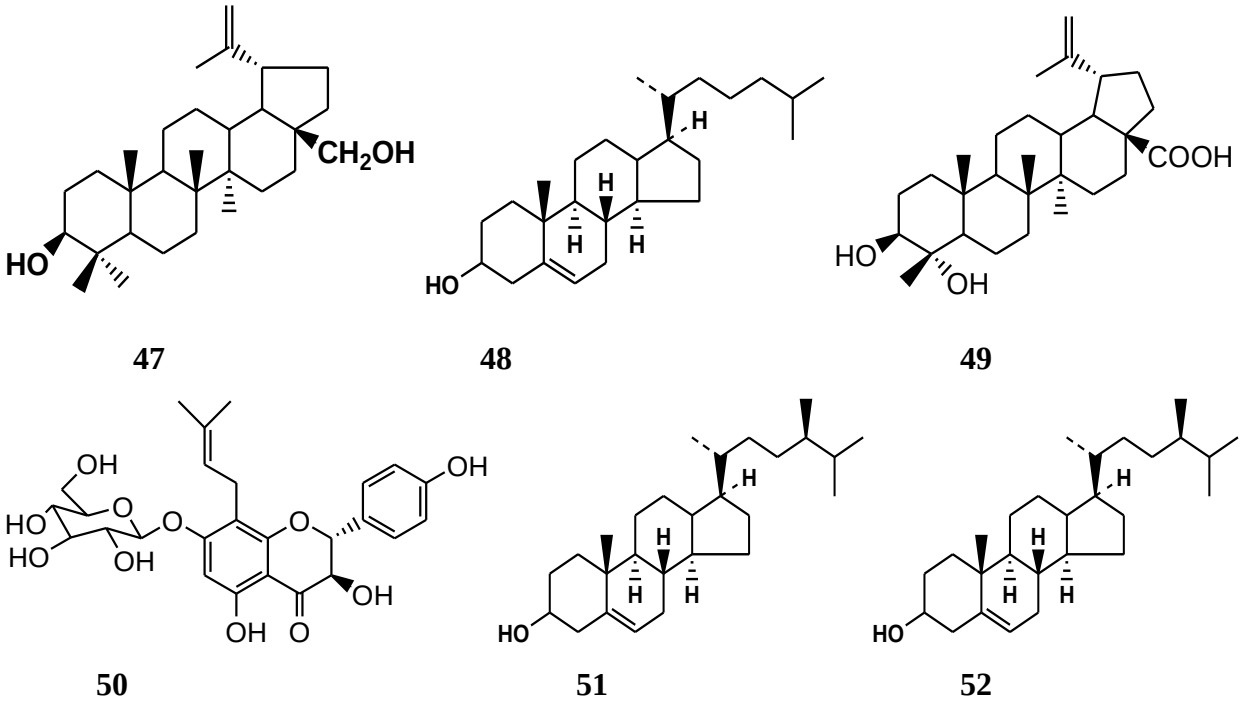

47 **48** **49**

50 **51** **52**

Figure 2. 5 The chemical structures of compounds (**47-52**) obtained from *C. africana and C. habessinica*

2.3.6 *C. confusa, C. molmol, C. sphaerocarpa, C. holtziana* and *C. kataf*

A study by Dekebo (2002) [15] on the resin of *C. confusa* afforded two new dammarane triterpenes, (3R,20S)-3,20-dihydroxydammar-24-ene (**53**) and (3R,20S)-3-acetoxy-20-hydroxydammar-24-ene (**54**) along with two known triterpenes, cabraleadiol 3-acetate **(55)** and α- amyrin **(56)** (Figure 2.6). After chromatography over silica, from the petrolether extract of *C. sphaerocarpa* resin six compounds were obtained, where chromatographic separation yielded a novel terpene, which showed the presence of a trisubstituted furan ring in ^{1}H-NMR and was characterized as (1E)-8,12-epoxygermacra-1,7,10,11-tetraen-6-one (**57)** [16]. The non-polar fraction of hexane extract of the resin of *Commiphora molmol* Engl, gave, the new furanoeudesmane (**58)** and furanoeudesma-1,3-diene (**59)** by column chromatography [106]. Not only the *Commiphora* species mentioned above but also Other *Commiphora* species have

provided pharmaceutically interesting compounds. Furanodienone (**60**) (Figure 2.6) belongs to the large group of furanosesquiterpenoids with different biological properties and found in extracts and essential oils of *Commiphora* species. Previously, oxygenated furanosesquiterpenes, curzerenone (**61**), and furanodienone (**60**) (Figure 2.4) from the resins of *C. sphaerocarpa* (Chiov.), *C. holtziana* (Engl.) and *C. kataf* [16, 83, 107] have been isolated by Messina (2017) [108] has shown that furanodienone (**60**) has anti-inflammatory, antimicrobial, and anticancer activities. Furanoeudesma-1,3-diene (**62**), the major compound of myrrh [16, 106], has been reported to exhibit analgesic activity in mice [109]. A mixture of furanodiene-6-one (**63)** (Figure 2.6) and 2-methoxyfuranoguaia-9-ene-8-one (**64**) exhibited antibacterial and antifungal activities against *Escherichia coli*, *Staphylococcus aureus*, *Pseudomonas aeruginosa* and *Candida albicans*, with MIC values ranging from 0.18 to 2.8 μg/mL [109].

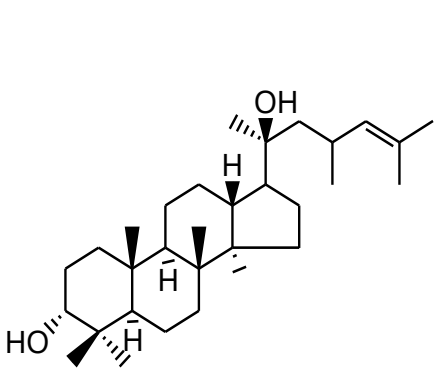

53

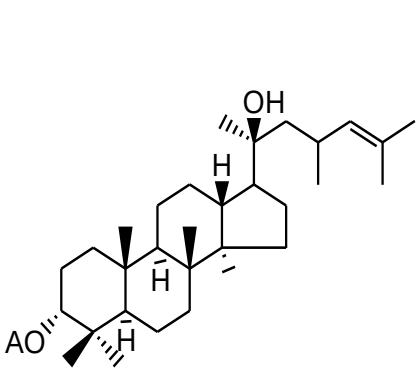

54

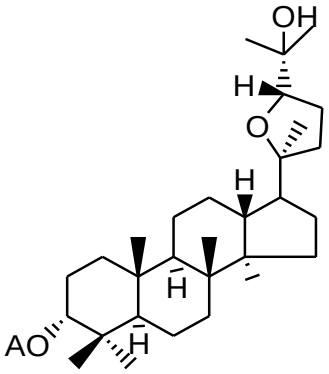

55

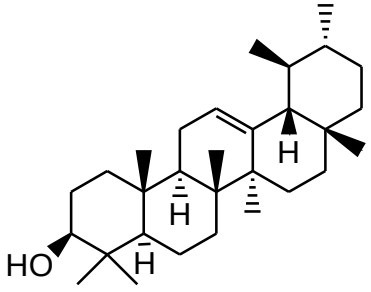

56

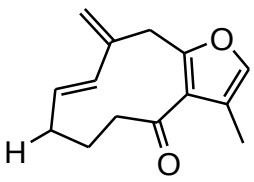

57

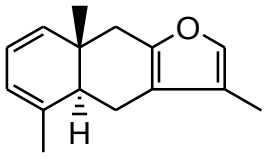

58

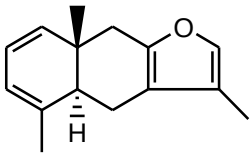

59

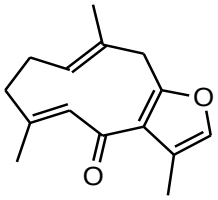

60

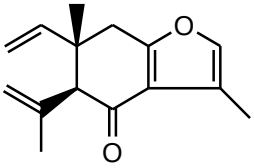

61

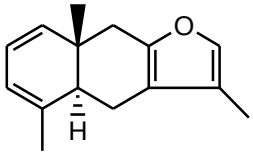

62

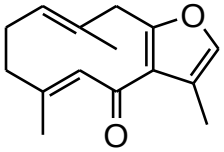

63

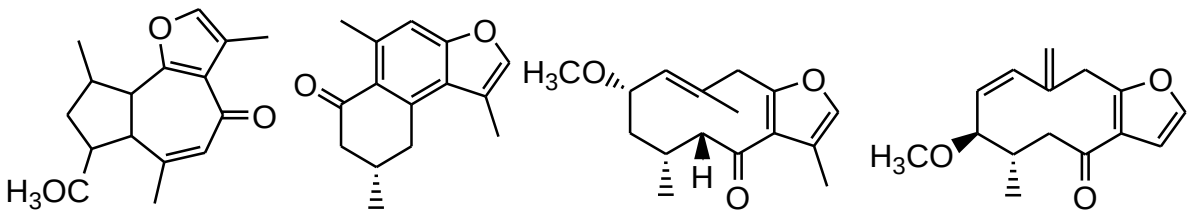

64 **65** **66** **67**

Figure 2. 6 The chemical structures of compounds (53-64) obtained from *C. confusa*, *C. molmol*, *C. sphaerocarpa*, *C. holtziana* and *C. kataf* essential oil (EO) (65-67).

The essential oils from *Commiphora* species have for centuries been recognized to possess medicinal properties. Oxygenated terpenoids are the components of essential oils most often responsible for their distinctive aroma and flavor, even though they are often minor constituents of the oil [110]. The essential oils and those classified as absolute and resinoid are used as fixatives in the manufacture of perfumes [111]. The oils are usually produced by steam and hydrodistillation process, and many studies have revealed that GC-MS analysis of the volatile oil from different species of the genus, commiphora [59]. The constituents of essential oil in myrrh by GC-MS resulted fifteen compounds most of compounds were furanosesquiterpenes isolated from its petroleum ether extract. The main constituents of myrrh was shown to be furanoeudesma-1,3-diene (**62**) (Figure 2.6) [112]. The essential oil of *C. myrrha* exhibited potent singlet oxygen quenching activity better than the control α-tocopherol. This effect was attributed to the reaction between furan ring of furano sesquiterpenoids of *C. myrrha* constituents in particular and singlet oxygen [113]. Three furano sesquiterpenoids (**65-67**) (Figure 2.6) from *C. myrrha* showed DPPH radical scavenging activity with EC_{50} values of 1.08, 4.29 and 2.56 mg/mL respectively [114]. The major components of essential oil from the stem distillation of *C. mukul* identified were myrcene (6**8**), limonene (**69**), *α*-pinene (**70**), linalool (**71**), 1,8-cineole (**72**), *α*-terpineol (**73**), *α*-phellandrene (**74**), methylheptanone (**75**), bornyl acetate (**76**), (±) geraniol (**77**) (Figure 2.7) [115]. The antibacterial activity of some constituents of *C. mukul* oleo-gum-resin essential oil, chloroform extract and isolated sesquiterpenoids were evaluated with a wide range of inhibitory activity against gram-positive and gram-negative bacteria being observed [116].

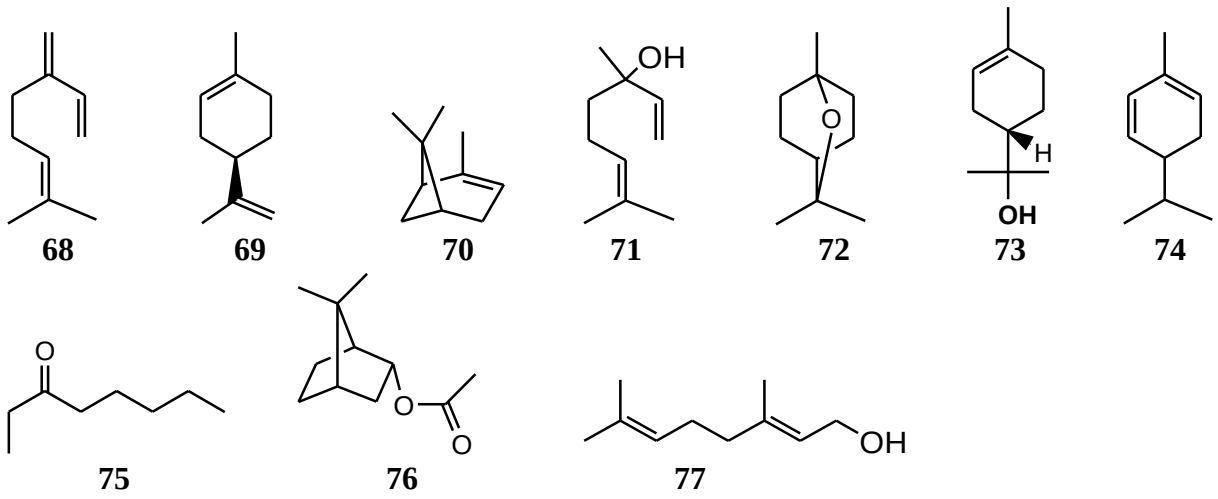

68 **69** **70** **71** **72** **73** **74**

75 **76** **77**

Figure 2. 7 The major components of hydrodistillate of *C. mukul* resin essential oil analysed using GC-MS

The chemical composition of the essential oil obtained from the oleo-gum resin of *C. myrrha* (Nees) Engl. var. *molmol* was examined using GC and GC-MS**,** curzerene (**78**), furanoeudesma-1,3-diene (**59**) and β-elemene (**79**) appear to be the major constituents (Figure 2.8). Assessment of bacterial growth inhibition using agar dilution method at various concentration levels showed that the oil from *C. molmol* possessed strong activity against clinical *S. aureus* including multidrug resistant strains [117]. The resin of *C. molmol* exhibited antitumor activity in Ehrlich-solid-tumor-bearing mice *in vivo*. With treatment at dose of 250 and 500 mg/kg/d, its antitumor property was comparable to the standard drug cyclo- phosphamide [18]. The volatile oil of *C. molmol* was shown to inhibit the production of IL-1β-stimulated IL-6 and IL-8 in human gingival fibroblasts cells [118]. The essential oil from the hexane extract of *C. habessinica* (Berg) Engl were identified to have more than twenty different constituents, including sesquiterpenoid hydrocarbons, β- elemene (**79**) and δ-elemene (**82**), α- copaene (**80**), β-bourbonene (**81**), δ-germacrene (**82**), caryophyllene (**83**), humulene (**84**), γ-cadinene (**85**) and δ-cadinene (**86**), and furanosesquiterpenoids, furanodienone (**47**), curzerenone (**61**), lindestrene (**87**), as well as isofuranogermacrene (**88**) [119].

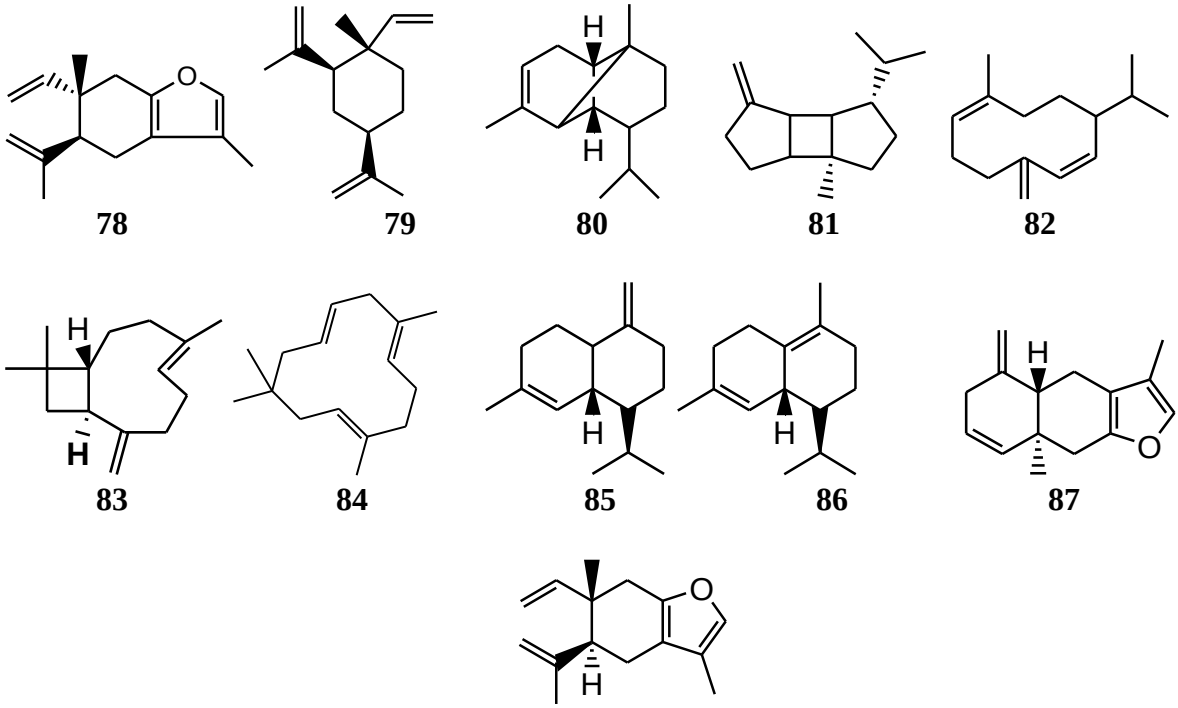

78 **79** **80** **81** **82**

83 **84** **85** **86** **87**

88

Figure 2. 8 Major constituents (**78-88**) of steam distillate of essential oils of *C. myrrha* and *C. habessinica*

The volatile fraction from the resin exudate of *C. tenuis* subjected to GLC and GLC-MS resulted in 42 components where only 37 of them were identified. The major components were identified to be α-pinene (**70**) (60.8%), α-thujene (**89**) (8.9%), β-pinene (**90**) (8.8%), β-thujene (sabinene) (**91**) (6.3%), limonene (**69**) (5.5%), 3-carene (**92**) (3.7%). β-myrcene (**68**) (1.3%), and β-elemene (**79**) (Figure 2.9). The essential oil exhibited antibacterial activities against *S. aureus, p. mirabilis* and *E. coli* with MIC between 0.5% and 1% [82]. Examination of the fluid exudate obtained upon wounding the bark of *C. tenuis* indicated α-pinene (**70**) as the major component [82]. The exudate exhibited antibacterial activities against *S. aureus, P. mirabilis* and *E. coli*.

It was observed that the composition of volatile oil from different *Commiphora* species varies largely. Monoterpenes including α-pinene (**70**), camphene (**93**), β-pinene (**90**), myrcene (**68**), limonene (**69**) and δ-elemene (**82**) are the most frequently detected. Hydrocarbon sesquiterpenes play a dominant role in volatile oil. β-elemene (**81**), α-copaene (**80**), α-humulene (**84**), β-selinene (**79**) and germacrene B (**94**) are widely distributed sesquiterpenes in the volatile oil of different *Commiphora* species. Essential oils predominantly rich with different phytochemicals

showed different biological activity, for example, α-terpineol (**73**) displayed antioxidant, anticancer, anticonvulsant, antiulcer, antihypertensive, anti-nociceptive activity [120], whereas, α-pinene (**70**) showed antiproliferative (NSCLC Carcinoma, A549), antiviral effects [121] alloaromadendrene oxide-(1) (**95**) [122], and spathulenol (**96**) were observed to have antibacterial, immunosuppressive Ursa-9(11),12-dien-3-one (**97**) anti-inflammatory, anti-oxidant [123], β-bisabolene (**98**) cytotoxicity in breast cancer [124], limonene (**69**), β-pinene (**90**) antiviral activity against herpes simplex virus *in vitro* [125], both caryophyllene (**83**) and caryophyllene oxide (**99**) (Figure 2.9) possess significant anticancer activities, affecting growth and proliferation of numerous cancer cells [126].

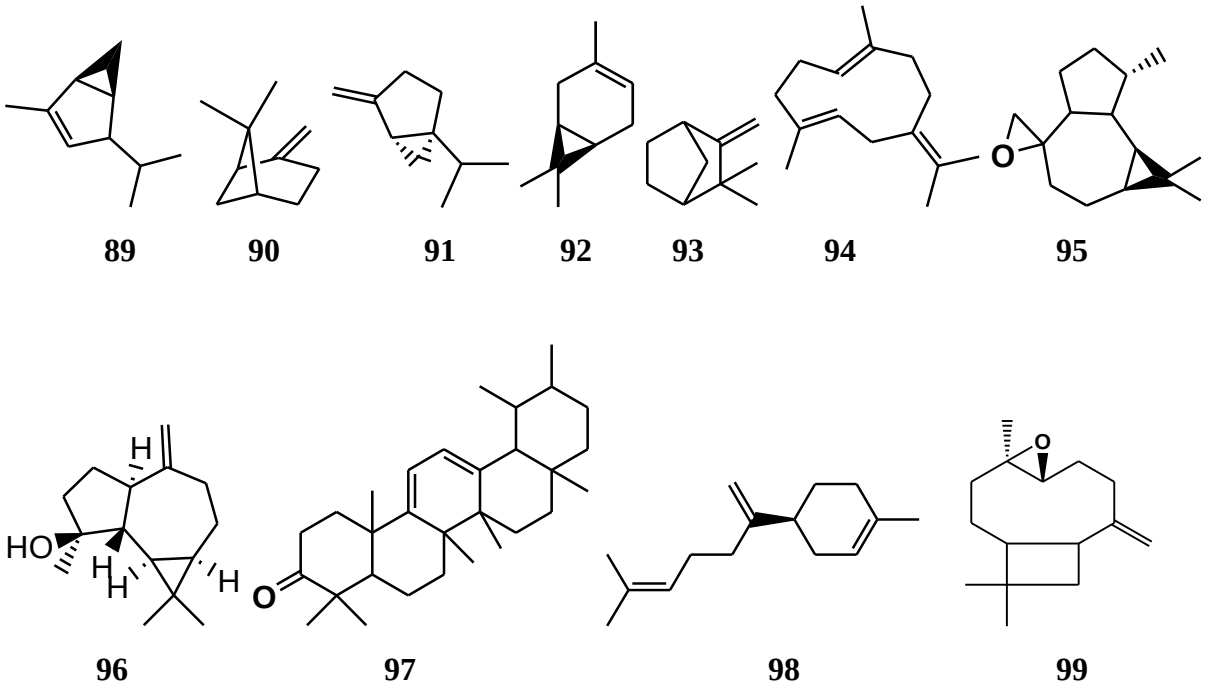

89 **90** **91** **92** **93** **94** **95**

96 **97** **98** **99**

Figure 2. 9 Major constituents of obtained from essential oils of *C. tenuis* and some other *commiphora* species (**89-99**)

2.4 Some Bioactive Phytosterols

Steroid molecules possess a common chemical skeleton of four fused rings, consisting of three six-membered rings and a five-membered ring **(100).** Chemically, this hydrocarbon scaffold is a cyclopentanoperhydro-phenanthrene, describing the three rings of phenanthrene (rings A, B, and C) and the cyclopentane ring (ring D). In steroids, the phenanthrene ring system is completely saturated (hydrogenated) and is thus referred to as a perhydrophenanthrene. This steroid scaffold

contains 17 carbon atoms, and the numbering of the carbon atoms begins with the carbons of the phenanthrene and is then followed by numbering the remaining carbons of the cyclopentane ring **(100)**. Additional carbon atoms on steroids include angular methyl groups attached to C13 and C10 and alkyl substituents on C17 **(101)**. The systematic names for steroids are based on the steroid hydrocarbon system, and the particular systematic name begins by selection of the stem name based on the hydrocarbon system. Cholestane is the term used for steroids with 27 carbon atoms **(102)** (i.e., the C27 steroid structure). Pregnanes are steroids with 21 carbon atoms **(103)**, androstanes have 19 carbon atoms (**104)**, estranes have 18 carbon atoms (**105)**, and gonanes have 17 carbon atoms (**106)** (Figure 2.10).

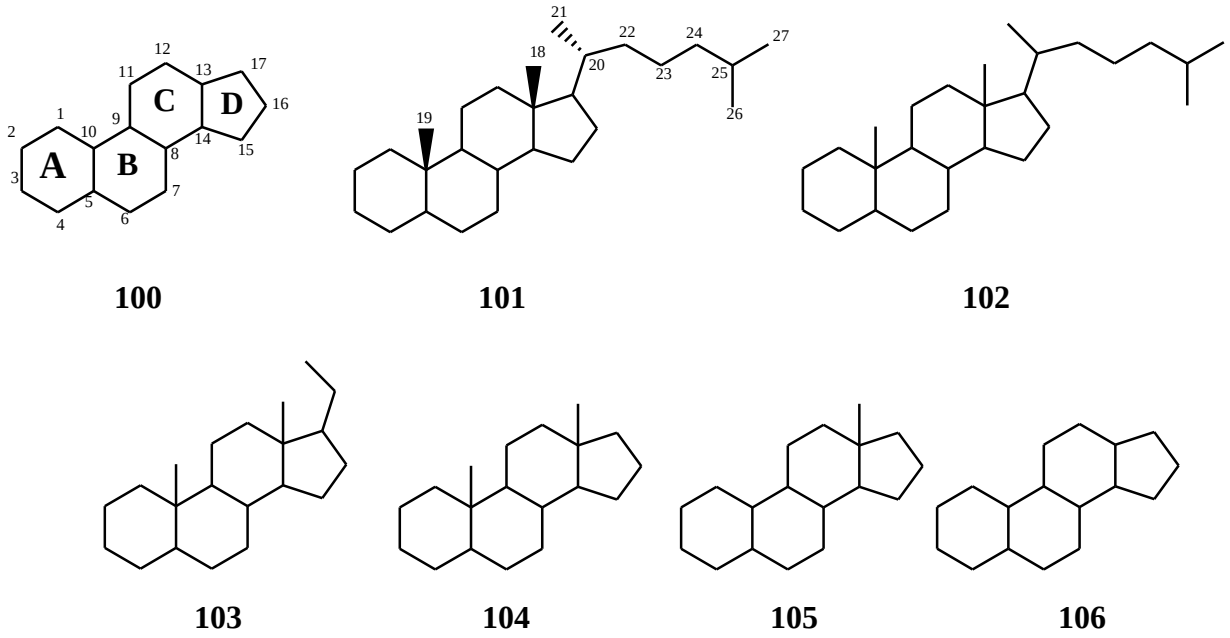

Figure 2. 10 Common scaffold structures of C-27, C-21, C-19 and C-18 steroids

Cholesterol (**48**) is the central steroid of the animal kingdom and functions as an essential component of cell membranes and as a biosynthetic precursor to other steroids in the body. Lathosterol (5α-cholest-7-en-3β-ol) an isomer of cholesterol (**48**) was used as a substrate in enzymatic assay for plasma. It is also an intermediate in cholesterol biosynthesis pathway. Lathosterol (**115**) in serum is carried on lipoproteins and is indicative of the rate of cholesterol biosynthesis[127]. It acts as a marker of synthesis of cholesterol and is not affected by dietary consumption of cholesterol [128].

Cholesterol (**48**) has 27 carbon atoms, a hydroxyl group at carbon 3, and contains a carbon-carbon double bond between carbons 5 and 6 (**48)**. Representative steroids in *Commiphora* having therapeutic potential is guggulsterone which ranges from E to Z (**17** and **18**). The two C21 steroid isomers from the resin of *C. mukul* [89], have attracted lots of interest for their potent anti-tumor, anti-inflammatory and hypolipidemic properties [96]. Numerous scientific studies have shown guggulipid effectively supports healthy levels of cholesterol and triglycerides. Guggulipid supports low levels of LDL ("bad") cholesterol and high levels of HDL ("good") cholesterol means hypolipidemic effect [129]. They are known as active principle of the *C. mukul* resin and accounts for the use of that plant in arthritis [130-132]. *C. mukul* possesses anti-inflammatory property and its steroidal fraction considered to be active principle for this activity and the steroidal fraction is twice active as raw extract.

2.5 Pharmacological activities of some triterpene acids

A study on anti-tumor effect of triterpene acid revealed that they have many excellent physiological and pharmacological activities, including anti-inflammatory [133, 134], anti-tumor [135-137], antiviral [138, 139], antibacterial [140] and regulating blood sugar level, and the role of calming the nerves [141]. Recent reports indicate that, triterpene acid type compounds can directly inhibit tumor growth both *in vivo* and *in vitro*, which can induce tumor cell apoptosis, and cause cell cycle arrest [142, 143]. Triterpene acid compounds with anti-tumor activities include, betullinic acid (**49**) and its derivative 23-hydroxyl betulinic acid (**107**) [144]. Oleanolic acid (OA) (**108**) and its derivatives [145]. Ursolic acid (**109**) [146-148]. Ganoderic acid D (**110**) [149]. In vitro study reported that celastrol (**111**) (Figure 2.11), a pentacyclic triterpenoids showed strong cytotoxic activity on differnt human tumor cell lines, including A549, HCT-8, MCF -7, KB, with IC_{50} values of 0.21, 0.25, 0.23 and 0.20 ng/mL, respectively [150]. Asttributable to its selective toxic effects on cancer cells and harmless to normal cells at the same time, triterpene acid type compounds has become one of the most popular topics recently doubled because of its selective toxic effects on cancer cells and harmless to normal cells at the same time [151]. Apoptosis (programmed cell death) provides a critical regulatory mechanism in inflammatory processes and cancer [152].

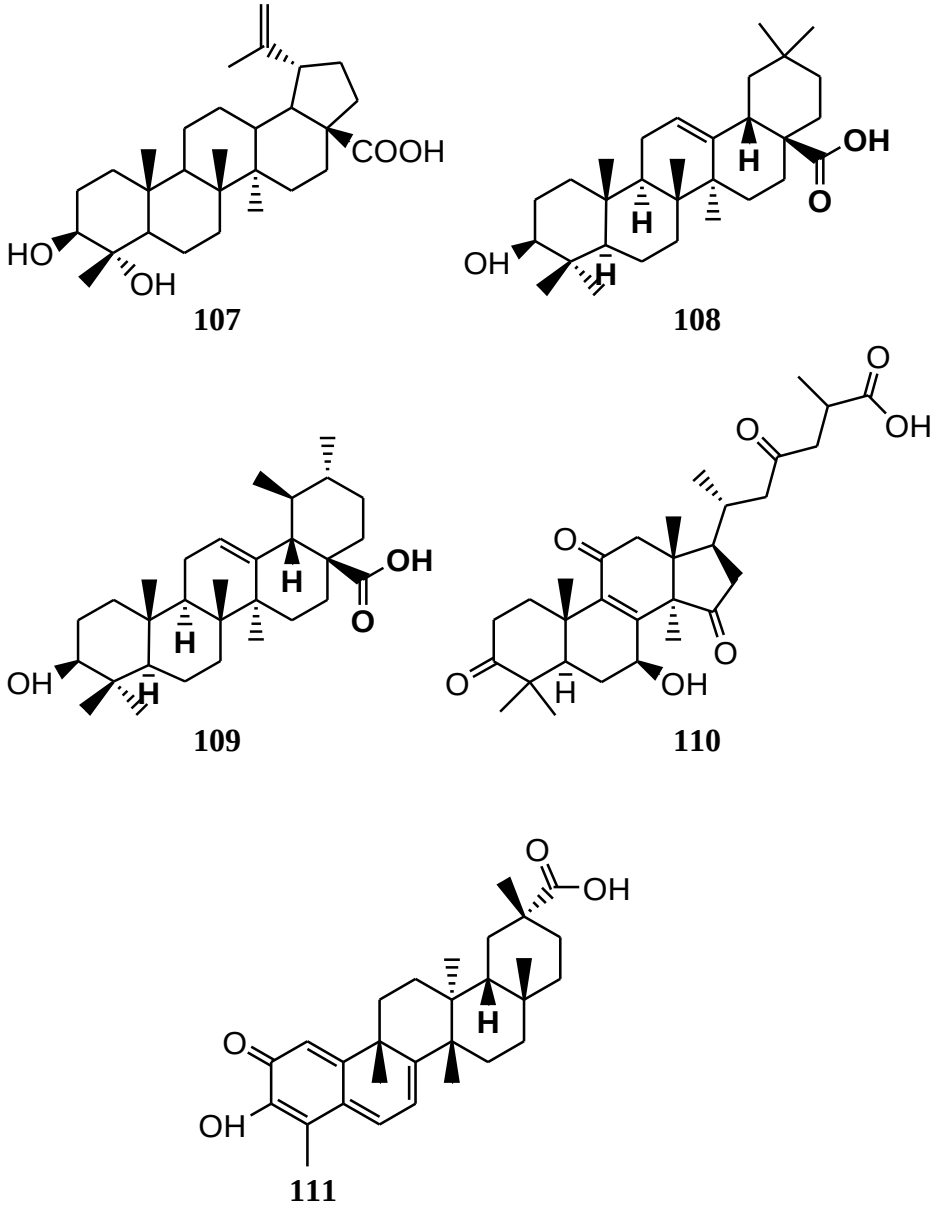

Figure 2. 11 Chemical structure of major triterpenoic acid pharmacologically active against tumor cell lines

2.6 Biosynthesis of terpenoids, phytosterols and tricyclic triterpenoids

Sterols and triterpenes are isoprenoids that are synthesized via the mevalonate pathway [153]. The last common intermediate for their two pathways is 2,3-oxidosqualene. Sterols are important structural components of membranes and also have roles in signaling (as steroidal hormones). In contrast, triterpenes are not regarded as essential for normal growth and development, and

although they do exist in plants in simple unmodified form, they often accumulate as conjugates with carbohydrates and other macromolecules, most notably as triterpene glycosides. Biosynthetic origin of isoprene unit is known. Isopentenyl pyrophosphate exits in living cells in equilibrium with the isomeric dimethylallyl pyrophosphate $(CH_3)_2C=CHCH_2OPP$. Terpenoid biosynthesis involves mostly head to tail addition of isopentenyl diphosphate (IPP, the active C_5 isoprene unit), to its isomer dimethylallyl disophosphate (DMAPP) synthesizing geranyl diphosphate (GPP, C_{10}). Isopentenyl pyrophosphate (IPP) is formed itself from acetate via mevalonic acid, $CH_2OH\text{-}CH_2C(OH,CH_3)CH_2COOH$. Further, condensation of enzyme-bound geranyl diphosphate with additional IPP units forms successively larger prenyl diphosphates e.g. farnesly diphosphate (FPP, C_{15}), geranylgeranyl diphosphate (GGPP, C_{20}), that might undergo cyclisation, coupling and/or rearrangement to produce the parent carbon skeleton of sesquiterpenes and diterpene (Figure 2.12) [154, 155]. GPP and FPP yield monoterpene and sesquitepene skeletons, respectively. Furthermore, FPP and GGPP dimerize to product parental precursors are subjected to structural modification through oxidation, reduction, isomerization, hydration, conjugation and/or other transformations to give rise to a variety of terpenoids [154].

In summary, terpenoids biosynthesis can be divided into four stages. Firstly, there is the formation of the isoprene unit, isopentenyl pyrophosphate, followed by the association of these units to form the $(C_5)_n$ isoprenoid backbone of the terpenoid families, the cyclization of these to generate the carbon skeletons; and finally, there are the interrelationships, hydroxylations and oxidations that lead to the individual terpenoids (Figure 2.12).

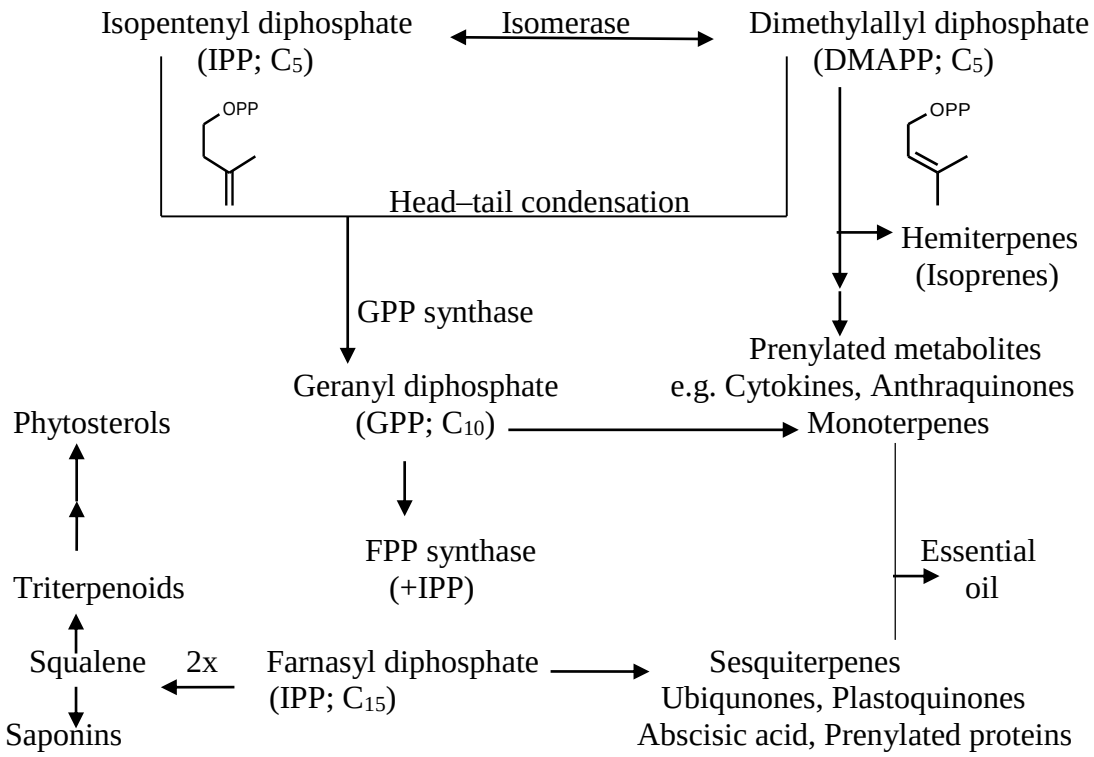

Figure 2. 12 Biosynthesis of various classes of terpenoids and sterolds in plants

CHAPTER THREE

MATERIALS AND METHODS

3.1 Plant collection and identification

The resins and other botanical specimens of four *Commiphora* species namely *C. africana, C. habessinica, C. schimperi* and *C. sphaerocarpa* Ethiopian origin were collected from two zones of Oromia regional state. The first three were obtained from natural vegetation of Yabello district, Borena zone on two occasions June 2016 and November 2016. Resin of *C. sphaerocarpa* resin was collected from Sofumer Bale zone in September, 2016. The plant species were identified by Mr. Shambel Alemu Department of Biology and the voucher specimen *C. africana* (A, Rich.) Engl (072772), *C. habessinica* (Berg) Engl (072771), *C. schimperi* (Berg) Engl (072773) and *C. sphaerocarpa* (072820) deposited at the National Herbarium, Addis Ababa University, Addis Ababa, Ethiopia.

3.2 Extraction and isolation

3.2.1 Preparation of plant extracts and liquid-liquid partitioning

Each plant resin materials were reduced to small size manually in order to facilitate ultimate solvent extraction, followed by maceration in 99.5 % methanol with a volume of ten times more than the dry weight resin material for 24 h in a flask. The flask was shaken and placed on an orbital shaker alternately and left for 24 h at a speed of 120 revolutions per min. After 24 hrs, the solution was filtered twice using Whatman No.1 filter paper. To exhaust the resin material, the above procedure was repeated for two times till no UV spot observed. The three filtrates of MeOH were combined dried with anhydrous sodium sulphate, and concentrated using Büchi Rotavapor (Rotavapor R114, Büchi Labortechnik, Flawil, Switzerland) at a reduced pressure and a temperature of at or below 40^{o}C.

The dried MeOH extract was suspended in distillated water (10 x mass) and consecutively partitioned with equal volumes of n-hexane, chloroform ($CHCl_3$), ethyl acetate (EtOAc) and butanol (BuOH). Each solvent fraction was filtered and evaporated under vacuum. Further dryness carried out using vacuum drier. The water extract has been discarded for good reason. This has been summarized in Figure 3.1.

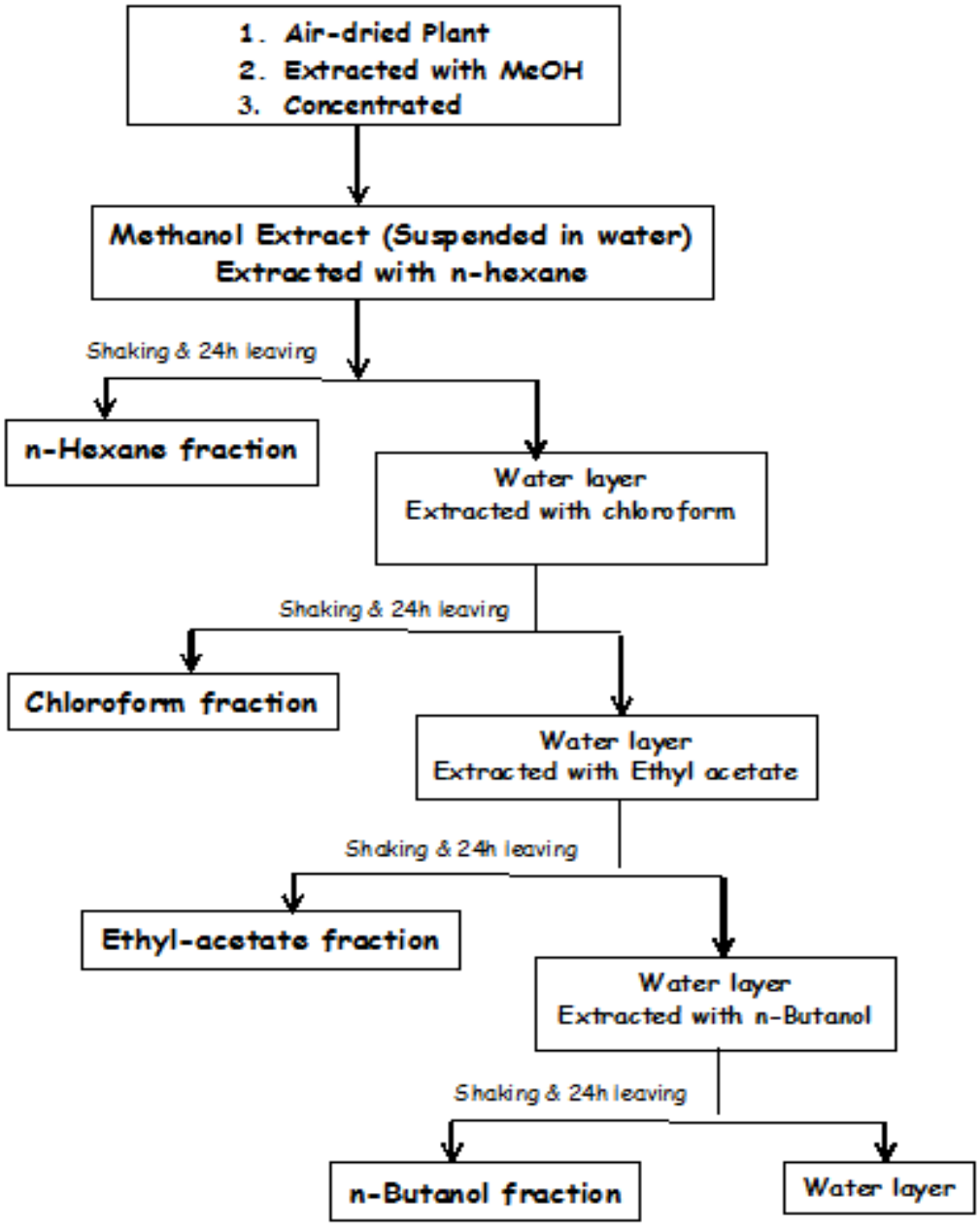

Scheme 3.1 Procedure of extraction and Partitioning on basis of polarity.

3.2.2 Hydro-distillation of the resins

Finely ground oleogum resins were subjected to hydro-distillation using Clevenger‟s type apparatus until complete exhaustion of extraction. The oils were collected, dried over anhydrous sodium sulfate, filtered, concentrated, percentage yield were calculated and kept in the refrigerator until analysis.

3.2.3 Chromatographic methods

3.2.3.1 Thin Layer Chromatography (TLC)

Thin layer chromatography analyses were performed on pre-coated TLC glass plates with silica gel 60 F_{254} (layer thickness 0.25 mm). Two mobile phases consisted of either a mixture of ethyl acetate : *n*-Hexane or dichloromethane : methanol solvent system were used. The bands separating on the TLC plate indicate the separation of compounds which were detected under UV absorbance at 254 and 366 nm UV light source. Chromatograms were further developed by immersing the TLC plates with phosphomolybdic acid reagent (PMA) and subsequent heating with a heat plate at 110^{o}C until colored spots were appeared.

3.2.3.2 Flash column chromatography (FCC)

In this experiment, somewhat loosely stuffed plug of cotton wool was placed at the bottom of appropriate size glass column. A telescoping lengths of glass tubing was used to make placement of the glass wool plug easy. Next, a slurry of silica gel 60 (approximately 30:1, silica gel to sample ratio) mixed with selected solvent system, usually *n*-hexane and ethylacetate was poured into a glass column using a funnel with gentle tapping to remove trapped air bubbles. A good amount of elution solvents was poured onto the silica gel. To force the solvent through the silica pressurized gas was used. The solvent system has been flushed continuously through the silica gel until the entire silica plug becomes homogeneous in appearance. It is also a common practice to recycle the solvent coming through the column onto the top of the column several times before all the silica gel is solvated. A minimum necessary pressure has been applied to keep a steady stream coming out of the column. The solvent system which remains above the silica was allowed to drain down until it is flush with the surface of the silica. Sea sand was applied to the top of the column, being careful not to disturb the top of the silica to protect the top surface of the silica when more solvent is added. Then, the sample was dissolved into the minimum volume

of the elution solvent was applied using a Pasteur pipette. In this study the silica gel used was 400-230 mesh silica gel 60 (E. Merck, Germany). In all separation of compounds sub fraction of 18 ml has been collected in a test tube. The fraction was eluted with the appropriate solvent system at a certain flow rate using increasing polarity of *n* hexane : EtOAc and sub fraction of 18 ml was collected in a test tube. The fractions with similar profile in TLC were combined together in a flask, and then concentrated using rotavap (rotary evaporator) which were then subjected to further chromatographic analysis.

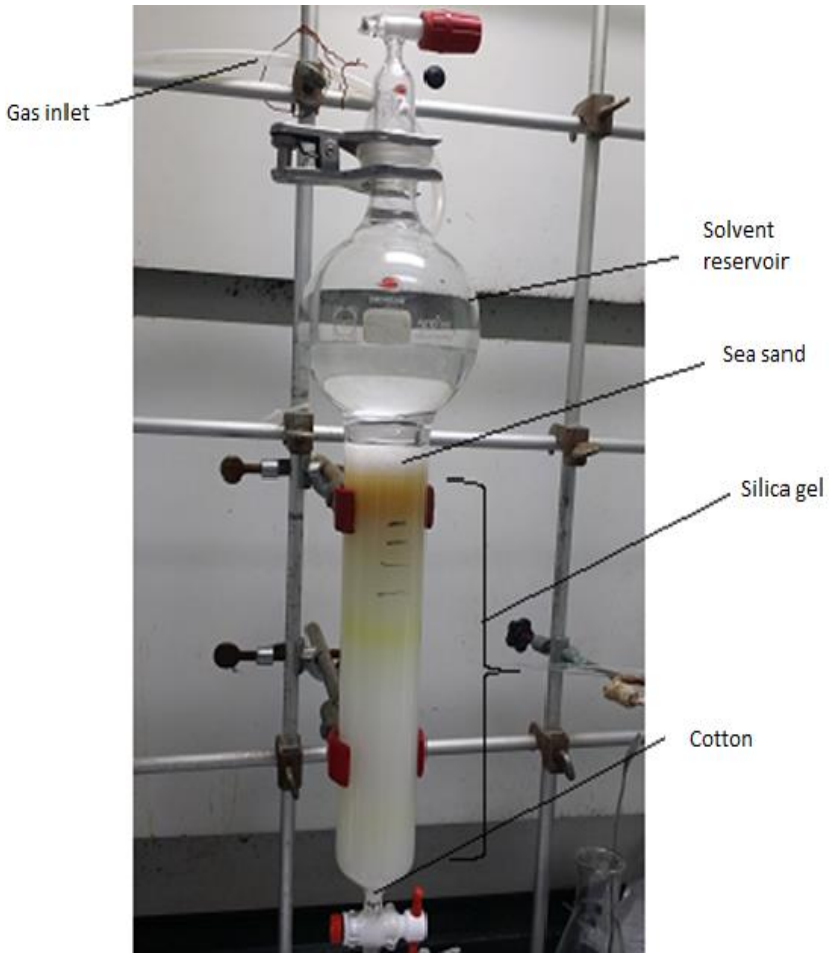

Figure 3. 1 Glass column used in silica gel flash column chromatography for the isolation of compounds.

3.2.3.3 Spray reagents used for detection

3.2.3.3.1 Phosphomolybdic acid (PMA)

Phosphomolybdic acid $H_3(P(Mo_3,O_{10})_4)$ stain is a good "universal" stain which is fairly sensitive to low concentrated solutions. It will stain most functional groups. A large number of organic substances can be oxidized with phosphomolybdic acid (PMA) were by portion of the Mo(VI) is reduced to Mo(IV), which forms blue-grey mixed oxides with remaining Mo (VI).

$$2MoO_3 \rightarrow MoO_2.MoO_3$$

PMA was prepared as follows: anisaldehyde (5 parts), glacial acetic acid (100 parts), methanol (85 parts), were mixed, to which 5 parts of concentrated H_2SO_4 were added slowly. The reagent was stored in an amber-colored bottle and kept refrigerated until use. TLC's were always conducted for each fraction prior to further chemical work, to monitor the identity of each and the qualitative purity of the fractions or the isolated compounds. Spot separations in TLC ware also very helpful in optimizing the solvent system that would be later applied for flash column chromatography. In order to activate the stain for visualization TLC plate was heated to 120 ^oC.

3.2.3.3.2 Vanillin

Vanillin (0.5 g) in 2.0 mL concentrated H_2SO_4 was added with cooling to methanol (8.0 mL) before sprayed to the TLC plate. Dried TLC plates were sprayed with vanillin reagent. The plate was heated at 100℃-110℃ until full development of color had occurred.

3.3 Spectroscopic methods

For structural characterization of the isolated compounds, several spectroscopic methods such as NMR and spectrometry were performed. IR was also used and LC-TIC carried out when puity of isolated compounds required. NMR spectra were obtained using a BrukerAvance 500 MHz (^1H at 500.13 Hz; ^{13}C at 125.77 MHz) and a BrukerAvance 600 MHz (600 and 150 MHz, respectively) spectrometer coupled with Topspin 2.1 acquisition software. The ^1H and ^{13}C NMR spectra were recorded using deuterated chloroform ($CDCl_3$) with the residual solvent peaks as reference (7.26 ppm for ^1H and 77.16 ppm for ^{13}C). In one case deuterated dichloromethane (CD_2Cl_2) was used instead (residual solvent peaks 5.32 ppm for ^1H and 53.84 ppm for ^{13}C). The chemical shifts were expressed in parts per million (ppm) as δ values and the coupling constants (J) in Hertz (Hz).

The ^{1}H and ^{13}C NMR data for commafric A (compound **113**) was acquired on an Avance III HD spectrometer (Bruker BioSpin GmbH, Germany) equipped with an inverse detected TCI cryoprobe with a cryogenic enhancement for ^{1}H, ^{2}H and ^{13}C, operating at 600 MHz for ^{1}H. All spectra were recorded using TopSpin 3.5pl7 at 298 K in dichloromethane-d_2 and chloroform-d_1, using gradient selected and adiabatic inversion versions of pulse sequences where applicable.

Analysis of NOE buildup for compound **113** was performed by complete relaxation matrix analysis using Mspin 2.3.2-694 (MestreLab Research S. L., Spain). The results are presented as Boltzmann averaged NOE enhancement across the conformational ensemble generated for analysis of IR (see Figure S12, Supporting information) and VCD section. The sample (10mg) for anisotropic NMR measurements was dissolved in $CDCl_3$ with 0.03% TMS to which increasing amounts of poly-γ-benzyl-L-glutamate (PBLG, 150,000-300,000 Da, Sigma-Aldrich CAS 25014-27-1) was added to yield weight-to-volume ratios of 7.9%, 12.1%, and 16.2%. For compound **113** ^{13}C-NMR, CLIP-HSQC, IPAP-HSQC and J-res carbon was acquired to extract the $^{1}J_{CH}$ coupling constants and anisotropic carbon shifts.

3.3.1 Experimental Vibrational Circular Dichroism (VCD) spectra.

VCD and absorption spectra of **113** were measured in $CDCl_3$ solution (~ 1 mg/100 μl) using a BaF_2 cell of an optical path of 50 μm and a BioTools ChiralIR-2X instrument. Spectra of pure $CDCl_3$ solvent were subtracted as a baseline, the accumulation time was ~12 hours using blocks of 1200 scans and 4 cm^{-1} resolutions.

3.3.2 Computational study

Using the Gaussian suite of programs [156] and our own scripts a systematic conformer search of commafric A (**113**) was performed considering the three torsional angles in the vicinity of the tricyclic system. Other C-C-C-C dihedral angles were all-trans and all-extended (180°) at the beginning of the optimizations and left to optimize without constraints. The B3LYP [157] PCM [158] (chloroform)/6-31++G** level was used for all quantum chemistry. For stable conformers thus obtained the magnetic field perturbation theory[159, 160] was used to simulate IR and VCD intensities; final spectra were obtained as a Boltzmann average, using a convolution with Lorentzian lines (FWHM = 10 cm^{-1}). Because consideration of the full molecular flexibility was

not possible with our computational means, atomic axial tensors of the linear side chain (from carbon number 16) were deleted for VCD generation. The chain itself is not chiral and thus supposedly the error introduced by this approximation is small, whereas the dominant signal from the chiral more rigid molecular part may help to assign the absolute configuration. Alternated simulations of the spectra based on molecular dynamics were attempted as well, but did not provide results significantly different from the limited conformer model. Boltzmann-averaged isotropic shielding and spin-spin coupling constants were computed at the same level as for VCD. IR spectra were recorded with a Bruker Optics ALPHA QuickSnap (A220/D-01) FT-IR spectrophotometer with OPUS spectroscopy software. A solid sample of each compound was cast onto the ATR platinum diamond crystal plate and was scanned from 4000 to 500 cm^{-1} with 64 scans for analysis.

3.3.3 Mass spectrometry

The non-conventional total ion current (TIC) detection and corresponding extracted ion current (EIC) chromatogram in LC-MS measurements was used for quantitative analysis of a pure compound and mixture of compounds. LC-(TIC/EIC)-MS experiments allows for the accurate determination of isomers, enantiomers, diastereomers and overall purity with defined stereochemistry. The described methodology offers an attractive solution in cases where conventional HPLC analysis with UV detection fails [161]. The technique is necessary for the unambiguous determination of purity and identity of the isolated compounds. Extracted Ion Current chromatogram (TIC/EIC) proved invaluable in this context. In the EIC chromatogram, only the ions of a particular molecular mass are taken into account, thus (mathematically) extracting specific information (EIC) out of the crude data (TIC)[161].

3.3.3.1 Elestrospray ionization (ESI)

The electrospray ionization method allows solutions containing compound(s) to be infused directly into the ion source of a mass spectrometer through a hollow metal needle that is held at a high positive or negative potential [162]. At the ending tip of the needle, highly charged droplets form and are drawn into the orifice of the MS by both a potential and an atmospheric pressure difference. During transition from atmospheric pressure to vacuum, the solvent evaporates, whereas the analyte of interest remains as an ionized species in the gas phase. ESI is a much

softer ionization technique, and yields primarily intact ions with little or no fragmentation when the ionization conditions have been optimized. Electrospray ionization, markedly favors detection of specific compound classes of high polarity, introducing a strong bias against many less polar classes of metabolites, for example many lipids and steroids.

3.3.3.2 Clean IN-Phase multiplets for heteronuclear single quantum multiple bond correlation (CLIP-HSQMBC)

CLIP-HSQMBC is a method used for the very easy, direct and accurate measurement of long-range proton–carbon coupling constants in organic molecules and natural products. The J value can be extracted directly from the analysis of resolved in-phase ^{1}H multiplets that show an additional splitting arising from the proton–carbon coupling [163].

3.3.4 GC-MS analysis

GC-MS analysis was done using a GC (7890B, Agilent Technologies, USA) coupled with an MS (5977A Network, Agilent Technologies). The GC had an HP 5MS column (non-polar column, Agilent Technologies), 30 m × 250 μm internal diameter (i.d.) and 0.25 μm film thickness. The carrier gas was helium flowing at a rate of 1 mL/ min. The injector temperature was 230℃ and the injection mode was split mode with split Ratio 10:1. The initial oven temperature was 40˚C held for 5 min. It was raised to 250˚C at 6˚C/min held at this temperature for 20 min. The total run-time was 60 min. Mass spectra were recorded in EI mode at 70 eV, scanning the 50-500 m/z range. The Mass Spectrometer was also equipped with a computer fed Mass Spectra data bank. The GC–MS methodology was adapted from Van Vuuren[164]

The chemical compositions of volatile oils were identified based on the comparison of retention indices calculated by linear interpolation relative to retention times of a series of C_7-C_{40} n-alkanes and their mass spectra with authentic samples and with data extracted from the literature [165] or by comparison with mass spectra recorded in the database as NIST 11 (National Institute of Technology and Standards, Gaithersburg,MD, USA). Linear indices (nonisothermal indices in accord with the definition of Van den Dool and Kratz [166] from temperature-programming measurements). Furthermore, the individual compounds were confirmed by comparison of their RIs, relative to C_8-C_{32} *n*-alkanes [167]. Relative amounts of detected compounds were calculated based on the peak areas of the total ion chromatograms (TIC).

$$RI = 100n + 100(t_{ri} - t_{rn})/(t_{trm} - t_{trn})$$

Where: RI = retention index of "i", i = constituent of essential oil that is being analyzed, *n* = carbon number of the alkane which elutes before "i", t_{ri} = retention time of "i", t_{rn}=retention time of the alkane which elutes before "i" and t_{rm}-retention time of the alkane which elutes after "i". The identification of components of essential oils, *n*-hexane and chloroform fractions were performed by comparing the mass spectra of the compounds with those in the database of NIST11 (National Institute of Standards and Technology, Gaithersburg, USA) having more than over 62,000 spectral patterns[168, 169] and the literature.

3.4 Biological assays

3.4.1 Anti-inflammatory assay

Primarily, to determine if EOs could reduce NO generation by LPS, RAW264.7 cells were pretreated with EOs at 10 and 20 μg/ml for 2 h and then co-treated with LPS (1 μg/ml) for the additional 18 h [170].

3.4.1.1 Cell culture and treatment

Mouse macrophage cell line, RAW264.7 was purchased from Korean Cell Line Bank (Seoul, Korea) and grown in DMEM supplemented with 10% fetal bovine serum (FBS), 100 U/ml penicillin, and 100 μg/ml streptomycin. These cells were maintained at 37℃ under a humidified atmosphereof 5% CO_2. *Commiphora* resin essential oil were dissolved in dimethyl sulfoxide (DMSO) and then treated to cells. DMSO was used as a vehicle and then final DMSO concentration was not exceeded 0.1% (v/v).

3.4.1.2 Measurement of nitric oxide (NO) production

Inhibitory effect essential oils of resins of *Commiphora* on the production of NO in LPS-stimulated RAW264.7 cells was evaluated using literature [171]. Briefly, RAW264.7cells were plated in 12-well plate for overnight. Cells were pre-treated with resin essential oils at the indicated concentrations for 2 h and then co-treat with LPS (1 μg/ml) for the additional 18 h. After 18 h, 200 μl of the media was mixed with equal amount of Griess reagent (1% sulfanilamide and 0.1% N-1-(naphthyl) ethylenediamine dil HCl in 2.5% H_3PO_4). The mixture

was incubated for the additional 5 min at the room temperature and the absorbance was measured at 540 nm [172].

3.4.1.3 Western blot analysis

Western blot analysis was performed according to the previous study [172]. To extract protein from RAW264.7 cells, the cells were washed three times with cold 1 × phosphate-buffered saline and lysed at 4 ^{o}C for 30 min using cold radio immunoprecipitation assay buffer (Boston Bio Products, Ashland, MA, USA) containing protease inhibitor (Sigma-Aldrich) and phosphatase inhibitor (Sigma-Aldrich). After centrifugation at 15,000 rpm for 10 min, the supernatant was recovered for protein quantitation using BCA protein assay (Thermo Fisher Scientific, Waltham, MA USA). The protein was separated on SDS-PAGE for about 1 h at 150 V and subsequently transferred to PVDF membrane (Bio-Rad Laboratories, Inc., Hercules, CA, USA) for 2 h at 100 V. After blocking the PVDF membranes using 5% non-fat dry milk in tris-buffered saline containing 0.05% Tween 20 (TBS-T) by stirring at room temperature for 1 h, the specific primary antibodies in 5% non-fat dry milk dissolved with TBS-T buffer were treated with PVDF membranes and reacted with stirring at 4 ^{o}C overnight. Then, PVDF membranes were washed three times with TBS-T buffer, and then treated with the secondary antibodies in 5% non-fat dry milk dissolved with TBS-T buffer for 1 h at room temperature. Chemi luminescence was detected with ECL Western blotting substrate (Amersham Biosciences, Piscataway, NJ, USA) and visualized using LI-COR C-DiGit Blot Scanner (Li-COR Biosciences, Lincoln, NE, USA).

3.4.1.4 Statistical analysis

All the data were shown as mean ± SD (standard deviation). Statistical analysis was performed with one-way ANOVA followed by Dunnett's test. Differences with *P or #P < 0.05 were considered statistically significant.

3.4.2 Cytotoxicity assay

The cytotoxicity of the extract, fractions and isolated compounds against cultured human cancer cell lines was evaluated by sulforhodamine B (SRB) method. The sulforhodamine B (SRB) assay is an antiproliferative assay used to assess the growth inhibition of cells. This colorimetric assay indirectly estimates the viable cell number by staining total cellular proteins. The cancer cell

lines including the human non-small cell lung cancer cell line (A549), ovarian cancer cell line (A2780), pancreatic cancer cell line (MIA-Paca-2), and stomach cancer cell line (SNU-638) were used for evaluation of anticancer activity. All cell lines were maintained using RPMI1640 cell growth medium (Gibco, Carlsbad, CA), supplemented with 5% fetal bovine serum (FBS) (Gibco), and grown at 37℃ in a humidified atmosphere containing 5% CO_2. The tissues selected are among the tissues most affected by cancer.

3.4.2.1 Treatment of cell lines

Stock solutions of the crude MeOH extract, *n*-hexane, chloroform, ethylacetate, and *n*-butanol fractions and isolated compounds dissolved in DMSO were prepared in the corresponding medium at different concentrations of 0.1, 0.3, 1.0, 3.0, 10.0, 30 μg/mL to determine percentage of growth inhibition for the 50% growth inhibition (IC_{50}). Each tumor cell line was inoculated over standard 96-well flat-bottom micro plates then incubated for 24 h at 37℃ in a humidified atmosphere of 5% CO_2. The attached cells were then incubated with serially diluted each samples. After continuous exposure to the compounds for 72 h, the culture medium was removed from each well, and the cells were fixed with 10% cold trichloroacetic acid at 4℃ for 1 h. After washing with tap water, the cells were stained with 0.4% SRB dye incubated for 30 min at room temperature. The cells were washed again, and then, the cell bound SRB was solubilized with 10 mM buffered Tris base solution of pH 10.5. The absorbance was measured spectrophotometrically at 520 nm with a micro titer plate reader. Each experiment was conducted in triplicate. The IC_{50} values of the extract and fractions were calculated by the nonlinear regression analysis. SRB assay is a high-throughput and sensitive method for evaluating cytotoxic activity against cancer and non- cancerous cell lines. It has a number of advantages over other current cytotoxicity assays; because SRB assay is independent of cell metabolic activity, not interfered by test compounds and easy to perform [173].

3.4.3 Antiviral assay

The antiviral activity of the crude extracts and related solvent fractions against influenza type A and influenza type B viral strains was evaluated by the cytopathic effect (CPE) reduction assay. The following viral strains were used in this study: PR8, A/Puerto Rico/8/34 (H1N1); HK, A/Hong Kong/8/68 (H3N2); and Lee, B/Lee/40.

3.4.3.1 Cells and viruses

Madin-Darby canine kidney (MDCK) cells and C6/36 mosquito cells (ATCC, Manassas, VA) were grown in minimum essential medium (MEM; Gibco/ Invitrogen, Carlsbad, CA) supplemented with 10% fetal bovine serum (FBS; Invitrogen) at 37 °C and 28 °C, respectively. African green monkey kidney Vero cells (ATCC) were grown at 37 °C in Dulbecco's Modified Eagle's Medium (DMEM; Gibco/Invitrogen) supplemented with 10% FBS (Invitrogen). Influenza viruses PR8, HK and Lee were obtained from ATCC. Influenza A viral PR8 and HK strains were propagated in 10-day-old chicken embryos at 37 °C for 3 days and influenza B virus (Lee) by infection of MDCK cells under serum-free conditions.

3.4.3.2 Treatment of viral strains

In the CPE reduction assay, MDCK cells were seeded in 96-well plates and either mock-infected or infected with influenza virus at a multiplicity of infection (MOI) of 0.001 50 plaque-forming units (PFU) of given virus per well]. After incubation for 1 h at 33 °C (mock) or 35 °C (given viral strains), the medium was removed, and test and standard chemicals were added, which were serially diluted in MEM containing 2 µg/ml TPCK-trypsin (Sigma). On day 2 or 3 post-infection (P. I), the cell viability was measured after treatment with fluorescein diacetate (FDA; Sigma), as described by Kim et.al. (2012) and Schols et. al. (1988) [174]. The 50% cytotoxic concentration (CC_{50}) and the 50% effective concentration (EC_{50}) values were calculated using SoftMax Pro Software (Molecular Devices, Sunnyvale, CA). The selectivity index (S.I.) is the ratio of CC_{50} to EC_{50}.

3.4.3.3 Antidengue assay

DENV-2 (New Guinea C strain) was purchased from the National Collection of Pathogenic Viruses, Culture Collections of Public Health England (Salisbury, Great Britain) and propagated in C6/36 cells. DENV viral titers were quantified by focus-forming assay on Vero76 cells as described previously. Vero cells were seeded on 96-well plates for DENV antiviral assay. After over night incubation, cells were inoculated with DENV-2 at a multiplicity of infection (MOI) 0.2 for 2 h at 37℃. Then crude extracts were added at two different concentrations (20 µg/ml and 100 µg/ml). An immunofluorescence assay (IFA) used to detect dengue infection was optimized for the dengue high-throughput content imaging assay. Briefly, DENV-infected cells

were detected by probing anti-DENV E (4G2) monoclonal antibody and AlexaFluor 488 (A488)-conjugated goat anti-mouse IgG (H+L) (Invitrogen Molecular Probes, USA) as secondary antibody. Cell nuclei counter stained with 5 μg/ml 4',5-diamidino-2-phenylindole (DAPI, Sigma-Aldrich, USA). After washing, digital images were acquired using Operetta® high content imaging system (Perkin Elmer, USA). The digital images were taken from 4 different fields of each well at 20X magnification. The percentage of inhibition was derived by using the formula; [1-(A488-positive cells/total cells)] x 100%. The cytotoxicity, antiviral and antidengue activity were conducted at Korean research institute of science and technology by virus research and testing group.

CHAPTER FOUR

RESULTS AND DISCUSSION

4.1 Isolation and characterization of compounds from active fractions of *commiphora* species

The dried resin of selected each *commiphora* species was extracted with MeOH in a ratio of volume (10 x mass of dry resin) at room temperature for three days and three times and the resulting MeOH extract was concentrated using Rota vapor at or below 40^{o}C. The yield, product status and amount used for further liquid – liquid separation tabulated as shown below (Table 4.1.1).

Table 4.1 1 List of *commiphora* species and MeOH extract dried mass

Plant resin	Plant Mass (g)	MeOH volume (L)	Dried mass (g), %	Product status & color	MeOH dry mass (for L-L separation), (g)
C. africana	322.25	2.9 L	151.2, 46.82	Solid, yellow	83.12
C. habessinica	218.57	2 L	63.92, 29.24	Gummy yellow	60
C. sphaerocarpa	95.14	0.95 L	34.5, 36.16	Solid, light yellow	34.5
C. schimperi	154.5	1.5 L	48.72, 31.52	Solid, light yellow	48.7

The MeOH extract suspended in distilled water with a volume (10 x MeOH extract dry mass) and consecutively partitioned with equal volumes of n-Hexane, chloroform ($CHCl_3$), ethyl acetate (EtOAc) and n-butanol (n-BuOH). The dry mass of each solvent fraction and corresponding percentage was tabulated (Table 4.1.2).

Table 4.1 2 Dried mass of solvent fractions of *commiphora* species

Plant resin	Dried mass (g), % (*n*-Hexane)	Dried mass (g), % (chloroform)	Dried mass (g), % (Ethyl acetate)	Dried mass (g), % (*n*-BuOH)
C. habessinica	1.87, 3.12	51.8, 86.33	0.59, 0.98%	1.68, 2.8%
C. africana	33.39, 40.17	41.26, 49.64	0.11, 0.13	0.074, 0.09
C. sphaerocarpa	12.4, 35.1	2.46, 7.13	0.17, 0.5	negligible
C. schimperi	31.64, 64.97	2.84, 5.83	0.019, 0.041	0.14, 0.29

4.1.1 Isolation of compounds from resin of *C. habessinica*

TLC of chloroform fraction of *C. habessinica* showed a clear five different spots in a 4:1 (*n*-hexane: EtOAc) system, where flash column chromatography (FCC) on silica gel 60 (230-400 mesh) four compounds were identified and characterized. A 5g of the chloroform fraction was completely dissolved in a small amount of the mobile phase (hexane/ethyl acetate), and introduced as a thin band to the silica gel using a Pasteur pipette. Once the fraction was loaded onto the silica gel, the mobile phase (*n*-hexane : EtOAc) was added at a constant flow rate. Gradient elution of increasing polarity was initiated consisting of successive elution of hexane**:** ethyl acetate (9:1 to 100% EtOAc) to give 134 fractions of each 18 ml. The first 15 fractions, fractions 38-48, 70-91, 96-101, 104-134 eluted with 9:1, 8:2, 7:3,6;4 *n*-hexane : EtOAc showed no spots after spraying with PMA reagent. Fractions 16-20, 21-30, 35-39 and 50-60 were eluted with 8:2 and 7:3 *n*-hexane: EtOAc showed similar spots were combined together and concentrated using Rota vapor at or below 40^{o}C. The fractions further chromatographed by FCC eluted with an isocratic solvent system of *n*-hexane: EtOAc (6:4), to afford n-hexadecane (25 mg), two C-27 cholestane type sterols, cholesterol (**48**) (45 mg), lathosterol (**112**) (39 mg) and a mixture of the two sterols (56 mg). TLC profiles of isolated compounds showed a single spot on spraying with (PMA). The compounds were identified by comparison of their spectral data with those reported in the literature [175].

4.1.1.1 Characterization of compound 48 (Cholesterol)

The compound was isolated as a white amorphous powder from $CHCl_3$ fraction using flash column chromatography eluting with *n*-hexane/EtOAc (6:4). The structure of cholesterol was principally identified using IR, 1D - NMR (^{1}H, ^{13}C, DEPT-45, DEPT-90, DEPT-135) experimental data. The compound was detected from HPLC-DAD chromatogram at RT = 1.97 min with 97.5 purity without the solvent (**Appendix A**, **Figure A1**). The molecular formula of compound (**48)** was established as $C_{27}H_{46}O$ from EI^{+}, $[M]^{+}$ generated a molecular cation peak at m/z 386, calcd (386) indicating five degree of unsaturation. From the EI-MS the presence of *m/z* 371 [M-CH_3], 353 [M-CH_3-H_2O], 329 [M-C_4H_9], 301 [M-C_6H_{13}], the existence of a prominent peak at 273 is due to loss of side chain [M-C_8H_{17}], 255 [M-C_8H_{17}-H_2O] related to the fragmentation pattern of C-27 steroids(**Appendix A**, **Figure A1**), which is a characteristic series for phytosterols side chains [176].

The compound exhibited a broad and intense IR band at 3434.07 cm^{-1} due to hydroxyl (OH) stretching, a strong peak at 2930.32 cm^{-1} is due to CH stretching vibration. The comound has one double bond (C=C) in the second ring (ring B). This was shown at 1728.68 cm^{-1} as short peak (**Appendix A**, **Figure A2**). This assignment of 1728.68 cm^{-1} for the double bond in the second ring of the compound is not in good agreement with the results reported by Zheng *et al*. [177] but relatively close to with the 1693–1671 cm^{-1} assignment for cyclopentene. The band at 1463.90 cm^{-1} is due to asymmetric stretching vibrations of CH_2 and CH_3 groups, the characteristic vibrational peak at 1439.51 cm^{-1} is due to the CH_2 and CH_3 deformation vibrations, and the band at 1377.58 cm^{-1} is attributed to the CH_2 and CH_3 bending vibration of cholesterol molecule. The sharp peak at 1053.46 cm^{-1} can be attributable to ring deformation of cholesterol [177].

The ^1H NMR spectral data of compound (**48)** (Table 4.1.3, **Appendix A**, **Figure A3**) displayed proton signals due to five methyl groups comprising two tertiary methyl groups at δ_H 0.67 (3H, s, H_3-18) and 1.01 (3H, s, H_3-19), three secondary methyl groups at δ_H 0.91 (3H, d, J= 6.5Hz, H-21), δ_H 0.87 (3H, d, J = 2.3 Hz H-26) and δ_H 0.86 (3H, d, J = 2.2 Hz H-27) were observed. The ^1H NMR spectrum showed a downfield proton signal at δ_H 5.35 ppm integrated to one proton, an indicative of an olefinic proton (H-6, m). Further confirmed by a downfield shift of C-5 and C-6 at δ_C 140.8 and 121.7 ppm. The ^1H NMR exhibited a multiplet at δ_H 3.59 ppm for an oxymethine proton and a downfield shift of ^{13}C NMR at δ_C 71.8 were consistent with oxygenated sp^3 carbon, i.e for C-3 [175]. The ^{13}C NMR spectral data revealed the presence of 27 carbon atoms suggestive of a steroidal compound (Table 4.1.3, **Appendix A**, **Figure A4**). Furthermore, with the aid of a distortionless enhancement by polarization transfer (DEPT) spectral (Table 4.1.3, **Appendix A**, **Figure A5)** data, the compound possessed five methyl carbons, eleven sp^3 methylene carbons, seven sp^3 and one sp^2 methine carbons, two sp^3 and one sp^2 quaternary carbons. From the ^{13}C NMR data one oxygenated and an olefinic carbon, and a double bond were identified. Based on the spectral and literature data [175] compound (**48)** was identified as cholesta-5-en-3β-ol commonly known as cholesterol (**48**).

Table 4.1 3 ^{1}H, ^{13}C NMR, DEPT-90, DEPT-135 and Literature data spectral data of compound **48**

Position	δ_C, Type	δ_H (J in Hz)	Lit., δ_C(125 MHz)	DEPT- 90	DEPT -135
1	37.3, CH_2	1.83	37.2	-	37.3
2	32, CH_2	1.98, 1.95	31.6	-	31.9
3	71.8, CH	3.52 (1H, m)	71.77	71.8	71.8
4	42.3, CH_2	2.28, 2.23	42.26	-	42.3
5	140.8, C		140.72	-	-
6	121.7, CH	5.35 (1H, m)	121.7	121.7	121.7
7	31.9, CH_2		31.88	-	31.9
8	31.7, C	1.81	31.86	31.7	31.7
9	50.1, CH	0.92	50.08	50.1	50.1
10	36.5, C		36.47	-	-
11	21.1, CH_2		21.05	-	21.1
12	39.8, CH_2	2.01	39.74	-	39.8
13	42.3, C		42.28	-	-
14	56.8, CH	0.98	56.73	56.8	56.8
15	24.3, CH_2		24.27	-	24.3
16	28.2, CH_2		28.22	-	28.2
17	56.2, CH	1.08	56.1	56.2	56.2
18	11.9, CH_3	0.67 (3H, s)	11.84	-	11.9
19	19.4, CH_3	1.01 (3H, s)	19.38	-	19.4
20	35.8, CH		35.77	35.8	35.8
21	18.7, CH_3	0.91 (3H, d, 6.5 Hz)	18.69	-	18.7
22	36.2, CH_2		36.16	-	36.2
23	23.8, CH_2		23.8	-	23.8
24	39.5, CH_2	1.13, 2.01	39.49	-	39.5
25	28, CH	1.84	27.99	28.0	28.0
26	22.6, CH_3	0.86 (6H, dd, 6.5, 2.3 Hz)	22.55	-	22.6
27	22.8, CH_3		22.81	-	22.8

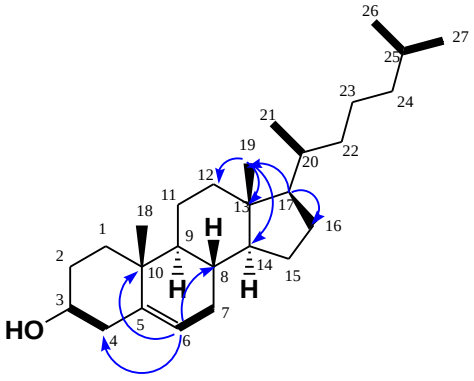

Figure 4.1. 1 Structure and some Key HMBC and ^{1}H-^{1}H COSY (bold) correlations observed in cholesterol

Cholesterol (**48**) was previously reported from *Guggulu*, the gum resin exudates from the tree *Commiphora mukul* (Hook, ex Stocks) Engl. along with two other isomeric steroids, which were identified as 4,17(20)-(*trans*)-pregnadiene-3,16-dione (*Z*-guggulsterone) (**17**) and 4,17(20)-(*cis*)-pregnadiene-3,16-dione (*E*-guggulsterone) (**18**) [178]. Cholesterol is a sterol also known as steroid alcohol, a type of lipid. Cholesterol is biosynthesized by all animal cells and is an essential structural component of animal cell membranes. Cholesterol is an important lipid molecule in cell membranes and lipoproteins. Cholesterol is also a precursors of steroid hormones, bile acids, and vitamin D. Cholesterol is essential for neuroactive steroid production, growth of myelin membranes, and normal embryonic and fetal development [179]. Abnormal levels of cholesterol or its precursors have been observed in various human diseases, such as heart diseases, stroke, type II diabetes, brain diseases and many others [180].

4.1.1.2 Characterization of compound 112 (Lathosterol)

Lathosterol was obtained as white powder from the chloroform fraction. Its molecular formula was assigned as $C_{27}H_{46}O$ with five degree of unsaturation based on the LC-ESI-MS, EI-MS and NMR data. The compound was detected from HPLC-DAD chromatogram at RT = 1.68 min (**Appendix B**, **Figure B1**). Its IR spectrum exhibited absorption bands of hydroxyl at 3367.51 cm^{-1} which is strengthened by 1040.69 cm^{-1} by the C-O group. The absorption band at 2931.22 cm^{-1} and 1377.54 cm^{-1} is the C-H stretching and bending of CH_3, respectively. A weak absorption band showed the presence of tri-substituted olefin stretch at 1711.75 cm^{-1} (**Appendix B**, **Figure B2**). From ESI-MS in positive ion mode, $[M+NH_4CN+H]^+$ (**Appendix B**, **Figure B1**) generated a quasi-molecular anion peak at m/z 431.46, calcd (431.33) indicating five degree of unsaturation. The structure of **112** was deduced from the detailed analysis of the ^1H and ^{13}C-NMR and DEPT-135, and further aided by two dimensional (2D) NMR experiments COSY, HSQC, and HMBC.

The ^1H NMR spectrum of compound **112** (Table 4.1.4, **Appendix B**, **Figure B3**) displayed one olefinic proton signal at δ_H 5.16 (dd, J = 4.8, 2.2 Hz, 1H) indicative of a single unsaturation unit on ring B of the sterol. A signal at δ_H 3.59 (tt, *J* = 10.9, 4.5 Hz, 1H) evidenced one oxymethine group of H-3. The spectrum showed five methyl groups comprising two tertiary methyl groups at δ_H 0.53 (s, H-18, 3H) and 0.79 (s, H-19, 3H), three secondary methyl groups at δ_H 0.92 (d, J= 6.5

Hz, H-21, 3H) and δ_H 0.87 (dd, J = 6.6 Hz, H-26 and H-27, 6H). The methyl doublets at δ_H 0.92, 0.87 and 0.86 were consistent with the presence of a side chain on the sterol skeleton [175].

The ^{13}C NMR spectrum revealed the presence of 27 different carbon signals. With the aid of DEPT-135 and HSQC (**Appendix B**, **Figure B4, B5 and B6)** the spectrum showed five methyl carbon, eleven methylene carbon, eight methine carbon and three quaternary carbon atoms were observed. The downfield-shifted signal observed at δ_C 139.62 was an olefinic quaternary carbon (C-8) and for sp^2 methine carbon at δ_C 117.42 supported the presence of a single olefinic moiety. The ^1H and ^{13}C NMR spectra were consistent with those data for related reported steroidal compounds [175].

Therefore, the 1D and 2D NMR data (Table 4.1.4, **Appendix B**) suggested that compound **112** was a cholestane type sterol, where the unsaturation of Δ7 double bond on ring B was determined by the HMBC correlations of H-7/C-6, C-9, C-14, and ^1H-^1H COSY correlations of H-7/H-6, H-9, H-14 (**Appendix B**, **Figure B7**). The position of the hydroxyl group was unambiguously assigned to C-3 on the basis of HMBC correlation of H-3 (δ_H 3.59) to C-2 (δ_C 31.48), C-4 (δ_C 38.00) ($^2J_{CH}$) and C-5 (δ_C 40.26) ($^3J_{CH}$) and ^1H-^1H COSY cross peaks of H-3/H-2, H-4 and literature data. The HMBC indicates a three bond correlation $^3J_{C\text{-}H}$ between H-26/C-24, H-27/C-26 and a two bond correlation between $^2J_{C\text{-}H}$ H-27/C-25 (**Appendix B**, **Figure B8**).

Table 4.1 4 ^{1}H and ^{13}C NMR assignments for lathosterol (**112**) and the observed HSQC, COSY ($^{1}H \rightarrow ^{1}H$) and HMBC ($^{1}H \rightarrow ^{13}C$) correlations.

Position	$\delta_{C,}$ Type	δ_{H} (J in Hz)	COSY	HMBC
1	37.15, CH_2	1.08, 1.83	2	
2	31.48, CH_2	1.40, 1.8	3	
3	71.07, CH	3.59 (tt, J = 10.9,4.5 Hz)	2, 4	2, 4, 5
4	38.00, CH_2	1.28, 1.72		3, 5
5	40.26, CH	1.39	6	
6	29.66, CH_2	1.25, 1.76		
7	117.42, CH	5.16 (dd, J = 4.8, 2.2 Hz)	6, 9, 14	9
8	139.63, C	-		
9	49.46, CH	1.63	11	
10	34.21, C	-		
11	21.56, CH_2	1.57, 1.4		12
12	39.58, CH_2	1.21, 2.03		13
13	43.39, C	-		
14	55.05, CH	1.39, 1.79		
15	22.96, CH_2	1.52, 1.40		14
16	27.95, CH_2	1.27, 1.88		
17	56.16, CH	1.20	1.26	12, 13, 15, 16, 18, 20, 22
18	11.84, CH_3	0.53 (s)		13, 17
19	13.04, CH_3	0.79 (s)		1, 10, 12
20	36.21, CH	0.99, 1.35	21	
21	18.85, CH_3	0.92 (d, J = 6.53 Hz)		
22	36.13, CH_2	1.35, 0.99		21
23	23.92, CH_2	1.34, 1.14		
24	39.509, CH_2	1.09, 1.12		
25	28.01, CH	1.26, 1.51	26, 27	
26	22.55, CH_3	0.87 (dd, = 6.6, 2.84 Hz)		24
27	22.82, CH_3			25

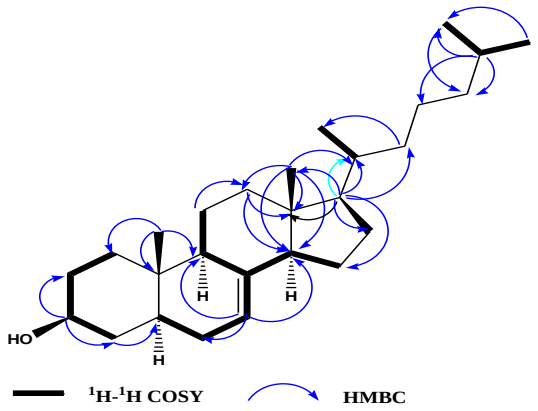

Figure 4.1. 2 Key HMBC (blue arrow) and ^{1}H-^{1}H COSY (Bold) correlations observed in lathosterol (**112**)

It acts as a marker of synthesis of cholesterol and is not affected by dietary consumption of cholesterol [128] (Figure 4.1.6). The compound is an isomer of cholesterol. The ^{1}H-NMR and ^{13}C-NMR spectral data of the compound was compared with NMR data of those previously reported for the same compound from Starfish *Aserinapectinifera*. The compound 5α-cholest-7-en-3β-ol was reported to have a potent antigenotoxic activity against mutagens both MNNG and NQO [181]. This is the first report of this compound from a plant belonging to the genus *Commiphora* resin.

Erasto [182] reported cholest-7-en-3β-ol and 4α-methyl-cholest-7-en-3β-ol from stem sap of *C. eminii.* The compound 4α-Methyl-cholest-7-en-3β-ol has previously been reported as a potential precursor in the biosynthesis of cholest-7-en-3β-ol (**112)** and other sterols in Echinoderms [183]. It has been reported that the starfish *Asterias rubens* can convert mevalonic acid into cholest-7-en-3β-ol (**112**) by a pathway similar to that established for sterol biosynthesis in mammals [184-186]. An alternative route for Δ7 sterol production in starfish demonstrated that *Pisaster ochraceus* could convert ingested cholest-5-en-3β-ol (**48**) into cholest-7-en-3β-ol (**112**) [187]. From the detailed ^{1}H-NMR and ^{13}C-NMR data (Table 4.1.9), where the assignments are based on ^{1}H-^{1}H COSY, ^{13}C-^{1}H HSQC and HMBC corrolations.

4.1.1.3 Isolation of a mixture cholesterol and lathosterol

A mixture was isolated as an amorphous white powder from the chloroform fraction. The TLC analysis using different solvent system of *n*-hexane / EtOAC showed a single spot. The ^{1}H and ^{13} NMR indicate the prescence of two cholestane type sterols (cholesterol and lathosterol) with

nearly equal amount. Detection with the non-conventional LC - DAD chromatogram in the LC-TIC measurement indicated the presence of two main peaks that corresponds to two major compounds at RT 1.32 and 1.94 min with peak area % of 47.85 and 52.15, respectively (**Appendix C, Figure C1**). The amount of compounds in the mixture was further confirmed from the integrated areas of olefinic and oxymethine protons where the 52.15% corresponds to lathosterol and 47.85% corresponds to cholesterol. Its ESI in a positive mode at 415.46 $[M-H_2O+HCOOH+H]^+$ Calcd (415.36) was due to dehydration of a protonated molecular ion attached to formic acid (**Appendix C, Figure C1**). On a separate measurement by EI-MS, a molecular ion peak at *m/z* 386 for $[M]^+$, corresponding to a molecular formula $C_{27}H_{46}O$ (Both sterols have the same molecular formula $C_{27}H_{46}O$, but a different retention time), suggesting they are isomers with different unsaturation pattern. The chemical identification and assignments were made from a combination of IR, mass spectral data given as m/z from low resolution LR-ESI-MS, EI-MS spectra, 1D and 2D spectra recorded. IR spectra of the mixture exhibited an O-H band at 3334.72 cm^{-1}. Compared to IR spectra of isolated compounds the mixture showed a broad absorption bands at 3334.72 cm^{-1} indicating the presence of hydroxyl group held together by intermolecular force, hydrogen bonding (**Appendix C, Figure C2**) and two consecutive weak absorption bands between 1680 and 1650 cm^{-1} attributed to the presence of two unsaturated (C=C) moieties and bands at 2930 cm^{-1} indicate CH_3 and CH_2 absorptions in the mixture. The absorptions at 1466.06 and 1040.69 cm^{-1} are attributed to the angular deformation of methyl groups and C-O stretch, respectively.

The ^1H NMR spectrum (**Appendix C, Figure C3**) of the mixture showed signals for two vinylic protons at δ_H 5.35 (1H, m) and 5.16 (1H, dd, J = 4.6, 2.1 Hz). These vinylic protons signals are characteristic for sterol compounds with H-6 and H-7 positions. The observation of a proton signal at δ_H 3.52 (1H, m) and 3.59 (1H, m) indicated the presence of two oxygenated methine protons in the mixture. The up field region of the ^1H NMR spectrum (**Appendix C, Figure C3**) of the mixture exhibited four methyl signals integrated to three protons each at δ_H 0.53 (3H,s), 0.68 (3H, s), 0.79 (3H, s), and 1.01 (3H, s). The signal at δ_H 0.86 (12H, dd, *J* = 6.6, 2.8 Hz) integrated to twelve protons and peak at δ_H 0.92 (6H, dd, *J* = 6.5, 2.9 Hz,) integrated to six protons. The integration of the ^1H NMR signals at δ_H 5.35 (assigned to H-6 of the cholesterol) and δ_H 5.16 (assigned to H-7 of the lathosterol) indicates a ratio of 47.85%

cholesterol and 52.15% lathosterol, excluding solvent impurities this leads to the LC-MS chromatogram peak with a retention time of 1.32 and 1.94 min corresponds to cholesterol and lathosterol respectively, i.e cholesterol precedes lathosterol.

The ^{13}C NMR spectrum revealed 50 carbon peaks, The DEPT-135 spectrum displayed the presence of eight methyl, 22 methylene, 14 methine and 6 quaternary carbons. In the ^{13}C NMR spectrum the four carbon signals at δ_C 56.2, 28.0, 22.8 and 22.6 ppm are intensively displayed these corresponds to C-17, C-25, C-26 and C-27 respectively (**Appendix C, Figure C4, C5**). This is due to overlap of the side chain carbons of the two sterols at the specified carbon positions. Furthermore, the ^{13}C NMR spectrum showed intense signals at δ_C 121.7 and 117.4 and less intense ones at δ_C 140.8 and 139.6 attributed to alkenyl carbon atoms where the less intense ones are quaternary carbons.

2D NMR of this mixture allowed identification of all the ^{1}H and ^{13}C NMR signals, whose assignments are given in Table 4.1.5. The structures of the side chains were assembled by 1D and 2D NMR correlation data as a result of the placement of the double bonds at δ_C 117.42, 121.71, 139.62 and 140.77 and configuration of their olefinic protons at δ_H 5.16 and 5.35. Furthermore, in addition to the two olefinic protons two separate spectra of oxygenated methine protons at δ_H 3.52, 3.59 and corresponding carbon signal peak at δ_C 71.8, 71.07 induced good spectral dispersion throughout the remaining carbon and allowed for the unambiguous identification of all carbon resonances. Both the olefinic and hydroxyl signals were distinguished by HSQC spectra (Table 4.1.5, **Appendix C, Figure C6**).

The absence of carbon peaks at 139.62 and 140.77 ppm from HSQC spectrum indicates these two are quaternary carbon of an alkene. The data further confirmed from DEPT-135 spectra. This study was used to examine whether ^{13}C NMR spectroscopy can be used to differentiate between cholesterol (**48**) and lathosterol which are isomers of 5α, 3β monenecholestane. Lathosterol (**112**) is a precursor (intermediate) in the biosynthesis pathway of cholesterol. Chemical shifts were assigned to the individual carbon with the help of previously documented literature [175]. It was found that the corresponding carbons 20-27, the alkyl side chain, afforded nearly identical chemical shifts for both compounds, whereas the major chemical shift difference was observed in the ring B of the sterols. Thus ^{13}C NMR can be used as an

additional tool to distinguish between the two 5α, 3β monenecholestane sterols isomers at Δ5 and Δ7 double bond positions. The larger shifts of the steroid ring protons compared to the side chains merely indicate that those protons are closer to the face of the anisotropic alkene group than the side chain protons. The chemical structure of lathosterol differs from that of cholesterol in having double bonds (at positions C7 and C8). ^{13}C-NMR spectra of the side chain of the two sterols are equivalent.

Table 4.1 5 Selected 1D and 2D NMR spectral data of the mixture (**48**) and (**112**)

Position	δ_H	Multiplicity (in Hz)	Integrated (proton)	HSQC	COSY	HMBC
H-3'	3.52	M	1	3' (71.8)	4' 2.28	1
H-3"	3.59	M	1	3"(71.08)	4' 1.72, 4" 1.26	4
H-6	5.35	M	1	6 (121.76)	7" 1.99	8, 10.4
H-7	5.16	dd, J=4.6, 3.1 Hz	1	7 (117.42)	6', 6" 1.77, 1.75	6
H-18'	0.68	S	3	18' (11.80)		12, 13, 14
H-19'	1.01	S	3	19' (19.40)		9, 10,
H-18"	0.53	S	3	18" (11.85)		12, 13, 14
H-19"	0.79	S	3	19" (11.80)		5, 9, 10
H-21	0.92	dd, J=6.5, 2.9 Hz	6	21 (18.58, 18.61)	20	17, 20, 22
H-26, 27	0.86	dd, J=9.3, 6.5 Hz	12	26 (22.53,22.50)	25	24, 25,

The three downfield aliphatic resonances can be assigned to the tertiary carbons C-9, C-14, and C-17. The two quaternary carbons (C-10 and C-13) have been located from DEPT-135 and HSQC spectra. The two up field resonances correspond to C-18 and C-19, with C-19 undergoing slight changes as a result of the position of the double bond, which is β to the alkene. Additionally, based on 2D NMR data such as HSQC, COSY and HMBC (Table 4.1.5, **Appendix C, Figure C6, C7 and C8**) and comparison of the spectra with literature data (Wilson et al., 1996) [175] the two C-27 sterol isomers were identified as cholesta-5-ene-3β-ol and cholest-7-ene-3β-ol which are commonly known as cholesterol (**48**) and lathosterol (**112**), respectively. The mixture showed a single TLC spot, HPLC peak and mass spectral characteristics. The mixture of cholstane type sterols also obtained from n-hexane fraction from a conventional HPLC with UV detector that showed a single major peak at retention time of 10.579 min injected on preparative HPLC using a mobile phase of a mixture of 80% methanol and 20% DIW (de-

ionized water), where the purity of isolated mixture was found to be 97.6% (**Appendix C, Figure C9, Table C1**).

4.1.2 Isolation of compounds from *C. africana* cytotoxic fractions

The *n*-hexane fraction (7g) was chromatographed repeatedly on a flash column chromatography (FCC) to afford a known pentacyclic triterpene α-amyrin (**56**) (22 mg) and two new migrated malabaricane triterpenes commafric A (**113**) (430 mg) and commafric B (**114**) (60 mg). During preparation of sample 7g of n-hexane fraction was dissolved in a minimum volume of the solvent system and applied with Pasteur pipette on the silica gel (60-120 mesh) column to separate possible Phytoconstituents. Flash chromatography was applied to drive the solvent through the column of stationary phase. The gradient elution was followed for the isolation. Initially *n*-hexane : ethylacetate (9:1) was used as a packing solvent and then column was eluted with increasing polarity (8:2, 7:3, 6:4, 1:1, 1:2 and finally 100% EA) of ethyl acetate. Total 240 fractions of 20 ml each were collected. All the fractions were monitored simultaneously on a TLC plate using appropriate n-hexane: ethyl acetate solvent system. The fractions showing identical spots on TLC were pooled together and finally 7 fractions were obtained. Fr 46-49, Fr 51-64, Fr 65-71, Fr 81-90, Fr 101-105, Fr 106-118. The fractions were further flash chromatographed to afford one ursane type triterpenes, α-amyrin (**56**) and two migrated malabaricane triterpenes namely Commaric A (**113**) and B (**114**). The known compound α-amyrin (**56**) was readily identified by comparison of its spectral data with those reported in the literature.

4.1.2.1 Isolation and characterization of compound 56 (α-amyrin)

α-Amyrin was obtained as a white powder and LC chromatogram displayed a single peak with peak area percent of 100 which indicate its purity at retention time of 1.77 (**Appendix D, Figure D1**). The molecular formula of the compound was determined based on ^{1}H NMR, ^{13}C NMR, DEPT spectral data and literature to be $C_{30}H_{50}O$ indicating six degree of unsaturation. ESI is suited for highly to moderately polar and ionic analytes containing acidic and basic functional groups. Positive ionization consist in protonation and is suitable for the compounds containing basic functional groups, typically producing $[M+H]^+$, $[M+Na]^+$ and $[M+K]^+$ ions. Negative

ionization consists in deprotonation and therefore is suitable for the compounds containing an acidic functional group, typically producing $[M-H]^-$ ions.

The ^{1}H-NMR spectrum (Table 4.1.6, **Appendix D, Figure D3**) showed signal for an olefinic proton at δ_H 5.14 (t, *J* = 3.6 Hz, 1H). A chemical shift at δ_H 3.22 (dd, *J* = 10.9, 5.1 Hz, 1H) is typical for oxygenated methine proton. Furthermore, the six singlet signal of protons containing three protons (s,3H) at δ_H 1.08, 1.02, 1.01, 0.97, 0.93, 0.8 ppm and a doublet signal at δ_H 0.81 ppm (d, *J* = 2.5 Hz, 6H) confirm the structure of the α-amyrin molecule which has eight methyl groups.

The ^{13}C-NMR spectrum (Table 4.1.6, **Appendix D, Figure D4**) of compound **56** with the aid of DEPT-135 (Table 4.1.6, **Appendix D, Figure D4**) revealed signals corresponding to 30 carbon signals that indicate the compound is clearly a pentacyclic triterpenes consisted of eight methyl carbons, nine methylene carbons, seven methine carbons and six quaternary carbons. The signal at 124.41 ppm can be attributed to a carbon of the type –CH=CR$_2$ (C-12). The signal at δ_C 79.06 implies a methine carbon atom bonded to oxygen (C-3). The downfield shifted carbon signals at δ_C 124.4 and 139.6 imply an olefinic methine and quaternary carbons positioned at C-12 and C-13 respectively. The signals that appear at δ 28.1, 15.7, 15.6, 16.9, 23.3, 28.1, 17.7 and 21.4 ppm are methyl carbon signals. Signals at δ 38.8, 28.8, 18.4, 32.9, 23.4, 27.3, 26.6, 31.3 and δ 41.5 ppm are methylene carbon signals, and signals at δ 79.1, 55.2, 47.7, 124.4, 59.1, 39.7 and 39.6 ppm is the methine carbon signals and signal at δ 38.8, 40.0, 36.9, 136.6, 42.1 and 33.8 ppm are signals of quaternary carbons. Chemical shifts and types of carbon above are identical to the carbon chemical shift of α-amyrin (**56**).

Table 4.1 6 ^{13}C NMR and ^{1}H NMR ($CDCl_3$) (500 MHz) spectral data of compound **56** and literature data

Position	^{1}H-NMR (*J* in Hz) Compound **112**	^{1}H-NMR (*J* in Hz) Compound **112** literature [188]	^{13}C-NMR Compound **1 12**, type	13C-NMR literature [188]
1		1.68(2H,m)	38.8, CH_2	38.9
2		2.03(2H,m)	28.8, CH_2	28.3
3	3.24 (dd,1H, J = 10.5, 5.1Hz)	3.22 (dd,1H, J = 11.2, 4.8Hz)	79.1, CH	79.2
4		-	38.8, C	38.7
5		0.74 (1H,d,J=11.8)	55.2, CH	55.3
6		1.57(2H,m)	18.4, CH_2	18.5
7		1.36(1H,m)	32.9, CH_2	33.1
8		-	40.0, C	40.2
9		1.54(1H,m)	47.7, CH	47.9
10		-	36.9, C	37.0
11		1.91(2H,m)	23.4, CH_2	23.5
12	5.14 (t, 1H, J = 3.62 Hz)	5.12 (t, 1H, J = 3.8 Hz)	124.4, CH	124.6
13		-	139.6, C	139.7
14		-	42.1, C	42.2
15		1.61 (2H,t,J=4,2)	27.3, CH_2	27.4
16		1.83 (2H,t,J=4.9)	26.6, CH_2	26.8
17		-	33.8, C	33.9
18		1.31(1H,s)	59.1, CH	59.2
19		1.36(1H,m)	39.7, CH	39.8
20		0.87(1H,m)	39.6, CH	39.8
21		1,39(2H,m)	31.3, CH_2	31.4
22		1,41(2H,t,J=10.1)	41.5, CH_2	41.7
23	1.01 (s,3H)	0.99(3H.s)	28.1, CH_3	28.3
24	0.93 (s, 3H)	0.95(3H,s)	15.7, CH_3	15.8
25	0.97 (s, 3H)	0.96(3H,s)	15.6, CH_3	15.8
26	1.02 (s,3H)	1.01(3H,s)	16.9, CH_3	17.0
27	1.08 (s,3H)	1.07(3H,s)	23.3, CH_3	23.4
28	0.8 (s,3H)	0.8(3H,s)	28.1, CH_3	28.9
29	0.81 (d, 3H, J= 2.5 Hz)	0.79 (3H, d,J=3.45)	17.5, CH_3	17.6
30	0.81 (d, 3H, J=2.54Hz)	0.91(3H,d,J=5.8)	21.4, CH_3	21.6

^{1}H NMR and ^{13}C NMR of Compound **56** data identified as the pentacyclic triterpene α-amyrin (**56**) by comparison of its spectral data with those reported in the literature. These data are presented in Table 4.1.12. The compound α-amyrin exhibits anti-inflammatory [189], and can be considered as cytotoxic [190]. A separate study indicated that the pentacyclic triterpenes α-amyrin stimulates proliferation of human keratinocttes but does not protect them against UVB damage [191]. ^{1}H NMR and ^{13}C NMR data are in agreement with published data [188, 192, 193].

4.1.2.2 Isolation and characterization of compound 113 (Commafric A)

Commafric A (**113**) was obtained as a white powder and LC chromatogram displayed a single major peak with peak area percent of 100% without solvent at retention time of 1.74 (**Appendix E, Figure E1**). Compound **113 (**"commafric A"), the most abundant isolated molecule was obtained as a white solid with n-hexane/EtOAc (7:3) solvent system. The molecular formula was defined as $C_{30}H_{48}O_4$ with seven degree of unsaturation based on by the aid of LR-ESI-MS interfaced in positive and negative ion modes scanned from 100 to 1000 m/z (**Appendix E, Figure E2**) and HR-ESI-MS^2 mass scanned from 170.00 to 600.00 m/z in positive mode (**Appendix E, Figure E3**). The structure of the isolated compound was elucidated by IR, ^{13}C, ^{1}H-NMR, 2D-NMR, computation and comparing with literature data. Two ESI mode was used to determine the molecular mass of the compound, the LR-ESI-MS and HR-ESI-MS^2. The molecular formula of compound **113** was calculated to be $C_{30}H_{48}O_4$ (m/z 471.35, $[M-H]^-$, calcd 471.34), suggesting seven degree of unsaturation. The molecular ion peak at 471.35 in a negative ion mode of compound **113** was the highest in intensity and produced less fragmentation and is more informative compared to the positive ion spectra (**Appendix E, Figure E2ii**). In ESI-MS negative ionization consists in deprotonation and therefore is suitable for compounds which contained an acidic functional group, typically producing $[M-H]^-$ ion [162]. Since molecular clusters are common in ESI, in the negative ion mode the peak at m/z 943.63 calcd 943.70 corresponds to deprotonated dimerized parent molecule $[2M-H]^+$. Regarding the m/z values, it should be noted that the MS signal of the dimer appeared in small intensity. The low resolution ESI-MS data in a Positive ion mode indicated a base peak at m/z 455.22 $[M+H-H_2O]^+$ calc for 454.35 indicated protonation of a dehydrated parent molecule. The molecular ion peak at m/z at 473.45 $[M+H]^+$ is less intense and calc. for 472.35. The peak at m/z 277.27 is due to the loss of long branched chain $[M-C_{13}H_{23}O]^+$ calc for 277.18 (**Appendix E, Figure E2ii**).

The second technique used to determine the major precursor ion and calculated fragment ion elemental composition was under the HR-ESI-MS of compound **113** and is tabulated. The chemical formula was established as $C_{30}H_{48}O_4$, on the basis of the positive-ion mode HR-ESI-MS data due to Na adduct formation or a qusimolecular ion was observed at m/z 495.3442, $[M+Na]^+$, (calcd 495.3445) and NMR data indicating seven degree of unsaturation (Table 4.1.7, **Appendix E, Figure E3**).

The collision induced decomposition (CID) spectra of FTMS-ESI^+-MS^2 spectrum of the selected $[M+H]^+$ ion peak at m/z 473.36 and m/z 455.35 consisted of four and six major peaks respectively (**Appendix E, Figure E3a, E3b**). The four major fragment ion peaks observed in m/z 473.36 are at *m/z* 455.3515, 437.3411, 427.3568, and 409.3464 (**Appendix E, Figure E3a**). The mass differences between the parent ion at *m/z* 473.36 $[M+H]^+$ and the fragment ions at *m/z* 455.3515, and 437.3411 are 18.0085 and 36 respectively. This shows protonation of a dehydrated molecule for *m/z* 455.3515 and protonation with loss of two H_2O molecules for m/z 437.3411. The last two fragment ions show losses of 45, and 63 (1×45 plus 18), m//z masses from the parent molecule. The first peak corresponds to loss of carboxylic acid. The peak at 409.3464 corresponds to loss of H_2O molecules and carboxylic acid group from the parent molecule. The peak at m/z 277.1798 is due to the loss of long side chain ($C_{13}H_{23}O$). The major fragment ion peaks observed in m/z 455.35 are at m/z 277.1801 and 259.1695 that corresponds to loss of the long side chain and dehydration of the three fused ring left after the loss of side chain. Other fragments related to this are 287.2008 ($C_{19}H_{27}O_2$), 305.211 ($C_{19}H_{29}O_3$), 313.2165 ($C_{21}H_{29}O_2$), and 331.2270 ($C_{21}H_{31}O_3$) (**Appendix E, Figure E3b**). Fragment ion peaks and corresponding calculated fragment ion elemental composition based on accurate mass detection are tabulated below (Table 4.1.7).

Table 4.1 7 Calculated fragment ion elemental composition based on accurate mass detection CID fragmentation with HRESIMS^2 for compound **126** (commafric A)

m/z	Calc. mass	Comp.	m/z	Calc. mass	Comp.
511.3385	511.3394	$C_{30}H_{48}O_5Na$	285.222	285.2213	$C_{20}H_{29}O$
495.3442	495.3445	$C_{30}H_{48}O_4Na$	277.18	277.1798	$C_{17}H_{25}O_3$
473.3625	473.3625	$C_{30}H_{49}O_4$	269.227	269.2264	$C_{20}H_{29}$
455.3519	455.352	$C_{30}H_{47}O_3$	267.211	267.2107	$C_{20}H_{27}$
455.3515	455.352	$C_{30}H_{47}O_3$	259.206	259.2056	$C_{18}H_{27}O$
437.3411	437.3414	$C_{30}H_{45}O_2$	259.17	259.1693	$C_{17}H_{23}O_2$
427.3568	427.351	$C_{29}H_{47}O_2$	257.154	257.1536	$C_{17}H_{21}O_2$
419.3308	419.3308	$C_{30}H_{43}O$	255.211	255.2107	$C_{19}H_{27}$
411.3623	411.3621	$C_{29}H_{47}O$	245.154	245.1536	$C_{16}H_{21}O_2$
409.3464	409.3465	$C_{29}H_{45}O$	241.195	241.1951	$C_{18}H_{25}$
395.8729	393.35166	$C_{29}H_{45}$	239.18	239.1794	$C_{18}H_{23}O_4$
391.3361	391.3359	$C_{29}H_{43}$	231.174	231.1743	$C_{16}H_{23}O$
363.3048	363.3048	$C_{27}H_{39}$	221.117	221.1172	$C_{13}H_{17}O_3$
359.2582	359.2581	$C_{23}H_{35}$	215.179	215.1794	$C_{16}H_{23}$
355.2997	355.2995	$C_{25}H_{39}O$	213.164	213.1638	$C_{16}H_{21}$
349.2892	349.289	$C_{26}H_{37}$	209.117	209.1172	$C_{12}H_{17}O_3$
345.2427	345.2424	$C_{22}H_{33}O_3$	199.148	199.1481	$C_{15}H_{19}$
337.2892	337.289	$C_{25}H_{37}$	191.179	191.1794	$C_{14}H_{23}$
331.227	331.2268	$C_{21}H_{31}O_3$	185.132	185.1325	$C_{14}H_{17}$
327.2321	327.2319	$C_{22}H_{31}O_2$	177.164	177.1638	$C_{13}H_{21}$
315.2321	315.2319	$C_{21}H_{31}O_2$	173.132	173.1325	$C_{13}H_{17}$
313.2165	313.2162	$C_{21}H_{29}O_2$	159.117	159.1168	$C_{12}H_{15}$
305.2114	305.2111	$C_{19}H_{29}O_3$	157.101	157.1012	$C_{12}H_{13}$
303.1958	303.1955	$C_{19}H_{27}O_3$	149.132	149.1325	$C_{11}H_{17}$
299.2008	299.2006	$C_{20}H_{27}O_2$	147.117	147.1168	$C_{11}H_{15}$
287.2372	287.2369	$C_{20}H_{31}O$	135.117	135.1168	$C_{10}H_{15}$
287.2008	287.2006	$C_{19}H_{27}O_2$			

In IR spectrum (Fig. 4.1.3) a broad band ranging from 2500 - 3600 cm^{-1} compatible with hydrogen bonded OH. This band is superimposed by a sharper peak at 3607 cm^{-1} that may belong to a free (unbonded) OH stretching signal. The 2956 and 2872 cm^{-1} bands are assigned to CH stretching vibrations; the split indicates presence of both aliphatic part and H-C=C bond system. The presence of the carboxyl is further indicated by the 1695 cm^{-1} C=O stretch band. These features of the spectrum are in agreement with a simulated spectrum (Fig. 4.1.3), as is the fine

splitting in the fingerprint region (900-1500 cm^{-1}). Note that the hydrogen bond broadening was not simulated in the computation and only the "free" OH signal (3835/3743 cm^{-1}) is thus predicted. The fingerprint region contains CH_3 scissoring deformation peak at (exp/cal) 1449/1499 cm^{-1} and other CH_3 modes occur around 1384/1410 cm^{-1}. The bands around 1265/1325 cm^{-1} are largely formed by CH_2 twist motion, and OH bending contributes at 1155/1215 cm^{-1}.

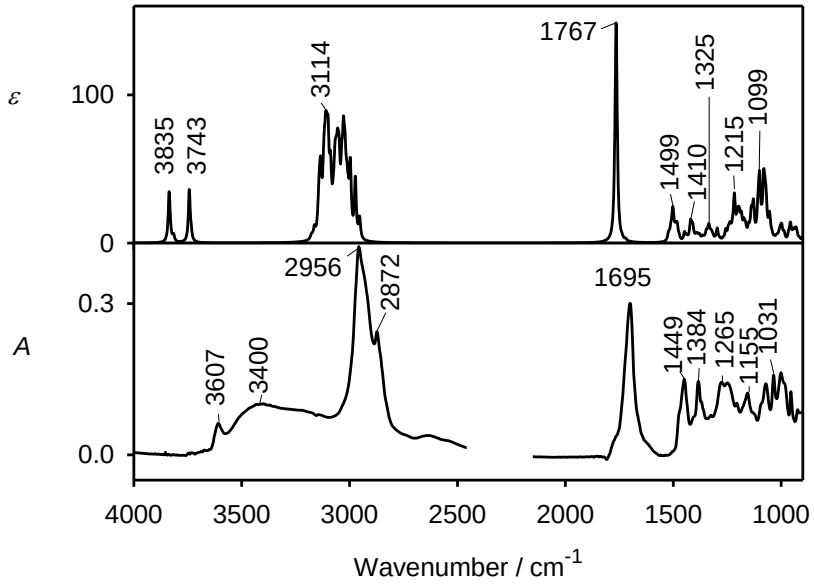

Figure 4.1. 3 Calculated- (upper panel, raw DFT frequencies) and experimental (lower panel) IR spectra of **113** (Commafric A)

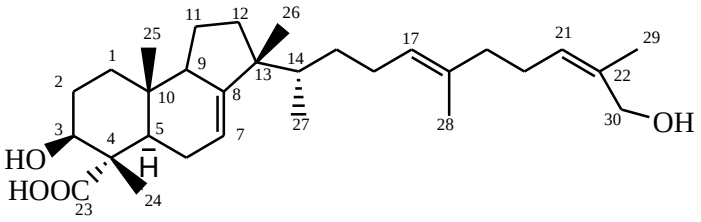

Commafric A (**113**)

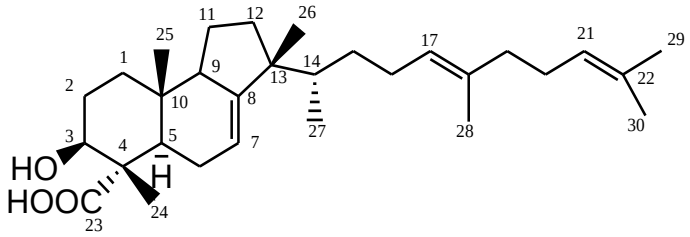

Commafric B (**114**)

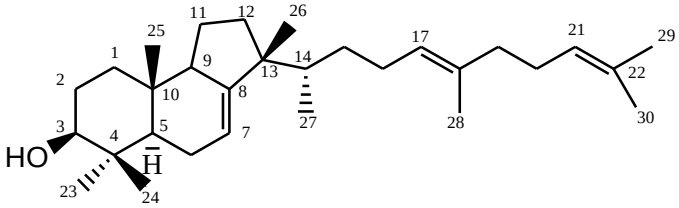

Podioda-7,17,21-triene (**115**)

The structure of compound **113** was elucidated by NMR spectroscopy. ^{1}H NMR resonances (Table 4.1.8, **Appendix E**, **Figure E4**) included two near triplets at δ_H 5.29 and 5.06, and one doublet of a triplet at δ_H 5.16, suggesting the presence of three olefinic protons. The splitting pattern of one of the three olefinic proton signals in **113** appeared at δ_H 5.16 (d) resembled those of 7-ene compounds [194].

Two geminally coupled protons appearing as doublets at δ_H 4.17 and 4.09 indicated the presence of one oxy methylene moiety. A signal integrated as one proton at δ_H 4.06 suggested the presence of an oxy methine group. Two moderately deshielded methyl signals were observed (1.57 and 1.79 ppm), indicating that two methyls are attached to sp^2 hybridized carbons (Table 4.1.8**, Appendix E, Figure E4**), and four aliphatic methyl signals (δ_H 0.75, 0.86, 0.91 and 1.18).

Table 4.1 8 NMR parameters of compound **113** in CD_2Cl_2: ^1H (600 MHz) and ^{13}C (150 MHz) NMR, HMBC, H2BC, ADEQUATE-1,1 and ROESY of **113**

No.	δ_C	δ_H (multi, J in Hz)	HMBC (H® C)[d]	H2BC (H® [H]C)[d]	1,1-ADEQUATE ([H]C® C)[d]	Key ROESY
1	38.1	1.72 (dt,*J*=13.3, 3.1)/1.32 (mc)	25	2'/''	2'/''	2'/'',25, 2'/''
2	27.3	1.67 (m[c])	3	1', 1'',3	1', 1'',3	1'/'', 25
3	76.2	4.02 (dd, *J*=11.2, 4.7)	1'',2'',5,24	2'/''	2'/''	2'/'',5
4	52.9	-	2' ,2'',3,5,24	-	3,5,24	-
5	46.6	1.88 (m[c])	24,25	6',6''	6',6''	3, 9
6	25.8	2.05 (m[c])/1.80 (m[c])	-	5,7	5,7	7, 24, 25
7	114	5.16 (dt, *J*=5.1, 2.6)	6'	6',6''	6',6''	14
8	151	-	6'/'',11'/'',12'/'',26	-	7,9	-
9	59.5	2.01 (m[c])	1',5,11',12'/'',25	11',11''	11',11''	1'',5, 11'',12''
10	34.1	-	1'/'',5,25	-	1',1'',5,9,25	-
11	23.1	1.25 (m[c])/1.53 (mc)	12'/''	12''	9, 12',12''	25, 26/9
12	33	1.25 (m[c])/1.48 (mc)	11'/'',14,26[a]	11',11''	11',11''	26/9, 15'/'', 27
13	48.3	-	12'',14,26,27	-	12',12'',14,26	-
14	41.2	1.36 (m[c])	9,12'',26,27	15',27	15',27	6',6'',7
15	33	1.34 (m[c])/1.00 (mc)	16'',27[a]	14,16',16''	14, 16',16''	
16	26.6	2.02 (m[c])/1.87 (mc)	15'/'',17[b]	15'',17	15',15'',17	-
17	125	5.04 (ddq, *J*=7.5, 6.3, 1.3)	15'/'',16'/'',19'/'',28	16',16'',28*	16',16''	-
18	135	-	16'/'',19'/'',28	-	17, 19',19'',28	-
19	40	1.96 (m[c])/1.93 (mc)	20'',28,29	20',20''	20',20''	-
20	26.7	2.14 (m[c])/2.09 (mc)	21[b]	19',19'',29**	19',19'',21	-
21	129	5.30 (t, *J*=7.0)	19'/'',20'/'',29,30'/''	19',19'',29*	20',20''	29
22	134	-	20'/'',29,30'/''	-	21,29, 30',30''	-
23	181	-	3,5,24	-	-	-
24	10.7	1.18 (s)	3,5	-	-	6',25
25	14.1	0.75 (s)	1'',5	-	-	1',2'/'',6',11',24
26	26.8	0.91 (s)	12'/''[b]	-	-	11',12'
27	15.1	0.86 (d, *J*=6.8)	14,15'/''	14	14	12''
28	16.4	1.57 (s)	17,19'/''	-	-	-
29	21.4	1.77 (s)	21,30'/''	-	-	21
30	61.5	4.07 (d, *J*=11.7)/4.17 (d, J=11.7)	21,29	-	-	-

[a] Overlap between C12 and C15, [b] Overlap between C16, C20 and C26

[c] Overlapping multiplets in ^1H, [d] Correlations listed on each receiving carbon row from the denoted proton(s)

The ^{13}C NMR (Table 4.1.8, **Appendix E**, **Figure E5**) and multiplicity edited HSQC/DEPT confirmed the presence of thirty carbons, of which seven were quaternary, ten methylene, seven methine, and six methyl. A set of 2D NMR experiments, HSQC, HMBC, H2BC, HSQC-TOCSY, ROESY, DQF-COSY and 1,1-ADEQUATE (**Appendix E**, **Figure E6-E10**), was used to establish the molecular framework of compound **113** as a tricyclic triterpenoid with structural similarity to podioda-7,17,21-trienol [195]. All carbon-carbon connections were unambiguously confirmed by 1,1-ADQUEATE, except for the two quaternary to quaternary carbon bonds (C4 to C23 and C8 to C13), which did not correlate in this pulse sequence because of the absence of

protons on both sides of the C-C bond (Fig. 4.1.4 b). The C-23 carboxyl group could be placed by HMBC correlations to H-3, H-5 and H-24 from C-23, while the C-8 to C-13 bond was confirmed by HMBC correlations between H-26 and H-12, and C-8. The location of the hydroxymethylene group as well as the position of the 21, 22 double bond was confirmed by 2D HMBC (**Appendix E**, **Figure E6**), which showed three bond couplings between the olefinic proton H-21 (δ_H 5.30) and the carbons at the C-29 methyl group (δ 21.4) and the C-30 hydroxymethylene carbon (δ_C 61.5). Furthermore, H2BC two-bond couplings appeared between C-22 and Me-29 and hyroxymethylene protons H-30$^{\prime,\prime\prime}$ (**Appendix E**, **Figure E8**).

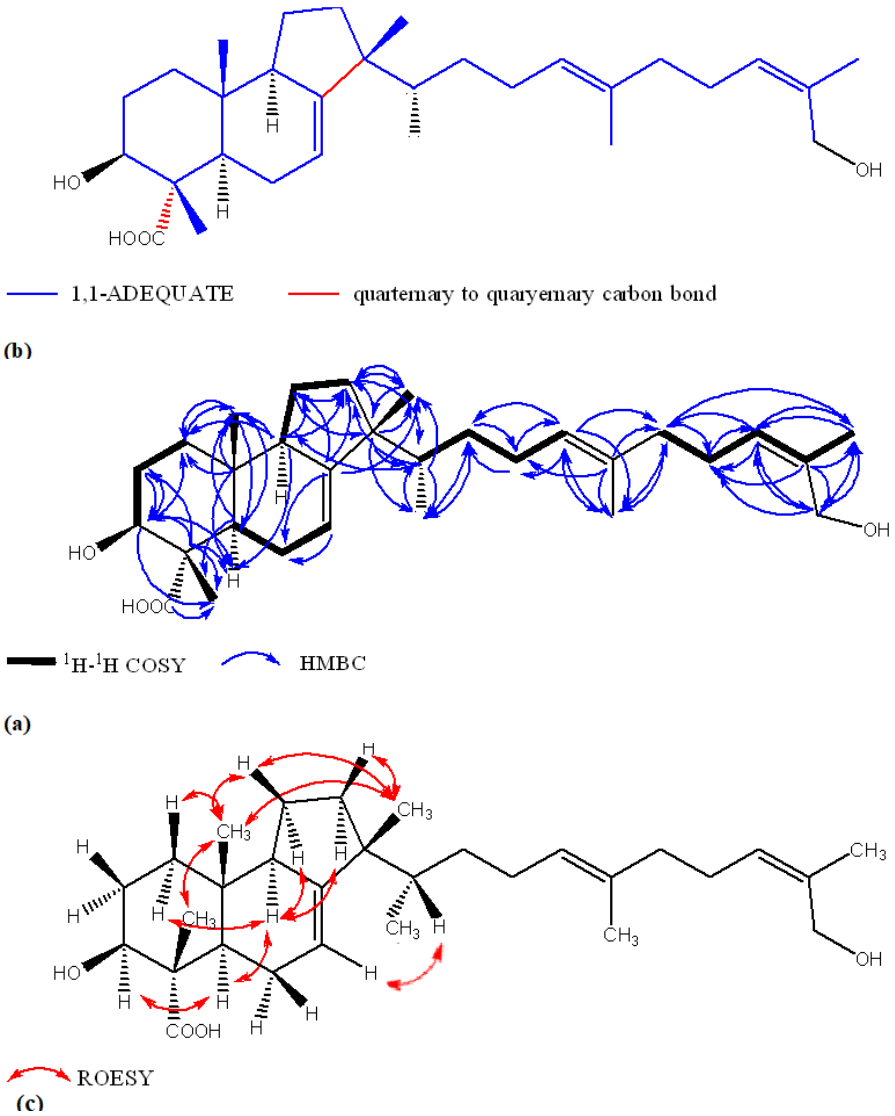

Figure 4.1. 4 2D NMR correlations through bonds, (a) COSY, HMBC and, (b) 1,1-ADEQUATE; and through space (c) NOESY/ROESY of compound **113**

Based on $^{3}J_{CH}$ couplings measured by selective CLIP-HSQMBC [163], as well as NOESY/ROESY analysis, the C-17/C-18 configuration was determined as E ($^{3}J_{C28H17}$ = 8.0 Hz and $^{3}J_{C19H17}$ = 6.0 Hz) and the C-21/C-22 configuration was determined as Z ($^{3}J_{C29H21}$=6.0 Hz and $^{3}J_{C30H21}$=9.3 Hz (**Appendix E, Figure E12**). These conclusions are based on the fact that the trans-$^{3}J_{CH}$ is expected to be stronger than the corresponding cis- $^{3}J_{CH}$. This was also consistent with the direct observations of the presence of the NOE_{H21H29} and ROE_{H21H29} correlations, and the absence of the NOE_{H21H29} and ROE_{H21H29} correlations. The Z-configuration of the C-21 to C-22-double bond is also consistent with the ^{13}C NMR chemical shifts of C-21, C-22, C-29, and C-30 in previously reported compounds with similar side chain configurations [91, 196, 197].

The relative configuration of the tricyclic system was established by NOESY and ROESY correlations supplemented with some $^{3}J_{HH}$ and $^{3}J_{CH}$ couplings. Most notably, an N/ROE correlation trace between H3-H5-H9-H11''-H12'' place these protons below the ring plane while the trace between H24-H25-H11'-H12'-H26 place these above the ring plane. The key correlations are displayed in Fig.4.1.4 c. A previous study on podioda-7,17,21-triene and podioda-8,17,21-triene tricyclic triterpenes showed the 14 (C-H) bond was drawn as a wavy line since the configuration of the substituent was unknown [198]. Configuration at the C-14 stereocenter could not be unambiguously determined from the N/ROE correlations without a full conformational analysis because of relatively free rotation about the C-13-C-14 bond.

In order to relate the measured VCD spectra to the structure, theoretical VCD spectra were simulated computationally. The theoretical modelling focused on the tricyclic system supposedly dominating in VCD spectrum, because a full conformer analysis (> 10^{6} possible conformers) was not possible with available computational means. A reduced ensemble of 27 conformers was generated by 120° rotations around the C-13-C-14, C-4-C-23 and C-3-O-3 bonds only, and relative conformer energies were obtained for both the *R* and *S* C-14 isomers. The molecular tail (C-14-C-30) was kept in the extended conformation and its contribution to VCD was not considered. The equilibrium geometries and spectral properties were calculated using the Gaussian software [199] and the B3LYP/6-311++G**/PCM($CHCl_3$) level of theory, relative enthalpies were used for property averaging. The simulation reproduced some spectral features observed experimentally (Figure 4.1.5), although the theoretical *R* and *S* VCD sign patterns of **113** are similar. The 1150-1000 cm^{-1} and other spectral region is however predicted to

be not significantly different for the R and S configurations, and comparison of the calculated for R and S configuration with experimental VCD signs no clear cut on the relative intensities for this region though it seems the experimental on C-14 comparably to the strength of the S configuration. Experimental wavenumbers are denoted in black and selected bands are assigned identifiers denoted in red. Positive experimental bands are traced with red lines and negative experimental bands are traced with blue lines.

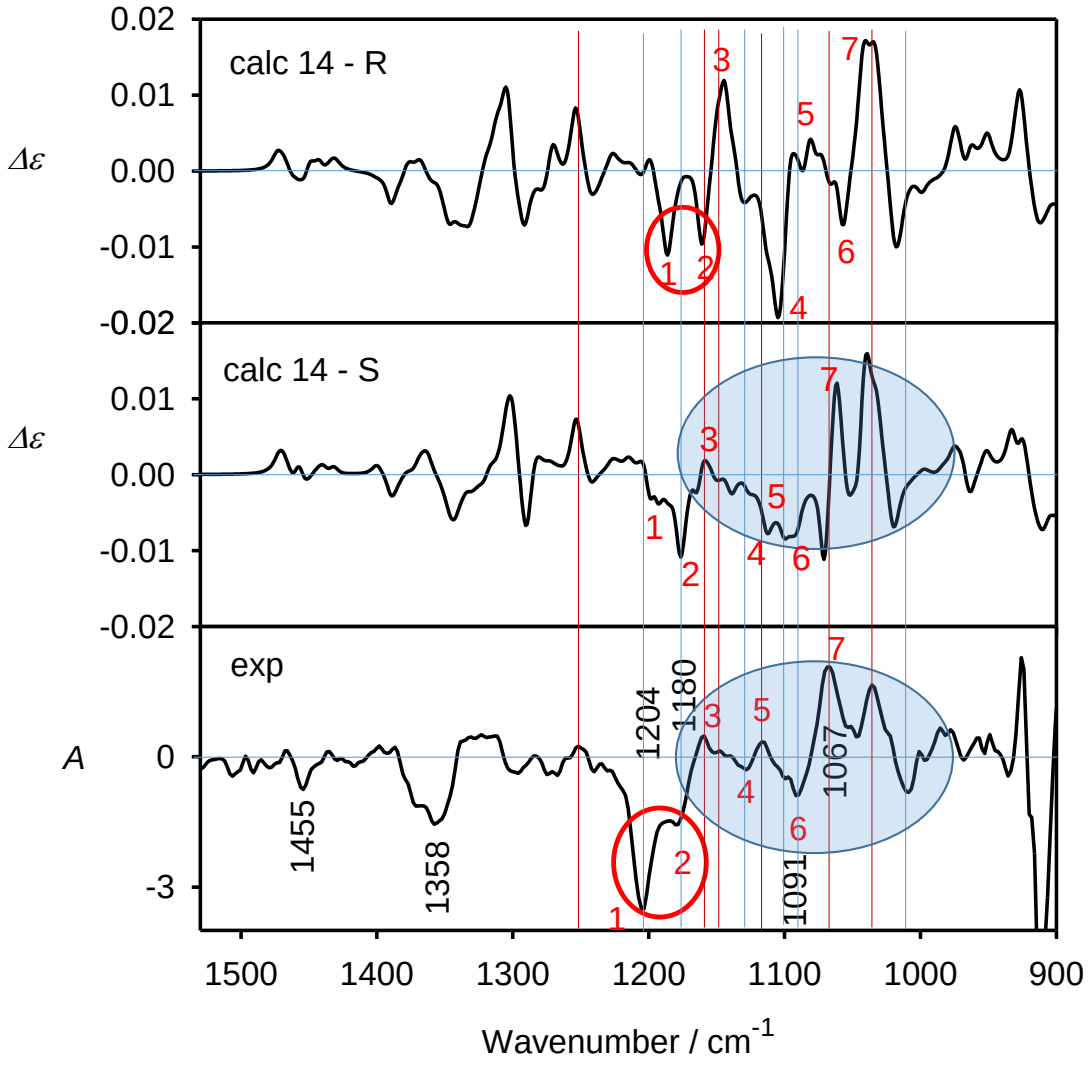

Figure 4.1. 5 VCD spectra calculated for the *R* and *S* C-14 isomers (upper and middle panels, frequency scaled by 0.967) and the experiment (lower panel) of **113**.

For a more detailed NMR data analysis of distances and coupling constants localized near the C-14, only the three Boltzmann averaged rotamers around the C-13/C-14 bond were used. The H-

14 proton is preferentially pointing towards the edge of the ring system (and H-7) in both the *R*- and the *S* C-14 configurations (Table 4.1.9). This was problematic for using the otherwise very informative $^{3}J_{CH}$ couplings originating from the only proton (H-14) directly attached to the rotating C-13/C-14 bond since the dihedral angles formed between the H-14/C-14 vector and the C-13/C-8, C-12, C-26 vectors will be very similar for *R*- and *S*. The predicted differences between the two configurations were smaller than 0.5 Hz. The experimental couplings (Table 4.1.10) are in agreement with the calculated rotamer populations of both configurations. These couplings were very challenging to measure accurately experimentally as the signal of H-14 overlaps with that of H-15s. That made it necessary to use heavily chemical shift filtered selective methods and there is unavoidable phase modulation from J-coupling. Coupling sums were utilized because of significant second order/phase contributions. For all these reasons, the experimental error is estimated to at least 1 Hz.

Table 4.1 9 Calculated C-13-C-14 Angular Distribution (*p*, %), for the C-14 Enantiomers

	R-C-14		S-C-14	
	P	τ (deg)$^{\alpha}$	*P*	τ (deg)$^{\alpha}$
Gauche +	12	71.9	11.1	44.9
Gauche -	87.7	-58.9	11.7	-64.9
Anti	0.3	-164.6	77.2	170.6

[a]∠ C-26-C-13-C-14-C-27, torsion angle between the two methyl groups as obtained for the optimized DFT geometries.

Table 4.1 10 Calculated and Experimental $^{3}J_{CH}$ Scalar Couplings for the C-14 Enantiomers

	Population	$^{3}J_{C8H14}$	J_{C12H14}	J_{C26H14}	Configuration
Gauche +	12	0.68	2.12	4.56	R
Gauche -	87.7	0.98	4.6	2.11	
Anti	0.3	4.79	0.82	3.29	
Averaged		**0.96**	**4.38**	**2.32**	
Gauche +	11.1	5.2	3.16	0.87	S
Gauche -	11.7	1.44	1.64	4.41	
Anti	77.2	0.68	4.4	2.55	
Averaged		**1.23**	**3.98**	**2.57**	
Experimental		**0.8**	**5.3**	**3.7**	

[a]∠ C-26-C-13-C-14-C-27, torsion angle between the two methyl groups as obtained for the optimized DFT geometries.

Furthermore, the possibility to determine the relative configuration from NOE buildup rates involving the C-27 methyl group were investigated. The C-27 methyl group is predicted to be predominantly *anti* to the C-26 methyl in the *S*-configuration and *gauche* to the C-26 methyl in the *R*-configuration. NOE buildups are intrinsically difficult to quantify for flexible molecules due to the fact that they depend on the distance as r^{-6}. A scarcely populated rotamer can contribute significantly to the observed NOE if the two protons are positioned very close to each other. The measured NOEs around and across the C-13/C-14 bond (**Appendix Viii**) are not conclusive alone as both theoretical configurations result in r^2 values in the order of 0.7. However, the most important NOE between H-26 and H-27 that is expected to be the most sensitive to the C-14 configuration indicates the *S*-configuration. The weighted experimental NOE was determined to **η = 0.0054** (corresponding to r = 2.9 Å), *i.e.*, closer to the value predicted for the *S*-model (**η = 0.0032,** r = 3.2 Å), than that predicted for the *R*-model (**η=0.0144,** r = 2.5 Å).

Anisotropic NMR parameters has emerged as powerful tools in structural elucidation [200, 201]. Residual dipolar coupling (RDC) depend on the relative orientation of the ^{13}C-^{1}H bond vectors, while residual chemical shift anisotropy (RCSA) depend on the relative orientations of the carbon chemical shielding tensors. When combined, they can provide the configuration of stereogenic centers that are difficult to establish by traditional methods. A method described by Liu *et al* [200] utilizing poly(γ-benzyl-L-glutamate) (PBLG) to form a liquid crystal that induces anisotropy in chloroform-d_1 was employed in the present study. ^{13}C residual chemical shifts were referenced to TMS, and combined with RDC data from HSQC-IPAP spectra (**Figure 4.1.6**, **Appendix E, Figures E15-E17**). In the comparison of the experimental and theoretical anisotropic parameters for the commafric A (**113**) the *S*-model provided lower quality factors (Q = 0.19) than the *R*-model (Q = 0.33, Figure 4.1.10). showing the best agreement between experimental and theoretical data for the S configuration. Based on the anisotropic parameters, together with the VCD and NOE data, we conclude that with very high probability the C-14 center of commafric A (**113**) is in the ***S*** configuration.

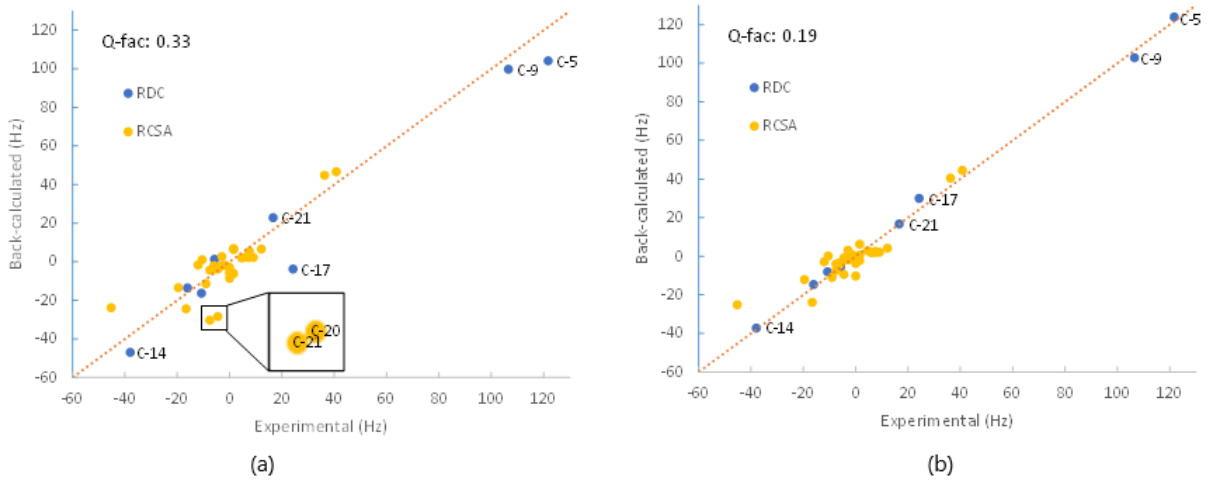

Figure 4.1. 6 Stereochemical differentiation between the (a) *R*- and (b) *S* configurations of C-14 in commafric A (**113**) using RDC and RCSA data collected in PBLG.

4.1.2.3 Isolation and Characterization of Compound 114 (Commafric B)

Commafric B (**114**) was obtained as a colourless powder and LC chromatogram displayed a single major peak with peak area percent of 100% at retention time of 3.51 with diode array detector (**Appendix F, Figure F1**). The molecular formula was determined to be $C_{30}H_{48}O_3$ with seven degrees of unsaturation as determined by low resolution mass spectrometry LR-ESI-MS at *m/z* 455.36 $[M-H]^-$ (calcd for $C_{30}H_{47}O_3$, 455.35) from the negative ion mode with the highest in intensity (**Appendix F, Figure F2**). In this mode the peak at m/z 911.70 corresponds to deprotonated dimerized parent molecule $[2M-H]^+$ (calcd for $2[C_{30}H_{47}O_3]$, 911.71) (**Appendix F, Figure F2**). Examination of the mass spectrum of commafric B in negative mode showed that the most stable ion is the deprotonation of the parent molecule, which is represented by the base peak; the intensity of this peak might also suggest that the loss of proton is the most stable one. Its IR spectrum (**Appendix F, Figure F3**) exhibited a characteristic weak and broad absorption band for hydroxyl (3378.41cm^{-1}) functional group which was strengthened by the absorption at 1073.10 cm^{-1} by the C-O group. The sharp peak at 1698.58 cm^{-1} was typical for C=O and indicated that the molecule contains a carboxyl carbonyl functional group. The absorption band at 2930.95 cm^{-1} is the CH stretching of the CH_3 and 2867.9 cm^{-1} for the CH stretching of CH_2 which is amplified by absorption in the absorption band at 1447.8 cm^{-1} is the CH bending of the CH_2 group and the absorption at 1378.6 cm^{-1} which is the CH bending of the CH_3 group.

The ^{1}H NMR data (**Table 4.1.11**, **Appendix F, Figure F4**) of compound **127** indicated presence of three olefinic protons at δ_H 5.17 (d, *J* = 3.6 Hz, 1H), 5.12 (m, 1H), 5.10 (d, *J* = 1.1 Hz, 1H), one oxymethine protons at δ_H 4.05 (dd, *J* = 11.5, 3.9 Hz, 1H). Unlike commifaric A, there is no diastereotopic proton signal observed, which indicates the absence of hydroxymethylene protons. The ^{1}H NMR ($CDCl_3$) and ^{13}C NMR (**Table 4.1.11**, **Appendix F, Figure F5**) spectra of commafric B (**114**), which were assigned by DEPT-135 NMR (Table 4.1.11, **Appendix F, Figure F6**) experiments, showed seven methyl signals at δ 0.74, 0.85, 0.89, 1.22, 1.58, 1.60 and 1.68. Among these, signals at δ 1.58, 1.60 and 1.68 showed distinct chemical shifts with three olefinic methyl signals. The signal of the methyl proton at δ_H 1.22 which appeared deshielded (downfield) indicated that this methyl group is geminal to a carboxyl function (3H, s, H-24). A doublet integrated for three proton observed at δ 0.85 attached to an sp^3 methine carbon (H-27) (3H, d, *J* = 6.7 Hz, H-27). The shielded signals of methyl protons at δ 0.74 and 0.89 corresponds to (3H, s, H-25) and (3H, s, H-26) respectively. The signal at δ 0.89 relatively deshilded due to its proximity towards a ring "C" of the tricyclic triterpene that contains the olefinic proton (H-7) (Table 4.1.11, **Appendix F, Figure F4**).

The ^{13}C NMR spectroscopic data with the aid of a DEPT-135 experiment (Table 4.1.11, **Appendix F, Figure F5 and F6**), displayed thirty carbon signals, including seven methyl carbons, none methylene carbons, seven methine carbons (one oxygenated) and seven quaternary carbons, three double bonds, one carboxyl carbon. The ^{13}C NMR spectrum revealed the presence of three tertiary-quaternary substituted double bonds at δ 114.1, 150.0 and 124.5, 131.2, as well as 124.5, 131.2 ppm, where the last two olefinic carbon signals are characteristics of double bonds at the exocyclic hydrocarbon side chains. The double bond carbon signal at δ 114.1, 150.0 refers to an endocyclic olefinic carbon positioned to C-7 and C-8 of ring B. From DEPT-135 signals at δ 150.0, 124.9, 131.2 pm are for quaternary carbons. The skeleton pf compound **114** was related to the known tricyclic triterpene podioda-7,17,21-triene (**115**), but modified by the presence of a carboxylic acid moiety in the A ring. A migration of the methyl group from C-8 to C-13 results in podioda-7,17,21-triene (**115**), which was first reported by Arai et al [202] from the fern *Polypodiodes niponica*. The relative stereochemistry at C-3 and C-4 was determined by comparing data obtained from literature and commafric A (**113)**. The two novel compounds

differ significantly in their side chain terminal functionality. Polypodane triterpenoids from this genus are only discovered in the species of *C. mukul* [75, 91].

Table 4.1 11 ^{1}H, ^{13}C NMR and DEPT-135 spectral data of compound B (**114**)

#C	Commafric B		Commafric A		δ_H of malabrica 7, 17,21 triene (Lit.)
	δ_H (multi, J in Hz)	δ_c, Type	δ_H (multi, J in Hz)	δ_c, Type	
1		37.6, CH_2	1.72 / 1.32	38.1	1.21 /1.67
2		26.8, CH_2	1.67	27.3	1.62 /1.58
3	4.05 (dd, J = 11.5, 3.9 Hz, 1H)	75.8, CH	4.02 (dd, J=11.2, 4.7)	76.2	3.254,dt,10.8,5.4
4		52.6, C	-	52.9	-
5		45.9, CH	1.88	46.6	1.19
6		25.4, CH_2	2.05 /1.80	25.8	2.13 / 1.95
7	5.18 (d, J = 3.6 Hz, 1H)	114.1, CH	5.16 (dt, J=5.1, 2.6)	114	5.220, dt, 4.4, 2.8
8		150.0, C	-	151	-
9		57.9, CH	2.01	59.5	1.94
10		33.8, C	-	34.1	-
11		22.5, CH_2	1.25 / 1.53	23.1	1.51 /1.17
12		32.3, CH_2	1.25 /1.48	33	1.56 / 1.17
13		48.1, C	-	48.3	-
14		40.4, CH	1.36	41.2	1.39
15		34.1, CH_2	1.34) / 1.00	33	1.54,0.95
16		26.9, CH_2	2.02 / 1.87	26.6	
17	5.12 (m, 1H)	124.9, CH	5.04 (ddq, J=7.5, 6.3, 1.3)	125	5.12
18		134.9, C	-	135	-
19		39.7, CH_2	1.96 / 1.93	40	1.98
20		26.8, CH_2	2.14 / 2.09	26.7	2.06
21	5.10 (d, J = 1.1 Hz, 1H).	124.5, CH	5.30 (t, J=7.0)	129	5.1
22		131.2, C	-	134	-
23		182.6, C	-	181	0.997 s
24	1.22 (s)	10.4, CH_3	1.18 (s)	10.7	0.876 s
25	0.74 (s)	13.8, CH_3	0.75 (s)	14.1	0.707 s
26	0.89 (s)	25.7, CH_3	0.91 (s)	26.8	0.927
27	0.85 (d, J = 6.7 Hz)	14.8, CH_3	0.86 (d, J=6.8 Hz)	15.1	0.808 d, 6.7 Hz
28	1.60 (s)	15.9, CH_3	1.57 (s)	16.4	1.604, br s
29	1.68 (s)	25.4, CH_3	1.77 (s)	21.4	1.684, br s
30	1.58 (s)	17.7, CH_3	4.07 (d, J=11.7)/4.17 (d, J=11.7)	61.5	1.604, br s

4.2 GC-MS analysis of essential oils and solvent fractions of *Commiphora* species

The relative amount and identity of constituents of *commiphora* resin essential oils was performed by comparing the retention indices from published data and by comparing the mass spectra of the compounds with those in the database of NIST11 and literature data.

4.2.1 GC-MS analysis of *C. habessinica* resin essential oil

The air dried resin of *C. habessinica* (36 g) was subjected to hydrodistillation to give oil in 2.08% (w/w) yield (0.75 g). GC-MS chromatogram of the essential oil is shown in Figure 4.2.1. A total of 30 constituents were identified, representing 87.2 % of the total peak area. The retention time, identity of the compound, molecular formula, experimental retention indices (RI) relative to C_8-C_{20} and C_7-C_{40} n-alkanes (RI), and peak area percentages are listed in Table 4.2.1. The essential oil of *C. habessinica* was dominated by high content of aliphatic hydrocarbons (70.8%) among which pentadecane (11.11%), hexadecane (14.08%) and heptadecane (5.01%) were found to be the main components. It also comprised of oxygenated monoterpenes (13.1%); where D-verbenone (**116**) (5.24%), terpinen-4-ol (**117**) (3.325%), and α-terpineol (**73**) (3.203%) were found to be major components. Whereas, α-pinene, p-cymen-8-ol, trans-pinocarveol, 2-bornanone found in trace amount (< 1 %). These results were quite different to *C. habesseinca* resin essential oil originated from Yemen that contains sesquiterpene hydrocacrbons β-elemene (**79**) (32.1%) and α-selinene (**118**) (18.9%) as major ones [203]. The reported chemical composition of the essential oils of several *Commiphora* species was characterized mainly by aliphatic hydrocarbons, oxygenated and hydrocarbon mono and sesquiterpenes, which invariably differ from species to species and geographical location [16, 204-209].

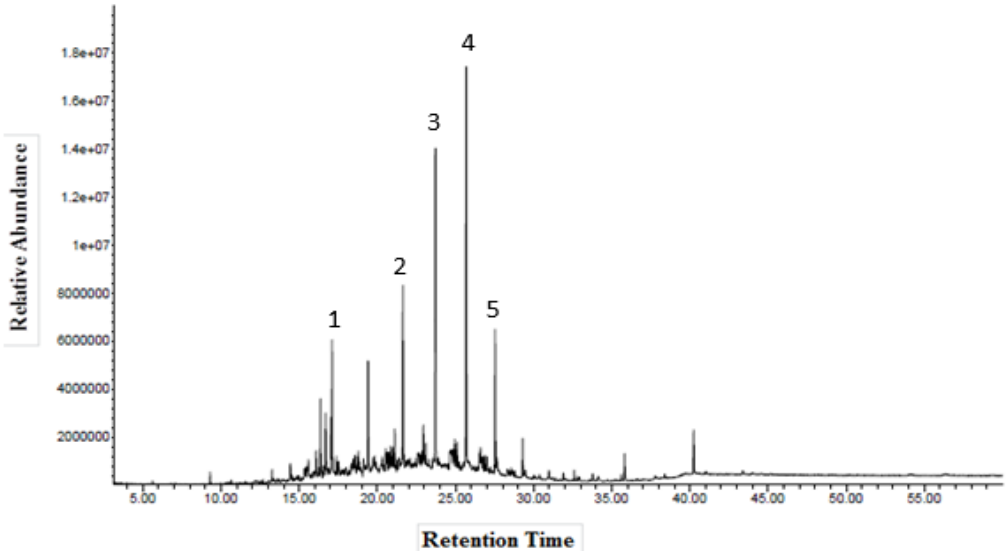

Figure 4.2. 1 GC of the hydro-distillate of *C. habessinica*

GC of the hydrodistillate of *C. habessinica***,** 1**:** Verbenone (5.2%) (**116**), 2: Tetradecane (6.4%)**, 3:** Pentadecane (11.1%) **4:** Hexadecane (14.1%) **5:** Heptadecane (5.0%)**.**

Table 4.2. 1 The composition of the essential oils of the resins of *C. habessinica* by GC-MS on a non-polar column

RI (Cal)	RI (lit)	Compounds	M.Wt	M.F.	RT	Peak Area (%)
		Monoterpenes				**13.6**
		Monoterpenes hydrocarbons				**0.4**
932	932	α-Pinene	136.1	$C_{10}H_{16}$	9.3	0.4
		Oxygenated monoterpenes				**13.1**
1132	1135	Cis-Pinocarveol	152.2	$C_{10}H_{16}O$	15.3	0.7
1134	1141	Camphor	152.1	$C_{10}H_{16}O$	15.4	0.6
1170	1174	Terpinen-4-ol	154.1	$C_{10}H_{18}O$	16.4	3.3
1185	1186	α-terpineol	154.1	$C_{10}H_{18}O$	16.7	3.2
1200	1204	**Verbenone**	150.1	$C_{10}H_{14}O$	17.1	**5.2**
		Aliphatic hydrocarbons				**70.8**
1055	-	Undecane, 5,7-dimethyl-	184.2	$C_{13}H_{28}$	13.3	0.4
1096	1101	Undecane	156.2	$C_{11}H_{24}$	14.4	0.4
1196	1200	Dodecane	170.2	$C_{12}H_{16}$	17.0	2.2
1210	-	Undecane, 2,6-dimethyl-	184.2	$C_{13}H_{28}$	17.4	1.0
1255	-	Decane, 2,3,4-trimethyl-	184.2	$C_{11}H_{14}$	18.5	1.0
1260	-	Dodecane, 2-methyl-	184.2	$C_{13}H_{28}$	18.6	1.5
1283	-	6-Methyltetralin	146.1	$C_{11}H_{14}$	19.1	0.6
1295	1300	Tridecane	184.2	$C_{13}H_{28}$	19.4	3.8
1309	-	1,4-Dimethyltetralin	160.1	$C_{12}H_{16}$	19.7	0.8
1313	-	Undecane, 2-methyl-	170.2	$C_{12}H_{26}$	19.8	0.7

1346	-	Dodecane, 2,5-dimethyl-	198.2	$C_{14}H_{30}$	20.6	0.9
1372	-	Dodecane, 2,6,10-trimethyl-	212.2	$C_{15}H_{32}$	21.1	1.7
1379	-	2-Methyl-Z-4-tetradecene	210.2	$C_{15}H_{30}$	21.3	0.5
1383	-	5,6-Dimethyltetralin	160.1	$C_{12}H_{16}$	21.4	1.0
1395	1412	**Tetradecane**	198.2	$C_{14}H_{30}$	21.6	**6.4**
1399	-	Decane, 3,8-dimethyl-	170.2	$C_{12}H_{26}$	21.7	0.7
1441	-	Cyclododecane, ethyl-	196.2	$C_{14}H_{28}$	22.6	0.6
1443	-	Cyclotetradecane	196.2	$C_{14}H_{28}$	22.6	0.4
1453	-	Tetradecane, 4-methyl-	212.3	$C_{15}H_{32}$	22.9	0.5
1458	-	10-Methylnonadecane	436.5	$C_{31}H_{64}$	22.9	2.2
1465	-	Tetradecane, 3-methyl-	212.2	$C_{15}H_{32}$	23.1	0.7
1487	-	Cyclopentadecane	210.2	$C_{15}H_{30}$	23.6	0.2
1495	1500	**Pentadecane**	212.2	$C_{15}H_{32}$	23.7	**11.1**
1541	-	Pentadecane, 7-methyl-	226.3	$C_{16}H_{34}$	24.6	0.7
1545	-	Decane, 4-cyclohexyl-	224.2	$C_{16}H_{32}$	24.7	1.1
1547	-	2-methyltetracosane	352.4	$C_{25}H_{52}$	24.7	1.1
1553	-	Pentadecane, 4-methyl-	226.3	$C_{16}H_{34}$	24.9	0.8
1558	-	Pentadecane, 2-methyl-	226.3	$C_{16}H_{34}$	25.0	1.5
1565	-	Pentadecane, 3-methyl-	226.3	$C_{16}H_{34}$	25.1	1.0
1594	1600	**Hexadecane**	226.3	$C_{16}H_{34}$	25.7	**14.1**
1639	-	Hexadecane, 7,9-dimethyl-	254.3	$C_{18}H_{38}$	26.5	0.6
1643	-	Pentadecane, 2,6,10-trimethyl-	254.3	$C_{21}H_{44}$	26.6	1.4
1648	-	Cyclopentane, undecyl-	224.3	$C_{16}H_{32}$	26.7	0.5
1652	-	Hexadecane, 4-methyl-	240.3	$C_{17}H_{36}$	26.8	0.5
1658	-	Hexadecane, 2-methyl-	240.3	$C_{17}H_{36}$	26.9	0.5
1665	-	Hexadecane, 3-methyl-	240.3	$C_{17}H_{36}$	27.0	0.5
1694	1700	**Heptadecane**	240.3	$C_{17}H_{36}$	27.5	**5.0**
1700	-	Pentadecane, 2,6,10,14-tetramethyl-	268.3	$C_{19}H_{40}$	27.6	0.7
1793	1800	Octadecane	254.3	$C_{18}H_{38}$	29.3	1.3
1992	2000	Eicosane	282.3	$C_{20}H_{42}$	32.6	0.4
		Others				**2.8**
1140	-	1,3-Cycloheptadiene	94.1	C_7H_{10}	15.6	1.0
1266	-	1-Iodo-2-methylundecane	296.1	$C_{12}H_{16}$	18.7	0.9
1269	-	Oxalic acid, decyl 2-ethylhexyl ester	342.3	$C_{20}H_{38}O_4$	18.8	0.9
				Total identified		**87.2%**

Where, M. Wt = Molecular weight and M.F = Molecular Formula

4.2.2 GC-MS analysis of *C. africana* resin essential oil

The yield of essential oil from the resin of *C. africana* was 0.93 % (w/w). Its GC-MS analysis led to the identification of 27 compounds, representing 96.3 % of the total peak area. The retention time, compound identity, molecular formula, retention indices (RI) relative to C_8-C_{20} n-

alkanes (RI), and peak percentages are listed in Table 4.2.2. As shown in (Table 4.2.2 and Fig. 4.2.2), the essential oil of *C. africana* was dominated by high content of hydrocarbon monoterpenes (46.3%) and oxygenated monoterpene (49.1%), among which α-pinene (**70**) (29.1%), β-pinene (**90**) (6.2%), β-thujene (**91**) (4.8%) from hydrocarbon monoterpenes and trans-verbenol (**119**) (12.7%), verbenone (**116**) (12.1%), terpinen-4-ol (**117**) (3.8%) (Figure 4.2.2) from oxygenated monoterpenes were identified and to be the major components. Furthermore, other specific constituents that were important markers of the resin β-thugene (**91**), p-cymene, camphene (**93**), terpinenin-4-o1 and verbenone (**112**) (Figure 4.2.2) were identified in our study. In a previous study by Provan, et al [206], of the essential oil of the resin of *C. africana* grown in arid parts of northern Kenya obtained by steam distillation was found to contain α-pinene (**70**) as major constituent. Whereas, a study on the essential oil of *C. africana* obtained from Saudi Arabia demonstrated significant variation in its constituents compared to our study and Kenyan origin with 1,4-methanoazulene, decahydro-4,8,8-trimethyl-9-methylene-, [1S-(1a,3aa,4a,8aa)]- (**120**) (31.83%) and cyclopropane, octyl (**121**) (20.95%) predominates as major components.

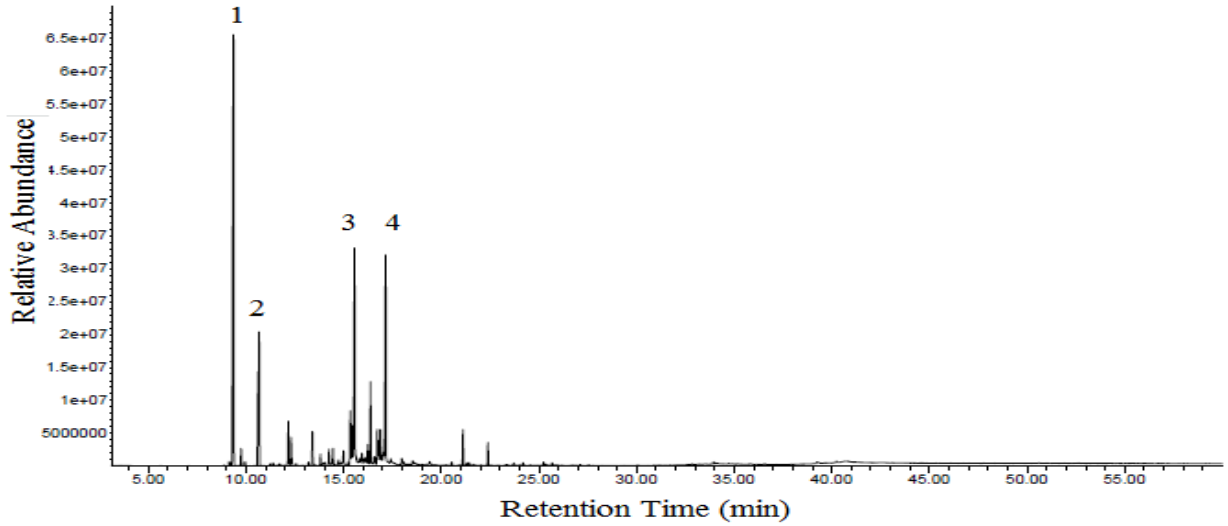

Figure 4.2. 2 GC profile of the hydro-distillate of the resin of *C. africana*

Table 4.2. 2 Chemical composition (peak area percentage) of the essential oil of *C. africana* resin

No	RI (Cal)	RI (lit)	Compounds	M.Wt	M.F	RT	Peak Area (%)
			Monoterpenes				**91.6**
			Monoterpenes hydrocarbons				**45.4**
1	925	926	α–Thujene	136.1	$C_{10}H_{16}$	9.13	0.2
2	932	932	**α-Pinene**	136.1	$C_{10}H_{16}$	9.35	**29.1**
3	945	946	Camphene	136.1	$C_{10}H_{16}$	9.75	0.9
4	951	957	Dehydrosabinene	134.1	$C_{10}H_{14}$	9.95	0.2
5	971	968	β-Thujene	136.1	$C_{10}H_{16}$	10.6	4.8
6	973	974	β-Pinene	136.1	$C_{10}H_{16}$	10.7	6.2
7	1019	1020	*p*-Cymene	138.1	$C_{10}H18$	11.4	2.2
8	1024	1024	D-Limonene	134.1	$C_{10}H_{14}$	12.2	1.6
9	1056	1054	γ-Terpinene	136.1	$C_{10}H_{16}$	12.3	0.2
			Oxygenated monoterpenes	136.1	$C_{10}H_{16}$	13.2	**46.2**
10	1060	1159	*p*-Menth-8-en-1-ol	154.1	$C_{10}H_{18}O$	13.4	1.6
11	1091	1140	trans-2-Menthenol	154.1	$C_{10}H_{18}O$	14.3	0.9
11	1117	1122	α-Campholenal	152.1	$C_{10}H_{16}O$	15	0.9
12	1132	1135	Cis-Pinocarveol	152.1	$C_{10}H_{16}O$	15.3	2.7
12	1134	1141	Camphor	152.1	$C_{10}H_{16}O$	15.4	2.3
13	1138	1140	***trans*-Verbenol**	152.1	$C_{10}H_{16}O$	15.6	**12.7**
13	1141	1137	*cis*-Verbenol	152.1	$C_{10}H_{16}O$	15.6	0.8
14	1153	1158	D-Pinocamphone	152.1	$C_{10}H_{16}O$	15.9	0.3
14	1155	1160	Pinocarvone	150.1	$C_{10}H_{14}O$	15.9	0.5
15	1165	1158	*trans*-3-Pinanone	152.1	$C_{10}H_{16}O$	16.2	1
15	1170	1174	Terpinen-4-ol	154.1	$C_{10}H_{18}O$	16.4	3.8
16	1178	1179	*p*-Cymen-8-ol	150.1	$C_{10}H_{14}O$	16.6	0.5
16	1185	1186	α-terpineol	154.1	$C_{10}H_{18}O$	16.7	1.8
17	1186	1182	Myrtenal	150.1	$C_{10}H_{14}O$	16.8	1.1
17	1190	1194	Myrtenol	150.1	$C_{10}H_{14}O$	16.9	2.2
18	1200	1204	**Verbenone**	150.1	$C_{10}H_{14}O$	17.2	**12.1**
18	1212	1215	trans-Carveol	150.1	$C_{10}H_{16}O$	17.4	0.4
19	1237	1239	D-Carvone	150.1	$C_{10}H_{14}O$	18	0.3
19	1295	1289	Thymol	150.1	$C_{10}H_{14}O$	19.4	0.3
			Sesquiterpenes				**3**
			Sesquiterpene hydrocarbons				**2.9**
20	1345	1350	α-Longpinene	204.2	$C_{15}H_{24}$	20.5	0.2
21	1370	1374	**α-Copaene**	204.2	$C_{15}H_{24}$	21.1	**1.6**
22	1426	1432	*trans*-α-Bergamotene	204.2	$C_{15}H_{24}$	22.4	1.0
23	1518	1537	α-Cadinene	204.2	$C_{15}H_{24}$	24.2	0.1
			Oxygenated sesquiterpene				**0.1**
24	1572	1577	Spathulenol	220.2	$C_{15}H_{24}O$	25.2	0.1
			Others				**1.7**
25	1156	-	6-Methyl-3,5-heptadiene-2-one	124.1	$C_8H_{12}O$	16	0.2
26	1159	-	1,3-Cyclopentadiene, 5,5-dimethyl-				0.7
27	1196	-	Cyclohexanol, 2-methylene-6-methyl-	126.1	$C_8H_{14}O$	17	0.8
					Total identified		**96.3**

RI_{Calc}.= based on HP 5MS capillary column (non-polar column) and alkane standards (C_8-C_{20} and C_7-C_{40}) according Vanden Dool and Kratz (1963) [166]. RI_{Lit}.= based on Adams (2007) and V. I. Babushok (2011) [167, 210].

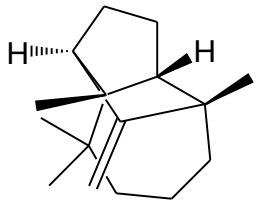

120

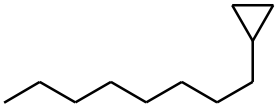

121

α-pinene (**70**) and β-pinene (**90**) are the dominant odorous compounds emitted by trees, shrubs, flowers and grasses [211]. Studies showed that β-pinene (**90**), along with α-pinene (**70**) and other terpenes, are cytotoxic on cancer cells [212]. They represent a great part of essential oils with sedative properties [213]. When α- and β-pinenes are the major constituents of an essential oil, they exhibit the anti-inflammatory and analgesic activity [214]. The essential oil of *C. africana* resin characterized by having large amount of α-pinene (**70**), which is among the top fragrant from the list of common names of fragrance ingredients used in consumer and professional cleaning and laundry products. It seems to be a general trend that essential oils containing monoterpenes and sesquiterpenes have a higher antibacterial [215], and anti-oxidative potential [216].

4.2.3 GC-MS analysis of *C. sphaerocarpa* resin essential oil

Essential oil from 16 g ground resin of *C. sphaerocarpa* was obtained by hydrodistillation for 3h using a Clevenger-type apparatus and the yield was (0.0064g) 0.04% (w/w) essential oil. The oil has intense fragrance. The GC-MS analysis of *C. sphaerocarpa* resin led to the identification of 36 compounds, representing 92.3 % of the total peak area. The retention time, compound name, molecular formula, retention indices (RI) relative to C_8-C_{20} and C_7-C_{40} n-alkanes (RI), and peak percentages are listed in Table 4.2.3. As shown in (Table 4.2.3, Fig. 4.2.3), the essential oil of *C. sphaerocarpa* resin was dominated by high content of hydrocarbon sesquiterpene (78.17%) and oxygenated sesquiterpene (15.89%), among which α-copaene (**80**) (22.71%), β-caryophyllene (**83**) (28.03%) from sesquiterpene hydrocarbons and caryophyllene oxide (**99**) (13.89%) from oxygenated sesquiterpene.

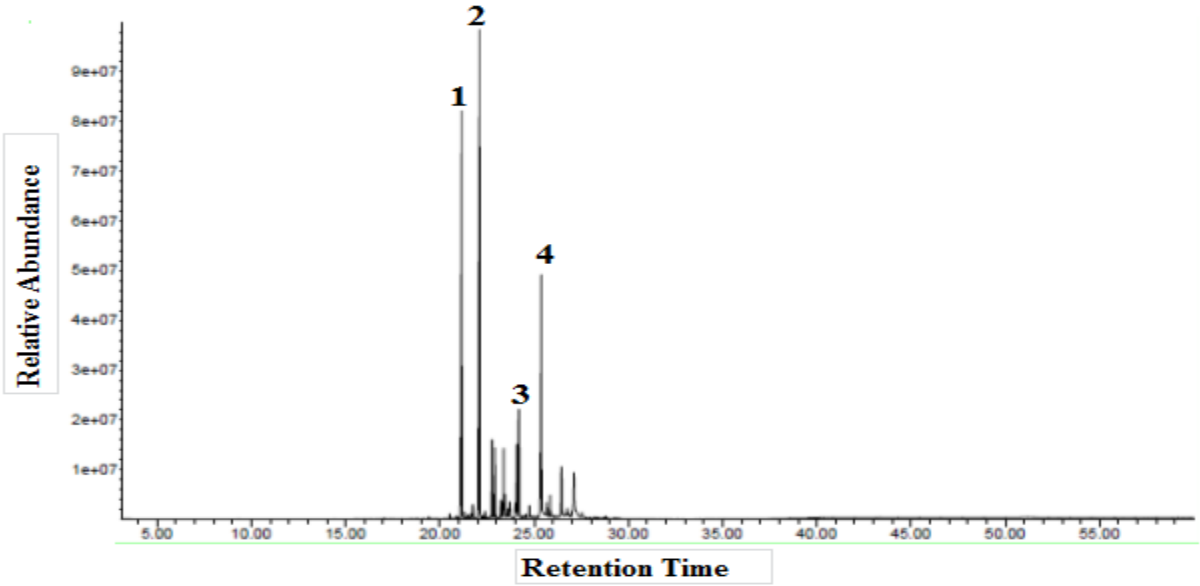

Figure 4.2. 3 GC of hydrodistillate of *C. sphaerocarpa*

Table 4.2. 3 Relative concentration (%) of components of the hydrodistillate of *C. sphaerocarpa* resin

RI (Cal)	RI (lit)	Compounds	M.Wt	M. F.	RT	Peak Area(%)
		Sesquiterpenes				**90.8**
		Sesquiterpene hydrocarbons				**75.5**
1345	1345	α-Cubebene	204.2	$C_{15}H_{24}$	20.5	0.2
1361	1379	β-Patchoulene	204.2	$C_{15}H_{24}$	20.9	0.2
1370	1374	**α-Copaene**	204.2	$C_{15}H_{24}$	21.2	**22.7**
1381	1387	β-Bourbonene	204.2	$C_{15}H_{24}$	21.3	0.3
1387	1389	β-Elemene	204.2	$C_{15}H_{24}$	21.5	0.2
1424	1419	**β-Caryophyllene**	204.2	$C_{15}H_{24}$	22.1	**28.0**
1431	1430	β-Copaene	204.2	$C_{15}H_{24}$	22.3	0.1
1449	1432	α-Bergamotene	204.2	$C_{15}H_{24}$	22.4	0.3
1457	1452	α-Humulene	204.2	$C_{15}H_{24}$	22.8	3.3
1472	1473	Alloaromadendrene	204.2	$C_{15}H_{24}$	22.9	3.0
1479	1478	γ-Muurolene	204.2	$C_{15}H_{24}$	23.2	2.7
1482	1481	4,11-selinadiene	204.2	$C_{15}H_{24}$	23.4	3.0
1489	1489	β-Selinene	204.2	$C_{15}H_{24}$	23.5	1.0
1490	1493	γ –Maaliene	204.2	$C_{15}H_{24}$	23.6	0.3
1495	1491	γ –Selinene	204.2	$C_{15}H_{24}$	23.6	0.4
1509	1500	α-Muurolene	204.2	$C_{15}H_{24}$	23.7	0.8
1513	1483	α-Amorphene	204.2	$C_{15}H_{24}$	24.0	0.7
1518	1520	7-epi-a-selinene	204.2	$C_{15}H_{24}$	24.1	3.1

1527	1522	**δ-Cadinene**	204.2	$C_{15}H_{24}$	24.2	**4.7**
1537	1533	trans-Cadinadiene-1,4	200.2	$C_{15}H_{20}$	24.4	0.1
1547	1544	α-Calacorene	164.2	$C_{12}H_{20}$	24.6	0.2
1635	1621	Epianastrephin	204.2	$C_{15}H_{24}$	26.2	0.2
		Oxygenated sesquiterpene				**15.3**
1589	1582	**Caryophyllene oxide**	220.2	$C_{15}H_{24}O$	25.4	**13.9**
1607	1608	α-Humulene epoxide II	178.2	$C1_5H_{24}O$	25.9	1.0
1653	1652	α-Cadinol	222.4	$C_{15}H_{26}O$	26.7	0.4
		Aliphatic hydrocarbons				**1.3**
1395	1400	Tetradecane	198.2	$C_{14}H_{30}$	21.6	0.2
1594	1600	Hexadecane	138.1	$C_{16}H_{34}$	25.7	0.9
1694	1700	Heptadecane	190.2	$C_{17}H_{36}$	27.5	0.2
		Others				**0.3**
1579	-	1,Z-5,E-7-Dodecatriene	220.2	$C_{15}H_{24}O$	24.7	0.6
1623	-	Benzenepropanoic acid				0.3

4.2.4 GC-MS analysis of *C. schimperi* resin essential oil

The resin (46 g) of *C. schimperi* was hydro-distilled and gave essential oil (0.21%). GC-MS analyses showed that the constituents of the oils of *C. schimperi* are clearly different from the oil of *C. africana* and *C. sphaerocarpa* with a slight similarity on the classes of constituent group of essential oil components of *C. habessinica* such as aliphatic hydrocarbons. It contains partly oxygenated monoterpenes, sesquiterpene and hydrocarbons. The chemical composition and retention indices of the constituents of *C. schimperi* resin EO is presented in (Table 4.2.4, Figure 4.2.4). A total of 44 volatile constituents were identified, representing, 96.55%. The main constituents of *C. schimperi* are a sesquiterpene hydrocarbon δ-Cadinene (**86**) (31.52%), and long chain hydrocarbons classes of secondary metabolites such as hexadecane (11.59%) and pentadecane (8.06%).

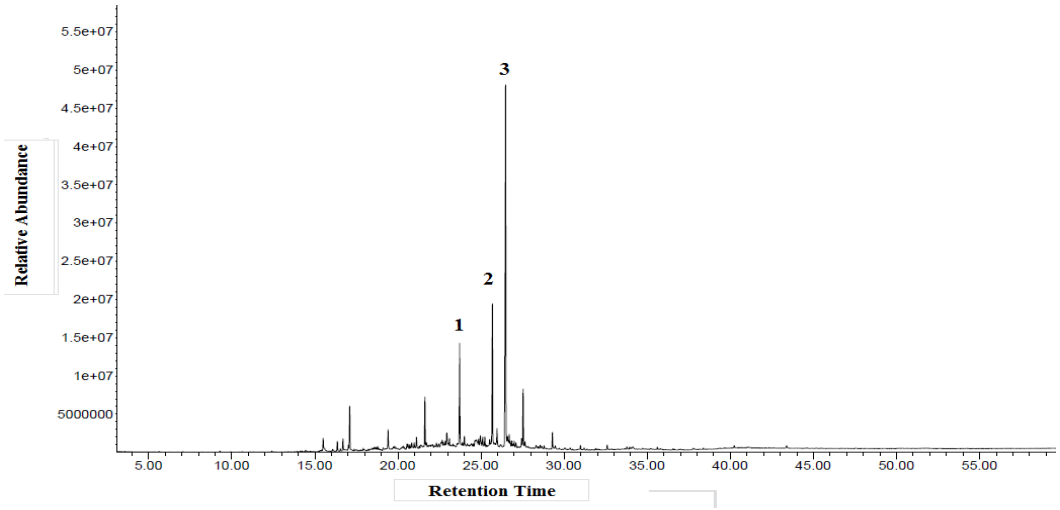

Figure 4.2. 4 GC of hydrodistillate of *C. sphaerocarpa*

Table 4.2. 4 Relative concentration (%) of components of the hydrodistillate of *C. schimperi*

No	RI (Cal)	RI (lit)	Compounds	D (%)	Identification
			Monoterpenes	**5.4**	RI, MS
			Oxygenated monoterpenes	**5.4**	
1	1138	1140	***trans*-Verbenol**	**0.8**	RI, MS
2	1170	1174	Terpinen-4-ol	0.8	RI, MS
3	1185	1186	α-terpineol	0.8	RI, MS
4	1200	1204	**Verbenone**	3.1	RI, MS
			Sesquiterpenes	**38.75**	
			Sesquiterpene hydrocarbons	**36.49**	
5	1509	1513	γ –Cadinene	1.5	RI, MS
6	1509	1500	α-Muurolene	0.8	RI, MS
7	1513	1483	α-Amorphene	0.7	RI, MS
8	1527	1522	**δ-Cadinene**	**31.5**	RI, MS
9	1537	1533	trans-Cadinadiene-1,4	2.0	RI, MS
			Oxygenated sesquiterpene	**2.3**	
10	1572	1577	(-)-Spathulenol	1.1	RI, MS
11	1586	1590	(-)-Globulol	1.2	RI, MS
12	1653	1652	α-Cadinol	1.1	RI, MS
			Aliphatic hydrocarbons	**47.6**	
13	1196	1200	Dodecane	0.7	MS
14	1295	1300	Tridecane	1.4	MS
15	1309	-	1,4-Dimethyltetralin	0.5	MS
16	1328	-	Tridecane, 2-methyl-	0.4	MS
17	1334	-	3,5-Dimethyldodecane	0.7	MS
18	1337	-	Dodecane, 2,6,10-trimethyl-	1.1	MS

19	1346	-	Tetracontane, 3,5,24-trimethyl-	0.4	MS
20	1351	-	Tridecane, 4,8-dimethyl-	0.7	MS
21	1371	-	Cyclododecane, ethyl-	0.7	MS
22	1375	-	Tetradecane, 5-methyl-	0.8	MS
23	1379	-	Dodecane, 2,6,11-trimethyl-	2.4	MS
24	1383	-	5,6-Dimethyltetralin	0.8	MS
25	1395	1412	Tetradecane	3.6	MS
26	1399	-	Decane, 3,8-dimethyl-	0.4	MS
27	1441	-	Cyclododecane, ethyl-	0.7	MS
28	1453	-	Tetradecane, 4-methyl-	0.7	MS
29	1465	-	Tetradecane, 3-methyl-	0.9	MS
30	1487	-	Cyclopentadecane	0.6	MS
31	1495	1500	**Pentadecane**	**8.1**	MS
32	1547	-	Tridecane, 5-methyl-	0.5	MS
33	1553	-	Pentadecane, 4-methyl-	0.8	MS
34	1565	-	Pentadecane, 3-methyl-	1.1	MS
35	1594	1600	**Hexadecane**	**11.6**	MS
36	1639	-	Hexadecane, 7,9-dimethyl-	0.5	MS
37	1658	-	Hexadecane, 2-methyl-	0.6	MS
38	1665	-	Hexadecane, 3-methyl-	0.6	MS
39	1694	1700	**Heptadecane**	**4.1**	MS
40	1752	-	Nonadecane, 4-methyl-	0.2	MS
41	1793	1800	Octadecane	1.1	MS
42	1893	1900	Nonadecane	0.5	MS
43	1992	2000	Eicosane	0.4	MS
			Others	**1.1**	
44	1373	-	1-Octadecanesulphonyl chloride	1.1	MS
			Total identified	**92.9 %**	

4.2.5 GC-MS analysis of *C. habessinica* resin n-hexane fraction

Previously, a study on the mass spectrum of the resin of *C. habessinica* containing 6.5% of steroid fraction using mass spectrum showed the presence of cholest-5-en-3β-ol (cholesterol) (**48)**, Δ5-campestan-3β-ol (**51)** (Campesterol), and Δ5-sitostan-3β-ol (**52**) (β-sitosterol) [105]**.** Analysis of *n*-Hexane fraction obtained from successive partitioning of the crude MeOH extract using GC-MS confirmed the prescence of 18 constituents. The major constituents were found to be a C-27 cholestane sterols: cholesterol (**48**) (33.47%) and lathosterol (**112**) (55.74%) (Figure 4.2.5, Table 4.2.5). Other C-27 sterols with trace amount were 5α-cholestan-6-one (0.93%), 3β-

cholesta-5,20-dien-3-ol (0.61%), lathosterone (1.21%), 3β, 5α-Cholesta-7, 24-dien-3-ol, (1.02%) and Cholesterone (1.99%), progesterone (0.25%) and ergesterol (2.05%). The hexane fraction also contains oxygenated monoterpenes such as *trans*-verbenol (**119**), verbenone (**116**) and hydrocarbon monoterpene α-copaene (**80**) in trace amount (< 0.1%) (Table 4.2.5). Ergosterol (2.05%), cholesterone (1.99%), lathosterone (1.21%), cholestan-6-one, (5α) (0.93%), and progesterone (0.25%) found relatively in a fair amount (> 0.2%). The sum totals of the identified compounds account 95.99% where cholesterol (**48**) and lathosterol (**112**) accounts 89.21%. The two major compounds and a mixture of the two, i.e. cholesterol (**48**) and lathosterol (**112**) and hexadecane were separated by flash column chromatography (FCC) from the chloroform fraction.

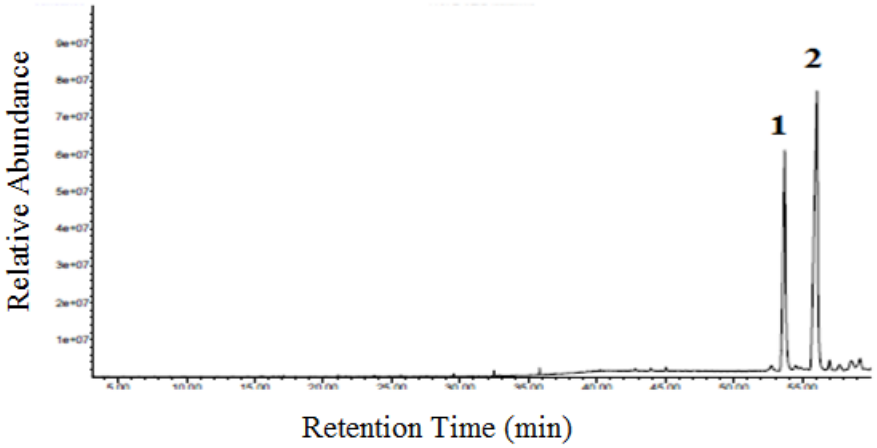

Figure 4.2. 5 GC chromatogram of the n-hexane fraction of *C. habessinica* 1**:** Cholesterol (33.47%) (**48**), 2: Lathosterol **(55.74%) (112).**

Table 4.2. 5 Relative concentration (%) of components of the *n*-hexane fractions of *C. habessinica*

Compound	RT (min)	Mol.F	Mol.Wt.	% Total
trans-Verbenol	15.498	$C_{10}H_{16}O$	152.12	0.05%
Verbenone	17.096	$C_{10}H_{16}O$	150.1	0.04%
α–Copaene	21.102	$C_{15}H_{24}$	204.19	0.05%
Pentadecane	23.708	$C_{15}H_{32}$	212.25	0.03%
Hexadecane	25.67	$C_{16}H_{34}$	226.27	0.06%
Tetradecanal	29.535	$C_{14}H_{28}O$	212.21	0.09%
13-Octadecenal, (Z)-	32.475	$C_{18}H_{34}O$	266.26	0.15%
Hexahydroindole	35.807	$C_8H_{13}N$	123.11	0.23%
Progesterone	45.042	$C_{21}H_{30}O_2$	314.23	0.25%
Cholest-8-en-3-ol, (3β.)-	52.728	$C_{27}H_{46}O$	386.36	1.09%
Cholesterol	53.72	$C_{27}H_{46}O$	386.36	**33.47%**

Cholestan-6-one, (5α)-	54.52	$C_{27}H_{46}O$	386.36	0.93%
Cholesta-5,20-dien-3-ol, (3β)-	54.846	$C_{27}H_{44}O$	384.34	0.61%
Lathosterol	56.081	$C_{27}H_{46}O$	386.36	**55.74%**
Lathosterone	56.984	$C_{27}H_{44}O$	384.34	1.21%
Cholesta-7, 24-dien-3-ol, (3β,5α)	57.718	$C_{27}H_{44}O$	384.34	1.02%
Ergosterol	58.575	$C_{28}H_{44}O$	400.37	2.05%
Cholesterone	59.22	$C_{27}H_{44}O$	384.34	1.99%
		Total identified		99.10%

Epidemiologic and experimental studies suggest that dietary phytosterols may offer protection from the most common cancers in Western societies, such as colon, breast and prostate cancer [217-219]. Therefore, they may play significant roles in the management and prevention of human cancers. The presence of phytosterols in resin extract may be contributing towards antimicrobial and antioxidant activity. They are well known towards their medical, cosmetic, functional food applications and also known for their saturated fat reducing and cholesterol lowering activity; thus they may reduce risk of heart disease [220]. A study by Brieskorn and Noble [119], from hexane extract of *C. abyssinica* (Berg) Engler resin collected from Yemen with the help of column and preparative chromatography resukted in isolation of monoterpenes, sesquiterpenes, furanosesquiterpene and organic acids [59]. However, none of the phytosterols were identified in the present GC-MS analysis of the *n*-hexane fraction appeared as major component with those reported by Brieskorn and Noble. This might be due to differences geographical location, soil type, climate condition etc. The GC-MS profile study indicated that this fraction contained a diversity of sterols, with cholesterol and lathosterol being particularly abundant.

4.2.6 GC-MS analysis of *C. habessinica* resin chloroform fraction

A total of 37 phytochemical constituents were identified when the chloroform soluble portion of methanol extract of *C. habessinica* resin was subjected to GC- MS (Figure 4.2.6, Table 4.2.6). The major components were found to be pentacyclic triterpenes: β-amyrin (**122**) (11.10%), α-amyrin (**56**) (24.13%), 3-epimoretenol (**123**) (22.35%), and lupeol (**124**) (5.40%) appeared at higher retention time, whereas an alkaloid isoquinoine (**125**) was found at a relatively high concentration at low retention time. The fraction also contains 2(1H) naphthalenone,

3,5,6,7,8,8a-hexahydro-4,8a-dimethyl-6-(1-methylethenyl) (3.52%), palmitic acid vinyl ester (2.29%), benzene, 1-(chloromethyl)-2-methyl (1.31%), lathosterol (**112**) (1.04%) and 1,3-cyclopentadiene, 2,3,4,5-tetramethyl-1-(4-pentenyl) (1.04%). Organic acids such as hexadecanoic acid, heptadecanoic acid, cyclohexamine, caprolactam, phenol-2,6-bis(1,1-dimethylethyl)-4, methyl carbamate, 3,7,11,15-tetramethyl-2- hexadecen-1-ol (phytol) found in a relatively small amount. These components with of their retention time, molecular weight, and percentage peak area are illustrated in Fig. 4.2.6 and Table 4.2.6.

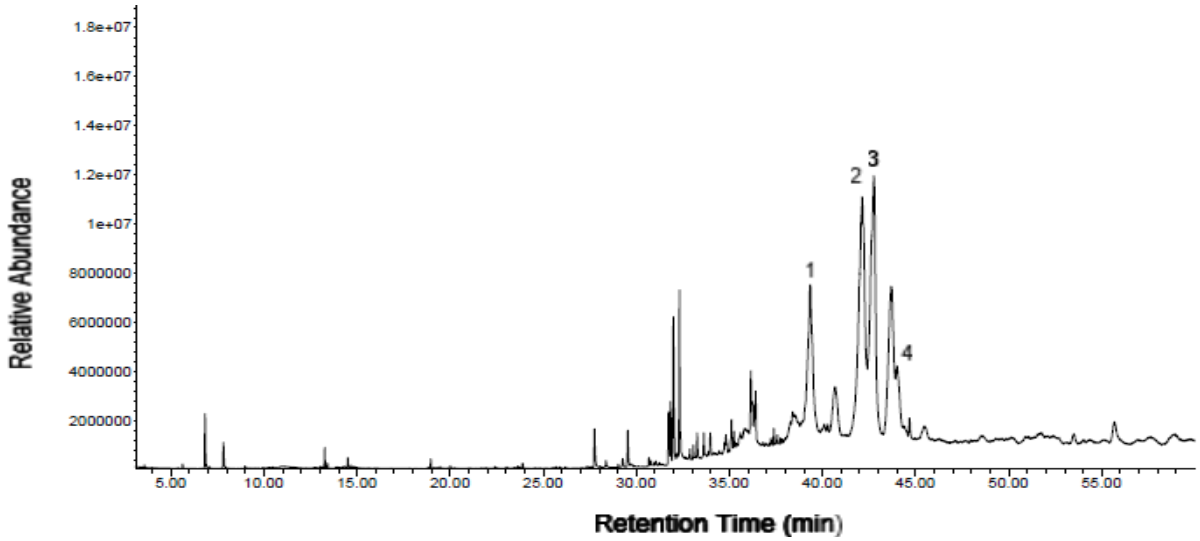

Figure 4.2. 6 GC chromatogram of chloroform fraction of *C. habessinica.*

Hexadecanoic acid, was found in trace amount. This fatty acid was observed to be a potential antimicrobial and antidiarrhoeal activities [221], is reported to cause growth inhibition and apoptosis induction in human gastric cancer cells [222]. Of the major compounds, α-amyrin stimulates proliferation of human keratinocytes but does not protect them against UVB damage [223], a mixture of α and β-amyrin isolated from the resin of *Protium kleinii* and given by intraperitoneal (i.p.) or oral (p.o.) routes, caused dose-related and significant antinociception against the visceral pain in mice produced by i.p. injection of acetic acid [192].

Table 4.2. 6 Relative concentration (%) of components of the chloroform fractions of *C. habessinica*

Compound	RT (min)	M. F	Mol Wt. (amu)	Peak Area %
Ethylbenzene	6.835	C_8H10	106.078	0.65%
Styrene	7.819	C_8H_8	104.063	0.35%
Oxalic acid, 2-ethylhexyl isohexyl ester	13.261	$C_{16}H_{30}O_4$	286.214	0.20%
Decane, 3,6-dimethyl-	14.502	$C_{12}H_{26}$	170.203	0.10%
Pentadecanal-	27.749	$C_{15}H_{30}O$	226.23	0.62%
Heptadecanal	29.54	$C_{17}H_{34}O$	254.261	0.48%
2-[1-(4-Cyano-1,2,3,4-tetrahydronaphthyl)]propanenitrile	31.73	$C_{14}H_{14}N_2$	210.116	0.72%
Quinolinium, 1-ethyl-, iodide	31.834	$C_{12}H_{14}IN$	285.001	0.86%
Isoquinoline	31.99	C_9H_7N	129.058	**2.43%**
Palmitic acid vinyl ester	32.315	$C_{18}H_{34}O_2$	282.256	2.29%
2-Trimethylsilyloxypentadecane	33.065	$C_{18}H_{40}OSi$	300.285	0.16%
3-[1-(4-Cyano-1,2,3,4-tetrahydronaphthyl)]propanenitrile	33.266	$C_{14}H_{14}N_2$	210.116	0.32%
3-[1-(4-Cyano-1,2,3,4-tetrahydronaphthyl)]propanenitrile	33.624	$C_{14}H_{14}N_2$	210.116	0.38%
Palmitic acid vinyl ester	33.969	$C_{18}H_{34}O_2$	282.256	0.29%
Hexadecane	34.737	$C_{16}H_{34}$	226.266	0.17%
Methyl 12-oxo-9-dodecenoate	34.81	$C_{13}H_{22}O_3$	226.157	0.27%
2H-Pyran, 2-(8-dodecynyloxy)tetrahydro-	35.113	$C_{17}H_{30}O_2$	266.225	0.47%
17-Pentatriacontene	35.25	$C_{35}H_{70}$	490.548	0.22%
Octacosanoic acid	35.599	$C_{28}H_{56}O_2$	424.428	0.44%
Benzene, 1-(chloromethyl)-2-methyl-	36.154	C_8H_9Cl	140.039	1.31%
Cyclohexanecarboxylic acid, hexyl ester	36.217	$C_{13}H_{24}O_2$	212.178	0.87%
(2,3-Diphenylcyclopropyl)methyl phenyl sulfoxide, trans-	36.332	$C_{22}H_{20}OS$	332.123	0.61%
Benzeneacetonitrile, .alpha.-methylene-	36.412	C_9H_7N	129.058	0.74%
(2,3-Diphenylcyclopropyl)methyl phenyl sulfoxide, trans-	37.385	$C_{22}H_{20}OS$	332.123	0.21%
Octadecanoic acid	37.574	$C_{18}H_{36}O_2$	284.272	0.17%
13,27-Cycloursan-3-one	38.398	$C_{30}H_{48}O$	424.371	0.31%
Ursa-9(11),12-dien-3-ol	38.489	$C_{30}H_{48}O$	424.371	0.18%
β–amyrin	39.347	$C_{30}H_{50}O$	426.386	**11.10%**
2(1H)Naphthalenone, 3,5,6,7,8,8a-hexahydro-4,8a-dimethyl-6-(1-methylethenyl)-	40.675	$C_{15}H_{22}O$	218.167	3.52%
α–amyrin	42.117	$C_{30}H_{50}O$	426.386	**24.13%**
3-Epimoretenol	42.769	$C_{30}H_{50}O$	426.386	**22.35%**
5(1H)-Azulenone, 2,4,6,7,8,8a-hexahydro-3,8-dimethyl-4-(1-methylethylidene)-, (8S-cis)-	43.679	$C_{15}H_{22}O$	218.167	0.13%
Lupeol	44.011	$C_{30}H_{50}O$	426.386	**5.40%**
Decanedioic acid, bis(2-ethylhexyl) ester	44.675	$C_{26}H_{50}O_4$	426.371	0.49%
1,3-Cyclopentadiene, 2,3,4,5-tetramethyl-1-(4-pentenyl)-	45.476	$C_{14}H_{22}$	190.172	1.04%
Lathosterol	55.678	$C_{27}H_{46}O$	386.355	1.04%
1,4-Bis(6-methylpyridyl-3)butadiene	58.957	$C_{16}H_{12}N_2$	232.1	0.64%
			Total Identified	85.66%

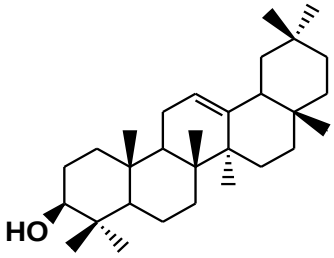

122

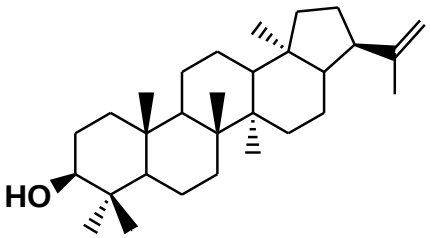

123

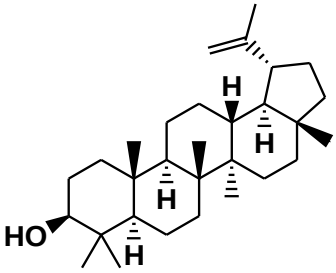

124

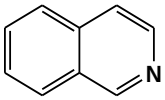

125

Vázquez et al. [188] demonstrated that a mixture of α-amyrin and β-amyrin from various plant exhibited various pharmacological activities *in vitro* and *in vivo* against inflammation, microbial, fungal, viral infections and cancer cells.

4.2.7 GC-MS analysis of *C. africana* resin n-hexane fraction

The chemical composition of the *n*-hexane fraction of *C. africana* resin was analyzed by GC-MS (Table 4.2.7 and Fig. 4.2.7), in which 97.08 % of the total *n*-hexane fraction, was identified based on mass spectra. The major components were oxygenated monoterpenes (53.76%) such as verbenone (**116**) (11.13%) and *trans*-2-caren-4-ol (**126**) (13.23%) followed by hydrocarbon sesquiterpene (16.52%) such as α-copaene (**80**) (7.69%) and α-bergamotene (**127**) (5.34%). The pentacyclic triterpene ursa-9(11),12-dien-3-ol accounts (**128**) (11.26%). All the constituents were identified by comparison of their MS with those in the NIST 11 library and literature data.

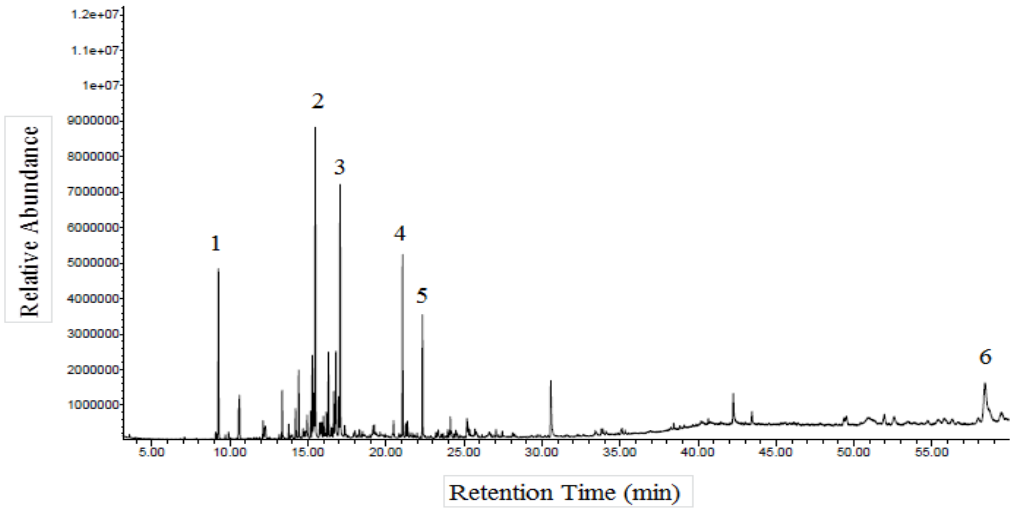

Figure 4.2. 7 GC of *n*-hexane fraction of the resin of *C. africana*

Table 4.2. 7 Phytochemicals identified in *n*-hexane fraction of *C. africana* resin using GC-MS

No	Peak Name	M.Wt	M.F	RT	Peak area%
1	α–pinene	136.125	$C_{10}H_{16}$	9.261	**7.26**
2	β-Pinene	136.125	$C_{10}H_{16}$	10.605	3.21
3	p-Cymene	134.11	$C_{10}H_{14}$	12.128	0.88
4	β-Terpineol	154.136	$C_{10}H_{18}O$	13.346	2.1
5	cis-β-Terpineol	154.136	$C_{10}H_{18}O$	14.205	1.31
6	2,3-Dehydro-1,8-cineole	152.12	$C_{10}H_{16}O$	14.411	2.85
7	Pinocarveol	152.12	$C_{10}H_{16}O$	15.28	3.54
8	Camphor (*1S,4S*)	152.12	$C_{10}H_{16}O$	15.378	2.38
9	*trans*-2-Caren-4-ol	152.12	$C_{10}H_{16}O$	15.464	**13.23**
10	(-)-Borneol	154.136	$C_{10}H_{18}O$	15.996	1.05
11	*cis*-Pinane	152.12	$C_{10}H_{16}O$	16.179	1.05
12	4-Terpineol	154.136	$C_{10}H_{18}O$	16.31	3.7
13	α–terpineol	154.136	$C_{10}H_{18}O$	16.654	1.98
14	Myrtenol	152.12	$C_{10}H_{16}O$	16.791	5.25
15	Isoborneol	154.136	$C_{10}H_{18}O$	16.974	1.6
16	*cis*-Verbenone	150.104	$C_{10}H_{14}O$	17.06	**11.13**
17	α–longipinene	204.188	$C_{15}H_{24}$	20.487	1.12
18	α–copaene	204.188	$C_{15}H_{24}$	21.065	**7.69**
19	β-Cubebene	204.188	$C_{15}H_{24}$	21.369	0.91
20	α–bergamotene	204.188	$C_{15}H_{24}$	22.336	5.34
21	δ–cubebene	204.188	$C_{15}H_{24}$	24.132	1.46
22	Cyclohexadecane	224.25	$C_{16}H_{32}$	30.564	4.05
23	Aromadendrene oxide-(1)	220.183	$C_{15}H_{24}O$	42.26	2.73
24	Ursa-9(11),12-dien-3-ol	424.371	$C_{30}H_{48}O$	58.396	**11.26**
				Tota; identified	**97.08**

GC-MS of the *n*-hexane fraction of *C. africana*, **1**: α-pinene (**70**) (7.26%) (**1**) **2**: trans-2-Caren-4-ol (**126**) (13.23%) **3**: cis-Verbenone (**116**) (11.13%) **4**: α-Copaene (**80**) (7.69%) **5**: α-Bergamotene (**127**) (5.34%) **6**: Ursa-9(11),12-dien-3-ol (**128**) (11.26%).

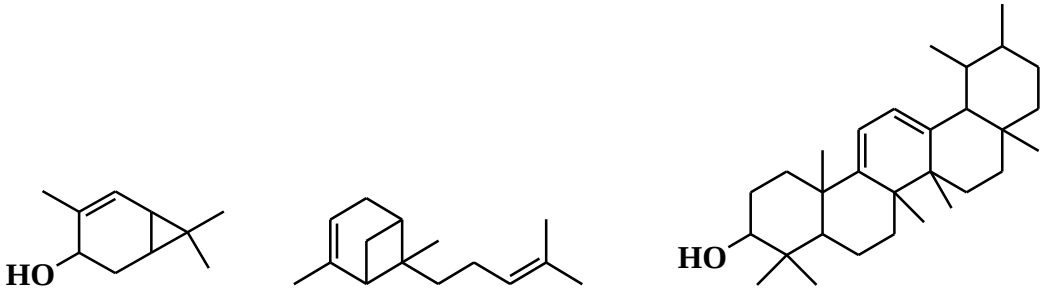

126 **127** **128**

4.2.8 GC-MS analysis of *C. africana* resin chloroform fraction

The chloroform fraction of the resin from *C. africana* led to the identification of 49 components. Palmitic acid, chlorohexanoic acid and other organic acids in trace amount. The total ion chromatogram (TIC) of chloroform fraction and the constituents identified in the resin of C. *africana* chloroform fraction are presented in Figure 4.2.8 and Table 4.2.8.

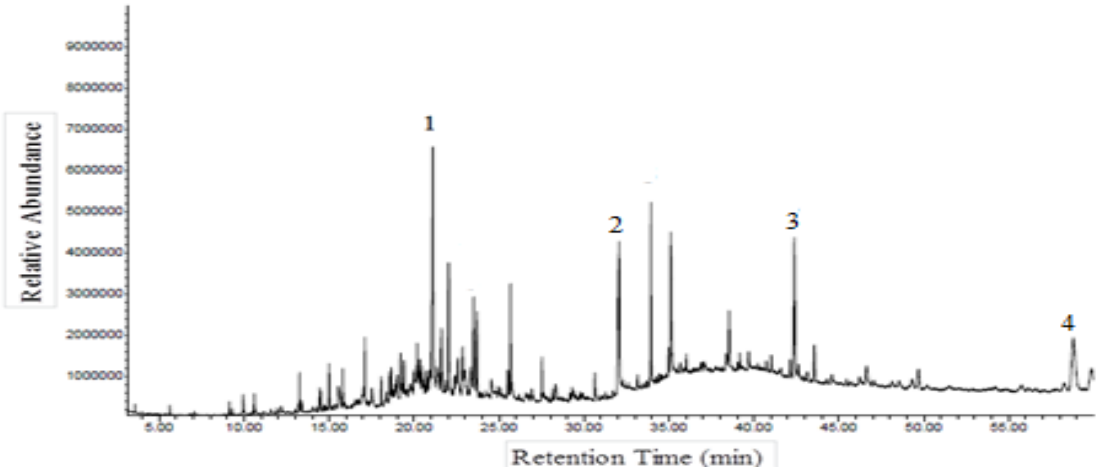

Figure 4.2. 8 GC of chloroform fraction of the resin of *C. africana.*

Table 4.2. 8 Phytoconstituents identified in chloroform fraction of *C. africana* resin using GC-MS

No	Compound	RT (min)	M.Wt	M. F	Peak Area %
1	Benzene, butyl-	9.95	134.1	$C_{10}H_{14}$	0.59
2	Bicyclo[3.1.0]hexane, 4-methylene-1-(1-methylethyl)-	10.60	136.1	$C_{10}H_{16}$	0.53
3	Decane, 4-ethyl-	13.26	170.2	$C_{12}H_{26}$	0.85
4	2,6-Octadienal, 3,7-dimethyl-, (*Z*)-	14.45	152.1	$C_{10}H_{16}O$	0.57
5	Cyclohexanone, 5-methyl-2-(1-methylethenyl)-, trans-	15.01	152.1	$C_{10}H_{16}O$	1.39
6	Verbenol	15.55	152.1	$C_{10}H_{16}O$	1.56
7	Cyclohexanone, 5-methyl-2-(1-methylethenyl)-	15.79	152.1	$C_{10}H_{16}O$	1
8	Bicyclo[3.1.1]hept-3-en-2-one, 4,6,6-trimethyl-, (1*S*)-	17.10	150.1	$C_{10}H_{14}O$	1.61
9	Pyrrolidine-2,4-dione	18.07	99.0	$C_4H_5NO_2$	0.84
10	3-Hexyne-2,5-diol, 2,5-dimethyl-	18.58	142.1	$C_8H_{14}O_2$	0.98
11	3-Pentenal, 4-methyl-	18.65	98.1	$C_6H_{10}O$	0.75
12	Methoxyacetic acid, 2-tetradecyl ester	18.95	286.3	$C_{17}H_{34}O_3$	0.52
13	3-Hexyne-2,5-diol, 2,5-dimethyl-	19.02	142.1	$C_8H_{14}O_2$	0.69
14	Tridecane	19.41	184.2	$C_{13}H_{28}$	0.8
15	Bicyclo[3.1.0]hex-3-en-2-one, 4-methyl-1-(1-methylethyl)-	20.19	150.1	$C_{10}H_{14}O$	1.54
16	5H-[1,2,4]Triazolo[4,3-a]azepin-3-ol, 6,7,8,9-tetrahydro-	20.33	153.1	$C_8H_{11}N_3O_2$	0.95
17	4-Hepten-3-ol, 4-methyl-	20.48	128.1	$C_8H_{16}O$	0.49
18	Cycloheptanol, 2-methylene	20.72	126.1	$C_8H_{14}O_2$	0.79
19	1,5,9-Decatriene, 2,3,5,8-tetramethyl-	20.92	192.2	$C_{14}H_{24}$	0.78
20	Ethanone, 1-(1,4-dimethyl-3-cyclohexen-1-yl)-	21.10	152.1	$C_{10}H_{1O}$	**10.88**
21	2-Cyclohexen-1-one, 4-(2-oxopropyl)-	21.34	152.1	$C_9H_{12}O_2$	1.14
22	Tetradecane	21.62	198.2	$C_{14}H_{30}$	2.59
23	8-Hydroxycarvotanacetone	22.03	168.1	$C_{10}H_{16}O_2$	4.83
24	1,3,6,10-Dodecatetraene, 3,7,11-trimethyl-, (Z,E)-	22.38	204.2	$C_{15}H_{24}$	0.58
25	3-Cyclopentylpropionic acid, 2,2-dimethylpropyl ester	22.46	212.2	$C_{13}H_{24}O_2$	0.6
26	Ethanone, 1-(2-methyl-1-cyclopenten-1-yl)-	22.58	124.1	$C_8H_{12}O$	2.36
27	4-t-Pentylcyclohexene	22.85	152.2	$C_{11}H_{20}$	1.73
28	1-Buten-3-one, 1-(1-acetyl-5,5-dimethylcyclopentyl)-	22.93	208.1	$C_{13}H_{20}O_2$	0.73
29	7-Oxabicyclo[4.1.0]heptane, 3-oxiranyl-	23.01	140.1	$C_8H_{12}O$	1.16
30	8-Methylene-3-oxatricyclo[5.2.0.0(2,4)]nonane	23.32	136.1	$C_9H_{12}O$	1.67
31	Naphthalene, decahydro-2,3-dimethyl-	23.50	166.2	$C_{12}H_{22}$	4.48
32	Pentadecane	23.70	212.3	$C_{15}H_{32}$	2.04
33	10-Mercaptopinane	24.55	170.1	$C_{10}H_{18}S$	0.93
34	Cyclohexanone, 2-propyl-	25.52	140.1	$C_9H_{16}O$	0.67
35	Hexadecane	25.67	226.3	$C_{16}H_{34}$	2.26
36	Heptadecane	27.53	240.3	$C_{17}H_{36}$	0.77
37	Cyclohexadecane	30.64	224.3	$C_{16}H_{32}$	0.75
38	*n*-Hexadecanoic acid	32.06	256.2	$C_{16}H_{32}O_2$	**8.61**
39	6-Chlorohexanoic acid, 4-cyanophenyl ester	33.94	251.1	$C_{13}H_{14}NO_2Cl$	4.48
40	Tetradecanoic acid	34.98	228.2	$C_{14}H_{28}O_2$	0.83
41	Phenol, 4,4'-(1-methylethylidene)bis-	35.12	228.1	$C_{15}H_{16}O_2$	5.11
42	Nonadecane, 1-chloro-	38.38	302.3	$C_{19}H_{39}Cl$	0.74
44	Eicosane	39.69	282.3	$C_{20}H_{42}$	0.21
45	Cyclohexene, 6-butyl-1-nitro-	42.38	183.1	$C_{10}H_{17}NO_2$	6.08
46	Bicyclo[5.2.0]nonane, 4-methylene-2,8,8-trimethyl-2-vinyl-	43.55	204.2	$C_{15}H_{24}$	1.46
48	Bicyclo[4.1.0]hepta-2,4-diene, 7,7-dimethyl-2,3,4,5-tetraphenyl-	58.81	424.2	$C_{33}H_{28}$	6.88
49	Ursa-9(11),12-dien-3-ol	59.87	424.4	$C_{30}H_{48}O$	1.01
				Total identified	**92.81%**

As shown in Fig. 4.2.8 and Table 4.2.8 92.81 % of the total chloroform fraction, were identified based on their mass spectra. The major components were identified to be ethanone, 1-(1,4-dimethyl-3-cyclohexen-1-yl)- (**129**) (10.88%) and 8-Hydroxycarvotanacetone (4.83%) followed by sesquiterpene (10.25%) such as Phenol, 4,4'-(1-methylethylidene) bis (**130**) (5.11%) (Figure 4.2.8). The pentacyclic triterpene ursa-9(11),12-dien-3-ol (**128**) accounts (1.01%) (Figure 4.2.8).

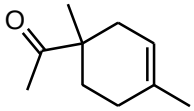

129

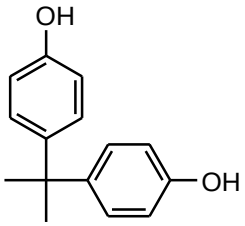

130

4.2.9 GC-MS analysis of *C. sphaerocarpa* resin n-hexane fraction

The phytochemicals of the resin of *C. sphaerocarpa* were investigated using GC-MS technique, while the mass spectra of the compounds found in the fraction was matched with the National Institute of Standards and Technology (NIST) library. Analysis of *n*-Hexane fraction comprised of 38 components among which 23 constituents were identified. The major constituents were pentacyclic triterpenes such as lupeol (**124**) (15.91%), Urs-12-en-3-one (**131**) (14.39%), α-amyrin (**56**) (13.42 %) and β-amyrin (**117**) (10.96 %) (Table 4.2.9 and Fig. 4.2.14). The *n*-hexane fraction also contains hydrocarbon sesquiterpenes such as α-copaene (**80**) (1.16%), caryophyllene (**83**) (0.96%), humulene (**84**) (0.12%), Alloaromadendrene (0.12%), γ-muurolene (0.03%), γ- selinene (0.12%), β-humulene (0.04%) and oxygenated sesquiterpene caryophyllene oxide (0.50%) in trace amount (Table 4.2.9 and Fig. 4.2.9).

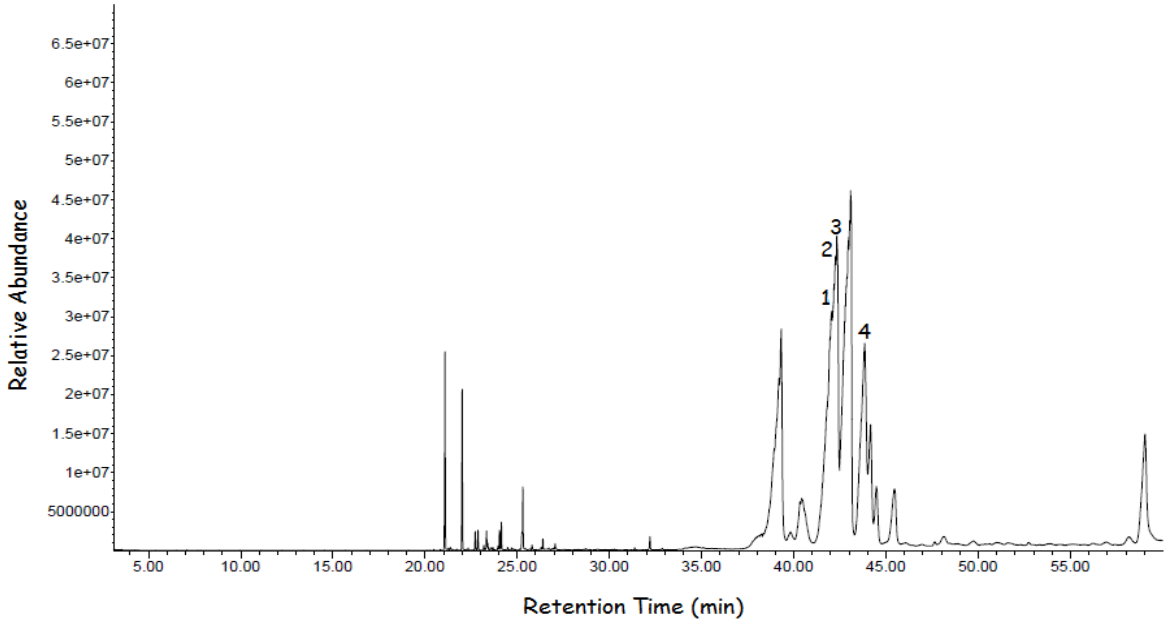

Figure 4.2. 9 GC of *n*-hexane fraction of *C. sphaerocarpa*.

Table 4.2. 9 Relative concentration (%) of components of the *n*-hexane fractions of *C. sphaerocarpa* resin

Name of Compound	M.Wt	M. F.	RT	Peak area %
α–Copaene	204.19	$C_{15}H_{24}$	21.1	1.16%
Caryophyllene	204.19	$C_{15}H_{24}$	22	0.96%
Humulene	204.19	$C_{15}H_{24}$	22.7	0.12%
Alloaromadendrene	204.19	$C_{15}H_{24}$	22.9	0.12%
γ–Muurolene	204.19	$C_{15}H_{24}$	23.2	0.03%
γ–Selinene	204.19	$C_{15}H_{24}$	23.3	0.12%
β–Humulene	204.19	$C_{15}H_{24}$	23.4	0.04%
α-Amorphene	204.19	$C_{15}H_{24}$	23.9	0.03%
α–Panasinsen	204.19	$C_{15}H_{24}$	24	0.12%
δ–Cadinene	204.19	$C_{15}H_{24}$	24.1	0.18%
Caryophyllene oxide	220.18	$C_{15}H_{24}O$	25.3	0.50%
(+)-epi-Bicyclosesquiphellandrene	204.19	$C_{15}H_{24}$	26.4	0.07%
(1S,6R,9S)-5,5,9,10-Tetramethyltricyclo[7.3.0.0(1,6)]dodec-10(11)-ene	218.2	$C_{16}H_{26}$	39.2	9.59%
2(1H)Naphthalenone, 3,5,6,7,8,8a-hexahydro-4,8a-dimethyl-6-(1-methylethenyl)-	218.17	$C_{15}H_{22}O$	39.3	4.83%
Olean-12-ene	410.39	$C_{30}H_{50}$	40.3	1.23%
Olean-12-en-3-one	424.37	$C_{30}H_{48}O$	40.4	2.39%
β.-Amyrin **(117)**	424.37	$C_{30}H_{48}O$	42	**13.45%**
Urs-12-en-3-one (**129**)	426.39	$C_{30}H_{50}O$	42.3	**14.39%**

Lupeol (**119**)	426.39	$C_{30}H_{50}O$	43	**15.91%**
Hop-22(29)-en-3β.-ol	426.39	$C_{30}H_{50}O$	43.1	7.89%
α.–Amyrin **(56)**	426.38	$C_{30}H_{48}O$	43.8	**10.96%**
Taraxasterol	426.39	$C_{30}H_{50}O$	44.2	3.72%
A'-Neogammacer-22(29)-en-3-one	424.37	$C_{30}H_{48}O$	48.1	0.34%

[a] Compounds listed in order of elution from a HP 5MS column; RT = Retention time; Mol.Wt = Molecular weight; Mol. Formula = Molecular formula.

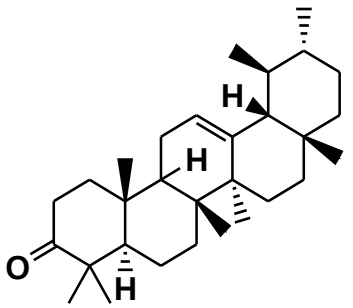

131

GC-MS analysis results indicated that β-amyrin had a shorter retention time than α-amyrin (Table 4.2.9) which was consistent with the earlier reports [224]. Some constituents such as α-copaene, α-humulene, β-selinene, and δ-cadinene were identified previously from the essential oil of *C. sphaerocarpa* resin [16]. Sesquiterpenes, which are one of the most common terpenes, are a class of natural products with a diverse range of attractive industrial properties [225, 226]. Several biological activities are attributed to sesquiterpenes, such as antimicrobial [227], antibacterial [228], antioxidant, antifungal [229, 230] and antigenotoxic [231] activities. A report by Nishida (2000) [232] showed α-copaene (**80**) is not genotoxic and it increases the antioxidant capacity in human lymphocyte cultures. Whereas, Fernandes (2007) reported pronounced oral anti-inflammatory effects for the sesquiterpenes isolated from the essential oil of *Cordia verbenacea* α-humulene and *trans*-caryophyllene [233]. Their oral anti-inflammatory properties are probably related to an important inhibition of the activation and/or release of different inflammatory mediators such as bradykinin, platelet activating factor, histamine, IL- 1β, TNFα and PGE2. The anti-inflammatory effects of these compounds seem to be closely associated with their ability to inhibit the up-regulation of both COX-2 and iNOS enzymes. These workers suggest that sesquiterpenes isolated from the essential oil of *C. verbenacea*, α-humulene and *trans*-caryophyllene, might constitute a relevant therapeutic alternative for the treatment of inflammatory diseases [233]. In vivo disease resistance assays, using ZmTps21 and Zmtps21

near-isogenic lines, supported the endogenous antifungal role of selinene-derived metabolites involved in the biosynthesis of nonvolatile antibiotics, ZmTps21 exists as a useful gene for germplasm improvement programs targeting optimized biotic stress resistance [234].

4.2.10 GC-MS analysis of *C. schimperi* resin n-hexane fraction

In this investigation, GC-MS was used to examine constituents of *n*-hexane fraction of *C. schimperi*. Analysis of the *n*-hexane fraction obtained by solvent partitioning from the resin of *C. schimperi* crude methanol extract showed the presence of 38 compounds however; only 3 were identified from NIST library having quality ≥ 90%. The main compositions were 1: 9,19-Cyclolanost-24-en-3-ol, (3β.)- (**131**) (13.01%) 2: Tirucallol (**132**) (11.23%), and 3: Lanost-7-en-3-one, (9β.13α,14β,17α) (**133**) (24.76%) where the three compounds belongs to a tetracyclic triterpene with a chemical formula of $C_{30}H_{50}O$ (Figure 4.2.10, Table 4.2.10)

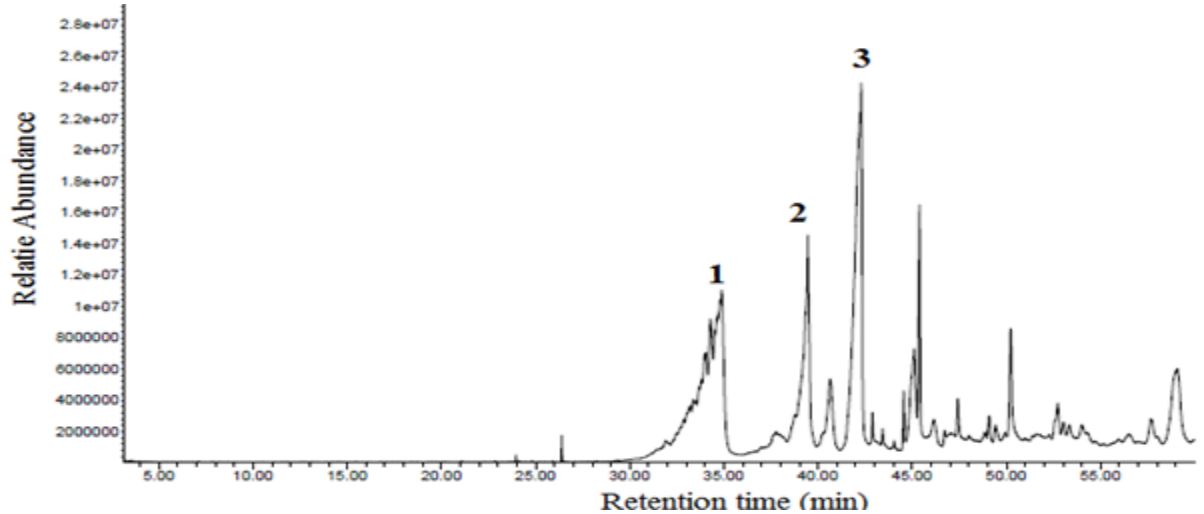

Figure 4.2. 10 GC of *n*-hexane fraction of the resin of *C. schimperi*

Table 4.2. 10 GC-MS analysis showing major compounds identified in hexane fraction of *C. schimperi* resin

No	Name of Compound	M.Wt.	Mol. Formula	RT	Peak Area %
1	9,19-Cyclolanost-24-en-3-ol, (3β)-	426.39	$C_{30}H_{50}O$	34.87	13.01
2	Tirucallol	426.39	$C_{30}H_{50}O$	39.46	11.23
3	Lanosterol	426.39	$C_{30}H_{50}O$	42.28	24.76

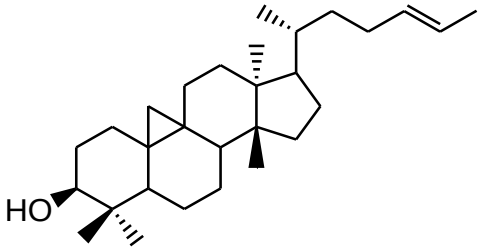

9,19-Cyclolanost-24-en-3-ol, (3β)-**(131)**

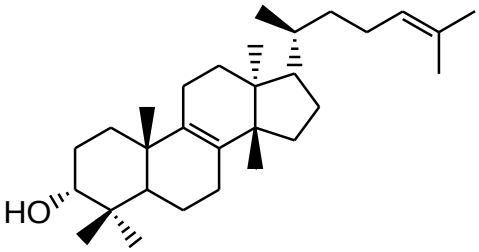

Tirucallol **(132)**

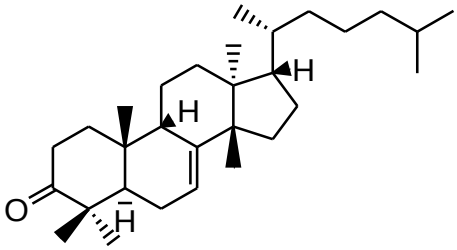

Lanost-7-en-3-one, (9β.13α,14β,17α) **(133)**

4.2.11 GC-MS analysis of *C. schimperi* resin chloroform fraction

GC-MS chromatogram analysis of the chloroform fraction of *C. schimperi* (Figure 4.2.11) showed 14 peaks. On comparison of the mass spectra of the constituents with the NIST library, 12 of the peaks that accounts (91.47%) of the phytochemicals were characterized and identified (Table 4.2.11). The identification of phytochemical compounds is based on the peak area (which represents the percentage of that compound), molecular weight and molecular formula.

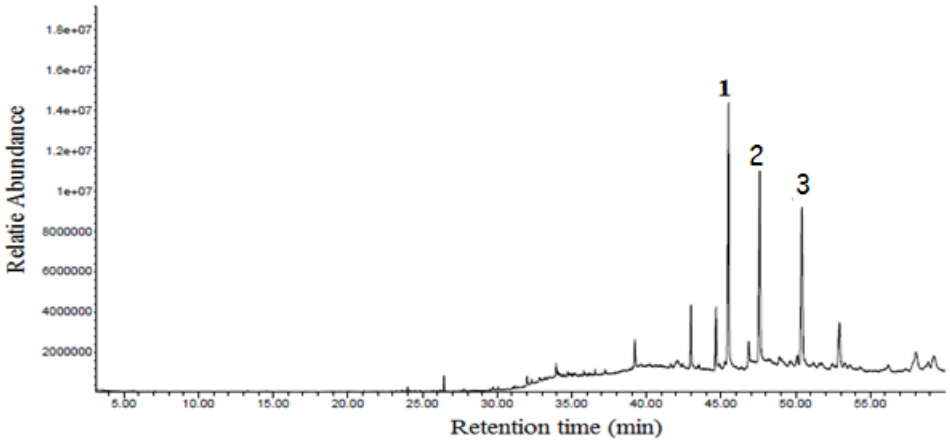

Figure 4.2. 11 GC of the chloroform fraction of *C.schimperi*

The main compositions of *C. schimperi* were 1: Carbanilic acid, p-phenyl- (134) (25.97%) 2: Isobenzofuran-1(3H)-one, 3,3-diheptyl- (135) (19.88%), and 3: Cannabichromene (136) (20.86%). The $CHCl_3$ inner bark extract of *C. schimperi* was reported to display antimalarial activity *in vitro* with anIC_{50} value of 4.63 mg/mL [79].

Table 4.2. 11 Compounds identified in *C. schimperi* resin chloroform fraction using GC-MS

Peak Name	RT (min)	M.Wt	M. F.	Peak Area %
(+)-epi-Bicyclosesquiphellandrene	26.433	204.188	$C_{15}H_{24}$	0.61%
n-Hexadecanoic acid	32.006	256.24	$C_{16}H_{32}O_2$	0.74%
Butyl 6,9,12-hexadecatrienoate	33.946	306.256	$C_{20}H_{34}O_2$	0.36%
Diethylene glycol dibenzoate	39.21	314.115	$C_{18}H_{18}O_5$	2.22%
Acrophylline	42.975	283.121	$C_{17}H_{17}NO_3$	4.12%
Pyrene, 1,1'-(1,2-ethanediyl)bis-	44.652	430.172	$C_{34}H_{22}$	5.41%
Carbanilic acid, p-phenyl-	45.493	213.079	$C_{13}H_{11}NO_2$	25.97%
Isobenzofuran-1(3H)-one, 3,3-diheptyl-	47.581	330.256	$C_{22}H_{34}O_2$	19.88%
2-Methylphenothiazine	50.105	213.061	$C_{13}H_{11}NS$	1.25%
Cannabichromene	50.414	314.225	$C_{21}H_{30}O_2$	20.86%
N-[1,3-Dimethylpyrazo-5-yl]anthranilic acid	58.041	231.101	$C_{14}H_{16}O_2N_3$	5.96%
2,4,6-Triisopropylbenzoyl chloride	59.283	266.144	$C_{16}H_{23}ClO$	4.09%

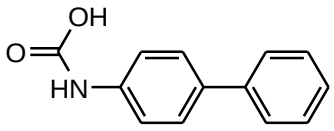

134

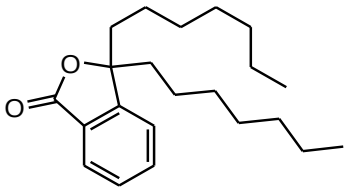

135

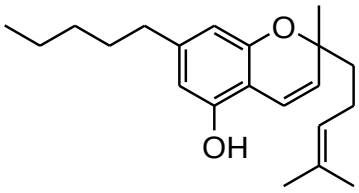

136

4.3 Biological activity of resins of *Commiphora* species

In this study, cytotoxicity of crude extract, fractions and isolated compounds, anti-inflammatory effect of the essential oils, antiviral and antidengue activity of crude extract and fractions obtained after performing liquid-liquid extraction of the crude resin MeOH exract have been generated. The results are discussed in the following sections.

4.3.1 The Cytotoxicity activity of resins of *Commiphora* species

4.3.1.1 Cytotoxicity of MeOH extract and solvent fractions of resin of *C. habessinica*

Commiphora habessinica (O.Berg), also known as *Commiphora abyssinica* Engl and *Commiphora madagascariensis* Jacq, is among transgressing *Commiphora* species widely distributed in the arid and semi-arid lowland areas of Ethiopia [64], Kenya [235] and Yemen [203]. It produces a yellow to brown oleo-gum resin rich in essential oil, gum and resin components [235].

The anti-proliferative activities of the extracts and fractions from the resin of *C. habessinica* were evaluated on four human cancer cell lines, A549, A2780, MIA-Paca-2 and SNU-638. The concentrations of the extract which inhibited 50% of the cell growth (IC_{50}) on the methanol and chloroform fraction was evaluated. The IC_{50}'s of methanol extract on A549, A2780, MIA-Paca-2, and SNU-638 were 3.37, 5.00, 9.18 and 4.46 μg/ml, respectively (Table 4.3.1). Wheras the *n*-hexane and *n*-butanol fractions showed less toxicity on the cancer cell lines with IC_{50} greater than 8.0 μg/ml. The chloroform fraction exhibited significant cell proliferation inhibition against the all four cell lines with dose-dependent relationship *in vitro*. The IC_{50}'s of chloroform extract on A549, A2780, MIA-Paca-2, and SNU-638 were 0.77, 3.03, 3.35 and 3.02 μg/ml, respectively (Figure 4.3.1, Table 4.3.1). The data indicated that the chloroform fraction demonstrated anti-proliferative effect comparable to Etoposide (the positive control), in prevention proliferation of non – small cell lung cancer (A549). The strong cytotoxicity of the chloroform fraction might be due to synergetic effect of the various constituents.

Table 4.3. 1 IC_{50} values of the extracts from resin of *Commiphora habessinica* against four cancer cell in a SRB assay

Extract/Fractions	Cell lines and IC_{50} (µg/ml)			
	A549	A2780	MIA-PaCa-2	SNU638
Hexane	10.01	10.98	NC	8.03
Methanol	3.37	5	9.18	4.46
Chloroform	0.77	3.03	3.35	3.02
Ethyl acetate	ND	ND	ND	ND
Butanol	9.41	14.79	NC	14.99
Etoposide, µM (Positive control)	0.34	0.58	0.72	0.24

IC_{50} (Inhibition of cell growth by 50%). Data was generated by experiments performed in triplicates. ND = not determined as a result of insufficient solvent extract under question. NC. No cytotoxic activity at highest concentration tested (>30 µg/ml).

The data indicated that the chloroform fraction has shown anti-proliferative effect comparable to Etoposide (the positive control), in prevention proliferation of non-small cell lung cancer (A549). The percent inhibition on A549 cancer cell line starts to increase from (7.72%) at 0.1 µg/ml, 0.3 µg/ml (23.21%), (55.428%) at 1 µg/ml and reached maximum 84.05% at 3.0 µg/ml (Table 4.3.2)

Table 4.3. 2 Percent viability and IC_{50} values of resin of *C. habessinica* chloroform fraction against four human cancer cell lines.

Concentration (µg/ml)	Cells			
	A549	A2780	MIA-PaCa-2	SNU-638
0.1	92.28	101.15	101.32	98.77
0.3	76.79	99.11	101.02	88.41
1	44.58	96.81	100.71	82.6
3	15.95	57.48	82.52	51.91
10	-76.8	-81.16	-20.36	-71.95
30	-87.58	-94.88	-65.77	-83.31
IC_{50}	0.77	3.03	3.35	3.02

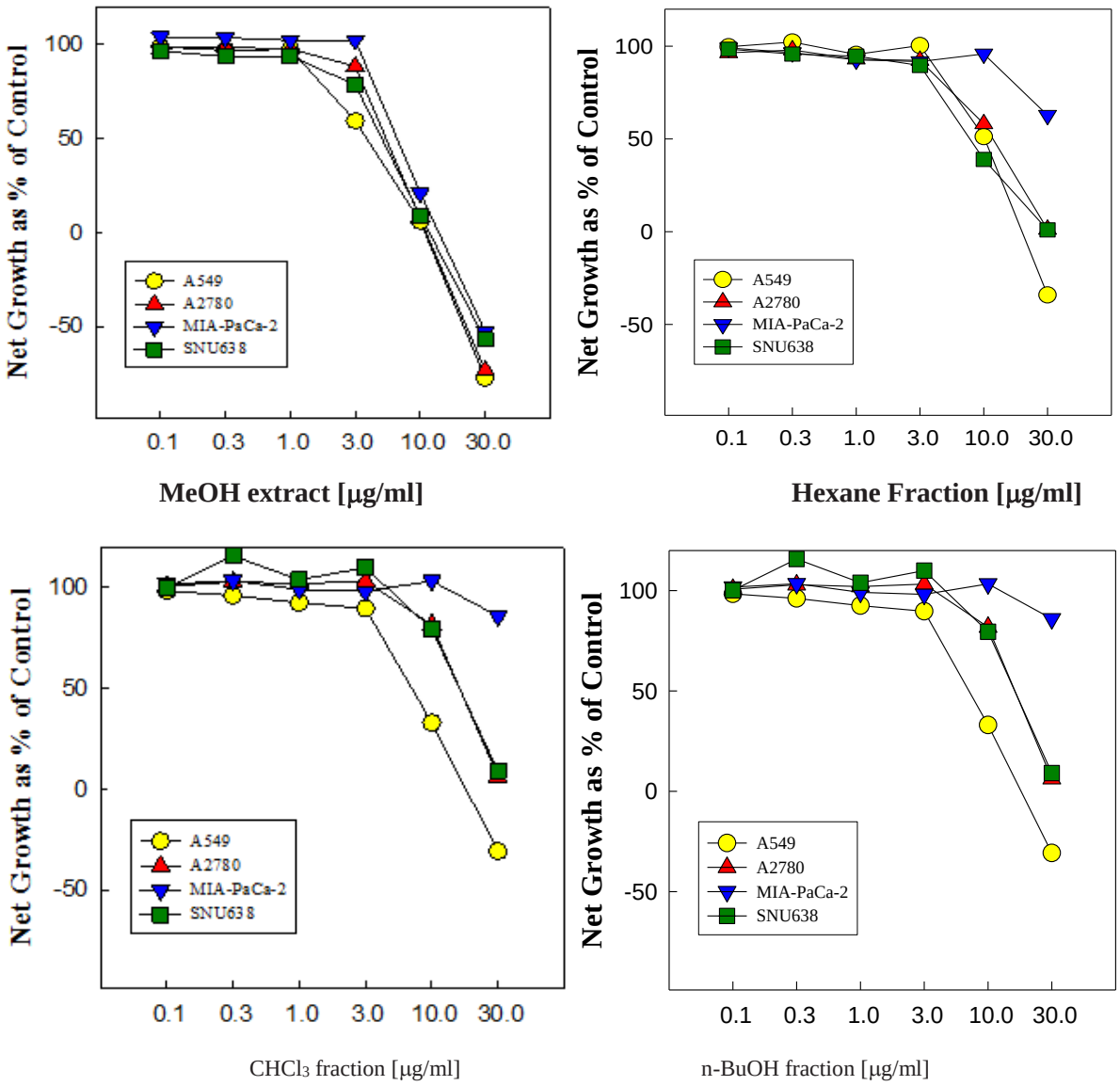

Figure 4.3. 1 Dose response curve of MeOH extract and solvent fractions of *C. habessinica* against the tested cancer cell lines.

4.3.1.2 Cytotoxicity of crude extract and fractions from resin of *C. africana*

C. africana (A. Rich.) Engl. from the family of Burseraceae is a bush about 1.5 m tall that is wide-spread in African countries such as Sudan, Ethiopia, Eritrea, Somalia, Kenya, Uganda and Mozambique [236]. Cytotoxicity of the extracts and fractions from resin of *C. africana* showed dose-dependent inhibition against cancer cell lines tested (Figure 4.3.2 and Table 4.3.3). The methanol extract, *n*-hexane and ethylacetate fractions were comparatively less toxic compared to the chloroform fraction against all the four cancer cell lines. In particular, antiproliferative effect of the chloroform fraction towards A549 (NSCLC) (2.04 μg/ml) is more than four times than the *n*-hexane fraction (9.64 μg/ml) and three times than the ethyl acetate fraction (6.6 μg/ml). Thus, it was the chloroform fraction that showed cytotoxicity compared to the crude methanol extract, *n*- hexane and ethylacetate fractions on A549 cell line (Table 4.1.5). Due to its highest cytotoxic effect the cholorofrm fraction was selected for isolation and separations of compounds. It was also worth mentioning isolation and purification of compounds from the n-hexane fraction was made on the basis of its cytotoxicity against three of the cancer cell lines tested compared to the ethylacetate fraction. Furthermore, all of the compounds isolated in the *n*-hexane fraction were also isolated from the chloroform fraction and were subjected for cytotoxicity screening against the four cancer cell lines.

The IC_{50}'s of n-hexane extract exhibited anti-proliferative activity on the four cell lines; A549, A2780, MIA-Paca-2, and SNU-638 with 9.64, 9.62, 17.21 and 10.3 μg/ml, with dose-dependent relationship *in vitro* respectively (Table 4.3.3 and Figure 4.3.2). The observed data indicated that in all cancer cell lines, in good agreement with American national cancer institute (IC_{50} < 30 μg/ml). Compared to other fractions the data for the ethyl acetate fractions showed no apparent bioactivities on three of cancer cell lines (IC_{50} > 12.0 μg/ml) with the exception on non-small cell lung cancer A549 with IC_{50} 6.6 μg/ml.

Table 4.3. 3 IC_{50} values of the extract and fractions from resin of *Commiphora africana* against four cancer cell in SRB method.

Sample	Cell lines and IC_{50} (µg/ml)			
	A549	A2780	MIA-PaCa-2	SNU638
MeOH extract	3.55	9.98	19.2	10.09
Hexane fraction	9.64	9.62	17.21	10.3
Chloroform fraction	2.04	8.81	11.5	4.85
Ethylacetate fraction	6.6	15.81	23.91	12.15
Etoposide µM	0.34	0.58	0.72	0.24

IC_{50} (Inhibition of cell growth by 50%). Data was generated by experiments performed in triplicates. The n-BuOH fraction not determined as a result of insufficient solvent extract under question.

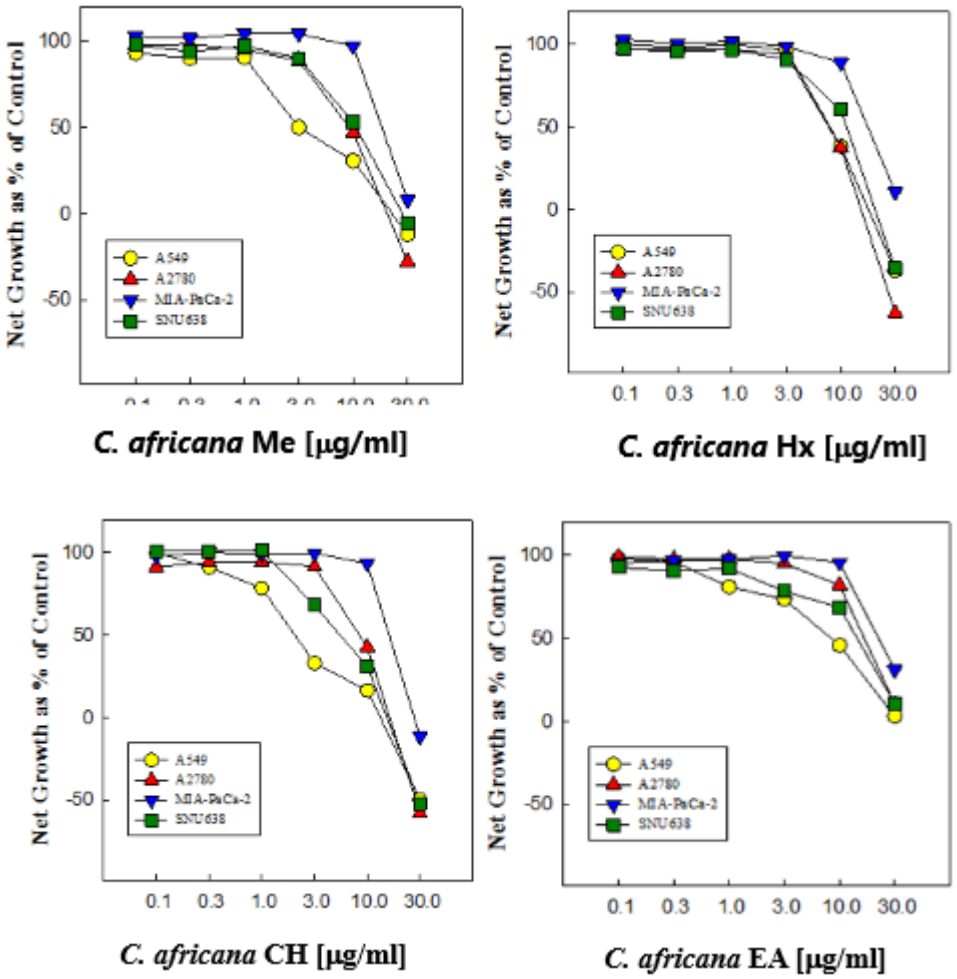

Figure 4.3. 2 Dose response curve of MeOH extract, Hx, $CHCl_3$ and EtOAc fractions against the tested four cancer cell lines

4.3.1.3 Cytotoxicity of MeOH extract and solvent fractions of resin of *C. sphaerocarpa*

Commiphora sphaerocarpa is one of oleo–gum resins of *commiphora* species resembling or sold under the product name myrrh [59]. *C. sphaerocarpa,* fruit edible; resin: against cough, diarrhea and headache, against ticks of cattle. This resin is sometimes found in true myrrh as adulterant. A previous study revealed idoation of six from the petrolether extract of *C. sphaerocarpa.* One of them, (1E)-8,12-epoxygermacra-1,7,10,11-tetraen-6-one, a new furanosesquiterpene [16].

The IC_{50}'s, the concentrations which inhibit 50% of cell growth ranges from 10.19 μg/ml to 26.2 μg/ml against most of the cancer cell lines tested (Table 4.3.4). Of all the fractions the *n*-hexane fraction showed apparent bioactivities on A549, A2780 and SNU-638 μg/ml cancer cell lines with IC_{50} value ranging from 10.19 μg/ml to 10.28 μg/ml with dose-dependent relationship *in vitro* (Figure 4.3.3 and Table 4.3.4). Particularly, for the n-hexane fraction the cell viability of the cancer cell line decreased sharply at higher concentration, i.e., at 10 μg/ml to the level of 69%, 89% and 60% towards A549, A2780 and SNU-638 cancer cell respectively. These results suggest that *n*-hexane fraction is responsible for the observed high anti-proliferative activity.
Slight inhibitory activity was observed by the MeOH crude extract and chloroform fraction in the range of 10.84 - 11.56 against A549, A2780 and SNU-638 cancer cell line (Figure 4.3.3 and Table 4.3.4). The activity presented by the the EtOAc fraction was least potent against the A549 and SNU-638 cancer cell lines with IC50 24.27 and 21.36 μg/mL The EtOAc fraction was non cytotoxic towards A2780 and MIAPaCa-2 cell line with IC_{50} greater than 30 μg/mL. Like the two resins dscussed above i.e *C. habessinica* and *C. africna,* it is unlikely to have a better cytotoxicity by the crude extract and fractions against MIAPaCa-2 cell line (Table 4.3.4).

Table 4.3. 4 Cytotoxic activity of the crude extracts and fractions from *C. sphaerocarpa* resin against four human cancer cell lines using SRB assay

Plant resin	Extract/Fractions	Cell lines and IC_{50} (μg/ml)			
		A549	A2780	MIA-PaCa-2	SNU-638
C. sphaerocarpa (CspR)	MeOH	11.03	11.32	23.51	11.56
	n-Hexane	10.19	10.28	26.2	10.28
	$CHCl_3$	11.23	11.06	24.57	10.84
	EtOAc	24.27	NC	NC	21.36
	Etoposide, μM	0.34	0.58	0.72	0.24

IC_{50} (Inhibition of cell growth by 50%). Data was generated by experiments performed in triplicates. NC. No cytotoxic activity at highest concentration tested (>30 μg/ml).

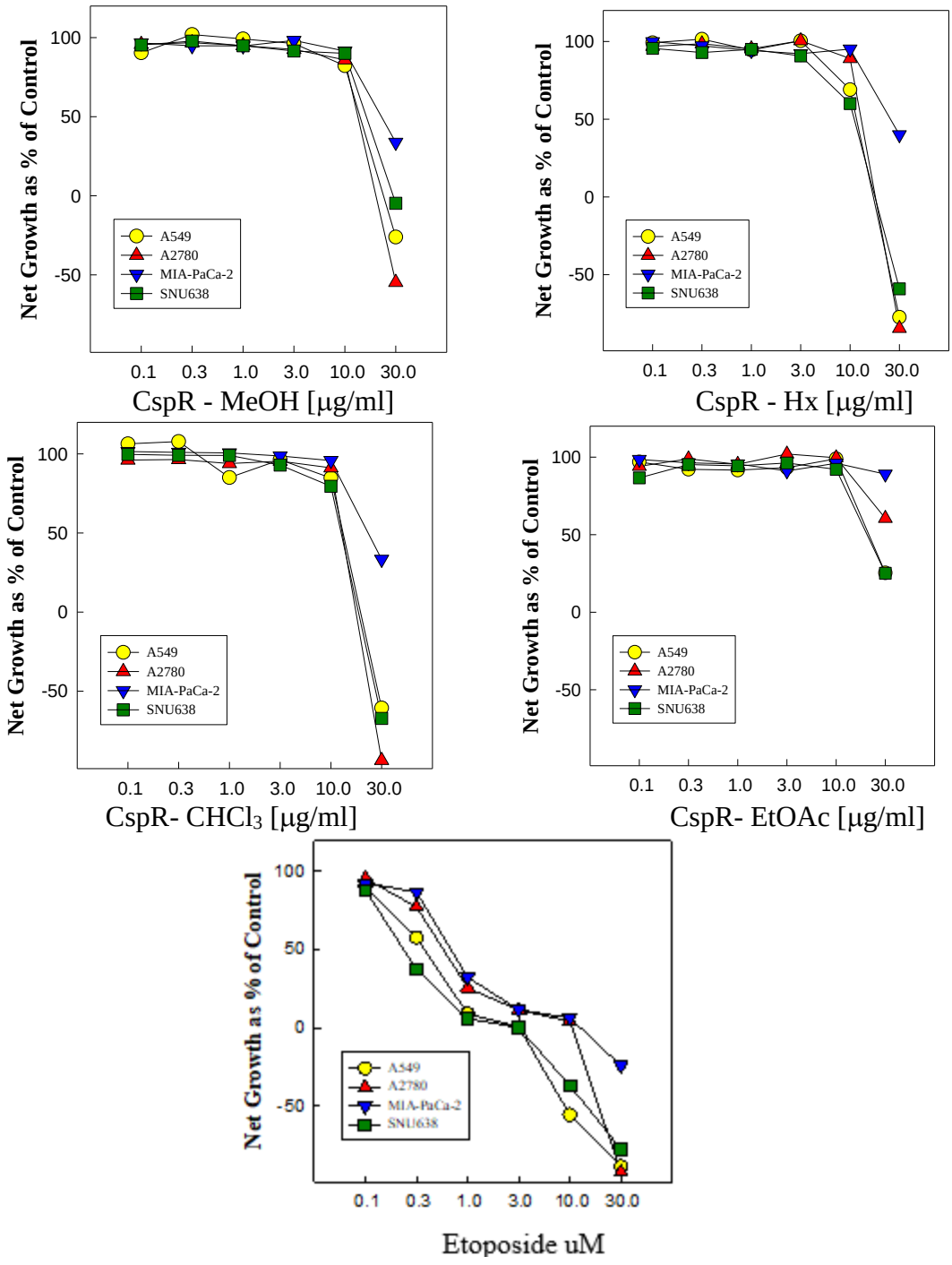

Figure 4.3. 3 Cytotoxic activity of Extracts and fractions from *C. sphaerocarpa* resin against A549, A2780, MIA-PaCa-2 and SNU 638 cancer cell lies.

The cytotoxicity of *C. sphaerocarpa* crude methanol extract, *n*-hexane and chloroform fractions have not been studied before, but the cytotoxicity of some compounds identified in the *n*-hexane fraction extracted from a variety of plant species showed different pharmacological activities. *In vivo* studies have identified that lupane type pentacyclic triterpenoid have strong antitumor and anti-inflammatory effects [237]. Experimental results showed that, in the mouse skin carcinogenesis model, local application of lupeol for 28 weeks can inhibit the growth of tumor prolongs the latency of tumor cells. The mechanism might be related to the nuclear factor kappa B (NF-κB)/phosphatidylinositol 3-kinase (PI3K)/proteinkinase B (Akt) signaling pathway [238]. Aratanechemuge et al (2004) [239], reported that hypodiploid apoptotic peak can be detected after the lupane type pentacyclic triterpenoid treatment on HL-60 leukemia cells, with time-dose-dependency. Gallo and Sarachine (2009) reviewed that lupeol and some of its analogues have been shown to possess a wide range of biological activities such as anti-cancer, hepatoprotective, antimicrobial, cardioprotective, anti-melanoma, etc. Therefore, lupeol and its derivatives have a potential to be consumed as a dietery supplement to prevent cancer, coronary and hepatic disease. Though, the sesquiterpenes such as caryophyllene (**83**) and caryophyllene oxide (**99**) found in trace amount in *n*hexane fraction, essential oils or fractions with high amount of the sesquiterpenes possessed higher cytotoxic activity against animal and human tumor cells [240].

4.3.1.4 Cytotoxicity of MeOH extract and solvent fractions of resin of *C. schimperi*

The IC_{50} value differ both in type of solvent used and cancer cell lines tested. The experiment result indicated that the n-hexane, EtOAc, and BuOH fraction were less cytotoxic. Whereas, the MeOH extract and $CHCl_3$ fractions comparably are cytotoxic against A549 and A2780 cell lines i.e., in the range of 9.66 - 11.51 μg/mL. The $CHCl_3$ fraction showed significant antiproliferative activity against SNU-638 with IC_{50} 9.88 μg/mL. Except the BuOH fraction and the crude MeOH extract three of the fractions strongly suggest *in vitro* non-cytotoxic potential towards pancreatic cancer cell line (MIA-Paca-2) with IC_{50} value greater than 30 μg/ml (Table 4.3.5 and Figure 4.3.4).

Table 4.3. 5 Cytotoxic activity of the crude extracts and fractions from *C. schimperi* resin against four human cancer cell lines in the SRB assay

Extract/Fraction	Cell lines and IC_{50} (μg/ml)			
	A549	A2780	MIA-PaCa-2	SNU-638
MeOH	9.97	11.51	24.21	12.05
n-Hexane	12.37	24.11	>30	13.82
$CHCl_3$	9.66	11.27	>30	9.88
EtOAc	18.21	20.63	>30	10.39
n-BuOH	16.27	>30	16.26	10.13
Etoposide, μM	0.34	0.58	0.72	0.24

IC_{50} (Inhibition of cell growth by 50%). Data was generated by experiments performed in triplicates. n.d = not determined as a result of insufficient solvent extract under question. NC. No cytotoxic activity at highest concentration tested (>30 μg/ml).

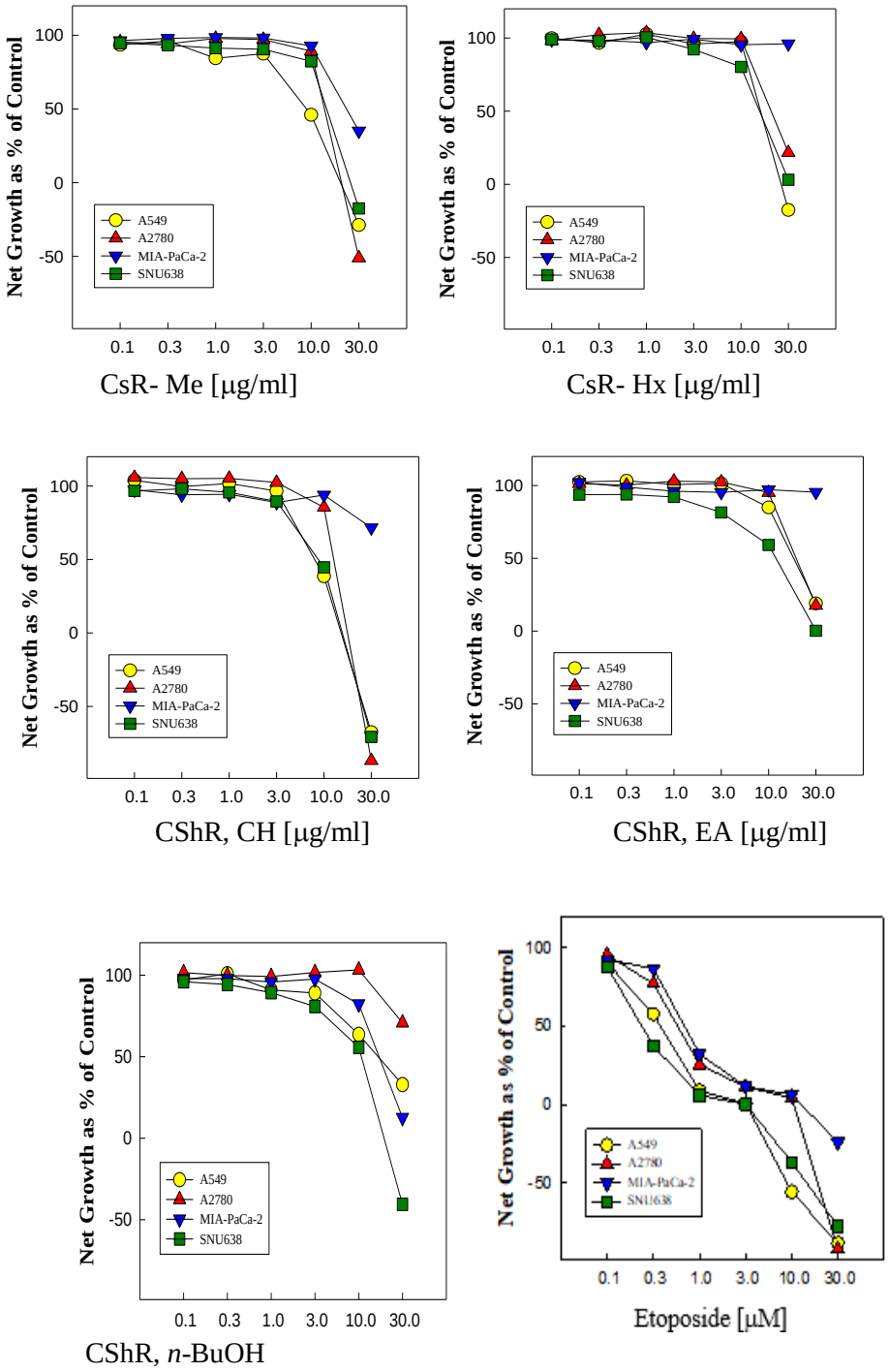

Figure 4.3. 4 Cytotoxicity of MeOH extract, n-hexane, $CHCl_3$, and EtOAc fraction from *C. schimperi* resin against A549, A2780, MIA-PaCa-2 and SNU 638 cancer cell lines.

4.3.1.5 Antiproliferative activity of cholesterol (48), lathosterol (112) and a mixture

The antiproliferative activity of mixed and purified sterols from chloroform fraction of *C. habessinica* resin was determined on the four human cancer cells. The IC_{50} values (Table 4.3.6) of the tested samples and the corresponding dose response curve (Figure 4.3.5) were summarized.

Table 4.3. 6 IC_{50} values of the constituents chloroform fraction from *C. habessinica* resin against four cancer cell lines using SRB assay

Sample	Cell lines and IC_{50} (μg/ml)			
	A549	A2780	MIA-PaCa-2	SNU638
Cholesterol (compound **48**)	N.C	N.C	N.C	N.C
Lathosterol (compound **112**)	22.25	N.C	N.C	N.C
Mixture of **48** and **112 (**47.85 to 52.15%**)**	13.77	20.36	N.C	N.C
Etoposide (μM)	0.16	0.14	1.87	1.14

IC_{50} (Inhibition of cell growth by 50%). Data was generated by experiments performed in triplicates. N.C. No cytotoxic activity at highest concentration tested (>30 μg/ml).

To the best of our knowledge there is no previous report on the cytotoxicity activity of the isolated sterols (cholesterol and lathosterol) on A549, A2780, MIAPaca-2, and SNU-638 cancer cell lines. The isolated compounds here from the chloroform fraction of *C. habessinica*, displayed no apparent antiproliferative activity in the SRB assay. Cholesterol did not show significant effect on all cancer cell lines which is far less than 30 μg/ml. Lathosterol (**112**) identical with cholesterol in molecular weight was cytotoxic on A549 cancer cell line with IC_{50} 22.25 μg/ml. Both cholesterol and lathosterol have the same chemical formula but differ only on the site of unsaturation. It may be that difference in the position of double bond account for the cell proliferative activity observed for lathosterol against A549 cancer cell line. Unlike the two independent sterols. The mixture showed a significant cytotoxicity against A549 cancer cell line with IC_{50} 13.77 μg/ml, which is is nearly twice the cytotoxicity of lathosterol. Cytotoxicity was also recorded for the mixture against on A2780 with IC_{50} being 20.36 μg/ml. The results indicated that effective component(s) of *C. habessinica* resin, which were responsible for cytotoxicity of the chloroform fraction against the four cancer cell lines used in this study, have not been identified.

Table 4.3. 7 Percent Cell viability of A549 and A2780 cancer cell lines after treated with a range of concentration of cholesterol, lathosterol and a mixture

Concentration (µg/ml)	Cholesterol	Lathosterol	A mixtrure	
	A549	A549	A549	A2780
0.1	108.65	97.42	101.73	99.18
0.3	101.18	95.71	97.74	100.72
1	99.27	94.28	103.34	95.7
3	99.58	91.92	89.17	91.52
10	75.34	84.35	74.3	88.03
30	72.8	27.29	18.56	27.74
IC_{50}	>30.0	22.25	13.77	20.36

There is a continuous decrease in % cell viability against A549 and A2780 cancer cell lines after treated with a range of concentration by cholesterol, lathosterol and a mixture of two, at the highest concentration 30 µg/ml, the % cell viability of A549 cancer cell line reached minimal by the mixture to 18.56 %, nearly four times than cholesterol 72.8 % (Table 4.3.7).

As the about 50% of cholesterol and lathosterol mixture have a promising cytotoxic activity in aforementioned cell line, more study on cytotoxicity study of theses sterols at various concentrations might be important to find out their optimum cytotoxic activity. Even though the mechanism of action of cholesterol on the mixture has not been studied, a study conducted on digitonin (a steroidal saponin, $C_{56}H_{92}O_{29}$) on its potential as cytotoxicity-enhancing agents and its molecular mechanisms of action on the membrane with and without incorporated cholesterol showed digitonin can induce membrane rupture only in the presence of cholesterol [241]. The study further noted that cholesterol concentration also greatly affected digitonin's ability to cause membrane disruption. The study affirmed that the ability of digitonin to increase membrane permeability with cholesterol can be used to facilitate the passage of drug molecules or other natural products through the cell membrane [241]. A separate study reaffirmed that betullin has potent anti-tumor activity especially in combination with cholesterol [102]. The sterols **48** and **112** were screened for antimycobacterial activity against *Mycobacterium madagascariense* and *Mycobacterium indicus pranii* and only cholest-7-en-3β-ol (**112**) exhibited antimycobacterial activity with MIC values of 1.6 mg/ml against both mycobacteria strains [182].

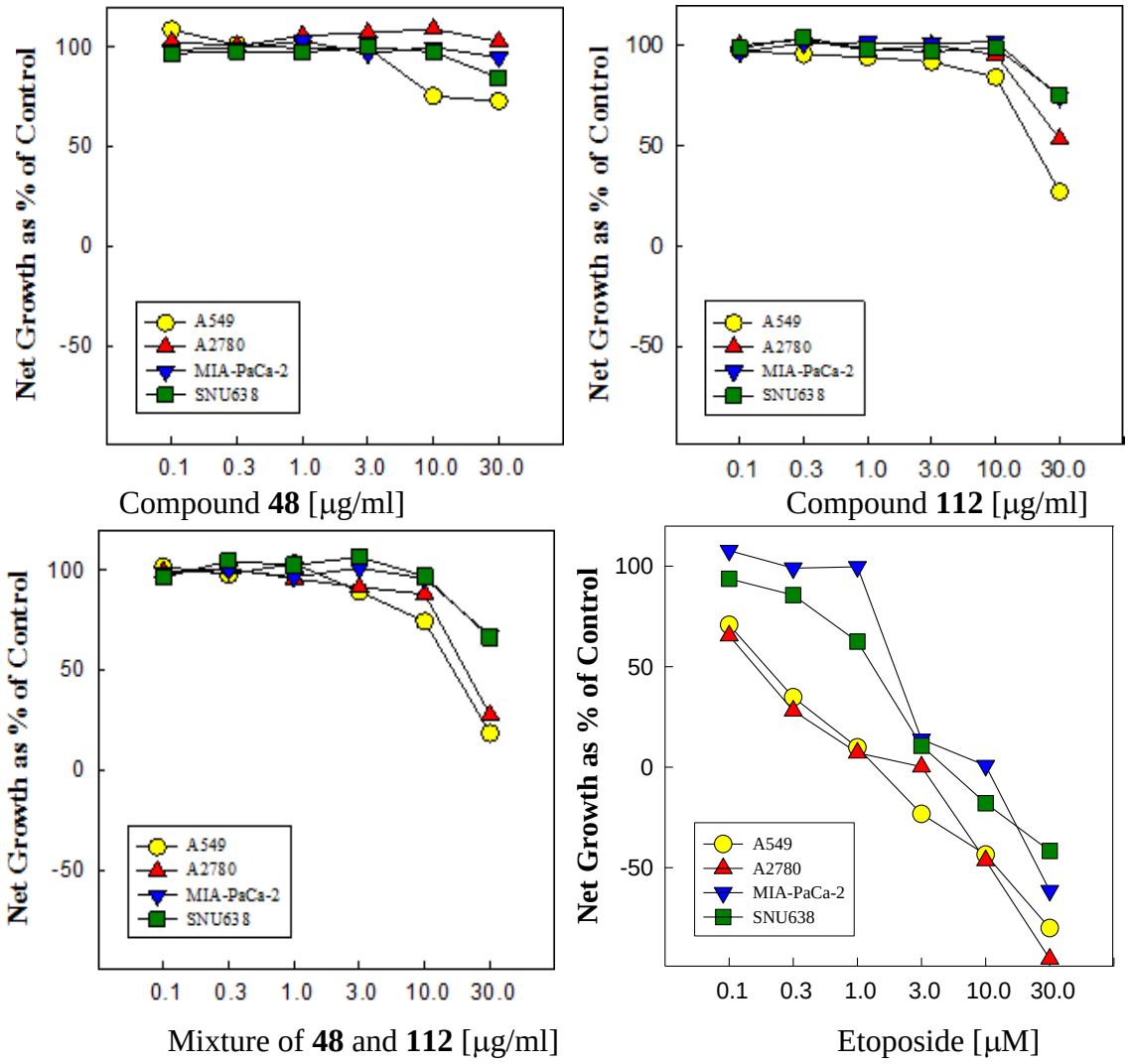

Figure 4.3. 5 Dose response curve of a mixture, compound **48** and compound **112** isolated from the $CHCl_3$ fraction of *C. habessinica* resin using SRB assay.

In this experiment Etoposide was used as a positive control. *Mixture of **48** and **112** were found in a ratio of ~ 1:1. Literature report revealed that cholesterol is required for viability and cell proliferation [128]. This study validates the enhanced effectiveness of a cytotoxic compound when used in combination against some of selected cancer cell lines. It is, therefore evident that lathosterol (**112**) may not be the major contributor of the antiproliferative activity against the two cancer cell lines (A549 and A2780) observed, but rather suggests that there are a number of compounds, occurring within the plant that may be acting synergistically to produce the antiproliferative activity observed. Further study is required for the antiproliferative mechanism and identification of active components of *C. habessinica* chloroform fraction. Thus, it is still a

long way to successfully develop *C. habessinica* as anti-cancer drug. As lathosterol, isolated from *C. habessinica* resin known to exhibit anti-cancer activity, the activity of *C. habessinica* chloroform fraction may be attributed partly to the presence of this compound.

4.3.1.6 Antiproliferative activity of α-amyrin (56) and commafric A (113)

One pentacyclic and two tricyclic triterpenes were isolated from n-hexane and chloroform fractions, as α-amyrin (**56**), Commafric A (**113**) and Commafric B (**114**), α-amyrin and Commafric A, a new triterpenoid were evaluated for cytotoxic effects *in vitro* against four human cancer cell lines: A549 (human lung adenocarcinoma cell line) A2780 (Ovarian cancer cell line), MIA-PaCa-2 (Human pancreatic carcinoma cell line) and SNU638 (human stomach carcinoma cell line). Etoposide was used as a positive control with IC_{50} values ranging from 0.24 to 0.72 μM for all the cancer cell lines tested (Table 4.3.8). To study the antiproliferative activity of commafric A, its purity (99%) and molecular weight (473.3625 Da) were confirmed by LC–MS. Commafric A (**113)** showed cytotoxic activity towards A549 cancer cell lines, with IC_{50} < 10 μM. The cytotoxicity was found moderate to the rest of the three cancer cell lines with IC_{50} in a range of 20 - 22 μM. The selective activity however suggests that commafric A might be modified to increase its activity against particular cancer diseases.

Table 4.3. 8 IC_{50} values of isolated compounds from *n*-hexane extract of resin of *C.africana* against four cancer cell using SRB assay

Sample	Cell lines and IC_{50} (μM)			
	A549	A2780	MIA-PaCa-2	SNU638
α–amryin (**56**)	21.78	51.55	37.89	66.2
Commafric A (**113**)	9.58	21.55	21.27	20.61
Etoposide μM	0.34	0.58	0.72	0.24

IC_{50} (Inhibition of cell growth by 50%), data was generated by experiments performed in triplicates.

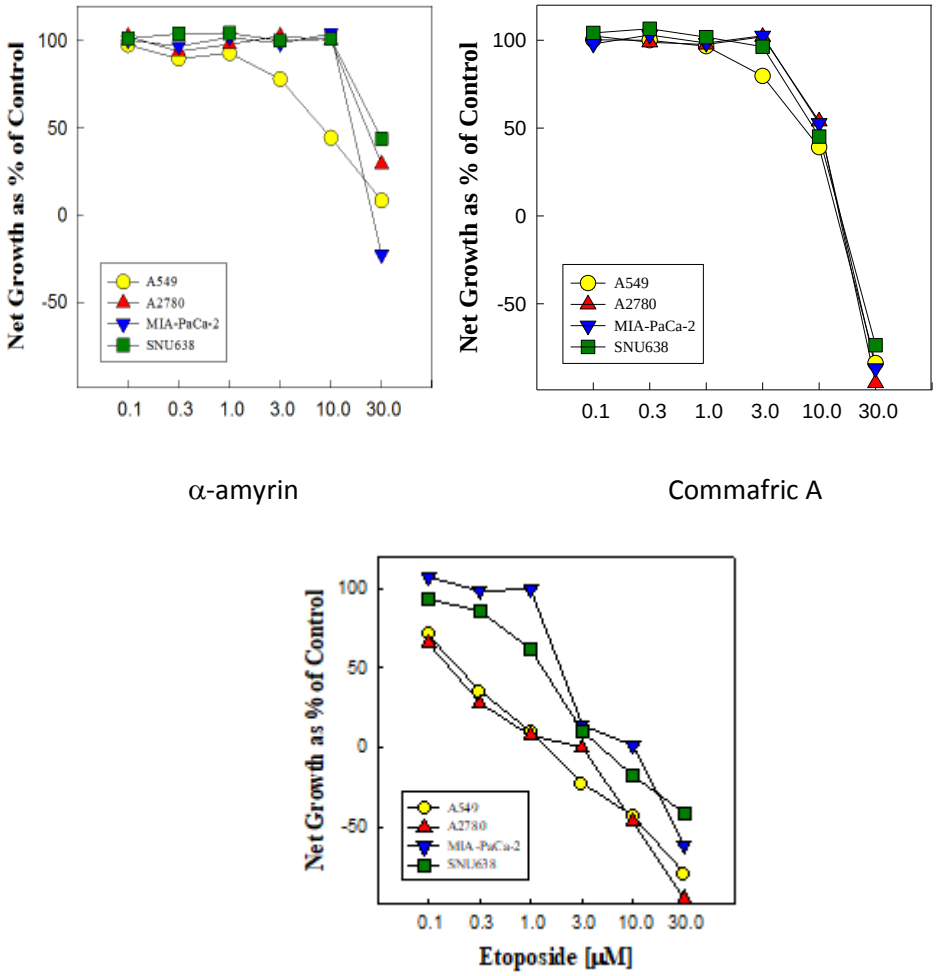

Figure 4.3. 6 Dose response curve of commafric A and α-amyrin isolated from *C. africana* hexane fraction against A549, A2780, MIA-PaCa-2 and SNU-638.

In general, the cytotoxicity of the isolated compound, commafric A (**113**) from hexane fraction of *C. africana*, displayed potent leading compound antiproliferative activity in the SRB assay (Fig. 4.3.6). Whereas α-amryin had no significant effect on all cancer cell lines tested. commafrric A a tricyclic triterpene with an acid functional group showed anti proliferative activity against A549 (human non-small cell lung cancer 9.58 μM, which is more than twice as α-amryin with 21.78μM (Table 4.3.8, Figure 4.3.6). Literature reveals that, *α*-amyrin (**56**) can be considered cytotoxic [242, 243]. A separate study indicated that the pentacyclic triterpenes α-amyrin stimulates proliferation of human keratinocites but does not protect them against UVB dmage [191, 223]. A review on anti-tumour effect of triterpene acidic compounds with emphasis on tetra and pentacyclic revealed, that they have multiple pharmacological effects including anti-

inflammatory, regulating blood sugar level, antiviral and antitumor activity. More importantly, triterpene acid type compounds has become one of the most popular topics recently because of its selective toxic effects on cancer cells and harmless to normal cells at the same time [151].

4.3.2 Anti-inflammatory activity of essential oils of *commiphora* species

Although there were previous reports on anti-inflammatory effect of *Commiphora* species the essential oils of selected *Commiphora* species involved have not been identified yet. Therefore, in this study the effect of essential oil hydrodistillate from resin of four *Commiphora* species evaluated on mediators of inflammation *in vitro,* i.e. nitric oxide. Nitric oxide (NO) plays an important role in the inflammatory processes [244]. Inhibition of excess NO production has been used as an assay in the screening of anti-inflammatory drugs. Of the selected four *Commiphora* species, *C. africana* essential oil slightly inhibited the ability of LPS-stimulated macrophage cells to release nitric oxide, NO, (5.1% at 10 μg/ml and 12.12% at 20 μg/ml) (Figure 4.3.7).

The EO of *C. sphaerocarpa* resin demonstrated a significant inhibition of LPS mediated NO production in RAW264.7 cells by 27.2±3.6% at 10 μg/ml and 62.3±5.2% at 20 μg/ml. Nitric oxide (NO) production by LPS stimulated RAW264.7 macrophage cells was not changed in the treatment of *C. habessinica* and *C. schimperi* resin essential oil as shown in Fig. 4.3.7. As a result, the resin EO of C. sphaerocarpa was investigated for further cytokine studies inorder to determine the different single pathway. The Cells (1.8×10^5 cells/ml) were stimulated with 1 μg/μl LPS for 24 h in the presence of *Commiphora* essential oils (10 and 20 μg/ml), (-) cells without LPS and (+) cells with LPS (1 μg/ml).

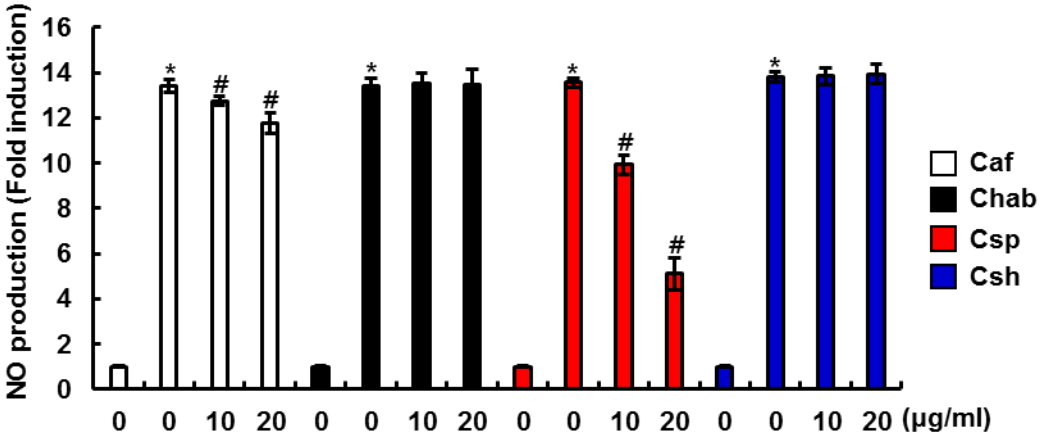

Figure 4.3. 7 Anti-inflammatory effect of *C. habessinica*, *C. africana*, *C. sphaerocarpa* and *C. schimperi* resin EO on NO production in LPS-induced RAW264.7 macrophages cells

4.3.2.1 Effects of *C. sphaerocarpa* EO on *i*NOS expression in LPS-stimulated RAW264.7 macrophages

To determine whether inhibitory effect of EO of resin of *C. sphaerocarpa* against LPS-mediated NO production results from the regulation of iNOS expression; we investigated whether *C. sphaerocarpa* affects *i*NOS expression in LPS-stimulated RAW264.7 cells. As a result, EO of resin of *C. sphaerocarpa* dose-dependently inhibited LPS-mediated *i*NOS overexpression in both protein and mRNA level (Fig.4.3.8).

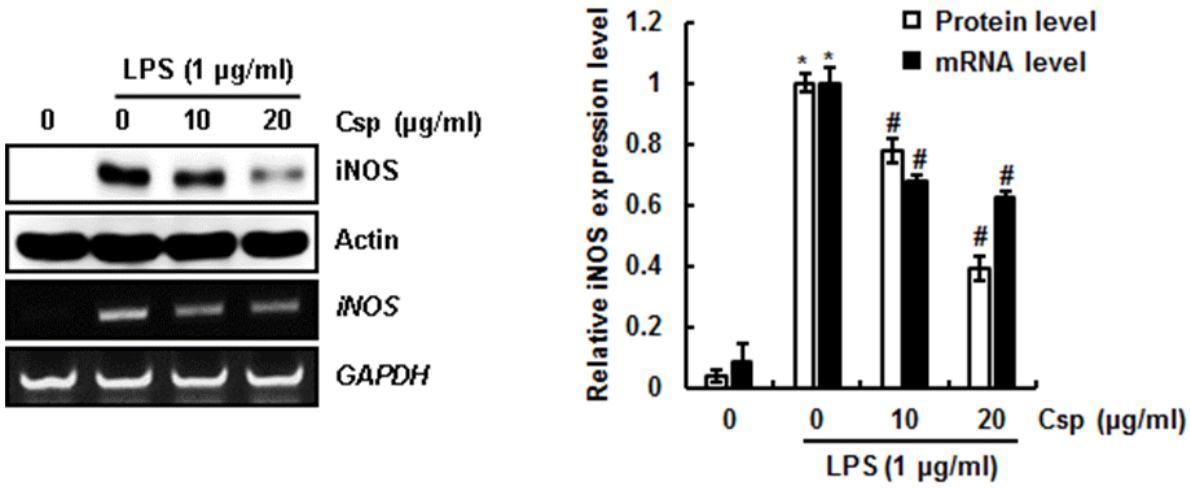

Figure 4.3. 8 Effect of EO of resin of *C. sphaerocarpa* on the expression of iNOS in LPS-stimulated 264.7 macrophage cells.

In identifying the expression of iNOS which stimulate NO production Actin and GAPDH was used as the control protein. The protein levels of iNOS were detected by Western blot analysis. Values given are the mean ± SD (n = 3). *p < 0.05 compared to LPS treatment without resin EOs

4.3.2.2 Inhibitory effect of C. sphaerocarpa EO on LPS-mediated IκB-α degradation and the nuclear accumulation of NF-κB p65 in RAW264.7 cells

Pro-inflammatory mediators such as NO and iNOS have been excessively produced by nuclear transcription factor Kappa-B (NF-κB) and mitogen-activated protein kinases (MAPKs) signaling pathway. Under normal conditions, NF-κB is sequestered in cytoplasm by inhibitor of κB-kinase complex inhibitor (IκB) [245]. However, IκB degradation by the inflammatory stimuli such as LPS leads to the release of NF-κB from its inhibitory complex, which contributes to the nuclear translocation of NF-κB. Thus, we investigated whether EOs of *C. sphaerocarpa* EO inhibits IκB-α degradation and nuclear accumulation of NF-κB p65 to elucidate the inhibitory effect of EO of resin of *C. sphaerocarpa* against NF-κB signaling activation. As a result, the treatment of LPS alone degraded IκB-α and subsequently induced the nuclear accumulation of NF-κB p65 compared with the cells without LPS. In addition, the presence of EOs of *C. sphaerocarpa* did not inhibit LPS-mediated IκB-α degradation and the nuclear accumulation of NF-κB p65 in RAW264.7 cells. These findings indicate that inhibitory effect of *C. sphaerocarpa* against LPS-mediated NO and *i*NOS production may be independent on NF-kB signaling pathway (Fig.4.3.9).

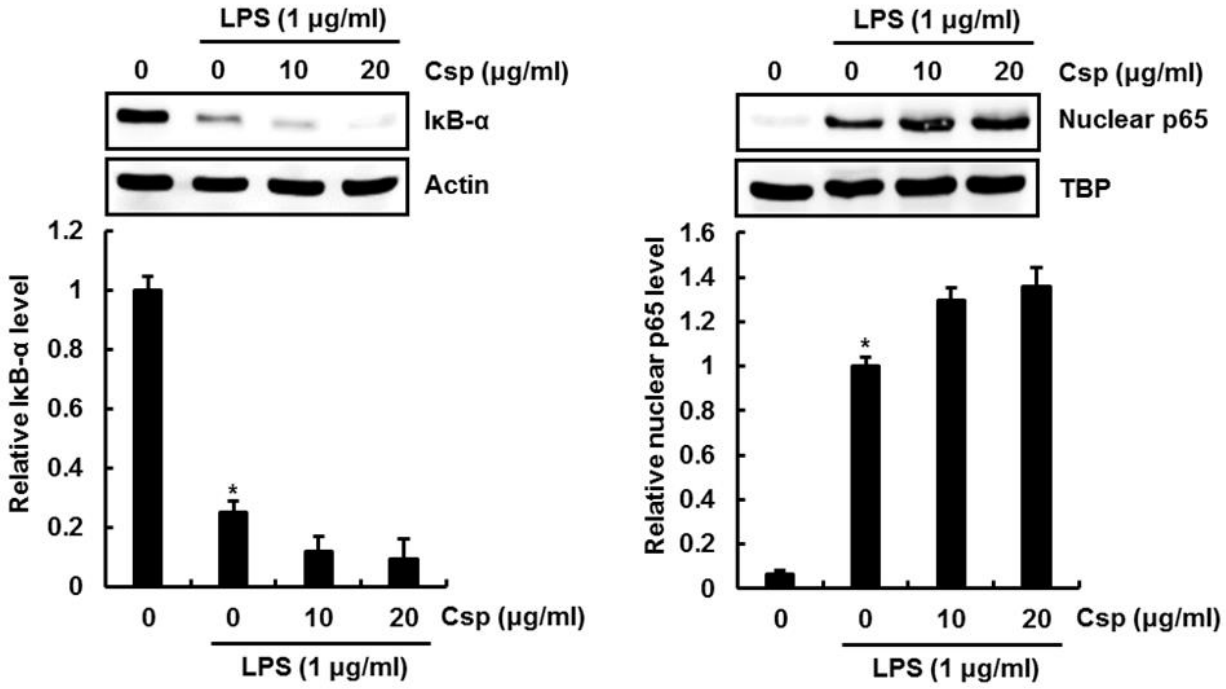

Figure 4.3. 9 Effect of EO of resin of *C. sphaerocarpa* on LPS-mediated IκB-α degradation and the nuclear accumulation of NF-κB p65 in RAW264.7 cells. Actin and TBP used as a positive control

4.3.2.3 Effects of *C. sphaerocarpa* essential oil on LPS-mediated phosphorylation of ERK1/2 and p38 -stimulated RAW264.7 cells

There is growing evidence that inflammatory stimuli such as LPS phosphorylate extracellular signal-regulated kinase 1/2 (ERK1/2) and p38 as MAPKs, which induces the expression of inflammatory mediators. Thus, we investigated whether EO of resin of *C. sphaerocarpa* affects LPS-mediated phosphorylation of ERK1/2 and p38. The findings revealed that EO of resin of *C. sphaerocarpa* inhibited the phosphorylation of ERK1/2 and p38 compared to LPS treatment alone, which indicates that *C. sphaerocarpa* EO may suppress MAPK activation (Figure 4.3.10 A). MAPK activation has been known to encourage the nuclear accumulation of activating transcription factor 2 (ATF2), which is associated with the production of the inflammatory mediators. As a result, we observed that LPS treatment alone induces ATF2 phosphorylation and accumulated ATF2 to the nucleus, while EO of resin of *C. sphaerocarpa* inhibited ATF2 phosphorylation and subsequent ATF2 nuclear accumulation (Figure 4.3.10 B and C). These findings indicate that the inhibition of MAPK activation by EO of resin of *C. sphaerocarpa* may

contribute to the mitigation of ATF2 nuclear accumulation, which exerts EO of resin of *C. sphaerocarpa* anti-inflammatory effect.

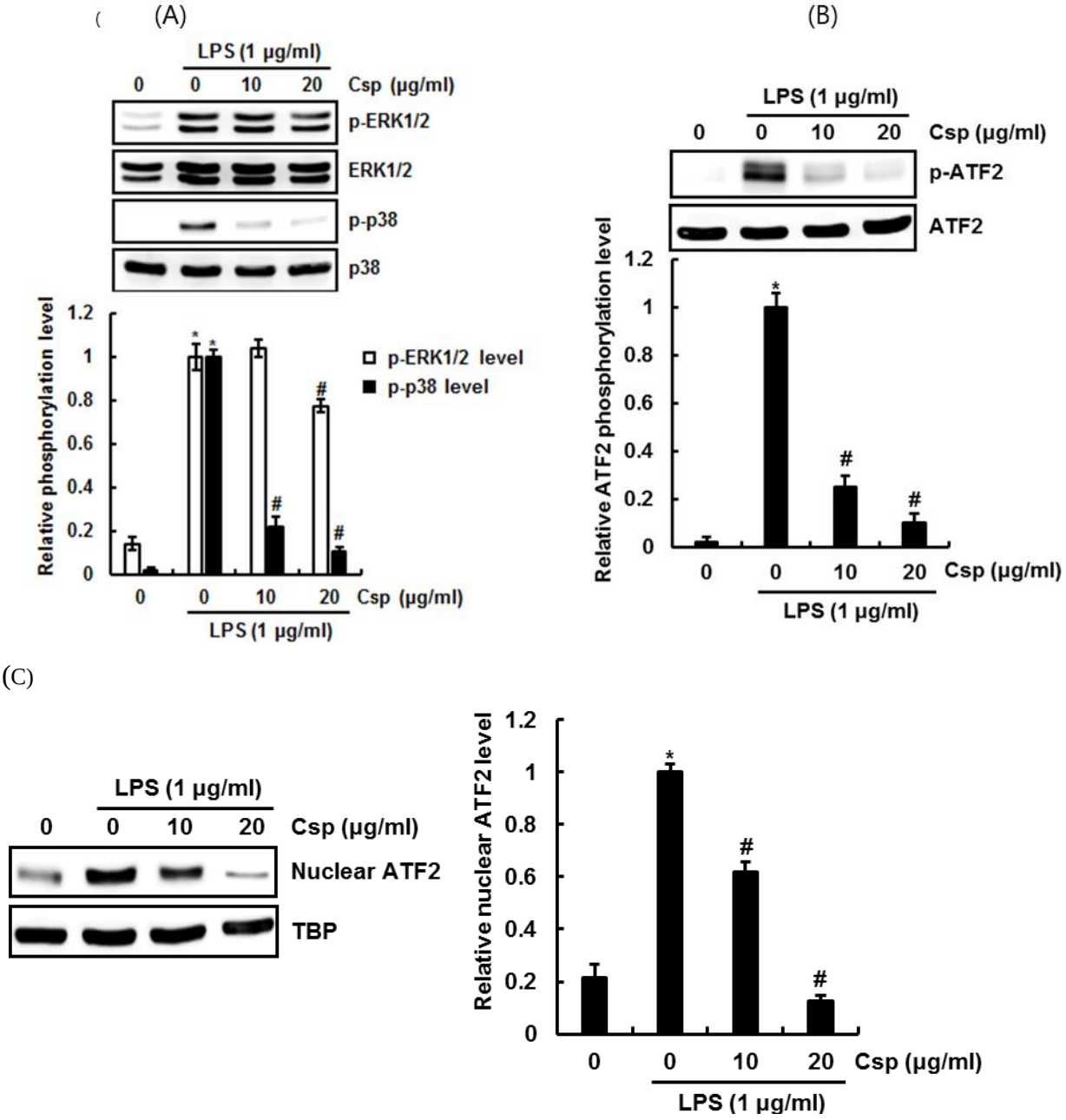

Figure 4.3. 10 Effect of EO of resin of *C. sphaerocarpa* (Csp) on phosphorylation of ERK1/2, p38 and accumulation of ATF2 in LPS-induced RAW264.7 cells.

The levels of p-ERK1/2, p-p38 and p-ATF2 were determined using Western blot method. The Cells were stimulated with LPS (1 μg/μl) in the presence of *C. sphaerocarpa* EO (at 10 and 20 μg/ml).

4.3.2.4 Effect of *C. sphaerocarpa* resin EO on HO-1 by ROS dependent Nrf2 activation and ZnPP in LPS-activated RAW264.7 cells

There is growing evidence that the overexpression of inducible heme oxygenase-1 (HO-1) blocked the production of pro-inflammatory mediators such as NO and iNOS. In addition, HO-1 knockdown induced severe inflammation in the animal model. These previous findings indicate that HO-1 may have anti-inflammatory effect. Thus, we evaluated whether *C. sphaerocarpa* affect HO-1 expression in RAW264.7 cells. As shown in (Fig 4.3.11 D), *C. sphaerocarpa* dose-dependently induced HO-1 overexpression in RAW264.7 cells. NF-E2-related factor 2 (Nrf2) has been reported to be associated with HO-1 expression. Although Nrf2 is sequestered in cytoplasm under normal condition, external stimuli induce Nrf2 activation through the nuclear accumulation of Nrf2. Indeed, overexpression of HO-1 by natural products has been reported to be involved in Nrf2 activation. Reactive oxygen species induce Nrf2 activation, which contributes to HO-1 expression. To investigate that HO-1 expression by *C. sphaerocarpa* results from ROS-dependent Nrf2 activation, RAW264.7 cells were pretreated with NAC as ROS scavenger and then co-treated with EO of resin of *C. sphaerocarpa*. As shown in (Fig 4.3.11 E), the presence of NAC inhibited Nrf2 nuclear accumulation and HO-1 expression induced by EOs of *C. sphaerocarpa* in RAW264.7 cells. These results indicate that *C. sphaerocarpa* mediated HO-1 expression may result from ROS-dependent Nrf2 activation. Next, we evaluated whether EOs of *C. sphaerocarpa* increases ROS level in RAW264.7 cells. As shown in (Fig 4.3.11 F), *C. sphaerocarpa* increased ROS level in RAW264.7 cells. Furthermore, we tested the inhibitory effect of *C. sphaerocarpa* against NO production in presence or absence of ZnPP as a HO-1inhibitor to investigate whether HO-1 expression by *C. sphaerocarpa* contributes to their anti-inflammatory activities. As shown in (Fig 4.3.11 G), the inhibition of HO-1 by ZnPP decreased the inhibitory effect of *C. sphaerocarpa* against NO production in LPS-stimulated RAW264.7 cells. These results indicate that HO-1 may be one of the molecular targets for the anti-inflammatory activity of essential oil resin of *C. sphaerocarpa*.

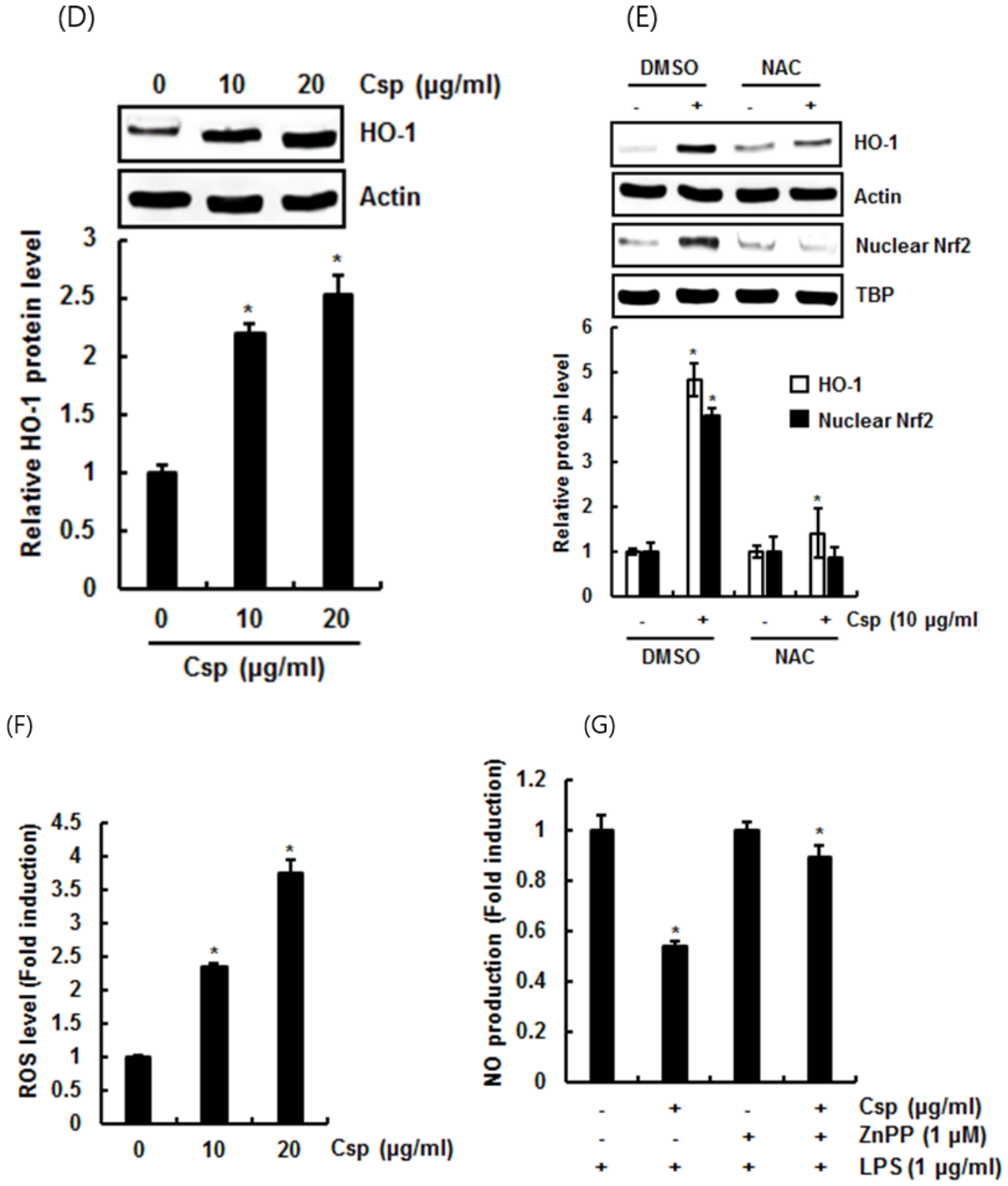

Figure 4.3. 11 Effect of *C. sphaerocarpa* resin EO on HO-1, ROS, Nrf2, ZnPP in LPS-induced RAW264.7 cells.

These findings indicate that the anti-inflammatory activity of *Commiphora* resin EOs depends on the type and amount of triterpene compounds present in the plant. *C. sphaerocarpa* resin

essential oil rich in sesquiterpenes is significantly anti-inflammatory than *C. africana* EO which is rich in monoterpenes. A review on β-caryophyllene and β-caryophyllene oxide (**99**) indicated both possesses significant anticancer activities, affecting growth and proliferation of numerous cancer cells. It was inidcated that β-caryophyllene oxide alters several key pathways for cancer development, such as mitogen-activated protein kinase (MAPK), PI3K/AKT/mTOR/ S6K1 and STAT3 pathways. In addition, treatment with this compound reduces the expression of procancer genes/proteins, while increases the levels of those with proapoptotic properties [126]. Thus, the result provides preclinical validation for the use of EOs of *C. sphaerocarpa* in the management of inflammatory disorders such as asthma, rheumatoid arthritis, rhinitis, conjunctivitis, and multiple sclerosis. In view of its safety and efficacy, this EOs can be useful adjuvants to conventional therapeutic approaches to the management of inflammatory disorders [29].

4.3.3 Antiviral activity of *commiphora* species

4.3.3.1 Antiviral activity of MeOH extract and solvent fractions of *C. habessinica*

As a preliminary means of initially identifying extracts with antiviral activity, the samoles were evaluated *in vitro* against viral strains of A/Puerto Rico/8/34 (H1N1, PR8), A/Hong Kong/8/68 (H3N2, HK) and B/Lee/40 (Lee) by cytopathic effect (CPE) reduction assay, in a two dose assay testing, lower and upper concentrations of 20 and 100 μg/ml. All antiviral activities were assessed at 72 h following treatment. Overall the antiviral activity varied between fractions and viral strains. The ethylacetate and n-butanol fraction showed greater than 50% inhibition at 100 μg/ml towards all tested viral strains (Table 4.3.9). As a result, the two fractions were selected for further screening.

Table 4.3. 9 Anti-viral activity of *C. habessinica* resin crude extract and fractions

S.No	Sample Code	20μg/ml			100μg/ml		
		PR8	HK	Lee	PR8	HK	Lee
1	C. hab-Me	1%	8%	7%	-21%	-10%	-11%
2	C. hab-Hx	50%	35%	46%	-17%	-6%	-8%
3	C. hab-CH	-1%	15%	12%	-21%	-10%	-11%
4	C. hab-EA	25%	17%	15%	78%	81%	63%
5	C. hab-Bu	52%	45%	21%	70%	68%	54%

Table 4.3. 10 Antiviral activity of *C. habessinica* resin EtOAc and n-BuOH fractions against influenza viruses in the CPE reduction assay

			Antiviral activity (EC_{50}: µg/ml)			Selectivity index		
			FluA		FluB	FluA		FluB
No	Code	Toxicity CC_{50} (µg/ml)	H1N1 PR8	H3N2 HongKong	- Lee	H1N1 PR8	H3N2 HongKong	- Lee
1	Chab-BU	53.0	17.0	15.3	23.2	3.1	3.5	2.3
2	Chab-EA	> 100.0	73.4	80.3	> 100.0	> 1.4	> 1.2	ND
3	AMT	> 100.0	> 100.0	6.7	> 100.0	ND	> 14.9	ND
4	RBV	> 100.0	23.0	22.4	30.0	> 4.3	> 4.5	> 3.3
5	OSV-C	> 100.0	0.1	< 0.005	1.0	> 909.1	> 20000.0	> 104.2

CC_{50}, 50% cell toxicity concentration; EC_{50}, 50% effective concentration; S.I., selectivity index = CC_{50}/EC_{50}; PR8, A/Puerto Rico/8/34 (H1N1); HK, A/Hong Kong/8/68 (H3N2); Lee, B/Lee/40; AMT, amantadine hydrochloride; OSV-C, oseltamivir carboxylate; RBV, ribavirin

Cell viability was measured using MTT to estimate the CC_{50} and EC_{50} values before and after infection of MDCK cells with PR8, HK and Lee (Table 4.3.10). The OSV-C (an NA inhibitor) and RBV (a viral polymerase inhibitor) efficiently inhibited the replication of all viral strains tested, confirming the reliability of the assay. The EtOAc and *n*-BuOH fraction obtained from the MeOH extract through liquid - liquid partitioning from *C. habessinica* resin exhibited EC_{50} values 73.4 and 17.0 µg/mL for PR8, 80.3 and 15.3 µg/mL for HK respectively. However, the EtOAc fraction was not cytotoxic to MDCK cells at the highest concentration used, 100.0 µg/mL (Table 4.3.10). The EtOAc fraction was active against Flu A viruses, even though it showed less selectivity index compared to the positive control (Table 4.3.10 and Figure 4.3.12).

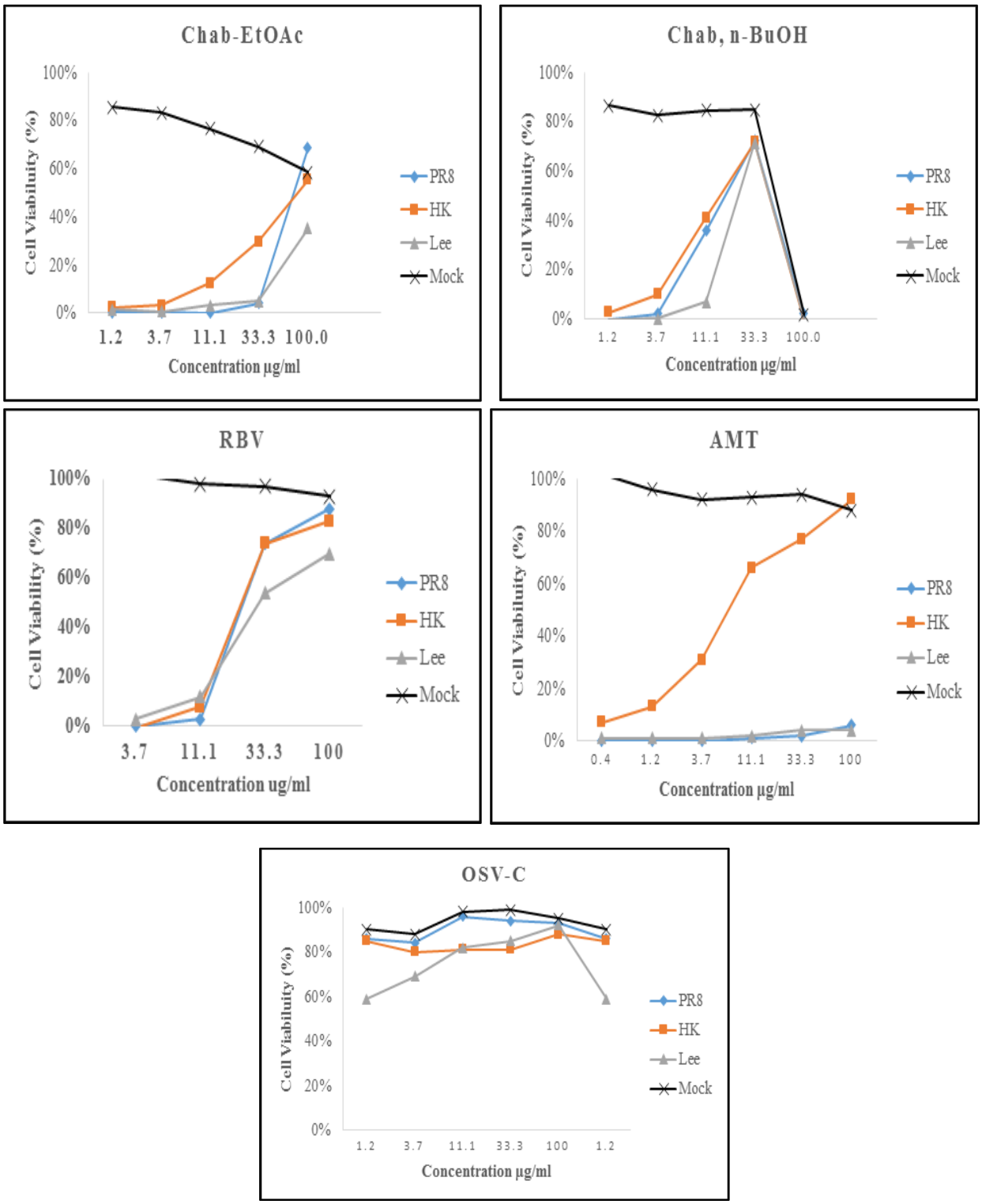

Figure 4.3. 12 Dose response curve of EtOAc fraction against PR8, HK and LEE and the MDCK host cell line. The values are means ± standard deviation (SD) from three replicates

4.3.3.2 Antiviral activity of MeOH extract and solvent fractions of *C. africana*

The anti-viral properties of crude extract and solvent fractions of *C. africana* have been demonstrated by *in vitro* assay using CPE effect.

Table 4.3. 11 Antiviral activity of methanol extract and related fractions of *C. africana* resin against influenza PR8, HK, Lee viruses infecting MDCK cells

Extract/Fractions	20 μg/ml			100 μg/ml		
	PR8	HK	Lee	PR8	HK	Lee
MeOH	1%	17%	4%	-3%	17%	20%
Hexane	1%	12%	13%	-21%	-10%	-10%
Chloroform	5%	25%	12%	-21%	-10%	-10%
EtOAc	7%	12%	21%	-7%	-8%	-1%

The above preliminary data illustrates that the crude extract and solvent fractions of *C. africana* lacks antiviral effect at 20 and 100 μg/ml with the lowest percent inhibition.

4.3.3.3 Antiviral activity of MeOH extract and solvent fractions of *C. sphaerocarpa*

There is an increasing need for substances with antiviral activity since the treatment of viral infections with available antiviral drugs often leads to the problem of viral resistance. Influenza A viruses are severe pathogens to public human health and approximately 10-20 % of the world population are infected in each year's flu season. However, we are limited in the countermeasures to fight against influenza infection, and oseltamivir is the only orally bioavailable drug in the United States. To meet the demand of novel antivirals that are needed to combat multidrug-resistant influenza A strains, we focus on evaluating crude extract and related solvent fractions of C. sphaerocarpa antiviral effect. The crude extract and related fractions obtained after liquid - liquid solvent separation of *C. sphaerocarpa* resin were investigated for potential antiviral effect against influenza type A, B and Lee viruses *in vitro*.

Table 4.3. 12 Antiviral activity of methanol extract and related fractions of *C. sphaerocarpa* resin against influenza PR8, HK, Lee viruses infecting MDCK cells

No	Extract/Fractions	20 μg/ml			100 μg/ml		
		PR8	HK	Lee	PR9	HK	Lee
1	MeOH	-1%	11%	2%	19%	7%	28%
2	*n*-Hexane	23%	4%	14%	95%	78%	97%
3	$CHCl_3$	41%	21%	45%	-21%	-10%	-11%
4	*n*-EtOAc	10%	7%	15%	127%	140%	156%

Table 4.3. 13 Antiviral activity of *C. spaherocarpa* resin n-hexane and EtOAc fractions against influenza viruses in the CPE reduction assay

			Antiviral activity ($EC_{50:}$ ug/ml)			Selectivity index		
		Toxicity	FluA	FluA	FluB	FluA	FluA	FluB
		CC_{50}	H1N1	H3N2	-	H1N1	H3N2	-
No	Code	(ug/ml)	PR8	HongKong	Lee	PR8	HongKong	Lee
1	Csp-Hx	> 100.0	> 100.0	> 100.0	> 100.0	ND	ND	ND
2	Csp-EA	> 100.0	> 100.0	77.0	95.7	ND	> 1.3	> 1.0
3	AMT	> 100.0	> 100.0	6.7	> 100.0	ND	> 14.9	ND
4	RBV	> 100.0	23.0	22.4	30.0	> 4.3	> 4.5	> 3.3
5	OSV-C	> 100.0	0.1	< 0.005	1.0	> 909.1	> 20000.0	> 104.2

The anti-influenza viral activity of *n*-hexne and EtOAc fraction from *C. sphaerocarpa* resin evaluated by CPE inhibition assay showed moderate inhibition with EC_{50} values 77.0 μg/mL and 95.7 μg/mL for H3N2 and Lee Influenza A and B type viruses respectively (Table 4.3.13). The *n*-hexane and EtOAc fraction were not cytotoxic to MDCK cells at the highest concentration used, 100.0 μg/Ml (Figure 4.3.13 and Table 4.3.13).

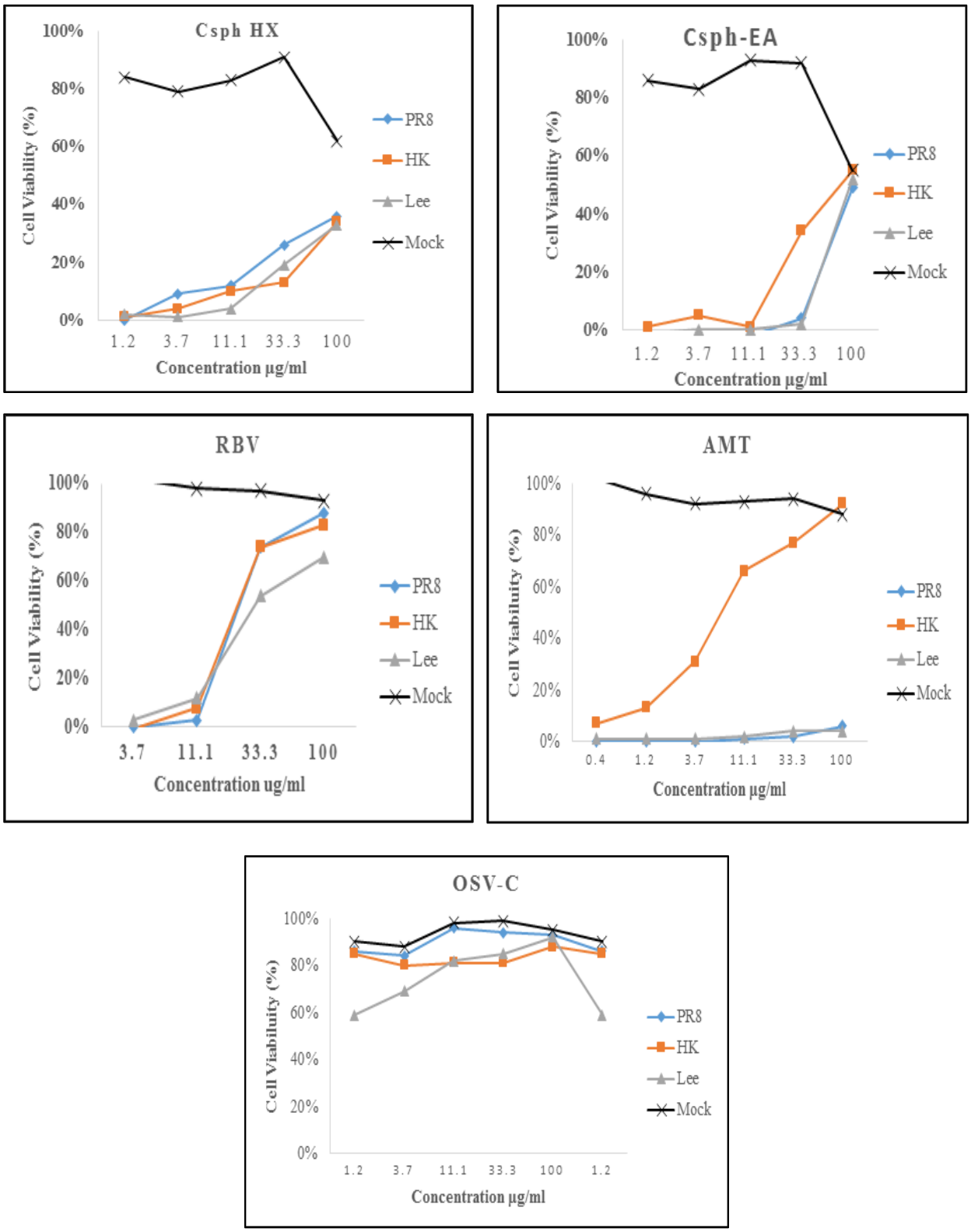

Figure 4.3. 13 Dose response curves of csp-Hx, Csp-EtOAC fractions from *C. sphaerocarpa* against PR8, HK and Lee and the MDCK host cell line.

In this study cell viability was measured by MTT assay. AMT (amantadine), RBV and OSV-C (Oseltamivir carboxylate) were used as a positive control. The values are means ± standard deviation (SD) from three replicates.

4.3.3.4 Antiviral activity of MeOH extract and solvent fractions of *C. schimperi*

C. schimperi resin is one of a common medicinal plant in Southern Ethiopia, Borena Zone and has been used in traditional medicine along with other medicinal plants to treat various ailments. The plant contains phytochemicals with various biological properties; however, its antiviral effect has not yet been demonstrated. This study was aimed to evaluate the anti-influenza virus activity of crude extract of *C. schimperi* resin and related solvent fractions, to characterize its antiviral effect. Anti-influenza virus activity of the crude extract of *C. schimperi* resin and related solvent fractions against virus strains A/Puerto Rico/8/34 (H1N1, PR8), A/Hong Kong/8/68 (H3N2, HK) and B/Lee/40 (Lee) was evaluated on the basis of cytopathic effect (CPE). In the primary screening, the crude MeOH extract, $CHCl_3$ and EtOAc fractions displayed no anti-influenza activity at 20 and 100 μg/ml (Table 4.3.14). The *n*-hexane fraction displayed mariginal activity. As a result, crude MeOH extract, $CHCl_3$, *n*-hexane and EtOAc fractions were excluded from further antiviral assays and the *n*-BuOH fraction with significant cell vibility at 100 μg/ml against the influenza viral strains selected for secondary screening.

Table 4.3. 14 Antiviral activity of crude extract and solvent fractions of *C. schimperi* resin against influenza viruses

Extract/Fraction	20μg/ml			100μg/ml		
	PR8	HK	Lee	PR8	HK	Lee
MeOH	7%	6%	6%	14%	11%	34%
n-Hexane	19%	18%	18%	79%	54%	82%
$CHCl_3$	22%	38%	49%	-21%	-10%	-10%
EtOAc	6%	-3%	4%	26%	13%	21%
n-BuOH	30%	50%	26%	111%	109%	102%

The *n*-BuOH fraction from *C. schimperi* resin showed anti-influenza A virus activity with an EC_{50} of 19.1 μg/mL and 7.6 μg/mL and selectivity index of > 5.2, > 13.2 for PR8 and HK, respectively (Table 4.3.15). Moreover, the n-BuOH fraction was not cytotoxic to MDCK cells at

the highest concentration used, 100.0 µg/mL. AMT, RBV and OSV-C were used as a positive control. The result showed that the *n*-BuOH fraction is more potent than the positive control ribavirin with selectivity index of > 4.3 and > 4.5 for influenza A type viruses PR8 and HK, respectively. Furthermore, the n-BuOH fraction showed comparable potent antiviral activity with relatively high S.I. values (Table 4.3.7), to Amatidine (AMT) the positive control against H3N2 (>13.2).

Table 4.3. 15 Antiviral activity of *n*-BuOH fraction from *C. schimperi* resin against influenza viruses in the CPE reduction assay

		Antiviral activity (EC_{50}: ug/ml)			Selectivity index (S.I)		
	Toxicity	FluA	FluA	FluB	FluA	FluA	FluB
	CC_{50}	H1N1	H3N2	-	H1N1	H3N2	-
Sample	(µg/ml)	PR8	H.K	Lee	PR8	HK	Lee
n-BuOH	> 100.0	19.1	7.6	50.0	> 5.2	> 13.2	> 2.0
AMT	> 100.0	> 100.0	6.7	> 100.0	ND	> 14.9	ND
RBV	> 100.0	23.0	22.4	30.0	> 4.3	> 4.5	> 3.3
OSV-C	> 100.0	0.1	< 0.005	1.0	> 909.1	> 20000.0	> 104.2

CC_{50}, 50% cell toxicity concentration; EC_{50}, 50% effective concentration; S.I., selectivity index = CC_{50}/EC_{50}; PR8, A/Puerto Rico/8/34 (H1N1); HK, A/Hong Kong/8/68 (H3N2); Lee, B/Lee/40.; AMT-Amatidine; OSV-C oseltamivir carboxylate; RBV ribavirin. (ND) Not determined.

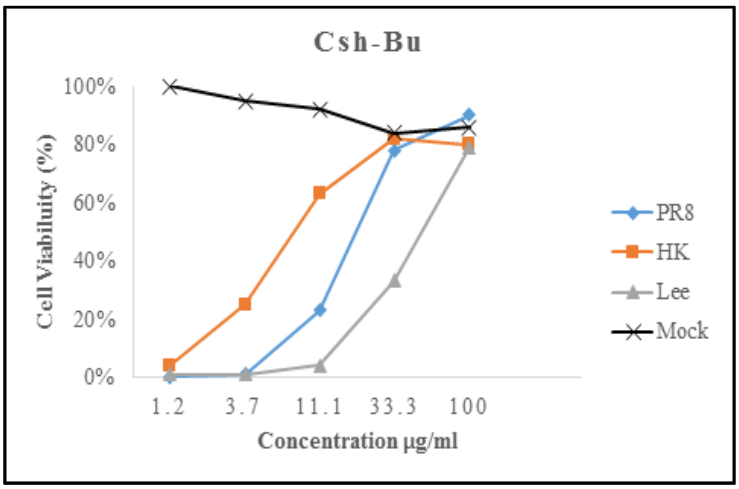

Figure 4.3. 14 Dose response curve of n-BuOH fraction against PR8, HK and Lee and the MDCK host cell line.

Cell monolayers were mock-infected or infected with influenza A and B viruses at a MOI of 0.001 for 1h. After washing with PBS, compounds serially diluted in MEM with 2 µg/mL TPCK-trypsin were added to the wells and incubated for 3 days. Cell viability was measured by MTT assay.

4.3.4 Antidengue activity of *commiphora* species

4.3.4.1 Antidengue activity of MeOH extract and solvent fractions of *C. habessinica*

In this study, preliminary *in vitro* inhibitory activities of *C. habessinica* resin extract and solvent fractions having different polarity towards DENV-2 replication was evaluated at 20 µg/ml and 100 µg/ml. The effect of crude extract and solvent fractions *in vitro* cell viability was assessed by IFA assay. In order to evaluate the antiviral activity, DENV infected cells were treated with non-cytotoxic concentrations of crude extract and solvent fractions for 48 h and virus yields were quantified by IFA assay. The 50% effective concentration (EC_{50}) was of selected fractions determined and the selectivity index (SI) was calculated as the ratio CC_{50}/EC_{50}.

Table 4.3. 16 Activities of crude extract and fractions of *C. habessinica* against Dengue virus

		20μg/ml		100μg/ml	
No	Sample Code	% Cell viability	% inhibition	% Cell viability	% inhibition
1	*C. hab*-Me	15%	99%	0%	100%
2	*C. hab*-Hx	77%	6%	0%	100%
3	*C. hab*-CH	39%	52%	0%	100%
4	*C. hab*-EA	94%	-5%	75%	100%
5	*C. hab*-Bu	99%	86%	78%	100%

In anti-dengue activity, extracts were selected for secondary screening on the basis of inhibition greater than 50 % at concentrations of the upper limit (100 μg/ml) tested. Extracts were considered moderately active showed cytotoxicity greater than 80% inhibition at 100 μg/ml with higher percent cell viability, eventhough the crude MeOH extract, n-hexane and chloroform fractions showed 100 % inhibition at 100 μg/ml, their cell viability towards MDCK cells was found to be zero at 100 μg/ml resulted them out of the secondary test. The EtOAC fraction showed weak inhibition at the lower concentration i.e., 20 μg/ml (Table 4.3.16).

Very active extracts showed 50% or greater inhibition at 20 μg/ml, these extracts were selected for further screening at a wider range of concentrations. Extracts exhibiting greater than 80% inhibition at 20 μg/ml were considered potent and identified as prime targets for further screening. Based on the above setted criteria, the *n*-BuOH fraction was positive non-cytotoxic at 20, 100 μg/ml and categorized as potent and chosen for the secondary screening test (Table 4.3.16).

4.3.4.2 Antidengue activity of MeOH extract and solvent fractions of *C. africana*

In this study the *in vitro* potential antidengue MeOH extracts and solvent fractions of *C. africana* resin have been evaluated whether or not effective against DENV-2 serotypes for further screening. Thus, *C. africana* resin extract and solvent fractions on DENV-2 serotype in Vero cell line compared with known antiviral drug Ribavirin (the positive control). The hexane fraction as indicated in Table 4.3.17 showed 100 % inhibition at the concentration of 100 μg/ml with 53% cell viability. Overall antiviral activity varied between fractions, with chloroform and hexane fractions showed greater percent cell viability and percent inhibition at 100 μg/ml respectively.

However, extracts and fractions exhibiting greater than 80% inhibition at 20 µg/ml were considered potent and identified as prime targets for further screening whereas those extracts and fractions with 80% and above inhibition at 100 µg/ml considered moderate anti-dengue activity. Based on these criteria, the hexane and chloroform fractions were categorized as moderately active it showed high % cell viability 68 % with 97 % inhibition at 100 µg/ml (Table 4.3.17).

Table 4.3. 17 Anti-Dengue virus activity of *C. africana* resin crude extract and fractions

No	SAMPLE	100µg/ml		20µg/ml	
		% Cell viability	% inhibition	% Cell viability	% inhibition
1	MeOH	32%	60%	79%	4%
2	n-Hexane	53%	100%	65%	20%
3	$CHCl_3$	68%	97%	70%	15%
4	EtOAc	68%	17%	71%	13%

4.3.4.3 Antidengue activity of MeOH extract and solvent fractions of *C. sphaerocarpa*

Although, so far there is no therapeutic drugs available against dengue viruses, there is ongoing effort to search for novel potential anti-dengue herbal products. Table 4.3.18 demosnstrates the percentage cell viability and percentage inhibition of the resin crude extract and solvent fractions of *C. sphaerocarpa* against DENV-2 serotypes at 20 and 100 µg/ml. The inhibitory activity of the EtOAc fraction against DENV-2 serotypes showed highest inhibition 89% with a percent cell viability of 59% (Table 4.3.18). The percent inhibition result is modest to undertake further investigation.

Table 4.3. 18 Anti-Dengue virus activity of *C. sphaerocara* resin crude extract and related fractions

No	*C. sphaerocarpa* Extract/Fractions	100ug/ml		20ug/ml	
		% Cell viability	% inhibition	% Cell viability	% inhibition
1	MeOH	78%	2%	94%	-14%
2	n-Hexane	95%	-15%	86%	-5%
3	$CHCl_3$	2%	100%	83%	-1%
4	EtOAc	59%	89%	64%	22%

4.3.4.4 Antidengue activity of MeOH extract and solvent fractions of *C. schimperi*

The effect of crude extract and solvent fractions *in vetro* cell viability was assessed by the IFA method and the % inhibition was determined inorder to evaluate the antiviral activity. DENV-2 infected cells were treated with crude extract and solvent fractions and % cell viability was quantified by IFA assay. In this study the *n*-butanol fraction showed 100 % inhibition against DENV-2 at 100 μg/ml with 92% cell viability compared to the rest of fractions and the crude extract which was with medium percent inhibition (72%) and the smallest non-cytoxic concentration i.e 2% cell viability. None of the other fractions exhibited virucidal effect against dengue virus serotype 2 (DENV-2) (Table 4.3.19). *C. schimperi* resin from which crude MeOH extract and solvent fractions have been prepared and tested to detect inhibition activity against DENV-2 are listed in Table 4.3.19.

Table 4.3. 19 Anti-Dengue virus activity of *C.schimperi* resin crude extract and fractions

Extract/Fraction	100 μg/ml		20ug/ml	
	% Cell viability	% inhibition	% Cell viability	% inhibition
MeOH	72%	10%	81%	1%
n-Hexane	97%	-10%	89%	-9%
$CHCl_3$	2%	100%	83%	-1%
EtOAc	48%	40%	67%	18%
n-BuOH	92%	100%	103%	-22%

CHAPTER FIVE
CONCLUSION AND RECOMMENDATION

5.1 Conclusion

This study is the first report on anti-inflammatory of essential oils, anti-proliferative, antiviral and antidengue virus activity of resins of the selected resins of *Commiphora* species MeOH extract, n-heane, $CHCl_3$, EtOAc and BuOH fractions. The anti-inflammatory activity of *Commiphora* resin EOs depends on the type and amount of triterpenes present in the plant. *C. sphaerocarpa* resin EO with 94.19 % sesquiterpenes predominantly α-copaene (22.7%), β-caryophyllene (28%) and caryophyllene oxide (13.9%) dose dependently inhibited NO production and was found to be significant. Whereas, *C. africana* resin EO with 91.6 % monoterpenes mainly α-pinene (29.1%), β-pinene (6.2%), cis-Verbenol (12.7%) and verbenone (12.1%) monoterpenes slightly inhibited NO production. EOs of *C. habessinica* and *C. schimperi* with high perentage of aliphatic hydrocarbons couldn't block NO production or showed no anti-inflammatory effect with the reated dose. The order of *in vitro* anti-inflammatory activity of EOs indicated, sesquiterpenes > monoterpenes > aliphatic hydrocarbons. Furthermore, EO of *C. sphaerocarpa* resin inhibited LPS-mediated iNOS overexpression, phosphorylation of ERK1/2, p38, ATF2, Nrf2 nuclear accumulation and HO-1 expression, ROS regulation. Thus, EO of *C. sphaerocarpa* resin may possibly be useful as anti-inflammatory agent.

It is important to note, the *in vitro* anti-proliferative activity of extracts and related fractions of the resisn of native *Commiphora* species on cell growth in A549, A2780, MIA-paca-2 and SNU-638 cancer cells indicated the prescence of therapeuically potential and specific active compoinds. The inhibition of cell proliferation was determined to be highly dose-dependent.

In the cytotoxicity assay, the A549 (NSCLC) cell line was the most sensitive to the *Commiphora* species in our study. A mixture of cholesterol and lathosterol isolated from chloroform fraction of *C. habessinica* with 1~1 ratio showed a promising cytotoxic activity against A549 cancer cell line (synergism) than the individual constituents and justify the prescence of cholesterol increases membrane permeability and enhance channel of drug(s) into cells. Thus, the

cytotoxicity of chloroform fraction against all cancer cell lines tested attributed to synergetic effect of multiple ingredients.

Commafric A, a tricyclic triterpene acid was found to be the highest among the isolated compounds towards NSCLC (A549) with IC_{50} value of 4.52 μg/ml. The compound can be modified to increase its cytotoxicity, since triterpene acid type compounds has become one of the most popular topics recently because of its selective toxic effects on cancer cells and harmless to normal cells at the same time.

The *n*-BuOH fraction of *C. schimperi* showed desirable antiviral activity in reducing type A influenza virus (PR8 and HK) replication in MDCK cells, with EC_{50} values 19.1 for PR8 7.6 μg/mL HK, which is, higher than the positive control ribavirin without cytotoxicity at the maximum concentration treated (100.0 μg/mL). Our study suggests that the *n*-BuOH fraction of *C. schimperi* could be a source of compounds promising inhibitors of influenza A type viruses and applied to development of a novel herbal medicine.

The *C. habessinica* resin *n*-BuOH fractions also showed highest activity against DENV-2 serotype. Further investigation is required, including the further isolation, separation and characterization of active component (s) from active fractions responsible for the anti-proliferative, anti-viral activities and anti-dengue activity.

5.2 Recommendations

This study intends to contribute towards the knowledge base of *Commiphora* species with therapeutic potential. It should be noted that it acutely only encompasses four species native to Ethiopia, and the biological activities and phytochemistry of other *Commiphora* species should also be investigated.

The active extracts and fractions of *Commiphora* species require further investigation, specifically in terms of the isolation, and characterisation of the compounds responsible for the anti-proliferative and anti-viral activities. GC-MS analysis of the chloroform fraction revealed the presence of cytotoxic compounds, such as lupeol (**119**), palmitic acid vinyl ester, octadecanoic acid that requires isolation, characterization and screening against cancer cell lines

tested. Additional work is required, including further separation and structural determination of the isolated component(s).

Mode of action of isolated compounds should be studied inorder to make a complete understanding of their pharmacological activity. Investigations involving different combinations of selected *Commiphora* extracts, or combinations of *Commiphora* resin extracts with other potentially active plant extracts and mixtures of isolated compounds should be carried out to assess prescence of synergistic or antagonistic effects. This study has proven the existence of a compound or compounds with potential *in vitro* antiproliferative activity in different *Commiphora* species, extracts and fractions of solvents of different polarity. Activity-guided fractionation, isolation and identification of these compounds is imperative and may lead to the development of novel treatments in the global struggle against cancer and cancer-related ailments and viral diseases. Further analysis must be conducted using different detectors and chromatographic techniques such as tandem LC-MS/MS spectrometry, to provide a greater insight of the phytochemical composition of this species.

REFERENCES

1. Amin, A.R., Omer K.F, Dong M., Perspectives *for cancer prevention with natural compounds.* Journal of clinical oncology, 2009. **27**(16): p. 2712.
2. Cragg, G.M. and D.J. Newman, *Biodiversity: A continuing source of novel drug leads.* Pure and applied chemistry, 2005. **77**(1): p. 7-24.
3. Ifeoma, O. and S. Oluwakanyinsola, *Screening of herbal medicines for potential toxicities*, in *New Insights into Toxicity and Drug Testing*. 2013, IntechOpen.
4. Schmidt, B.M., Ribnicky, D.M., Lipsky, P.E., Raskin, I., *Revisiting the ancient concept of botanical therapeutics.* Nature chemical biology, 2007. **3**(7): p. 360.
5. Singh, R., *Medicinal plants: A review.* Journal of Plant Sciences, 2015. **3**(1-1): p. 50-55.
6. Endashaw, B., *Study on actual situation of medicinal plants in Ethiopia.* Japan Association for International Collaboration of Agriculture and Forestry, 2007. **2**: p. 1-9.
7. Tadesse, M. and B. Mesfin, *A review of selected plants used in the maintenance of health and wellness in Ethiopia.* Ethiopian e-Journal for Research and Innovation Foresight, 2010. **2**(1): p. 85-102.
8. Sun, K., X.H. Tang, and Y.K. Xie, *Paclitaxel combined with harmine inhibits the migration and invasion of gastric cancer cells through downregulation of cyclooxygenase‑2 expression.* Oncology letters, 2015. **10**(3): p. 1649-1654.
9. Jacob, S., Aguado, M. F.k, David P.F., *The role of the DNA mismatch repair system in the cytotoxicity of the topoisomerase inhibitors camptothecin and etoposide to human colorectal cancer cells.* Cancer research, 2001. **61**(17): p. 6555-6562.
10. Shao, H., Yang, B.H, Rongrong W.Y, *Matrine effectively inhibits the proliferation of breast cancer cells through a mechanism related to the NF‑κB signaling pathway.* Oncology letters, 2013. **6**(2): p. 517-520.
11. Pezzuto, J.M., *Plant-derived anticancer agents.* Biochemical pharmacology, 1997. **53**(2): p. 121-133.
12. Cragg, G.M. and D.J. Newman, *Plants as a source of anti-cancer agents.* Journal of ethnopharmacology, 2005. **100**(1-2): p. 72-79.
13. Vollesen, K., I. Hedberg, and S. Edwards, *Flora of Ethiopia.* Addis Ababa, Ethiopia. National Herbarium, 1989. **3**: p. 442-478.

14. Tadesse, M. and S. Demissew, *Medicinal Ethiopian plants: inventory, identification and classification.* Plants used on African traditional medicine as practiced in Ethiopia and Uganda, East Africa. Botany 2000: NAPRECA, Monograph Series, 2000. **5**.
15. Dekebo, A., Dagne, E., Curry, Pat., Gautun, Odd., Aasen, A., *Dammarane triterpenes from the resins of Commiphora confusa.* Bulletin of the Chemical Society of Ethiopia, 2002. **16**(1): p. 81-86.
16. Dekebo, A., E. Dagne, and O. Sterner, *Furanosesquiterpenes from Commiphora sphaerocarpa and related adulterants of true myrrh.* Fitoterapia, 2002. **73**(1): p. 48-55.
17. Langenheim, J.H., *Plant resins: chemistry, evolution, ecology, and ethnobotany*. 2003: Oregon, US: Timber Press.
18. Al-Harbi, M.M., Qureshi, S., Raza, M.A., Mohammad M., Giangreco, AB., Shah, A.H *Anticarcinogenic effect of Commiphora molmol on solid tumors induced by Ehrlich carcinoma cells in mice.* Chemotherapy, 1994. **40**(5): p. 337-347.
19. Shen,T., Li, G-H., Wang, X-N., Lou, H-X.., *The genus Commiphora: a review of its traditional uses, phytochemistry and pharmacology.* Journal of ethnopharmacology, 2012. **142**(2): p. 319-330.
20. Nagata, M., *Inflammatory cells and oxygen radicals.* Current Drug Targets-Inflammation & Allergy, 2005. **4**(4): p. 503-504.
21. Nathan, C., *Nitric oxide as a secretory product of mammalian cells.* The FASEB journal, 1992. **6**(12): p. 3051-3064.
22. Lee, Y.G., Lee, W.M., Kim, J.Y., Lee, J.Y, Lee, I-K., Yun, B-S., Rhee, M.H., Cho, J.Y., *Src kinase-targeted anti-inflammatory activity of davallialactone from Inonotus xeranticus in lipopolysaccharide-activated RAW264. 7 cells.* British Journal of Pharmacology, 2008. **154**(4): p. 852-863.
23. Ferenčík, M., Štvrtinová, V., Hulin, I., Novak, M., et al., *Inflammation—a lifelong companion.* Folia microbiologica, 2007. **52**(2): p. 159.
24. Hogg, N. *Free radicals in disease*. in *Seminars in reproductive endocrinology*. 1998. Copyright© 1998 by Thieme Medical Publishers, Inc.
25. Kim, H.Y., Goo, J.H., Joo, Y.Ah., Lee, H.Y., Lee, S.M.O., Kim, N-H.H., Hwang, J.S., et al., *Impact on inflammation and recovery of skin barrier by nordihydroguaiaretic Acid as*

a protease-activated receptor 2 antagonist. Biomolecules & therapeutics, 2012. **20**(5): p. 463.

26. Ohshima, H. and H. Bartsch, *Chronic infections and inflammatory processes as cancer risk factors: possible role of nitric oxide in carcinogenesis.* Mutation Research/Fundamental and Molecular Mechanisms of Mutagenesis, 1994. **305**(2): p. 253-264.
27. Kröncke, K., K. Fehsel, and V. Kolb-Bachofen, *Inducible nitric oxide synthase in human diseases.* Clinical and experimental immunology, 1998. **113**(2): p. 147.
28. Kwon, O-K., Lee, M-Y.,Yuk, J-E., Oh, S-R., Chin, Y-W., Lee, H-K., Ahn, K.-S.., *Anti-inflammatory effects of methanol extracts of the root of Lilium lancifolium on LPS-stimulated Raw264. 7 cells.* Journal of ethnopharmacology, 2010. **130**(1): p. 28-34.
29. Coussens, L.M. and Z. Werb, *Inflammation and cancer.* Nature, 2002. **420**(6917): p. 860.
30. Siegel, R.L., K.D. Miller, and A. Jemal, *Cancer statistics, 2019.* CA: a cancer journal for clinicians, 2019. **69**(1): p. 7-34.
31. Lee, C., J. Baek, and S.-Y. Han, *The role of kinase modulators in cellular senescence for use in cancer treatment.* Molecules, 2017. **22**(9): p. 1411.
32. May, M., *Statistics: Attacking an epidemic. Nature [serial on the Internet] 2014 [acessado 2017 Mar 22]; 509 (7502): S50-S51*.
33. Siegel, R.L., K.D. Miller, and A. Jemal, *Cancer statistics, 2015.* CA: a cancer journal for clinicians, 2015. **65**(1): p. 5-29.
34. Vogelstein, B. and K.W. Kinzler, *Cancer genes and the pathways they control.* Nature medicine, 2004. **10**(8): p. 789.
35. Millimouno, F.M., Dong, J., Yang, L., Li., J., Li,X., *Targeting apoptosis pathways in cancer and perspectives with natural compounds from mother nature.* Cancer prevention research, 2014. **7**(11): p. 1081-1107.
36. Pan, S-Y., Zhou, S-F., Gao, S-H., Yu, Z-L., Zhang, S-F., Tang, M-K., Sun, J-N., Ma, D-L., Han, Y-F., Fong,W-F., *New perspectives on how to discover drugs from herbal medicines: CAM's outstanding contribution to modern therapeutics.* Evidence-Based Complementary and Alternative Medicine, 2013. **2013**.

37. Morrissey, K.M., Yuraszeck, T.M., Li, C-C., Zhang, Y., Kasichayanula, S., et al., *Immunotherapy and novel combinations in oncology: current landscape, challenges, and opportunities.* Clinical and translational science, 2016. **9**(2): p. 89-104.
38. Gordaliza, M., *Natural products as leads to anticancer drugs.* Clinical and Translational Oncology, 2007. **9**(12): p. 767-776.
39. Ijaz, S., Akhtar, N., Khan, M.S., Hameed, A., Irfan, M., Arshad, M.A., Ali, S., Asrar, M., *Plant derived anticancer agents: A green approach towards skin cancers.* Biomedicine & Pharmacotherapy, 2018. **103**: p. 1643-1651.
40. Khan, N. and H. Mukhtar, *Dietary agents for prevention and treatment of lung cancer.* Cancer letters, 2015. **359**(2): p. 155-164.
41. Memirie, S.T., Habtemariam, M.K., Asefa, M., Deressa. B.T., Abayneh, G.T., Biniam A., Mihiret, W., Ababi, G., Jemal, A., Rebbeck, T.R., *Estimates of Cancer incidence in Ethiopia in 2015 using population-based registry data.* Journal of global oncology, 2018. **4**: p. 1-11.
42. Barik, S., *New treatments for influenza.* BMC medicine, 2012. **10**(1): p. 104.
43. Kiyohara, H., Ichino, C., Kawamura, Y., Nagai, T., Sato, N., Yamada, H., *Patchouli alcohol: in vitro direct anti-influenza virus sesquiterpene in Pogostemon cablin Benth.* Journal of Natural Medicines, 2012. **66**(1): p. 55-61.
44. Rahman, N.A., Muliawan, S., Rashid, N.N., Muhamad, M., Yusof, R., *Studies on Quercus iusitanica extracts on DENV-2 replication.* Dengue Bulletin, 2006. **30**: p. 260.
45. Talarico, L.B., Duarte, M.E.R., Zibetti, R.G.M., Noseda, M.D., Damonte, E.B.., *An algal-derived DL-galactan hybrid is an efficient preventing agent for in vitro dengue virus infection.* Planta medica, 2007. **73**(14): p. 1464-1468.
46. Klawikkan, N., Nukoolkarn, V., Jirakanjanakir, N., Yoksan, S., Wiwat, C., Thirapanmethee, K., *Effect of Thai medicinal plant extracts against Dengue virus in vitro.* MU J Pharm, 2011. **38**(1-2): p. 13-18.
47. W.H.O, *Dengue and severe dengue. Fact sheet no. 117.* World Health Organization. Accessed March, 2012. **20**: p. 2013.
48. Goel, A., Patel, D. N., Lakhani, K. K., Agarwal, S.B., Agarwal, A., Singla, S., Agrawal, R., *Dengue fever—a dangerous foe.* J Indian Acad Clin Med, 2004. **5**(3): p. 247-258.

49. Halstead, S.B., *Dengue virus–mosquito interactions.* Annu. Rev. Entomol., 2008. **53**: p. 273-291.
50. Guzman, M.G. Halstead, S.B., Artsob, H., Buchy, P., Farrar, J., Gubler, D. J., Hunsperger, E., Kroeger, A., Margolis, H.S., Martínez, E., *Dengue: a continuing global threat.* Nature reviews microbiology, 2010. **8**(12supp): p. S7.
51. Gibbons, R.V., *Dengue conundrums.* International journal of antimicrobial agents, 2010. **36**: p. S36-S39.
52. Marks, R.M., Lu, H., Sundaresan, R., Toida, T., Suzuki, A., Imanari, T., Hernáiz, M.J., Linhardt, R.J., *Probing the interaction of dengue virus envelope protein with heparin: assessment of glycosaminoglycan-derived inhibitors.* Journal of medicinal chemistry, 2001. **44**(13): p. 2178-2187.
53. Shen, T. and H.X. Lou, *Bioactive constituents of myrrh and frankincense, two simultaneously prescribed gum resins in Chinese traditional medicine.* Chemistry & biodiversity, 2008. **5**(4): p. 540-553.
54. Watt, M. and W. Sellar, *Frankincense & Myrrh: Through the Ages, and a complete guide to their use in herbalism and aromatherapy today*. 2012: Random House.
55. Waterman, P.G. and M.F. Grundon, *Chemistry and chemical taxonomy of the Rutales*. 1983: Academic Press.
56. Vollesen, K., *Burseraceae.* Flora of Ethiopia, 1989. **3**: p. 442-478.
57. Soromessa, T., *Ecological phytogeography: a case study of Commiphora species.* Science, Technology and Arts Research Journal, 2013. **2**(3): p. 93-104.
58. Morikawa, T., H. Matsuda, and M. Yoshikawa, *A review of anti-inflammatory terpenoids from the incense gum resins frankincense and myrrh.* Journal of oleo science, 2017: p. ess16149.
59. Hanuš, L.O. Řezanka, T., Dembitsky., V. M., Moussaieff A., *Myrrh-commiphora chemistry.* Biomedical papers, 2005. **149**(1): p. 3-28.
60. El Ashry., E.S.H., Rashed, N., Salama, O.M., Saleh, A., *Components, therapeutic value and uses of myrrh.* Die Pharmazie-An International Journal of Pharmaceutical Sciences, 2003. **58**(3): p. 163-168.
61. Shen, T., Zhang, L. Wang, Y-Y., Fan, P-H., Wang, X-N., Lin, Z-M., Lou, H-X., *Steroids from Commiphora mukul display antiproliferative effect against human prostate cancer*

PC3 cells via induction of apoptosis. Bioorganic & medicinal chemistry letters, 2012. **22**(14): p. 4801-4806.

62. Cotton, C.M. and P. Wilkie, *Ethnobotany: principles and applications*. 1996: John Wiley & Sons Chichester.
63. Gerique, A., *An introduction to ethnoecology and ethnobotany: Theory and methods.* Integrative assessment and planning methods for sustainable agroforestry in humid and semiarid regions. Advanced Scientific Training. Loja, 2006.
64. Tadesse, W., G. Desalegn, and R. Alia, *Natural gum and resin bearing species of Ethiopia and their potential applications.* Forest Systems, 2007. **16**(3): p. 211-221.
65. Gemedo-Dalle, T., B.L. Maass, and J. Isselstein, *Plant biodiversity and ethnobotany of Borana pastoralists in southern Oromia, Ethiopia.* Economic Botany, 2005. **59**(1): p. 43-65.
66. Demissew, S., *A description of some essential oil bearing plants in Ethiopia and their indigenous uses.* Journal of Essential Oil Research, 1993. **5**(5): p. 465-479.
67. Mohamed, A.A., Ali, S.I., EL-Baz, F.K., Hegazy, A.K., Kord, M.A., *Chemical composition of essential oil and in vitro antioxidant and antimicrobial activities of crude extracts of Commiphora myrrha resin.* Industrial crops and products, 2014. **57**: p. 10-16.
68. Massoud, A., S. El Sisi, and O. Salama, *Preliminary study of therapeutic efficacy of a new fasciolicidal drug derived from Commiphora molmol (myrrh).* The American journal of tropical medicine and hygiene, 2001. **65**(2): p. 96-99.
69. Adebayo, H.A., Aliyu, R., Gatsing, D., Garba, H.I., *The effects of ethanolic leaf extract of Commiphora africana (Burseraceae) on lipid profile in rats.* International Journal of pharmacology, 2006. **2**(6): p. 618-622.
70. Akor, J. and T. Anjorin, *Phytochemical and antimicrobial studies of Commiphora africana root extracts.* International Journal of Agriculture and Biology, 2009. **11**(6): p. 795-797.
71. Abbiw, D., *Useful plants of Ghana, Intermediate Tech.* Publication. London: Royal Botanic Gardens, Kew, 1990. **207**.
72. Dharmananda, S., *Myrrh and frankincense, spiritual significance.* Internet Journal, 2003. **2**: p. 1-6.

73. Shoemaker, M., Hamilton, B., Dairkee., S.H., Cohen, I., Campbell, M.J., *In vitro anticancer activity of twelve Chinese medicinal herbs.* Phytotherapy Research: An International Journal Devoted to Pharmacological and Toxicological Evaluation of Natural Product Derivatives, 2005. **19**(7): p. 649-651.
74. Singh, B.B., Mishra, L.C., Vinjamury, S.P., Aquilina, N., Singh, V.J., Shepard, N., *The effectiveness of Commiphora mukul for osteoarthritis of the knee: an outcomes study.* Alternative therapies in health and medicine, 2003. **9**(3): p. 74-81.
75. Kimura, I., Yoshikawa, M., Kobayashi, S., Sugihara, Y., Suzuki, M., Oominami, H., Murakami, T., Matsuda, H., Doiphode., Vijay, V., *New triterpenes, myrrhanol A and myrrhanone A, from guggul-gum resins, and their potent anti-inflammatory effect on adjuvant-induced air-pouch granuloma of mice.* Bioorganic & medicinal chemistry letters, 2001. **11**(8): p. 985-989.
76. Lemenih, M., T. Abebe, and M. Olsson, *Gum and resin resources from some Acacia, Boswellia and Commiphora species and their economic contributions in Liban, south-east Ethiopia.* Journal of Arid Environments, 2003. **55**(3): p. 465-482.
77. McGuffin, M., Kartesz, J.T., Leung, A.Y., Tucker, A.O., *Herbs of Commerce2nd ed.* American Herbal Products Association, Silver Spring, Maryland, 2000.
78. Gradé, J.T., J.R. Tabuti, and P. Van Damme, *Ethnoveterinary knowledge in pastoral Karamoja, Uganda.* Journal of Ethnopharmacology, 2009. **122**(2): p. 273-293.
79. Koch, A., Tamez, P., Pezzuto, J., Soejarto, D., *Evaluation of plants used for antimalarial treatment by the Maasai of Kenya.* Journal of Ethnopharmacology, 2005. **101**(1-3): p. 95-99.
80. Carroll, J., A. Maradufu, and J. Warthen Jr, *An extract of Commiphora erythraea: a repellent and toxicant against ticks.* Entomologia experimentalis et applicata, 1989. **53**(2): p. 111-116.
81. Kokwaro, J.O., *Medicinal plants of east Africa.* 1976.
82. Asres, K., Tei, A. Moges, G., Sporer, F., Wink, M., *Terpenoid composition of the wound-induced bark exudate of Commiphora tenuis from Ethiopia.* Planta medica, 1998. **64**(05): p. 473-475.
83. Başer, K.H.C., Demirci, B., Dekebo, A., Dagne, E., *Essential oils of some Boswellia spp., myrrh and opopanax.* Flavour and Fragrance Journal, 2003. **18**(2): p. 153-156.

84. Maradufu, A., *Furanosesquiterpenoids of Commiphora erythraea and C. myrrh.* Phytochemistry, 1982. **21**(3): p. 677-680.
85. Guenther, E., *The Essential Oils, Vol. IV.* The Essential Oils, Vol. IV., 1950.
86. Tucker, C. and P. Sellers, *Satellite remote sensing of primary production.* International journal of remote sensing, 1986. **7**(11): p. 1395-1416.
87. Zhu, N., Sheng, S., Sang, S., Rosen, R., T Ho, C-T., *Isolation and characterization of several aromatic sesquiterpenes from Commiphora myrrha.* Flavour and Fragrance Journal, 2003. **18**(4): p. 282-285.
88. Su, S., Wang, T., Chen, Ting., Duan, J-a., Yu, L. Tang, Y., *Cytotoxicity activity of extracts and compounds from Commiphora myrrha resin against human gynecologic cancer cells.* Journal of Medicinal Plants Research, 2011. **5**(8): p. 1382-1389.
89. Patil, V., U. Nayak, and S. Dev, *Chemistry of ayurvedic crude drugs—I: Guggulu (resin from Commiphora mukul)—1: steroidal constituents.* Tetrahedron, 1972. **28**(8): p. 2341-2352.
90. Bajaj, A.G. and S. Dev, *Chemistry of ayurvedic crude drugs—V: Guggulu (resin from commiphora mukul)—5 some new steroidal components and, stereochemistry of guggulsterol-I at C-20 and C-22.* Tetrahedron, 1982. **38**(19): p. 2949-2954.
91. Matsuda, H., Morikawa, T., Ando, S., Oominami, H., Murakami, T., Kimura, I., Yoshikawa, M., et al., *Absolute stereostructures of polypodane-type triterpenes, myrrhanol A and myrrhanone A, from guggul-gum resin (the resin of Balsamodendron mukul).* Chemical and pharmaceutical bulletin, 2004. **52**(10): p. 1200-1203.
92. Singh, S. V., Zeng, Yan X., Dong, V., Victor G, N., Joel B, D., Rajiv, T., Yamini, B., *Caspase-dependent apoptosis induction by guggulsterone, a constituent of Ayurvedic medicinal plant Commiphora mukul, in PC-3 human prostate cancer cells is mediated by Bax and Bak.* Molecular cancer therapeutics, 2005. **4**(11): p. 1747-1754.
93. Matsuda, H., Morikawa, T., Ando, S., Oominami, H., Murakami, T., Kimura, I., Yoshikawa, M., *Absolute stereostructures of polypodane-and octanordammarane-type triterpenes with nitric oxide production inhibitory activity from guggul-gum resins.* Bioorganic & medicinal chemistry, 2004. **12**(11): p. 3037-3046.

94. Morad, S. A.F, Schmidt, C., Büchele, B., Schneider, B., Wenzler, M., Syrovets, T., Simmet, T., *(8 R)-3β, 8-Dihydroxypolypoda-13 E, 17 E, 21-triene Induces Cell Cycle Arrest and Apoptosis in Treatment-Resistant Prostate Cancer Cells.* Journal of natural products, 2011. **74**(8): p. 1731-1736.

95. Meselhy, M.R., *Inhibition of LPS-induced NO production by the oleogum resin of Commiphora wightii and its constituents.* Phytochemistry, 2003. **62**(2): p. 213-218.

96. Shishodia, S. and B.B. Aggarwal, *Guggulsterone inhibits NF-κB and IκBα kinase activation, suppresses expression of anti-apoptotic gene products, and enhances apoptosis.* Journal of Biological Chemistry, 2004. **279**(45): p. 47148-47158.

97. Lv, N., Song, M-Y., Kim, E-K., Park, J-W., Kwon, K-B., Park, B-H., *Guggulsterone, a plant sterol, inhibits NF-κB activation and protects pancreatic β cells from cytokine toxicity.* Molecular and cellular endocrinology, 2008. **289**(1-2): p. 49-59.

98. Dekebo, A., Lang, M., Polborn, K., Dagne, E., Steglich, W., *Four lignans from Commiphora erlangeriana.* Journal of natural products, 2002. **65**(9): p. 1252-1257.

99. Habtemariam, S., *Cytotoxic and cytostatic activity of erlangerins from Commiphora erlangeriana.* Toxicon, 2003. **41**(6): p. 723-727.

100. Battu, G.R., Zeitlin, I.J., Gray, A.I., Waterman P.G., *Inhibitory actions on rat myeloperoxidease of molecules isolated from anti-inflammatory extracts of Commiphora kua*. in *British Journal of Pharmacology*. 1999. Stockton Press Houndmills, Basingstoke Rg21 6xs, Hampshire, England.

101. Ahmed, I. M., Gadir, S. A., Elgilany, E. E., and Abdallah, T. M., *Commiphora africana Resin Phytochemical Analysis & Some Biological Aspects.* European Journal of Medicinal Plants, 2016. **13**(3).

102. Mullauer, F.B., J.H. Kessler, and J.P. Medema, *Betulin is a potent anti-tumor agent that is enhanced by cholesterol.* PloS one, 2009. **4**(4): p. e1.

103. Aiken, C. and C.H. Chen, *Betulinic acid derivatives as HIV-1 antivirals.* Trends in molecular medicine, 2005. **11**(1): p. 31-36.

104. Ma, J., S.H. Jones, and S.M. Hecht, *A Dihydroflavonol Glucoside from Commiphora a fricana that Mediates DNA Strand Scission.* Journal of natural products, 2005. **68**(1): p. 115-117.

105. Cagnoli Bellavita, B., P. Ceccherelli, and P. Damiani, *Cholesterol, campesterol, and β-sitosterol from a Commiphora abyssinica.* Ann Chim (Rome), 1968. **58**: p. 541-545.
106. Brieskorn, C.H. and P. Noble, *Two furanoeudesmanes from the essential oil of myrrh.* Phytochemistry, 1983. **22**(1): p. 187-189.
107. Dekebo, A., Dagne, E., Hansen, L., Gautun, O., and Aasen, A. J. *Crystal structures of two furanosesquiterpenes from Commiphora sphaerocarpa.* Tetrahedron Letters, 2000. **41**(50): p. 9875-9878.
108. Messina, F., Gigliarelli, G., Palmier, A. C., and Marcotullio, M. *Furanodienone: An Emerging Bioactive Furanosesquiterpenoid.* Current Organic Chemistry, 2017. **21**(4): p. 305-310.
109. Dolara, P., Luceri, C., Ghelardini, C., Monserrat, C., Aiolli, S., Luceri, F., Lodovici, a., Menichetti, S., Romanelli, M.N. *Analgesic effects of myrrh.* Nature, 1996. **379**(6560): p. 29.
110. Cavanagh, I. S., Cole, M. D., Cavanagh, I. S., Gibbons, S., Gray, A. I., Provan, G. J., and Waterman, P. G. *A novel sesquiterpene, 1, 2-epoxyfurano-10 (15)-germacren-6-one, from the resin of Commiphora holtziana Engl.* Flavour and fragrance journal, 1993. **8**(1): p. 39-41.
111. Coppen, J.J., *Gums, resins and latexes of plant origin.* 1995.
112. Tian, J. and S. Shi, *Constituents of essential oil of imported Myrrh and gum opoponax.* Zhongguo Zhong yao za zhi= Zhongguo zhongyao zazhi= China journal of Chinese materia medica, 1996. **21**(4): p. 235-7, 256.
113. Racine, P. and B. Auffray, *Quenching of singlet molecular oxygen by Commiphora myrrha extracts and menthofuran.* Fitoterapia, 2005. **76**(3-4): p. 316-323.
114. Fraternale, D., Sosa, S., Ricci, D., Genovese, S., Messina, F., Tomasini, S., Montanari, F., Marcotullio, M.C. *Anti-inflammatory, antioxidant and antifungal furanosesquiterpenoids isolated from Commiphora erythraea (Ehrenb.) Engl. resin.* Fitoterapia, 2011. **82**(4): p. 654-661.
115. Sarup, P., S. Bala, and S. Kamboj, *Pharmacology and phytochemistry of oleo-gum resin of Commiphora wightii (Guggulu).* Scientifica, 2015. **2015**.

116. Saeed, M.A. and A. Sabir, *Antibacterial activities of some constituents from oleo-gum-resin of Commiphora mukul.* Fitoterapia, 2004. **75**(2): p. 204-208.
117. Adam, M.E. and S.A. Selim, *Antimicrobial activity of essential oil and methanol extract from Commiphora molmol (Engl.) resin.* Int J Curr Microbiol Appl Sci, 2013. **2**(12): p. 1-6.
118. Tipton, D.A., Lyle, B., Babich, H., Dabbous, M.K. *In vitro cytotoxic and anti-inflammatory effects of myrrh oil on human gingival fibroblasts and epithelial cells.* Toxicology in vitro, 2003. **17**(3): p. 301-310.
119. Brieskorn, C. and P. Noble, *Constituents of the essential oil of myrrh.* Planta medica, 1982. **44**(2): p. 87-90.
120. Khaleel, C., N. Tabanca, and G. Buchbauer, *α-Terpineol, a natural monoterpene: a review of its biological properties.* Open Chemistry, 2018. **16**(1): p. 349-361.
121. Zhang, Z., Guo, S., Liu, X., and Gao, X. *Synergistic antitumor effect of α-pinene and β-pinene with paclitaxel against non-small-cell lung carcinoma (NSCLC).* Drug research, 2015. **65**(04): p. 214-218.
122. Lis-Balcnin, M., Ochocka, R. J., Deans, S.G., Asztemborska, M., and Hart, S. *Differences in bioactivity between the enantiomers of α-pinene.* Journal of Essential Oil Research, 1999. **11**(3): p. 393-397.
123. Goud, T. V., Reddy, N. S., Krishnaiah, P., and Venkateswarlu, Y. *Spathulenol: a rare sesquiterpene from soft coral Sinularia kavarattiensis.* Biochemical systematics and ecology, 2002. **5**(30): p. 493-495.
124. Yeo, S.K., Ali, A. Y., Hayward, O. A., Turnham, D., Jackson, T., Bowen, I. D., and Clarkson, R. *β-Bisabolene, a Sesquiterpene from the Essential Oil Extract of Opoponax (Commiphora guidottii), Exhibits Cytotoxicity in Breast Cancer Cell Lines.* Phytotherapy research, 2016. **30**(3): p. 418-425.
125. Astani, A. and P. Schnitzler, *Antiviral activity of monoterpenes beta-pinene and limonene against herpes simplex virus in vitro.* Iranian journal of microbiology, 2014. **6**(3): p. 149.
126. Fidyt, K., Fiedorowicz, A., Strządała, L., and Szumny, A. *β-caryophyllene and β-caryophyllene oxide—natural compounds of anticancer and analgesic properties.* Cancer medicine, 2016. **5**(10): p. 3007-3017.

127. Kempen, H-J, Glatz, J.F., Leuven, J.A.G, Van der Vert, H.A and Katan, M.B. *Serum lathosterol concentration is an indicator of whole-body cholesterol synthesis in humans.* Journal of lipid research, 1988. **29**(9): p. 1149-1155.

128. Li, L-H., Dutkiewicz, E.P., Huang, Y-C., Zhou, H-B., and Hsu, C-C. *Analytical methods for cholesterol quantification.* journal of food and drug analysis, 2019. **27**(2): p. 375-386.

129. Poonia, P., Mittal, S.K., Gupta, V.K., and Singh, J. *Sweety. Gum guggul: An Ayurvedic boom.* Int J Pharmacogn Phytochem Res, 2014. **6**: p. 347-54.

130. Gebhard, C., Stämpfli, S. F., Gebhard, C. E., Akhmedov, A., Breitenstein, A., Camici, G. G., Holy, E. W., Lüscher, T. F., and Tanner, F. C. *Guggulsterone, an anti-inflammatory phytosterol, inhibits tissue factor and arterial thrombosis.* Basic research in cardiology, 2009. **104**(3): p. 285-294.

131. Duwiejua, M., Zeitlin, I.J., Waterman, P.G., Chapman, J., Mhango, G.J., and Provan, G.J. *Anti-inflammatory activity of resins from some species of the plant family Burseraceae.* Planta medica, 1993. **59**(01): p. 12-16.

132. Satyavati, G., *Gum guggul (Commiphora mukul)--the success story of an ancient insight leading to a modern discovery.* The Indian journal of medical research, 1988. **87**: p. 327.

133. Banno, N., Akihisa, T., Yasukawa, K., Tokuda, H., Tabata, K., Nakamura, Y., Nishimura, R., Kimura, Y., and Suzuki, T. *Anti-inflammatory activities of the triterpene acids from the resin of Boswellia carteri.* Journal of ethnopharmacology, 2006. **107**(2): p. 249-253.

134. Checker, R., Sandur, S. K., Sharma, D., Patwardhan, R. S., Jayakumar, S., Vineet, S., Gautam, A., Bharat B., and Sainis, K. B. *Potent anti-inflammatory activity of ursolic acid, a triterpenoid antioxidant, is mediated through suppression of NF-κB, AP-1 and NF-AT.* PloS one, 2012. **7**(2): p. e31318.

135. de Melo, C. L., Queiroz, M., Goretti, R., Fonseca, S.G.C, B., Ayla M.C., Lemos, T.L.M., Tiago, S., Santos, F.A.R., and Vietla, S. *Oleanolic acid, a natural triterpenoid improves blood glucose tolerance in normal mice and ameliorates visceral obesity in mice fed a high-fat diet.* Chemico-biological interactions, 2010. **185**(1): p. 59-65.

136. Somova, L.O., Nadar, A., Rammanan, P., and Shode, F.O. *Cardiovascular, antihyperlipidemic and antioxidant effects of oleanolic and ursolic acids in experimental hypertension.* Phytomedicine, 2003. **10**(2-3): p. 115-121.

137. Akihisa, T., Uchiyama, E., Kikuchi, T., Tokuda, H., Suzuki, T., and Kimura, Y. *Anti-tumor-promoting effects of 25-methoxyporicoic acid A and other triterpene acids from Poria cocos.* Journal of natural products, 2009. **72**(10): p. 1786-1792.

138. Pavlova, N.I., Savinova, O.V., Nikolaeva, S.N., Boreko, E.I., and Flekhter, O.B. *Antiviral activity of betulin, betulinic and betulonic acids against some enveloped and non-enveloped viruses.* Fitoterapia, 2003. **74**(5): p. 489-492.

139. Gerrish, D., Kim, I.C., Kumar, D.V., Austin, H., Garrus, J. E., Baichwal, V., Saunders, M., McKinnon, R. S., Anderson, M. B., and Carlson, R. *Triterpene based compounds with potent anti-maturation activity against HIV-1.* Bioorganic & medicinal chemistry letters, 2008. **18**(24): p. 6377-6380.

140. Cunha, L. C., Scalon, e. S., Márcio, L. A., Furtado, N. A.J., Cardoso, V., Adriana, H.C., Martins, C. H., Gomes, da S., Filho, A. C., and Wilson, R. *Antibacterial activity of triterpene acids and semi-synthetic derivatives against oral pathogens.* Zeitschrift für Naturforschung C, 2007. **62**(9-10): p. 668-672.

141. Luo, J. and Z. Lin, *Advances of pharmacological effects of triterpenes from Ganoderma lucidum.* Acta Pharmaceutica Sinica, 2002. **7**.

142. Kikuchi, T., Uchiyama, E., Ukiya, M., Tabata, K., Kimura, Y., Suzuki, T., and Akihisa, T. *Cytotoxic and apoptosis-inducing activities of triterpene acids from Poria cocos.* Journal of natural products, 2011. **74**(2): p. 137-144.

143. Wu, G-S., Lu, J-J., Guo, J-J., Li, Y.B., Tan, W., Dang, Y.Y, Zhong, Z.F, Xu, Z-T., Chen, X-P., and Wang, Y-T. *Ganoderic acid DM, a natural triterpenoid, induces DNA damage, G1 cell cycle arrest and apoptosis in human breast cancer cells.* Fitoterapia, 2012. **83**(2): p. 408-414.

144. Eiznhamer, D. and Z. Xu, *Betulinic acid: a promising anticancer candidate.* IDrugs: the investigational drugs journal, 2004. **7**(4): p. 359-373.

145. Jutooru, I., Chadalapaka, G., Abdelrahim, M., Basha, M.D., Riyaz, S., Ismael, K., Marina, A., Michael, S., and Stephen. *Methyl 2-cyano-3, 12-dioxooleana-1, 9-dien-28-oate decreases specificity protein transcription factors and inhibits pancreatic tumor growth: role of microRNA-27a.* Molecular pharmacology, 2010. **78**(2): p. 226-236.

146. Shanmugam, M. K., Dai, X., Kumar, A., Prem, T., Benny, K.H., Sethi, G., Bishayee, A. *Ursolic acid in cancer prevention and treatment: molecular targets, pharmacokinetics and clinical studies.* Biochemical pharmacology, 2013. **85**(11): p. 1579-1587.

147. Wang, J.-s., T.-n. Ren, and T. Xi, *Ursolic acid induces apoptosis by suppressing the expression of FoxM1 in MCF-7 human breast cancer cells.* Medical Oncology, 2012. **29**(1): p. 10-15.

148. Manu, K. and G. Kuttan, *Ursolic acid induces apoptosis by activating p53 and caspase-3 gene expressions and suppressing NF-κB mediated activation of bcl-2 in B16F-10 melanoma cells.* International immunopharmacology, 2008. **8**(7): p. 974-981.

149. Chang, U-M., Li, C-H., Lin, L-I., Huang, C-P., Kan, L-S., and Lin, S-B. *Ganoderiol F, a ganoderma triterpene, induces senescence in hepatoma HepG2 cells.* Life sciences, 2006. **79**(12): p. 1129-1139.

150. Yang, H., Chen, D., Cui, Q.C., Yuan, X, Dou, Q.P. *Celastrol, a triterpene extracted from the Chinese "Thunder of God Vine," is a potent proteasome inhibitor and suppresses human prostate cancer growth in nude mice.* Cancer research, 2006. **66**(9): p. 4758-4765.

151. Zhang, W., X. Men, and P. Lei, *Review on anti-tumor effect of triterpene acid compounds.* Journal of cancer research and therapeutics, 2014. **10**(5): p. 14.

152. Budihardjo, I., Oliver, H., Lutter, M., Luo, X., and Wang, X. *Biochemical pathways of caspase activation during apoptosis.* Annual review of cell and developmental biology, 1999. **15**(1): p. 269-290.

153. Volkman, J.K., *Sterols and other triterpenoids: source specificity and evolution of biosynthetic pathways.* Organic geochemistry, 2005. **36**(2): p. 139-159.

154. McGarvey, D.J. and R. Croteau, *Terpenoid metabolism.* The Plant Cell, 1995. **7**(7): p. 1015.

155. Ganjewala, D. and R. Luthra, *Essential oil biosynthesis and metabolism of geranyl acetate and geraniol in developing Cymbopogon flexuosus (Nees ex Steud) Wats Mutant cv. GRL-1 Leaf.* Am J Plant Physiol, 2007. **2**: p. 269-75.

156. Frisch, M.J., Trucks, G.W., Schlegel, H.B., Scuseria, G.E., Robb, M.A., Cheeseman, J.R., Scalmani, G., Barone, V., Petersson, G.A., and Nakatsuji, H. *Gaussian 16, Revision A. 03, Gaussian.* Inc., Wallingford CT, 2016.

157. Becke, A.D., *Density-functional thermochemistry. I. The effect of the exchange-only gradient correction.* The Journal of chemical physics, 1992. **96**(3): p. 2155-2160.
158. Cossi, M., Rega, N., Scalmani, G., and Barone, V. *Energies, structures, and electronic properties of molecules in solution with the C-PCM solvation model.* Journal of computational chemistry, 2003. **24**(6): p. 669-681.
159. Stephens, P., *Gauge dependence of vibrational magnetic dipole transition moments and rotational strengths.* Journal of Physical Chemistry, 1987. **91**(7): p. 1712-1715.
160. Stephens, P.J., Ashvar, C.S., Devlin, F.J., Cheesemano, J.R., Frischo, M.J. *Ab initio calculation of atomic axial tensors and vibrational rotational strengths using density functional theory.* Molecular Physics, 1996. **89**(2): p. 579-594.
161. Verzele, D., J.L. Goeman, and A. Madder, *LC-(TIC/EIC)-MS as tool in the analysis of diastereomeric 3, 12-aza-analogues of deoxycholic acid.* Arkivoc, 2007. **10**: p. 325-336.
162. Likhtarovich, A., Luhin, V., Sovastei, O., Zukowski, P., and Dado, M. *Application of HPLC-MS with electrospray ionization for the qualitative and quantitative analysis of antibiotics in pharmaceutical formulation.* Acta Physica Polonica A, 2015. **128**(5): p. 901-904.
163. Saurí, J., T. Parella, and J.F. Espinosa, *CLIP-HSQMBC: easy measurement of small proton–carbon coupling constants in organic molecules.* Organic & biomolecular chemistry, 2013. **11**(27): p. 4473-4478.
164. Van Vuuren, S., G. Kamatou, and A. Viljoen, *Volatile composition and antimicrobial activity of twenty commercial frankincense essential oil samples.* South African Journal of Botany, 2010. **76**(4): p. 686-691.
165. Adams, R.P., *Identification of essential oils by ion trap mass spectroscopy*. 2012: Academic press.
166. Van den Dool, H. and P.D. Kratz, *A generalization of the retention index system including linear temperature programmed gas-liquid partition chromatography*. 1963.
167. Adams, R.P., *Identification of essential oil components by gas chromatography/mass spectrometry*. Vol. 456. 2007: Allured publishing corporation Carol Stream, IL.
168. McLafferty, F.W., *The Wiley/NBS registry of mass spectral data*. 1989.

169. Stein, S., *National Institute of Standards and Technology (NIST) Mass spectral database and software, version 3.02.* Gaithersburg, Maryland, USA, 1990.

170. Higgs, E., *Nitric oxide; Physiology, pathophysiology and pharmacology.* Phramacol Rev, 1991. **43**: p. 109-142.

171. Banskota, A. H., Tezuka, Y., Nguyen, N.T., Awale, S., Nobukawa, T., Kadota, S. *DPPH radical scavenging and nitric oxide inhibitory activities of the constituents from the wood of Taxus yunnanensis.* Planta medica, 2003. **69**(06): p. 500-505.

172. Kim, H.N., Park, G-H., Park, S-B., Kim, J-D., Eo, H-J., Son, H-J, Song, J-H., and Jeong, J-B. *Sageretia thea Inhibits Inflammation through Suppression of NF-κ B and MAPK and Activation of Nrf2/HO-1 Signaling Pathways in RAW264.7 Cells.* The American journal of Chinese medicine, 2019. **47**(02): p. 385-403.

173. Thanekar, D.R., Tupe, P., Dhodi, J., and Juvekar, A.R. *Evaluation of in vitro cytotoxic activity of petroleum ether and methanol extract of Mentha arvensis (whole plant) on human cancer cell lines.* Int. J. Pharm. Pharm. Sci, 2014. **6**: p. 169-172.

174. Schols, D., Pauwels, R., Vanlangendonck, F., Balzarini, Jan De Clercq, E. *A highly reliable, sensitive, flow cytometric/fluorometric assay for the evaluation of the anti-HIV activity of antiviral compounds in MT-4 cells.* Journal of immunological methods, 1988. **114**(1-2): p. 27-32.

175. Wilson, W.K., Sumpter, R.M., Warren, J.J., Rogers, P.S., Ruan, B., Schroepfer, G.J *Analysis of unsaturated C27 sterols by nuclear magnetic resonance spectroscopy.* Journal of lipid research, 1996. **37**(7): p. 1529-1555.

176. Märk, T.D. and G.H. Dunn, *Electron impact ionization*. 2013: Springer Science & Business Media.

177. Gupta, U., et al., *Spectroscopic studies of cholesterol: fourier transform infra-red and vibrational frequency analysis.* Materials Focus, 2014. **3**(3): p. 211-217.

178. Francis, J.A., S.N. Raja, and M.G. Nair, *Bioactive Terpenoids and Guggulusteroids from Commiphora mukul Gum Resin of Potential Anti-Inflammatory Interest.* Chemistry & biodiversity, 2004. **1**(11): p. 1842-1853.

179. Aneja, A. and E. Tierney, *Autism: the role of cholesterol in treatment.* International Review of Psychiatry, 2008. **20**(2): p. 165-170.

180. Goldstein, J.L. and M.S. Brown, *A century of cholesterol and coronaries: from plaques to genes to statins.* Cell, 2015. **161**(1): p. 161-172.
181. Han, Y-Hwan, Ham, J-H., Lee, N-J., Park, C-H., Shin, Y-H., and Lee, D-U. *Antimutagenic activity of 5α-cholest-7-en-3β-ol, a new component from the starfish Asterina pectinifera.* Biological and Pharmaceutical Bulletin, 2000. **23**(10): p. 1247-1249.
182. Erasto, P., *Antimycobacterial Sterols from Aromatic Stem Sap of Commiphora eminii Engl.* Journal of Advanced Scientific Research, 2012. **3**(4).
183. Goad, L., I. Rubinstein, and A. Smith, *The sterols of echinoderms.* Proceedings of the Royal Society of London. Series B. Biological Sciences, 1972. **180**(1059): p. 223-246.
184. Smith, A.G. and L.J. Goad, *The conversion of cholest-5-en-3β-ol into cholest-7-en-3β-ol by the echinoderms Asterias rubens and Solaster papposus.* Biochemical Journal, 1975. **146**(1): p. 35-40.
185. Smith, A. and L. Goad, *Sterol biosynthesis in the starfish Asterias rubens and Henricia sanguinolenta.* Biochemical Journal, 1971. **123**(4): p. 671-673.
186. Danielsson, H. and J. Sjovall, *Sterols and bile acids*. 1985: Elsevier.
187. Fagerlund, U. and D. Idler, *marine sterols: vi. sterol biosynthesis in molluscs and echinoderms.* Canadian journal of biochemistry and physiology, 1960. **38**(9): p. 997-1002.
188. Vázquez, L.H., J. Palazon, and A. Navarro-Ocaña, *The Pentacyclic Triterpenes α,β-amyrins: A Review of Sources and Biological Activities*, in *Phytochemicals-A global perspective of their role in nutrition and health*. 2012, IntechOpen.
189. Hasmeda, M., Kweifio-Okai, G., Macrides, T., and Polya, G. M. *Selective inhibition of eukaryote protein kinases by anti-inflammatory triterpenoids.* Planta Medica, 1999. **65**(01): p. 014-018.
190. Pae, H.-O. and H.-T. Chung, *Heme oxygenase-1: its therapeutic roles in inflammatory diseases.* Immune network, 2009. **9**(1): p. 12-19.
191. Sun, H., Fang, W-S., Wang, W-Z., and Hu, C. *Structure-activity relationships of oleanane-and ursane-type triterpenoids.* Botanical Studies, 2006. **47**(4): p. 339-368.
192. Otuki, M. F., Ferreira, J., Lima, F. V., Meyre-Silva, C., Malheiros, A., Muller, L. A., Cani, G. S., Santos, A.R.S., Yunes, R. A., and Calixto, J. B. *Antinociceptive properties of mixture of α-amyrin and β-amyrin triterpenes: evidence for participation of protein*

kinase C and protein kinase A pathways. Journal of Pharmacology and Experimental Therapeutics, 2005. **313**(1): p. 310-318.

193. Aragao, G. F., Carneiro, L.M.V., Júnior, A. P.F., Bandeira, P. N., Lemos, T. L.G., Viana, G. S. de.B. *Antiplatelet Activity of α.-and β.-Amyrin, Isomeric Mixture from Protium heptaphyllum.* Pharmaceutical biology, 2007. **45**(5): p. 343-349.
194. Dinku, W., Choi, S-U., Lee, S-H., Jung, Y-S., No, Z-S., Dekebo, A. *Antiproliferative Effect of Sterols from Resin of Commiphora habessinica.* Journal of Pharmacy and Nutrition Sciences, 2019. **9**: p. 000-000.
195. Lodeiro, S., Xiong, Q., Wilson, W. K., Kolesnikova, M. D., Onak, C. S., and Matsuda, S. P.T. *An oxidosqualene cyclase makes numerous products by diverse mechanisms: a challenge to prevailing concepts of triterpene biosynthesis.* Journal of the American Chemical Society, 2007. **129**(36): p. 11213-11222.
196. Stuppner, H. and E. Moller, *Cucurbitacins with unusual side chains from Picrorhiza kurroa.* Phytochemistry, 1993. **33**(5): p. 1139-1145.
197. Tai, T., Shingu, T., Kikuchi, T., Tezuka, Y., and Akahori, A. *Triterpenes from the surface layer of Poria cocos.* Phytochemistry, 1995. **39**(5): p. 1165-1169.
198. Mahato, S.B. and S. Sen, *Advances in triterpenoid research, 1990–1994.* Phytochemistry, 1997. **44**(7): p. 1185-1236.
199. Frisch, M.J., Trucks, G.W., Schlegel, H.B., Scuseria, G.E., Robb, M.A., Cheeseman, J.R., Scalmani, G., Barone, V., Petersson, G.A., and Nakatsuji, H. *Gaussian 16, Revision A. 03*, Gaussian, Inc., Wallingford CT, 2016.
200. Liu, Y., Cohen, R. D., Gustafson, K. R., Martin, G. E., Williamson, R. T. *Enhanced measurement of residual chemical shift anisotropy for small molecule structure elucidation.* Chemical communications, 2018. **54**(34): p. 4254-4257.
201. Liu, Y., Navarro-Vázquez, A., Gil, R. R., Griesinger, C., Martin, G. E., Williamson, R. T. *Application of anisotropic NMR parameters to the confirmation of molecular structure.* Nature protocols, 2019. **14**(1): p. 217.
202. Arai, Y., M. Hirohara, and H. Ageta, *Fern constituents: Three new skeletal triterpenoid hydrocarbons isolated from Polypodiodes niponica.* Tetrahedron letters, 1989. **30**(51): p. 7209-7212.

203. Ali, N.A.A., M. Wurster, and U. Lindequist, *Chemical composition of essential oil from the oleogum resin of Commiphora habessinica (Berg.) Engl. from Yemen.* Journal of essential oil bearing plants, 2009. **12**(2): p. 244-249.

204. Manguro, L.O., K.M. Mukonyi, and J.K. Githiomi, *Bisabolenes and furanosesquiterpenoids of Kenyan Commiphora kua resin.* Planta medica, 1996. **62**(01): p. 84-85.

205. Mothana, R.A., A.J. Al-Rehaily, and W. Schultze, *Chemical analysis and biological activity of the essential oils of two endemic Soqotri Commiphora species.* Molecules, 2010. **15**(2): p. 689-698.

206. Provan, G.J., A.I. Gray, and P.G. Waterman, *Monoterpene-rich resins from some kenyan burseraceae.* Flavour and fragrance journal, 1987. **2**(3): p. 115-118.

207. Abegaz, B., Dagne, E., Bates, C., Waterman, P. G. *Monoterpene-rich resins from two ethiopian species of commiphora.* Flavour and fragrance journal, 1989. **4**(3): p. 99-101.

208. Nasser, A., Awadh, A., Wurster, M., Arnold, N., Lindequist, U., and Wessjohan, L. *Essential Oil Composition from Oleogum Resin of Soqotraen Commiphorkua, Rec.* Nat. Prod, 2008. **2**(3): p. 70-75.

209. Al-Massarany, S. M., Abbas, F. A., Demirci, B., Baser, K. H.C, Khan, S. A-R., Adnan, J., Mossa, J. S., Abourashed, E. A. *Chemical composition and biological evaluation of the essential oil of Commiphora opobalsamum L.* Journal of herbs, spices & medicinal plants, 2008. **13**(4): p. 111-121.

210. Babushok, V., P. Linstrom, and I. Zenkevich, *Retention indices for frequently reported compounds of plant essential oils.* Journal of Physical and Chemical Reference Data, 2011. **40**(4): p. 043101.

211. Ennifar, S., Ferbach, S., Kraut, C., and Rolli, H. *Physiological and pharmacological properties of monoterpenes.* Strasbourg: Université Pasteur, 2001.

212. Setzer, W. N, Setzer, M. C., Moriarity, D. M., Bates, R. B., Haber, W. A. *Biological activity of the essential oil of Myrcianthes sp. nov."black fruit" from Monteverde, Costa Rica.* Planta Medica, 1999. **65**(05): p. 468-469.

213. Sayyah, M., L. Nadjafnia, and M. Kamalinejad, *Anticonvulsant activity and chemical composition of Artemisia dracunculus L. essential oil.* Journal of Ethnopharmacology, 2004. **94**(2-3): p. 283-287.

214. Erazo, S., Delporte, C., Negrete, R., García, R., Zaldívar, M., Iturra, G., Caballero, E., López, J. L., Backhouse, N. *Constituents and biological activities of Schinus polygamus.* Journal of ethnopharmacology, 2006. **107**(3): p. 395-400.

215. Lakhal, H., Ghorab, H., Chibani, S., Kabouche, A., Semra, Z., Smati, F., Abuhamdah, S., and Kabouche, Z. *Chemical composition and biological activities of the essential oil of Salvia officinalis from Batna (Algeria).* Der Pharmacia Lettre, 2013. **5**(3): p. 310-314.

216. Mercier, B., J. Prost, and M. Prost, *The essential oil of turpentine and its major volatile fraction (α-and β-pinenes): a review.* International journal of occupational medicine and environmental health, 2009. **22**(4): p. 331-342.

217. Awad, A.B. and C.S. Fink, *Phytosterols as anticancer dietary components: evidence and mechanism of action.* The Journal of nutrition, 2000. **130**(9): p. 2127-2130.

218. Awad, A.B., R. Roy, and C.S. Fink, *β-sitosterol, a plant sterol, induces apoptosis and activates key caspases in MDA-MB-231 human breast cancer cells.* Oncology reports, 2003. **10**(2): p. 497-500.

219. Choi, Y-H., Kong, K-R., Kim, Y., Jung, K-O., Kil, J-H., Rhee, S-H., Park, K-Y. *Induction of Bax and activation of caspases during β-sitosterol-mediated apoptosis in human colon cancer cells.* International journal of oncology, 2003. **23**(6): p. 1657-1662.

220. Saeidnia, S., Manayi, A., Gohari, A. R., Abdollahi, M. *The story of beta-sitosterol-a review.* European Journal of Medicinal Plants, 2014. **4**(5): p. 590.

221. Mamza, U., O. Sodipo, and I. Khan, *Gas chromatography–mass spectrometry (GC–MS) analysis of bioactive components of Phyllanthus amarus leaves.* International Research Journal of Plant Science, 2012. **3**(10): p. 208-215.

222. Oyugi, D. A., Ayorinde, F. O., Gugssa, A., Allen, A., Izevbigie, E. B., Eribo, B., Anderson, W. A. *Biological activity and mass spectrometric analysis of Vernonia amygdalina fractions.* J Biosci Tech, 2011. **2**(3): p. 287-304.

223. Biskup, E., Gołębiowski, M., Gniadecki, R., Stepnowski, P., and Łojkowska, E. *Triterpenoid α-amyrin stimulates proliferation of human keratinocytes but does not protect them against UVB damage.* Acta Biochimica Polonica, 2012. **59**(2).

224. Burnouf-Radosevich, M., N.E. Delfel, and R. England, *Gas chromatography-mass spectrometry of oleanane-and ursane-type triterpenes—application to Chenopodium quinoa triterpenes.* Phytochemistry, 1985. **24**(9): p. 2063-2066.

225. Wang, C., Yoon, S-H., Jang, H-J., Chung, Y-R., Kim, J-Y., Choi, E-S., Kim, S-W. *Metabolic engineering of Escherichia coli for α-farnesene production.* Metabolic engineering, 2011. **13**(6): p. 648-655.

226. Scalcinati, G., Partow, S., Siewers, V., Schalk, M., Daviet, L., Nielsen, J. *Combined metabolic engineering of precursor and co-factor supply to increase α-santalene production by Saccharomyces cerevisiae.* Microbial cell factories, 2012. **11**(1): p. 117.

227. Wu, Y-X., Chen, Y-J., Liu, C-M., and Gao, K. *Four new sesquiterpenoids from Ligularia cymbulifera.* Journal of Asian natural products research, 2012. **14**(12): p. 1130-1136.

228. Stojanović-Radić, Z., Čomić, L.J., Radulović, N., Blagojević, P., Denić, M., Miltojević, A., Rajković, J., and Mihajilov-Krstev, T. *Antistaphylococcal activity of Inula helenium L. root essential oil: eudesmane sesquiterpene lactones induce cell membrane damage.* European Journal of Clinical Microbiology & Infectious Diseases, 2012. **31**(6): p. 1015-1025.

229. Al-Maskri, A. Y., Hanif, M. A., Al-Maskari, M. Y., Abraham, A. S., Al-sabahi, J. N., Al-Mantheri, O. *Essential oil from Ocimum basilicum (Omani Basil): a desert crop.* Natural product communications, 2011. **6**(10): p. 1934578X1100601020.

230. Conforti, F., Menichini, F., Loizzo, M. R., Statti, A. G., Rapisarda, A., Menichini, F., Houghton, P. J. *Antioxidant, α-amylase inhibitory and brine-shrimp toxicity studies on Centaurea centaurium L. methanolic root extract.* Natural product research, 2008. **22**(16): p. 1457-1466.

231. Anter, Jaouad RJ, Magdalena F., Zahira V. Myriam A, Mohamed A. Angeles M., Andrés., Antigenotox*icity, cytotoxicity, and apoptosis induction by apigenin, bisabolol, and protocatechuic acid.* Journal of medicinal food, 2011. **14**(3): p. 276-283.

232. Nishida, R., Shelly, T. E., Whittier, T. S, Kaneshiro, K. Y. *α-Copaene, a potential rendezvous cue for the Mediterranean fruit fly, Ceratitis capitata?* Journal of Chemical Ecology, 2000. **26**(1): p. 87-100.

233. Fernandes, E.S., Passos, G.F., Medeiros, R.C., Fernanda. M.F., Maria M, P. Luiz F, Calixto, J.B., Fernandes, E.S., *Anti-inflammatory effects of compounds alpha-humulene*

and (−)-trans- caryophyllene isolated from the essential oil of Cordia verbenacea. European journal of pharmacology, 2007. **569**(3): p. 228-236.

234. Ding, Y., Huffaker, A., Köllner, T. G, Weckwerth, P., Robert, C. A.M., Spencer, J. L., Lipka, A. E., and Schmelz, E.A. *Selinene volatiles are essential precursors for maize defense promoting fungal pathogen resistance.* Plant physiology, 2017. **175**(3): p. 1455-1468.
235. Waweru, J.G., H.N. Njenga, and L.K. Omosa, *Standardization of Commiphora Abyssinica Engl. Gum Resin From Kajiado, Kenya.*
236. Burkill, H.M., *The useful plants of west tropical Africa. Volume 2: Families EI*. 1994: Royal Botanic Gardens.
237. Saleem, M., *Lupeol, a novel anti-inflammatory and anti-cancer dietary triterpene.* Cancer letters, 2009. **285**(2): p. 109-115.
238. Saleem, M., Afaq, F., Adhami, V., Mustafa, Mukhtar, H. *Lupeol modulates NF-κB and PI3K/Akt pathways and inhibits skin cancer in CD-1 mice.* Oncogene, 2004. **23**(30): p. 5203.
239. Aratanechemuge, Y., Hibasami, H., Sanpin, K., Katsuzaki, H., Imai, K., and Komiya, T. *Induction of apoptosis by lupeol isolated from mokumen (Gossampinus malabarica L. Merr) in human promyelotic leukemia HL-60 cells.* Oncology reports, 2004. **11**(2): p. 289-292.
240. El Hadri, A., del Rio, M.A., Gomez, S., Jesús, C., Azucena, G., Idaomar, M., Ozonas, B. R., Gonzalez, J.B., Reus, M.S. *Cytotoxic activity of α-humulene and transcaryophyllene from Salvia officinalis in animal and human tumor cells.* An R Acad Nac Farm, 2010. **76**(3): p. 343-356.
241. Sudji, I.R., *Bioactivity of Steroid and Triterpenoid Saponins: Influence on Membrane Permeability and Drug Absorption*. 2015.
242. Chaturvedula, V.S., Prakash, Z., Bing-Nan, G., Zhijie, T., Shannon, J., Hecht, S., M, Kingston, D.G.I. *New lupane triterpenoids from Solidago canadensis that inhibit the lyase activity of DNA polymerase β.* Bioorganic & medicinal chemistry, 2004. **12**(23): p. 6271-6275.

243. Chung, I.-M., Kim, M-Y., Park, S-D., Park, W-H., Moon, H-I. *In vitro evaluation of the antiplasmodial activity of Dendropanax morbifera against chloroquine-sensitive strains of Plasmodium falciparum.* Phytotherapy research, 2009. **23**(11): p. 1634-1637.

244. Moncada, S., *Nitric oxide: physiology, pathophysiology, and pharmacology.* Pharmacol rev, 1991. **43**: p. 109-142.

245. Katagiri, T., L. Hirono, and T. Aoki, *The NF-KB and IKB proteins: new discoveries and in-sights.* Ann Rev Immunol, 1996. **33**(7): p. 649-681.

APPENDIXES

Appendix A

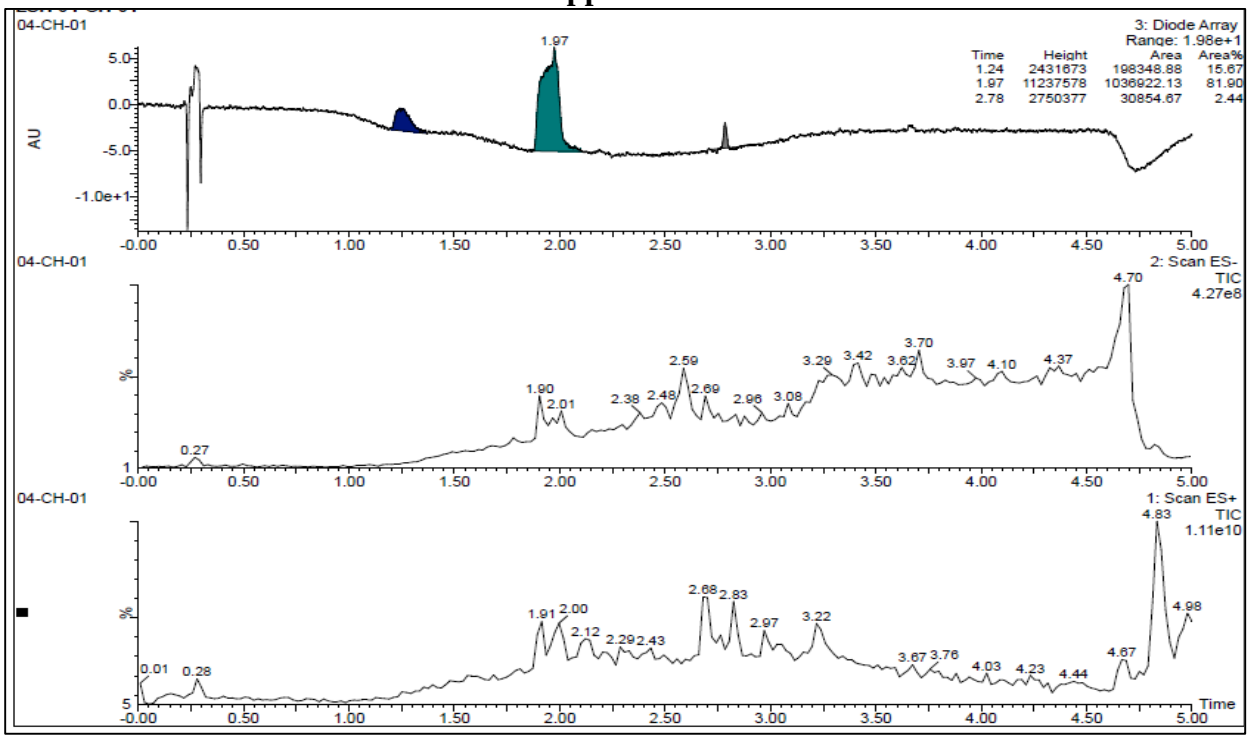

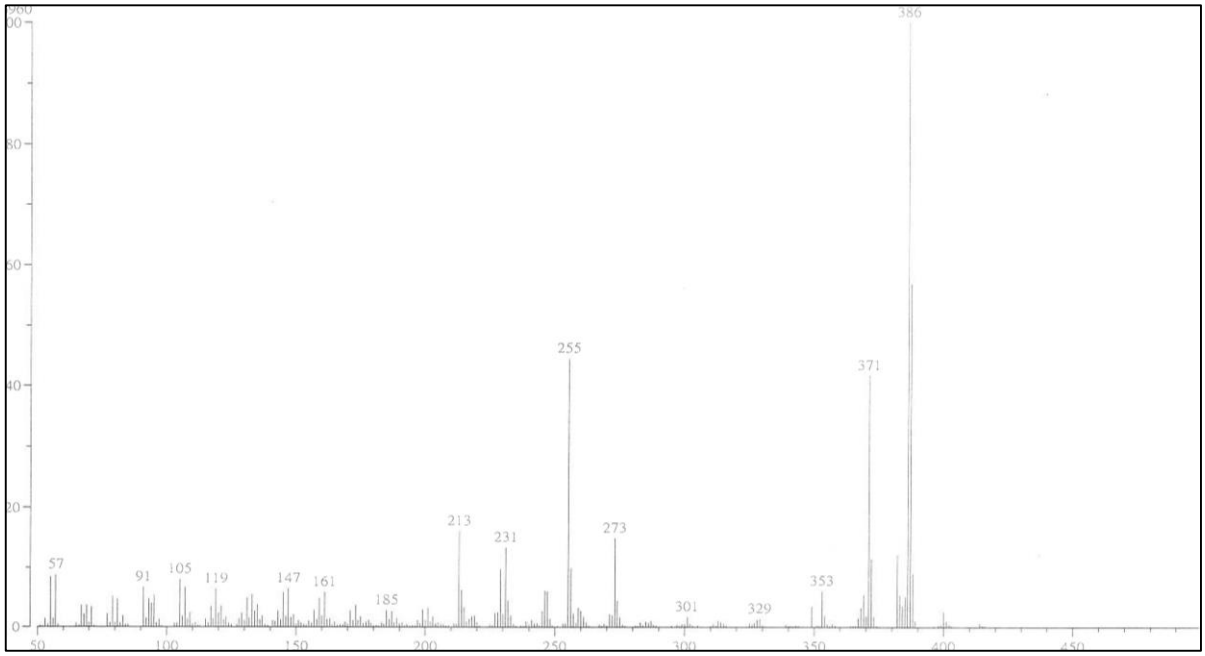

Figure A1: LC-TIC and EI chromatogram of compound **48 (**Cholesterol**)**

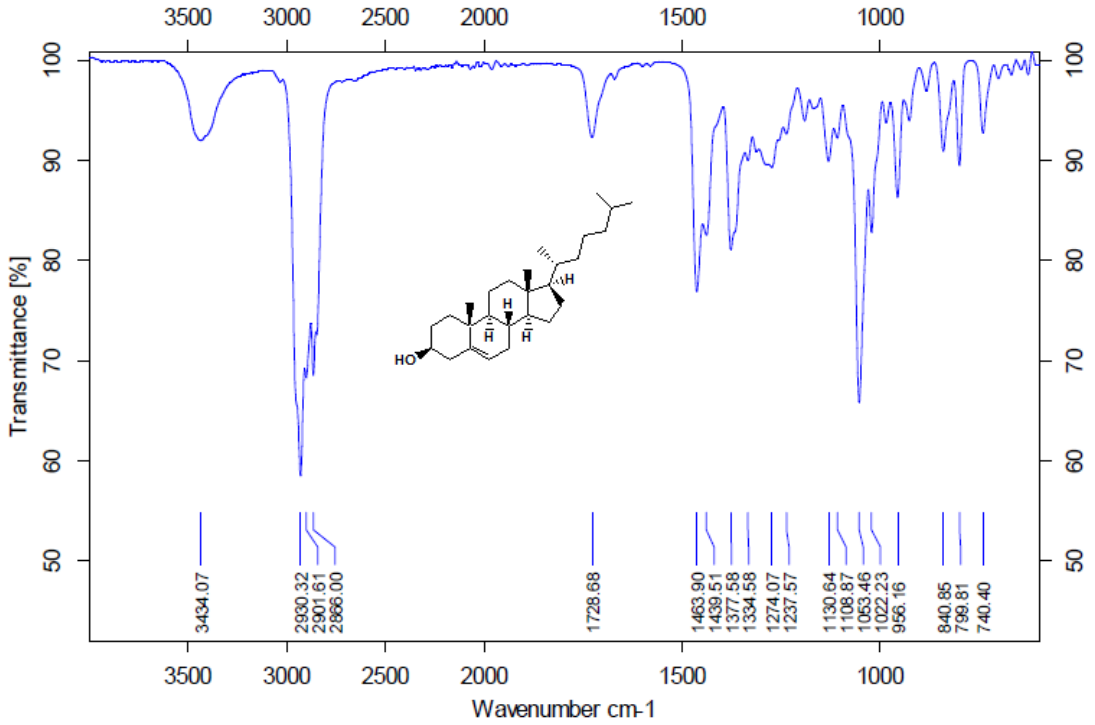

Figure A2: IR of compound **48** (Cholesterol)

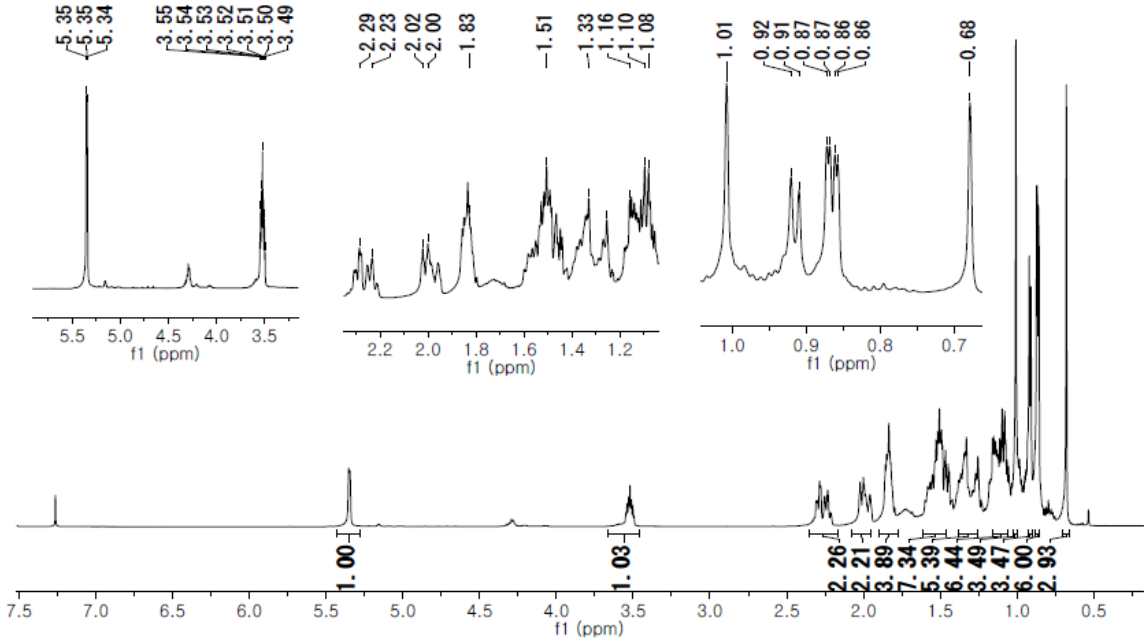

Figure A3: ^{1}H NMR spectrum of compound **48** (Cholesterol)

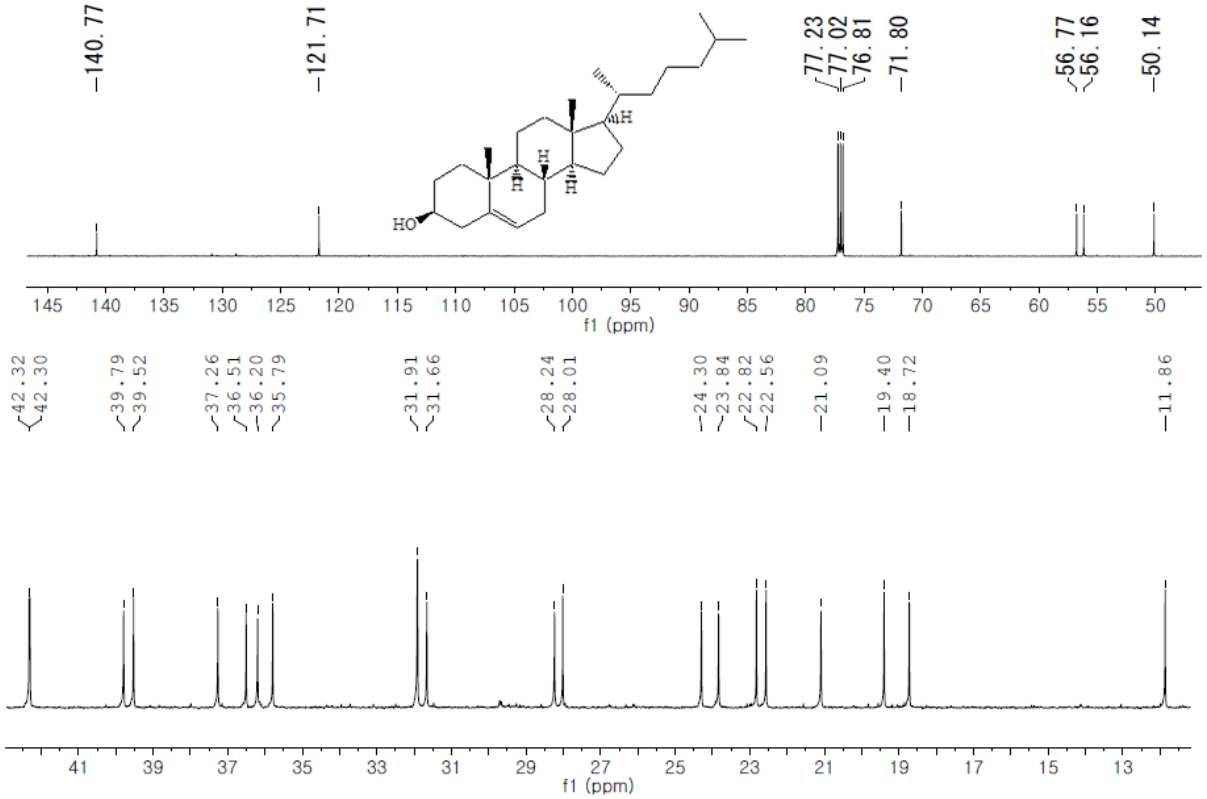

Figure A4: ^{13}C NMR spectrum of compound **48** (Cholesterol)

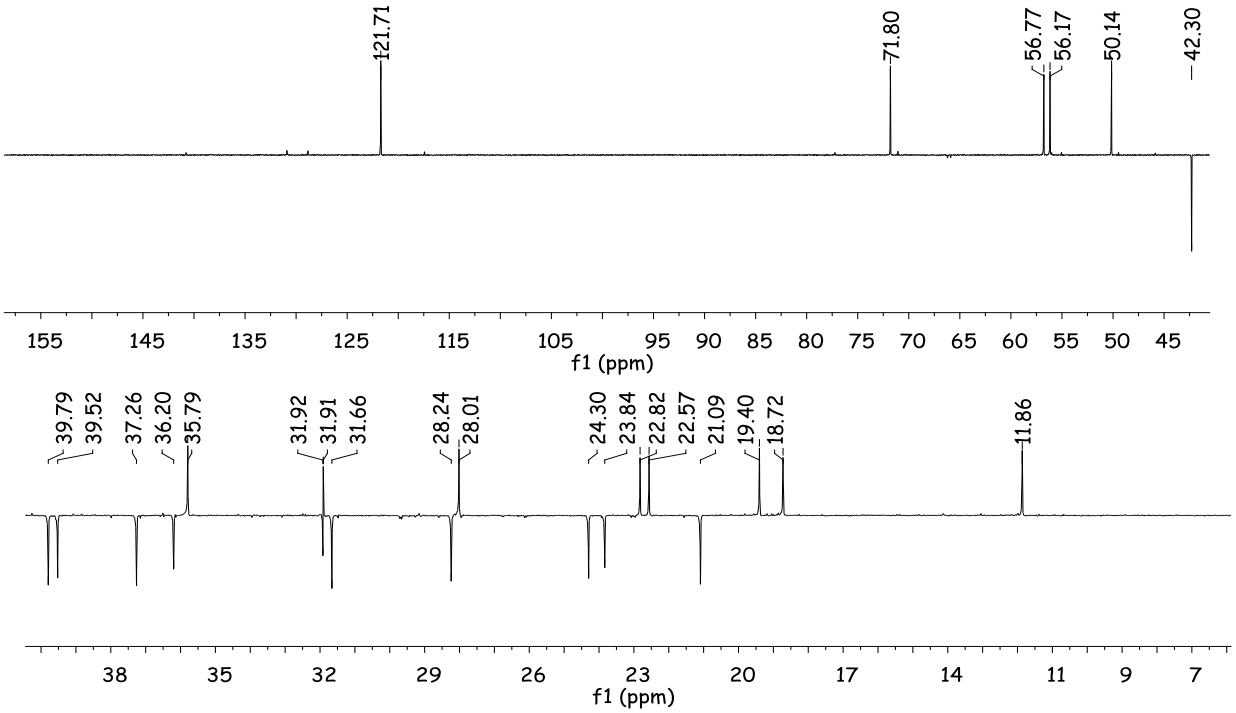

Figure A5: DEPT-135 spectrum of compound **48** (Cholesterol)

Appendix B

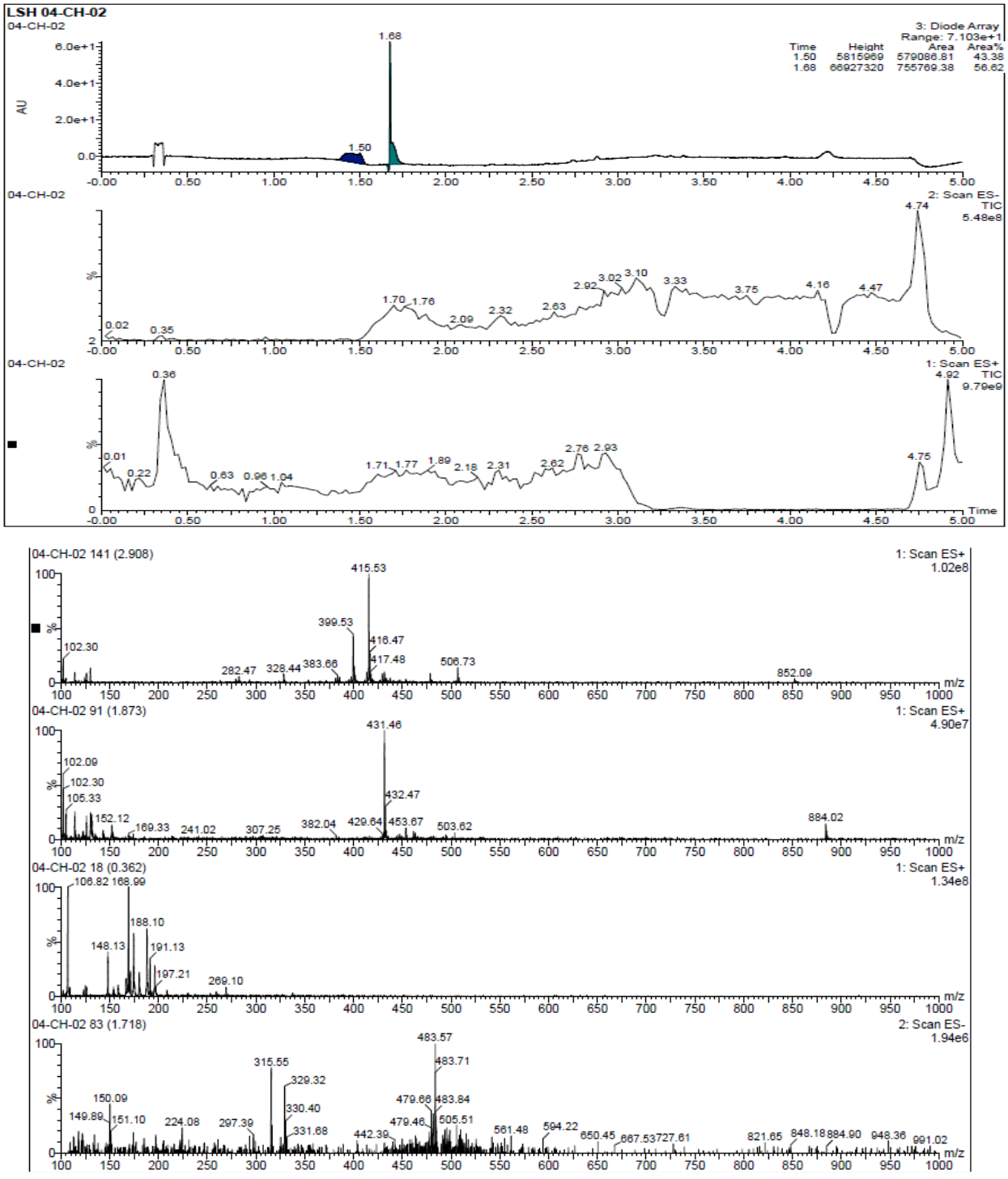

Figure B1: LC-TIC and ESI-MS of compound **112** (Lathosterol)

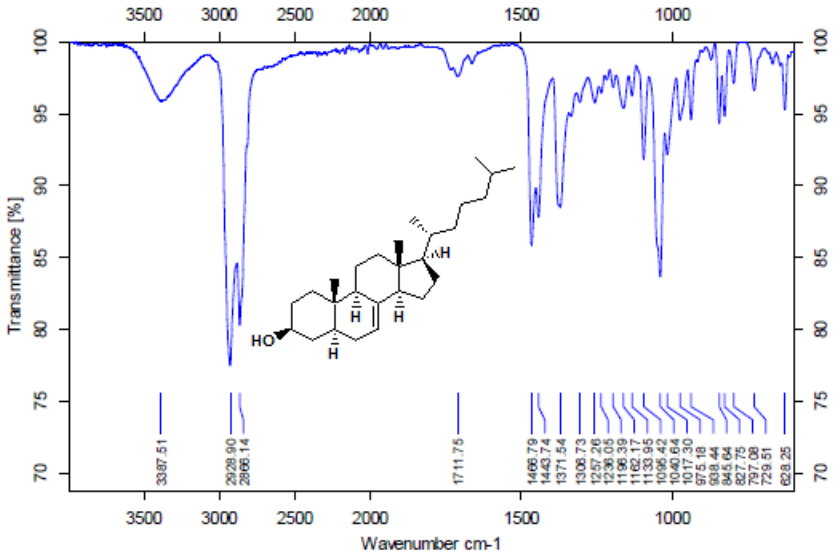

Figure B2: IR of compound **112** (Lathosterol)

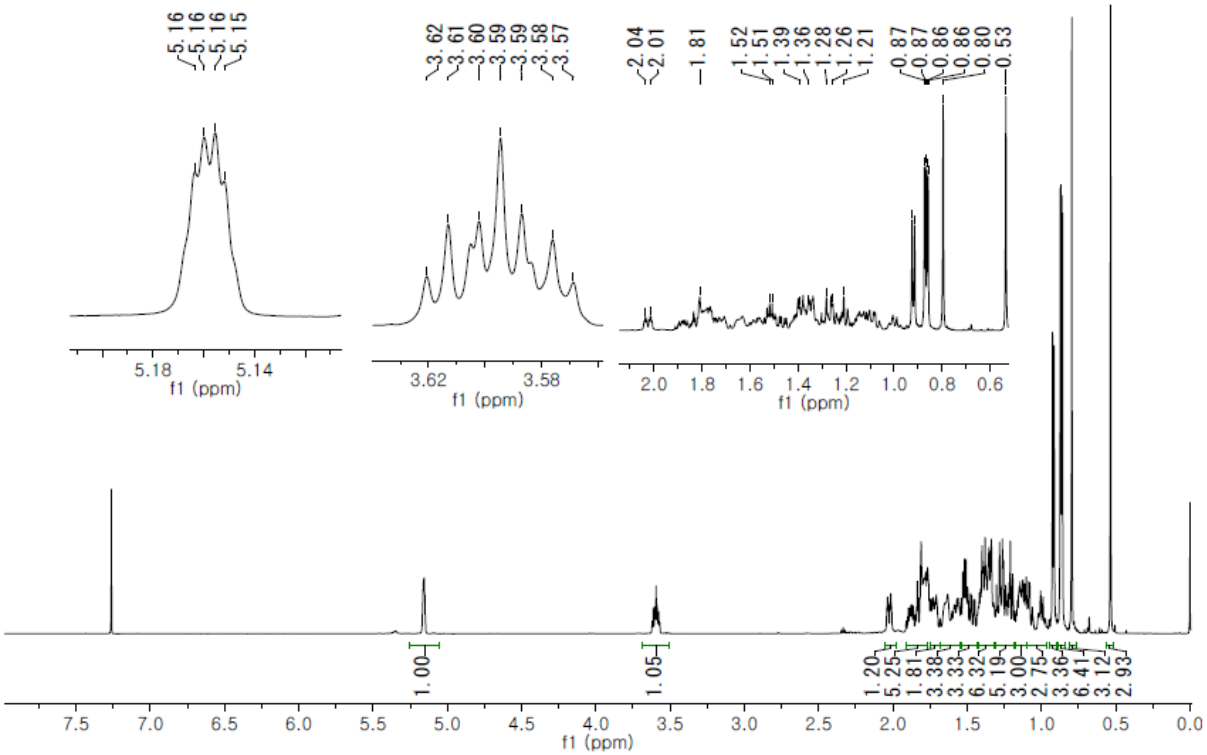

Figure B3: ^{1}H NMR spectrum of compound **112** (Lathosterol)

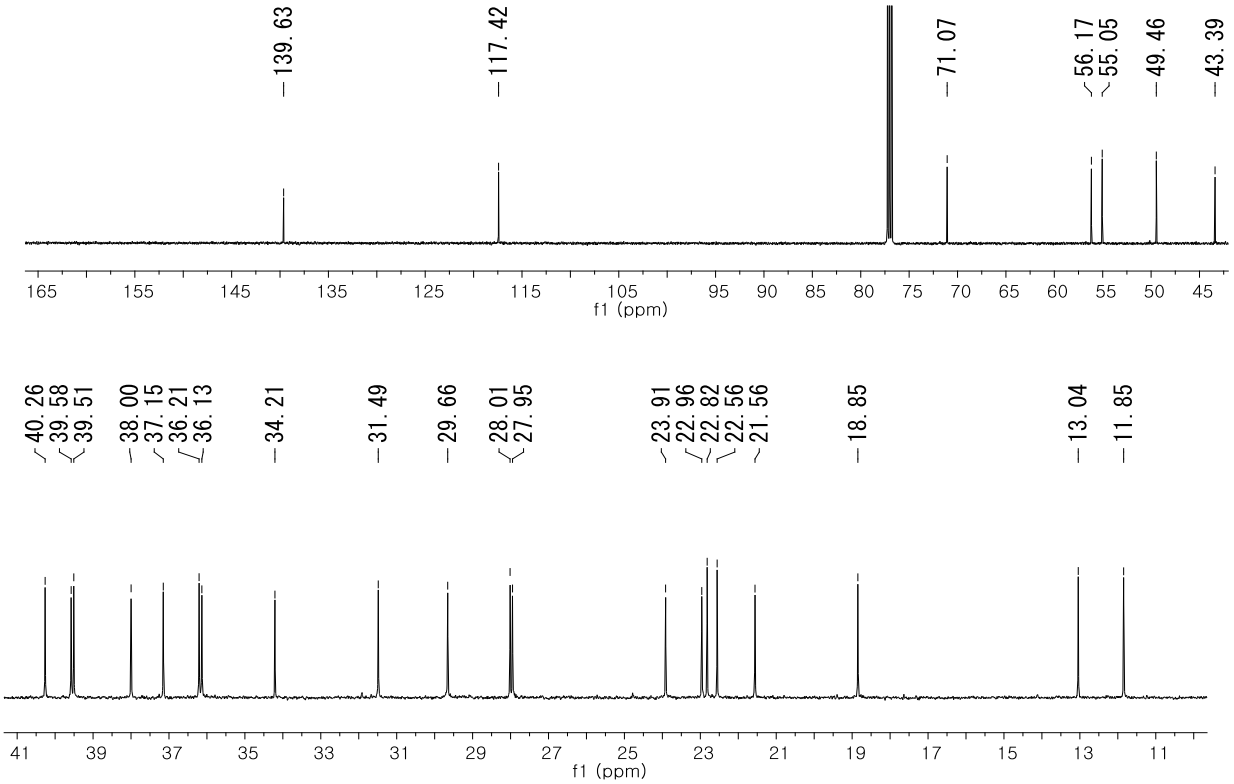

Figure B4: ^{13}C NMR spectrum of compound **112** (Lathosterol)

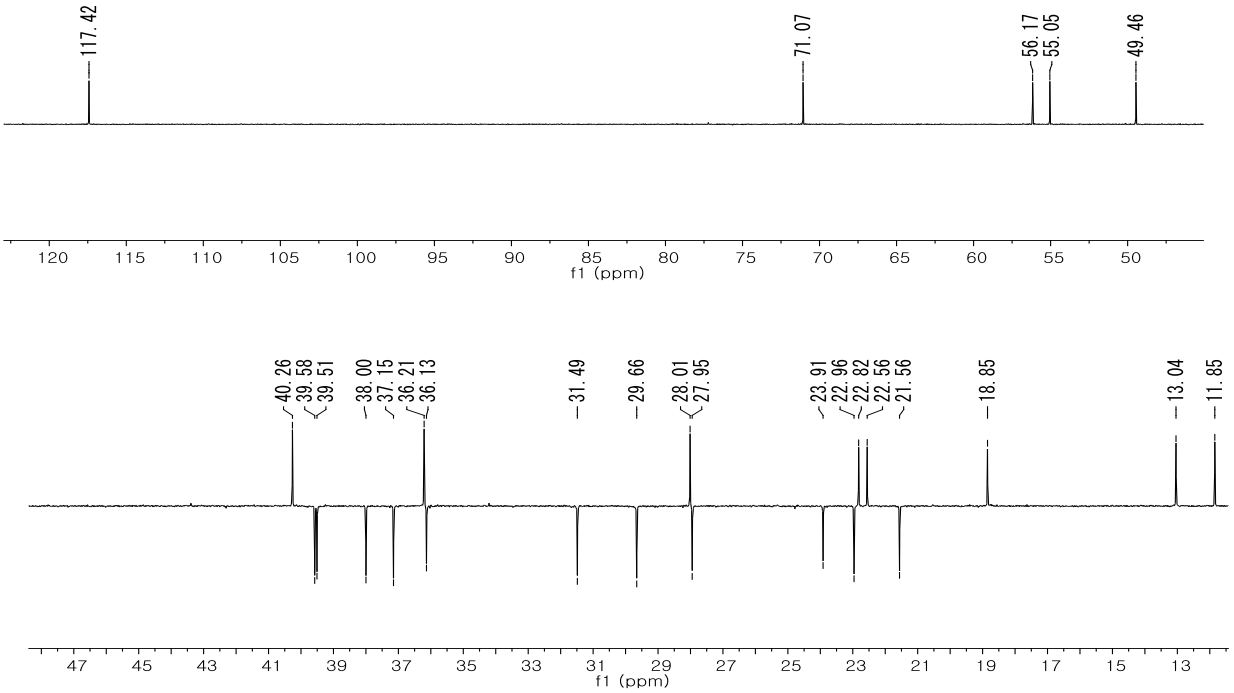

Figure B5: DEPT-135 spectrum of compound **112** (Lathosterol)

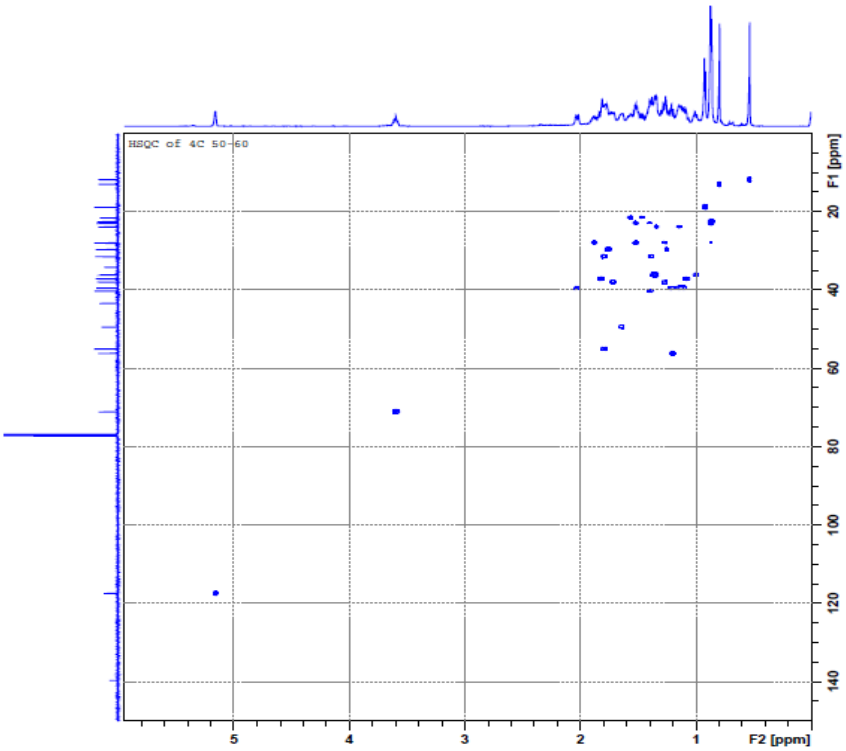

Figure B6: HSQC spectrum of Compound **112** (Lathosterol)

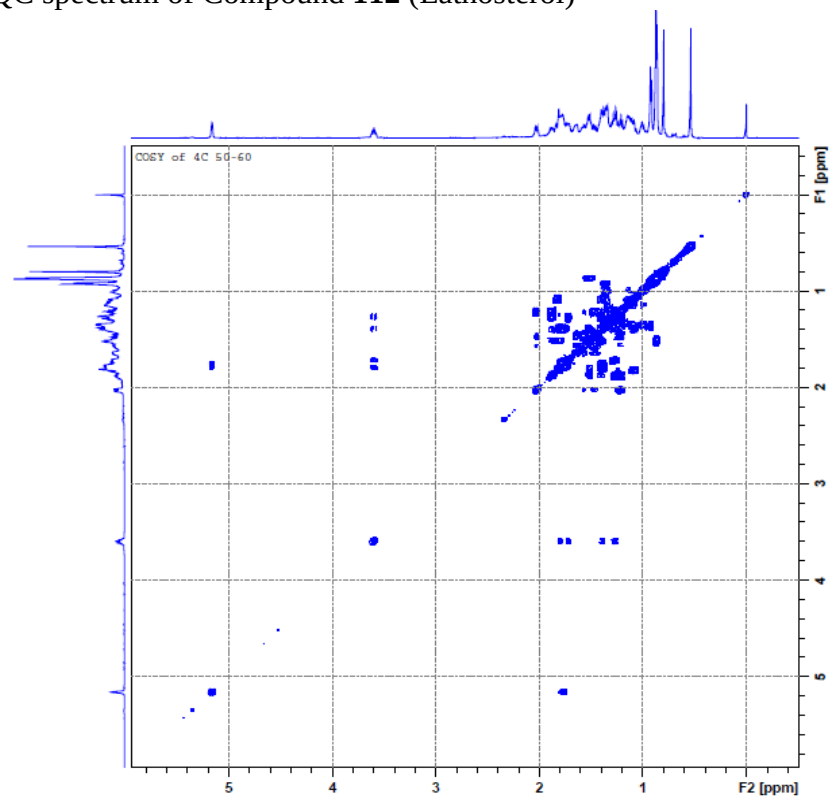

Figure B7: COSY spectrum of Compound **112** (Lathosterol)

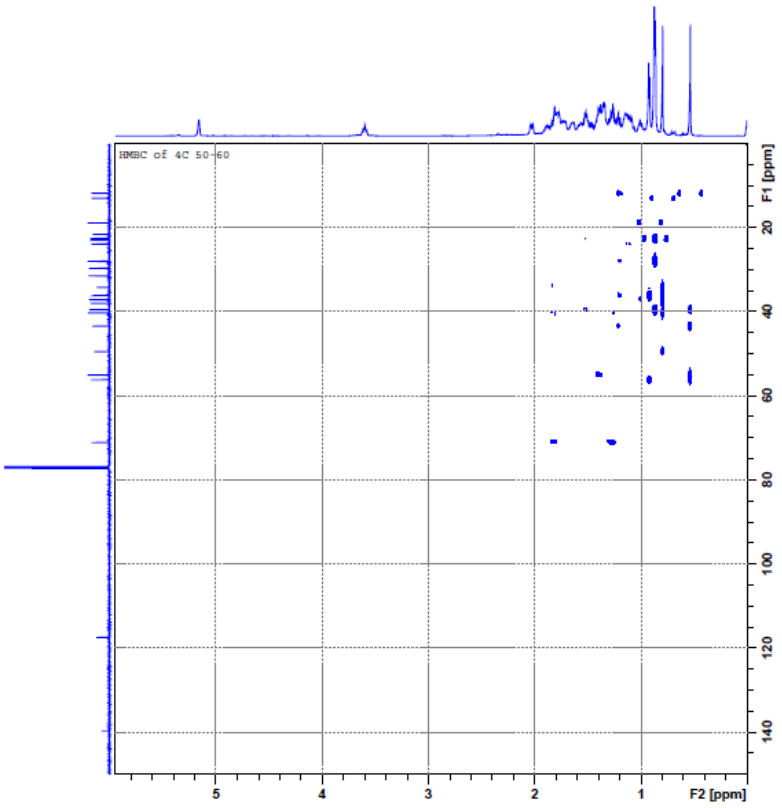

Figure B8: HMBC spectrum of Compound **112** (Lathosterol)

Appendix C

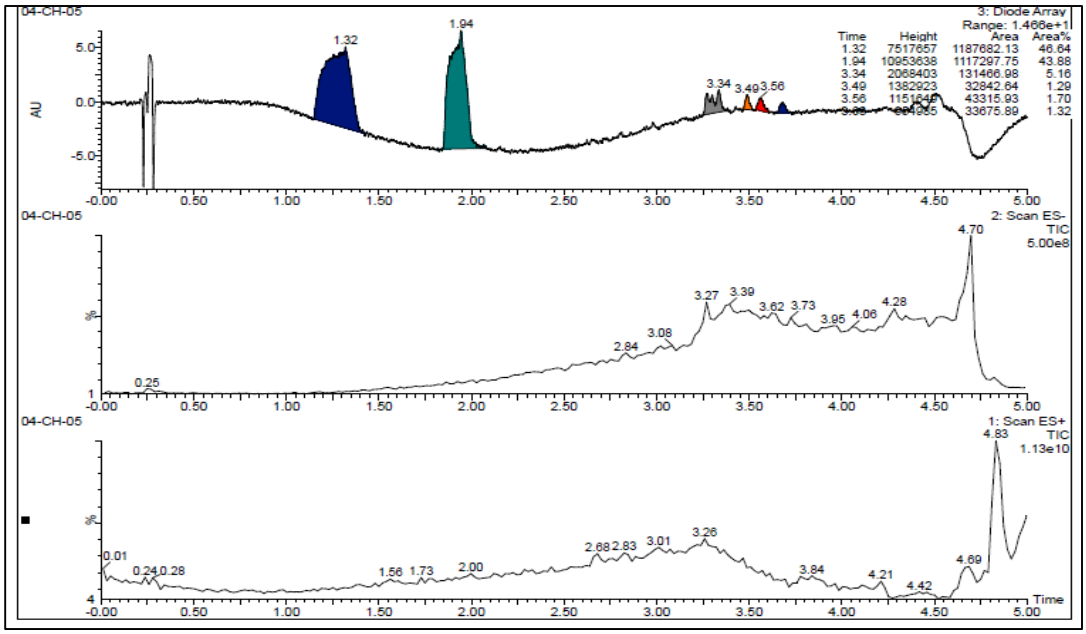

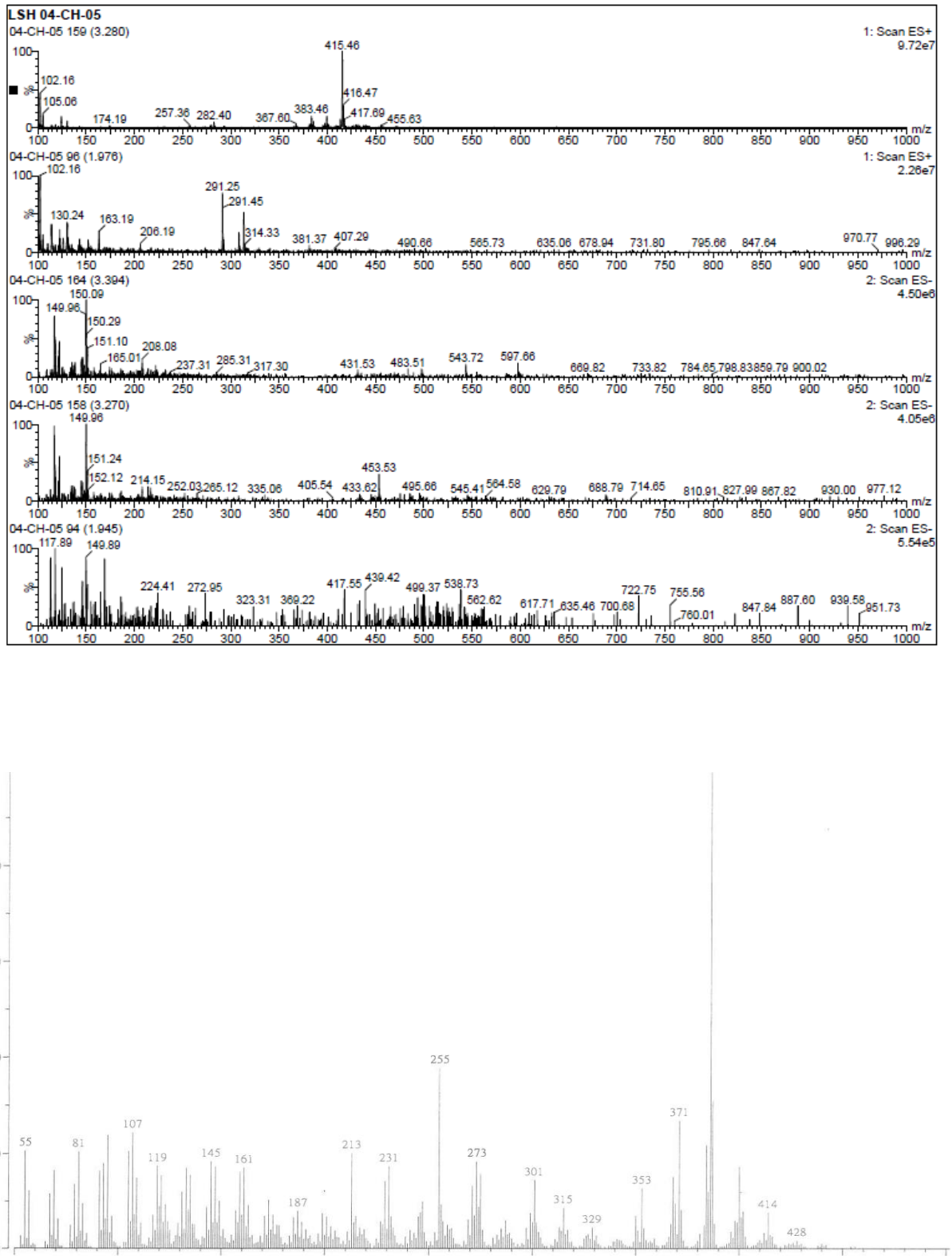

Figure C1: LC-TIC, ESI-MS and EI-MS of a mixture of Compound **48** and **112**

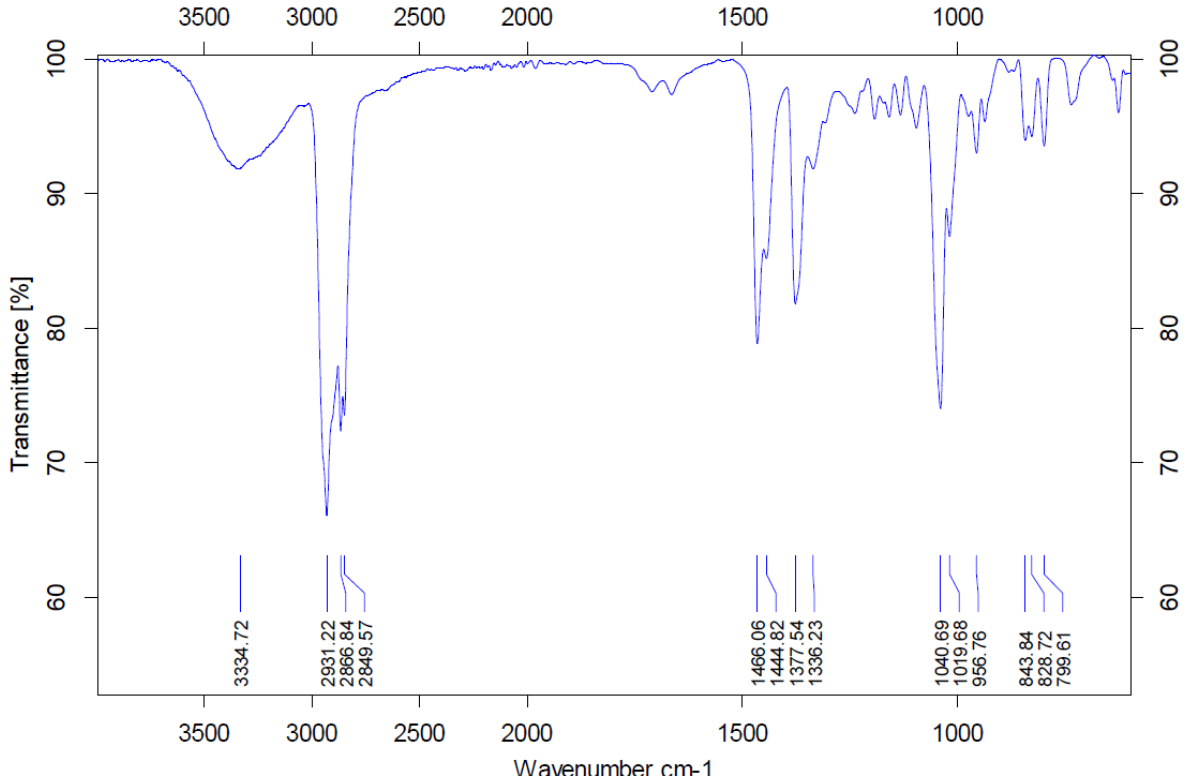

Figure C2: IR of a mixture of Compound **48** and **112** (cholesterol and Lathosterol)

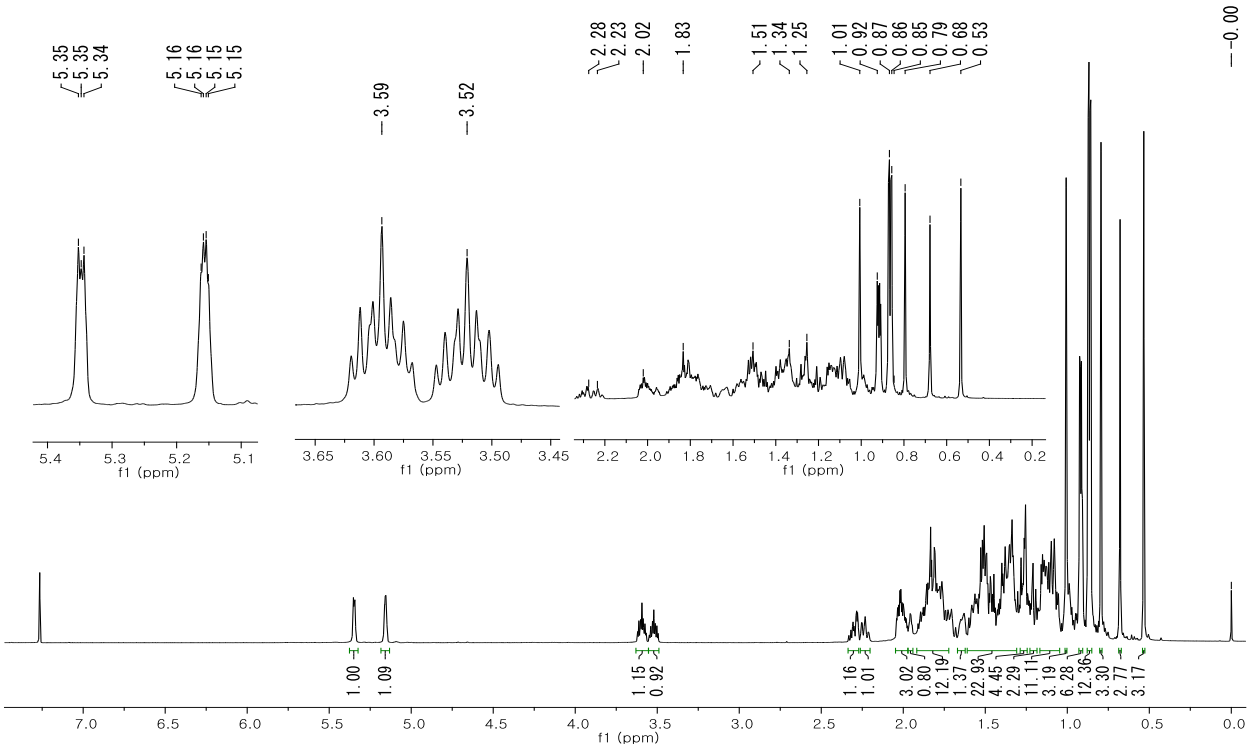

Figure C3: ^{1}H NMR spectrum of a mixture of Compound **48** and **112**

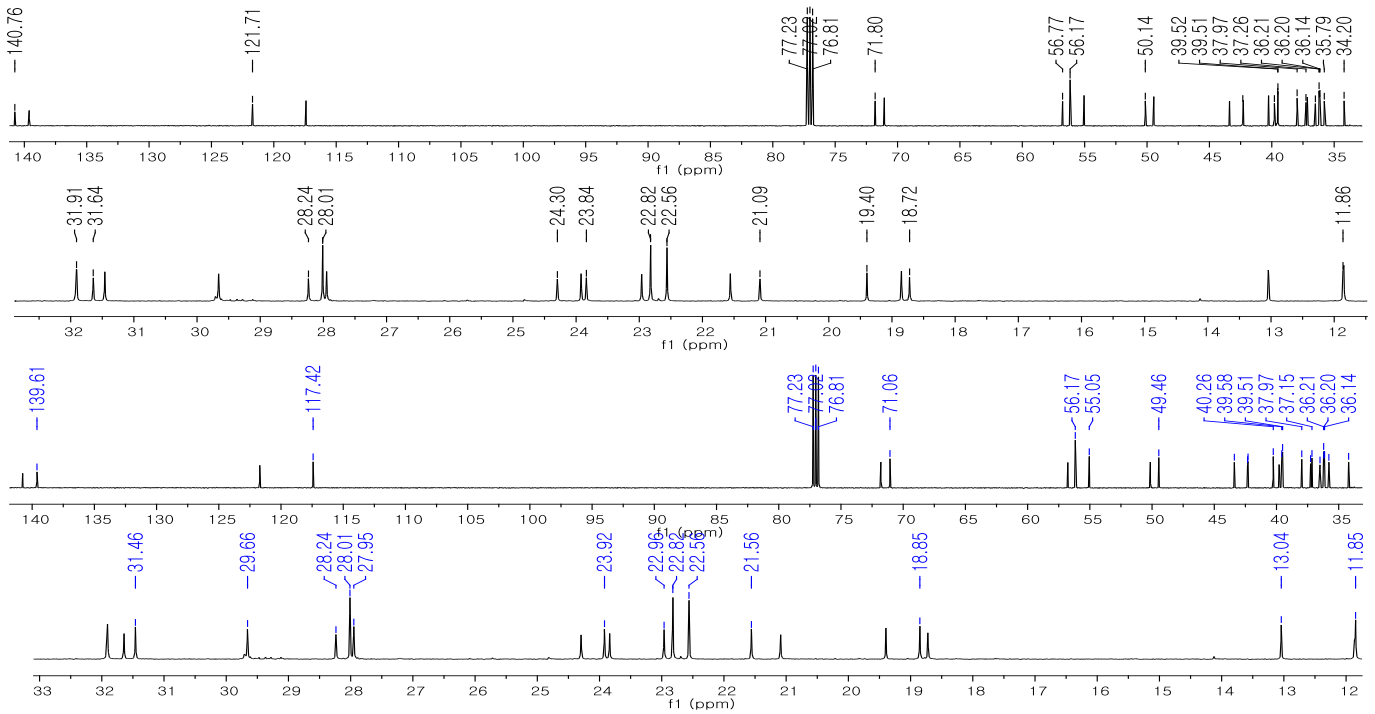

Figure C4: ^{13}C NMR spectrum of a mixture of Compound **48** and **112**

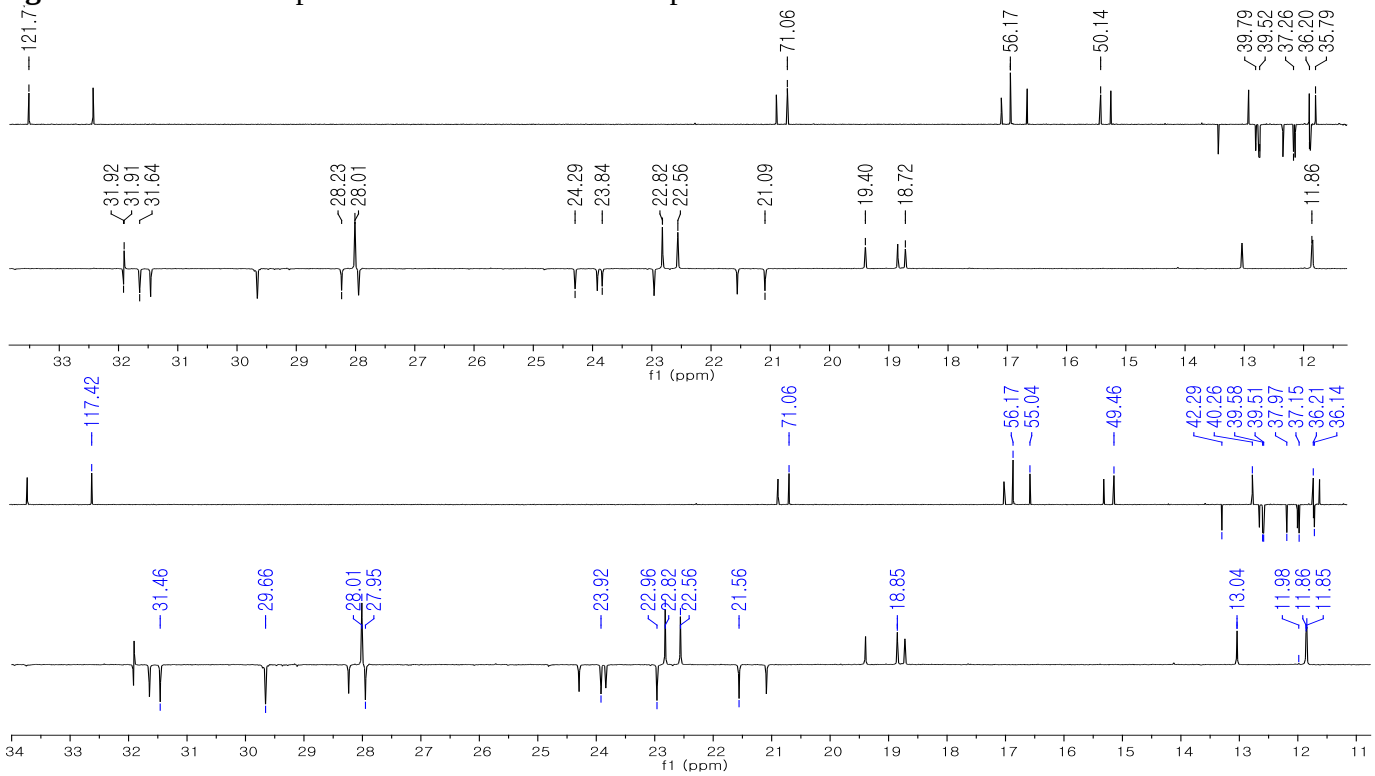

Figure C5: DEPT-135 spectrum of a mixture of Compound **48** and **112**

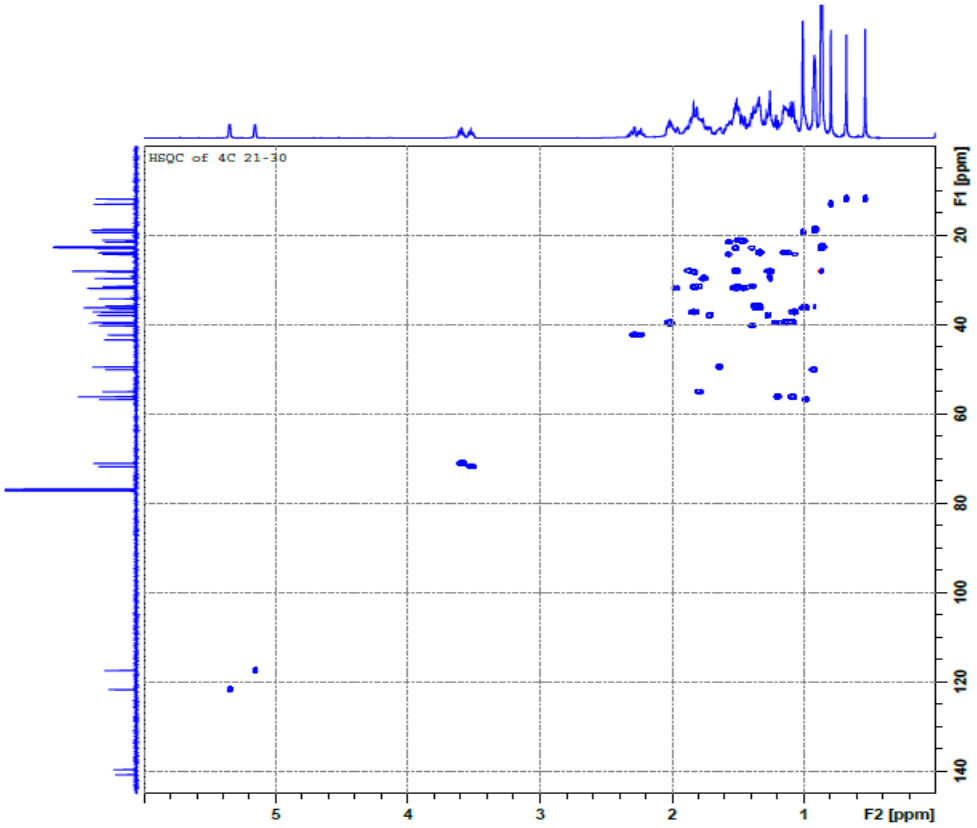

Figure C6: HSQC spectrum of a mixture of Compound **48** and **112**

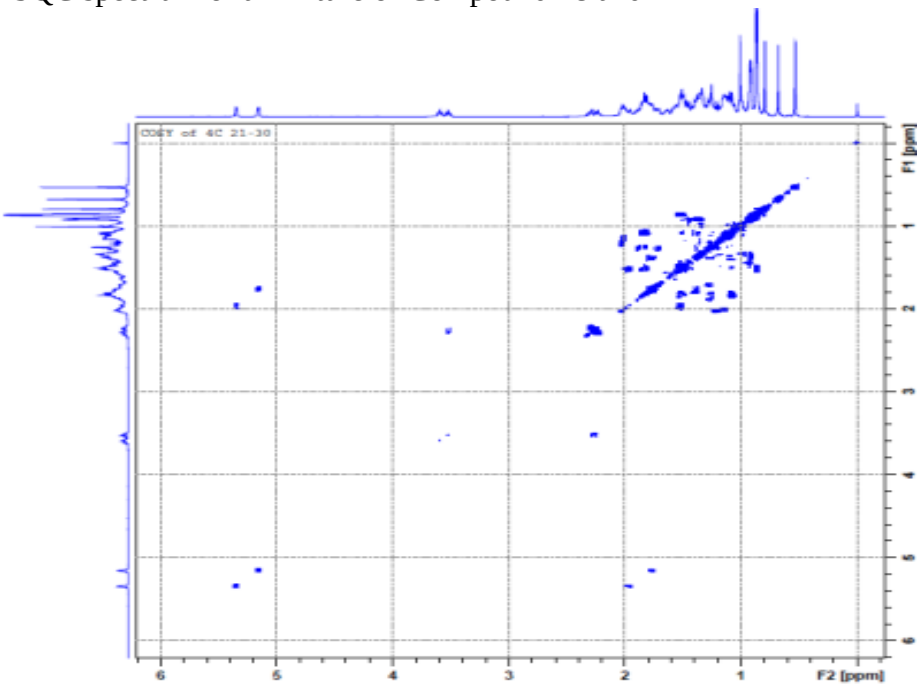

Figure C7: COSY spectrum of a mixture of Compound **48** and **112**

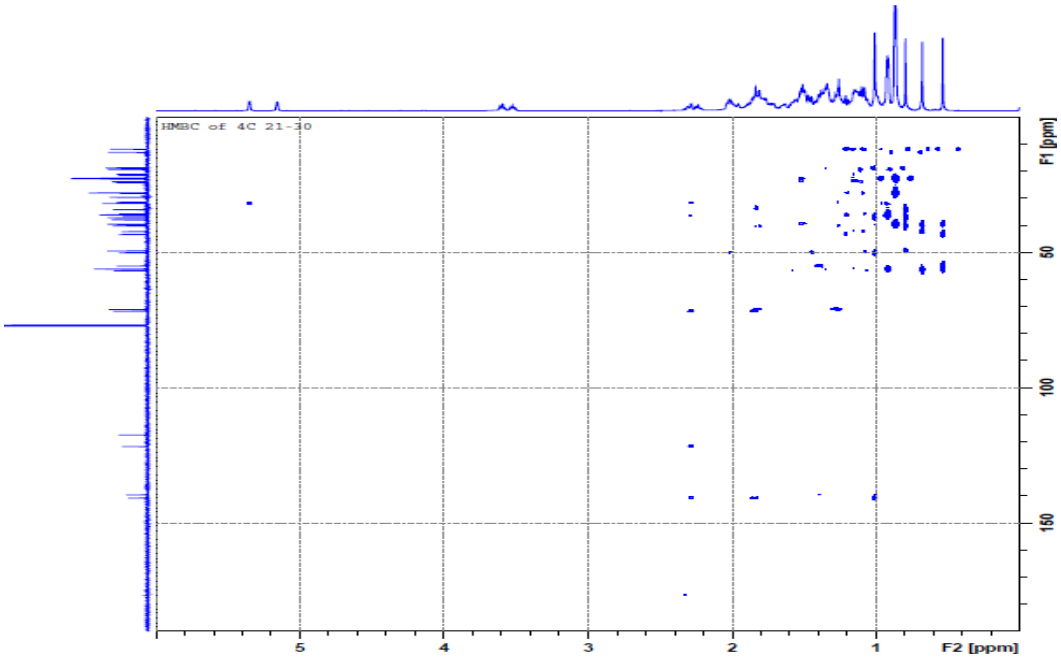

Figure C8: HMBC spectrum of a mixture of Compound **48** and **112**

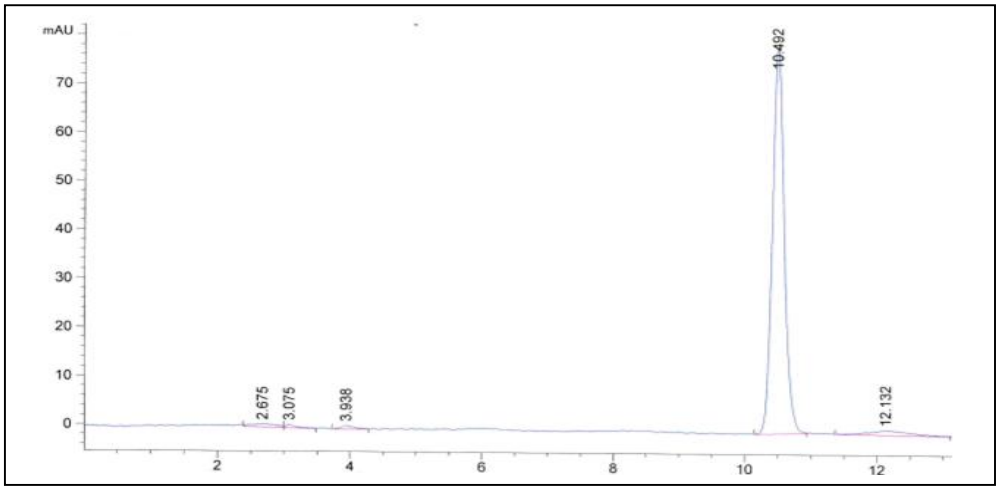

Figure C9: HPLC chromatogram of *Commiphora habessinica* resin n-hexane fraction.

Table C1: Retention time, percentage integration area of *Commiphora habessinica* n-hexane fraction

Peak #	Ret Time (min)	Width (min)	Area (MAU*S)	Height (MAU*S)	Peak Area %
1	2.833	0.1423	7.02883	7.57E-01	0.3442
2	3.488	0.2102	27.37843	1.85E+00	1.3408
3	7.798	0.1496	11.80309	1.15E+00	0.578
4	8.102	0.1805	1995.6825	1.66E+02	97.7369

Appendix D

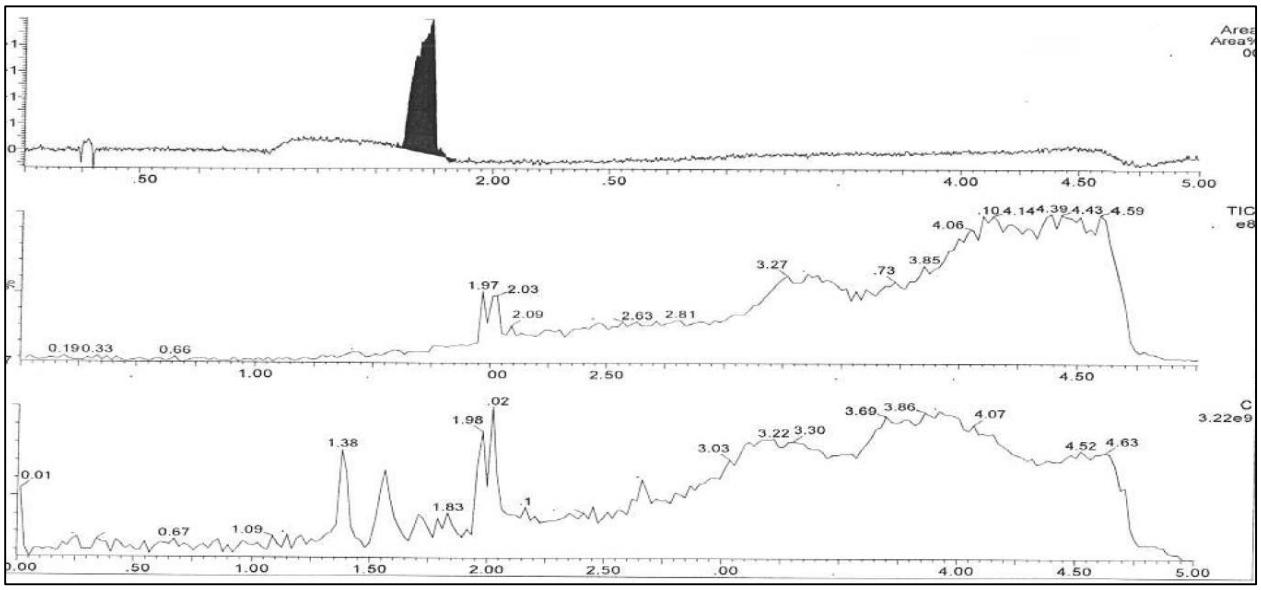

Figure D1: LC-TIC (in negative mode) of compound **56** (α-amyrin)

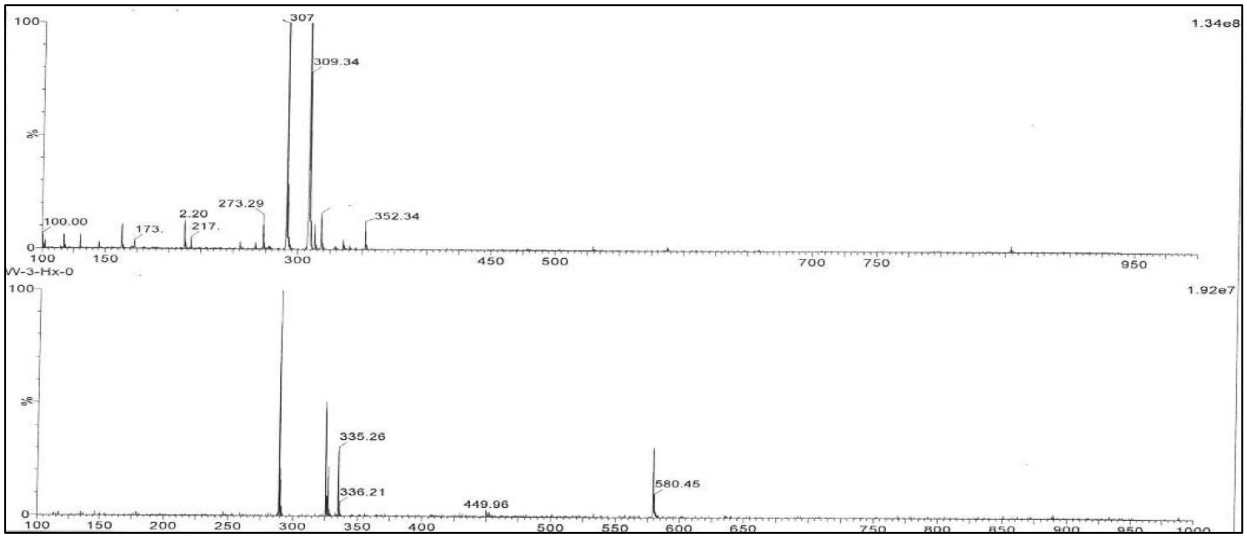

Figure D2: ESI-MS (in negative mode) of compound **56** (α-amyrin)

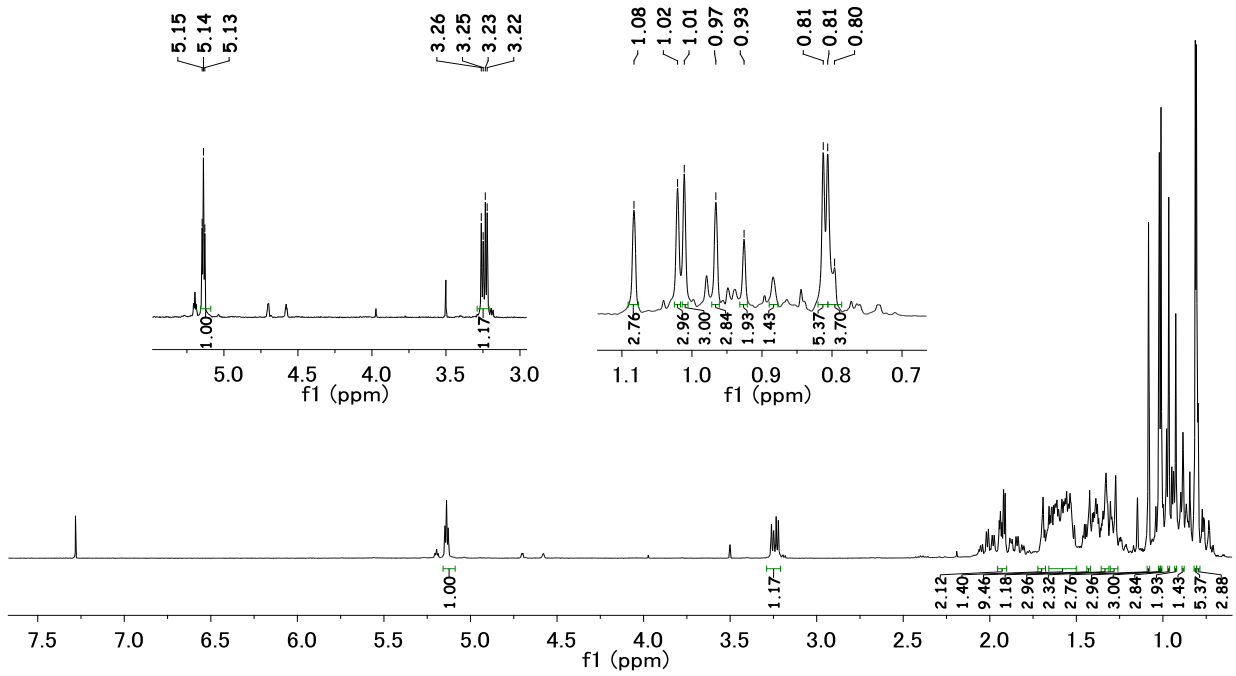

Figure D3: ^{1}H NMR spectrum of compound **56** (α-amyrin)

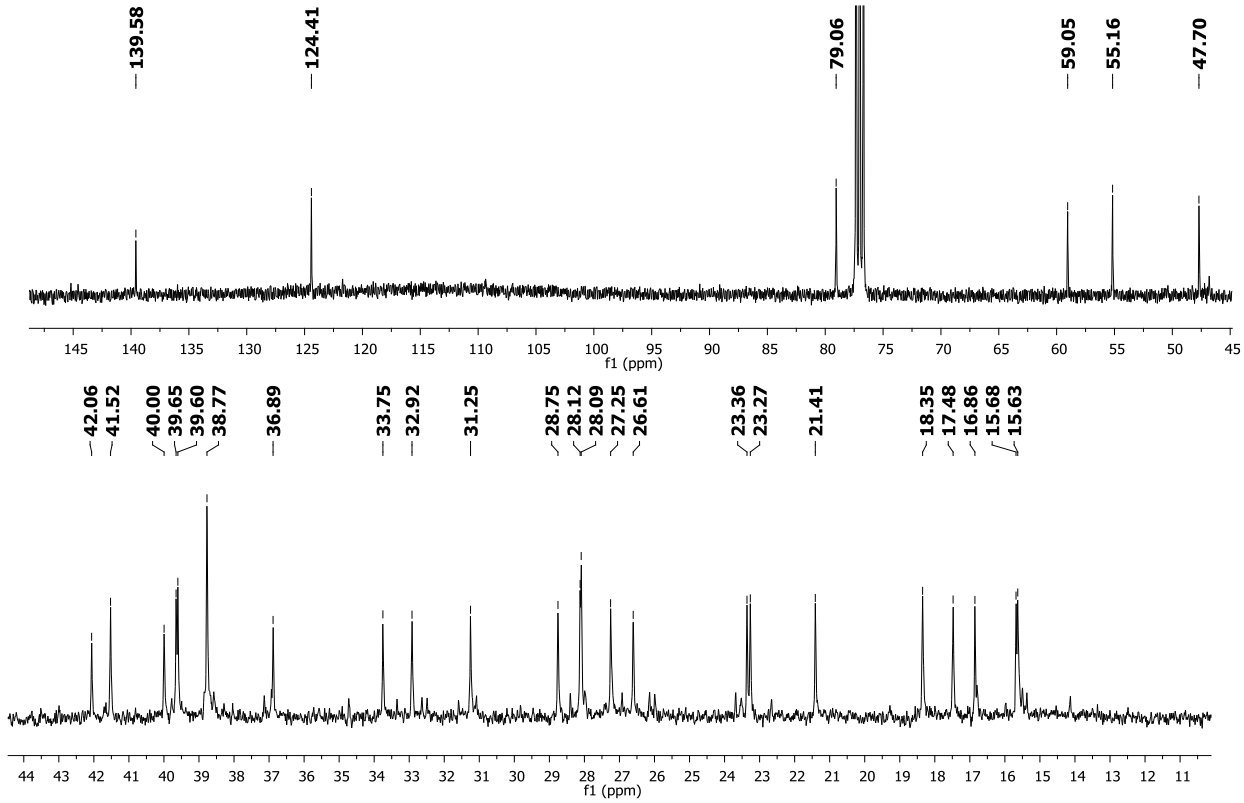

Figure D4: ^{13}C NMR spectrum of compound **56** (α-amyrin)

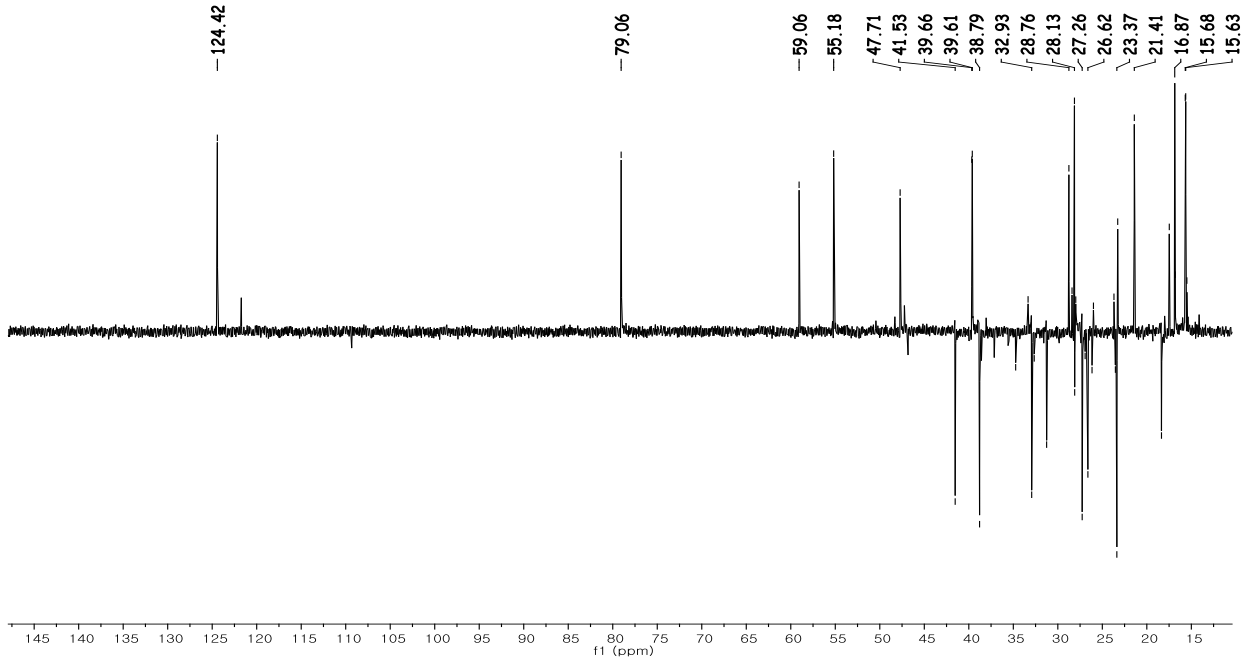

Figure D5: DEPT-135 spectrum of compound **56** (α-amyrin)

Appendix E

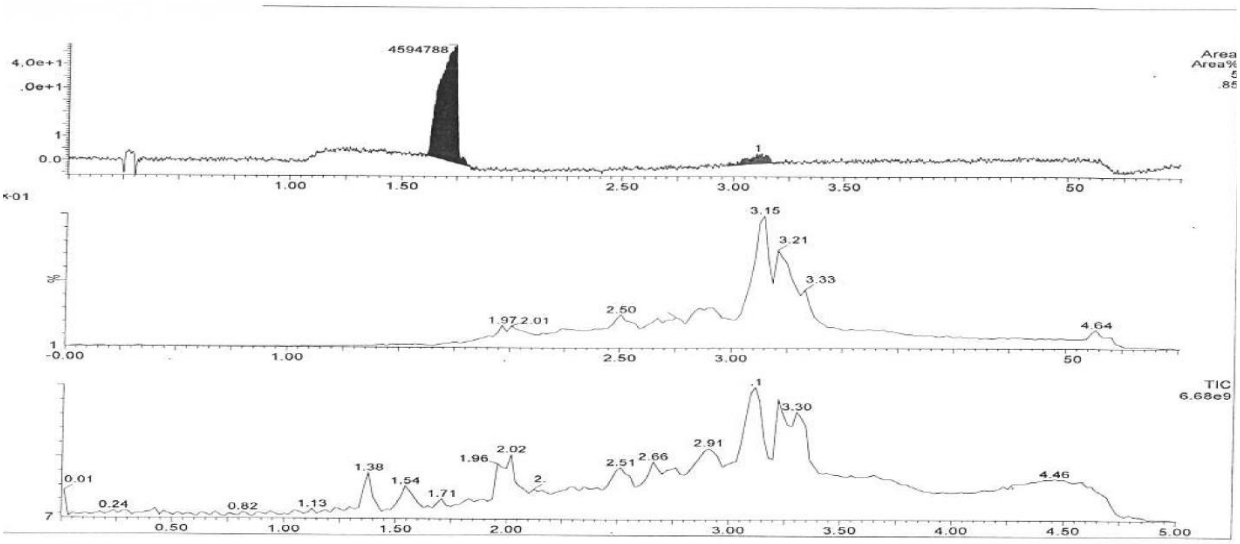

Figure E1: LC-TIC of compound **113** (commafric A)

i)

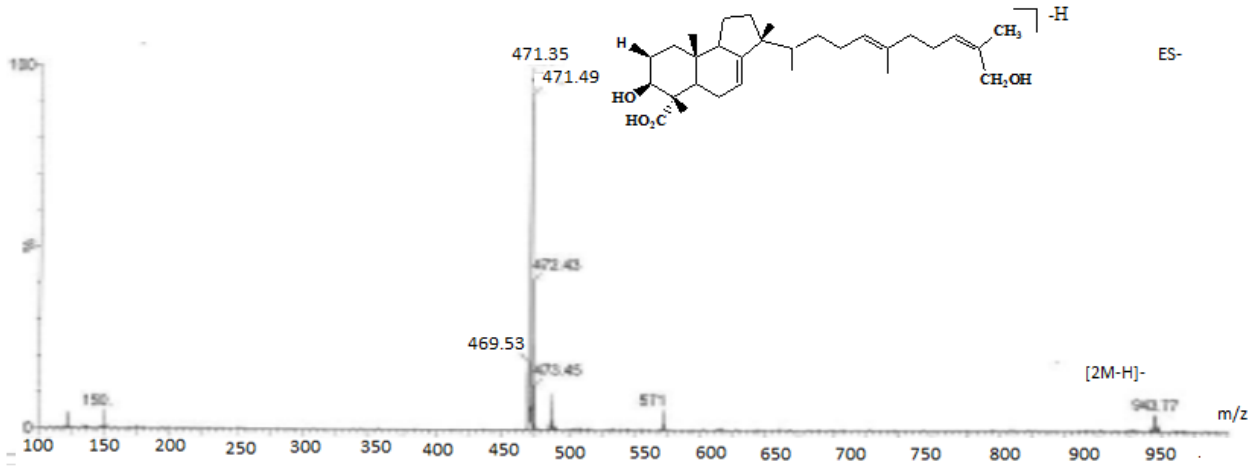

ii)

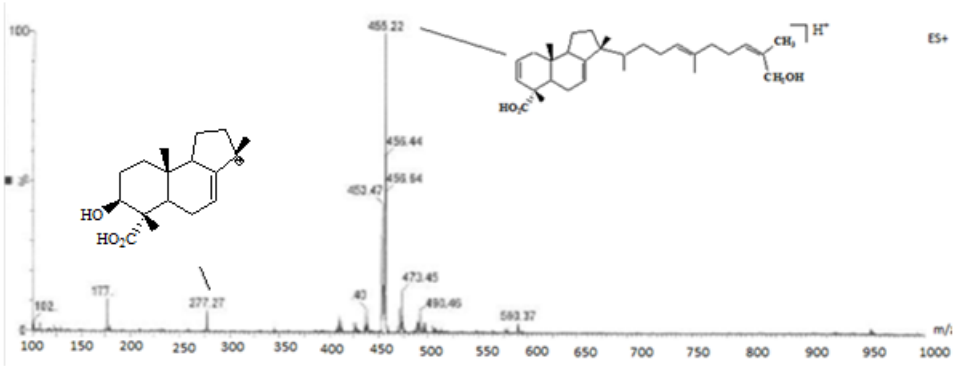

Figure E2a: LR-MS of commafric A(**113**) by ESI i) in negative mode and ii) positive mode.

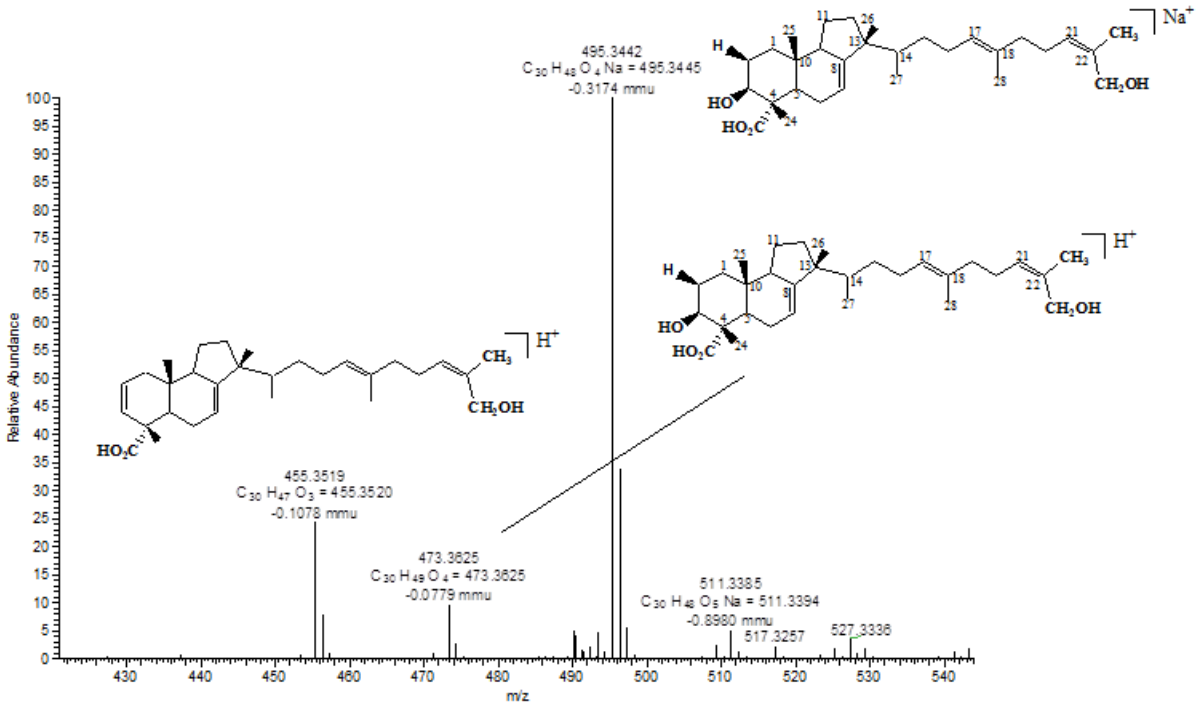

Figure E3: HR-ESI-MS Spectrum of compound **113** (commafric A)

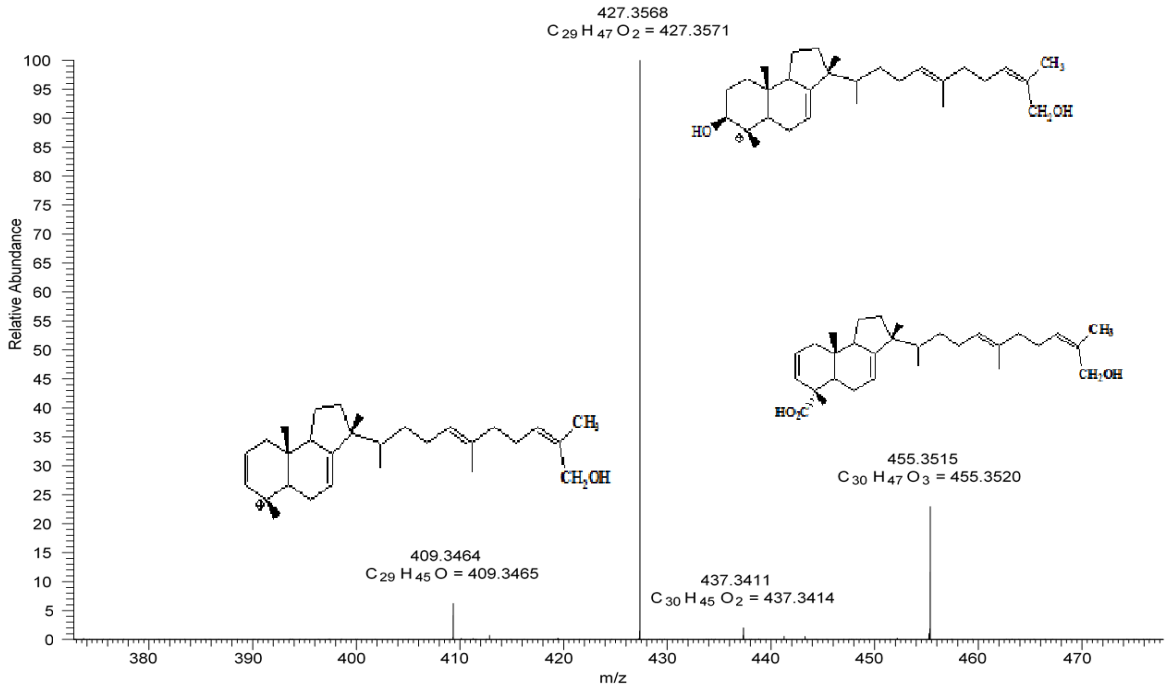

Figure E3a: Fragment ion elemental composition with MS/MS(commafric A) **113** of the parent ion at RT: 0.59-0.73 with *m/z* 473.36.

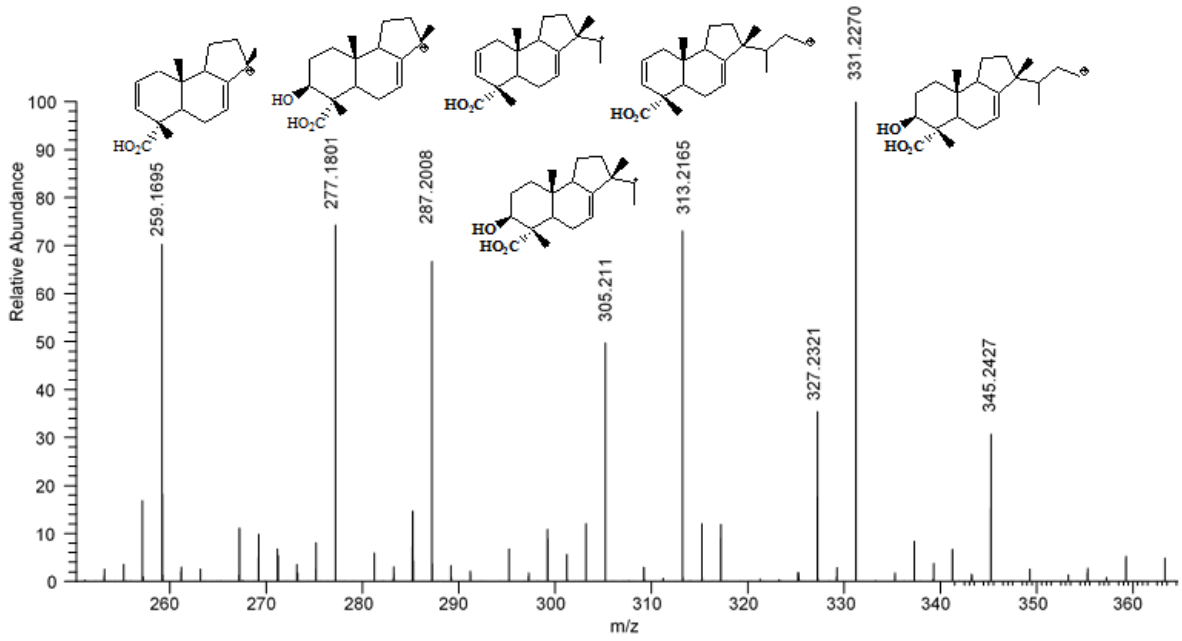

Figure E3b: Fragment ion elemental composition with MS/MS(commafric A) **113** of the parent ion at RT: 1.35 - 1.56 with *m/z* 455.35.

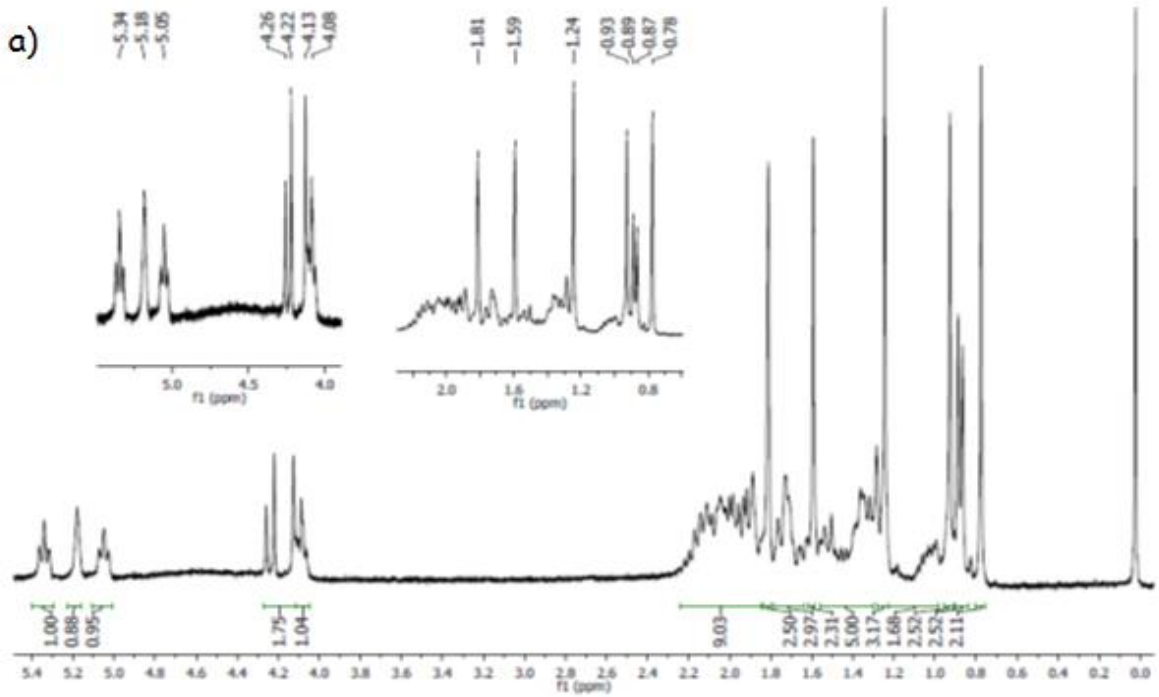

b)

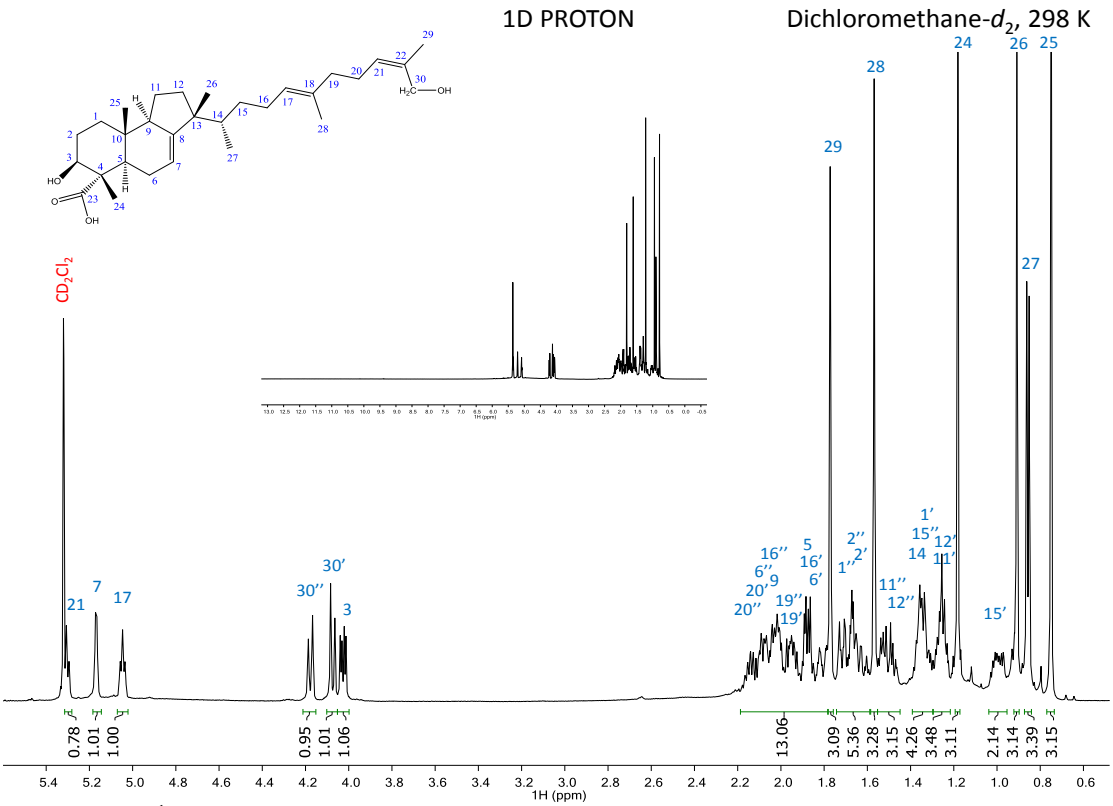

Figure E4: ^{1}H NMR spectrum of compound **113** (commafric A) a) at 300 MHzn in $CDCl_3$, b) 600MHz in CD_2Cl_2.

a)

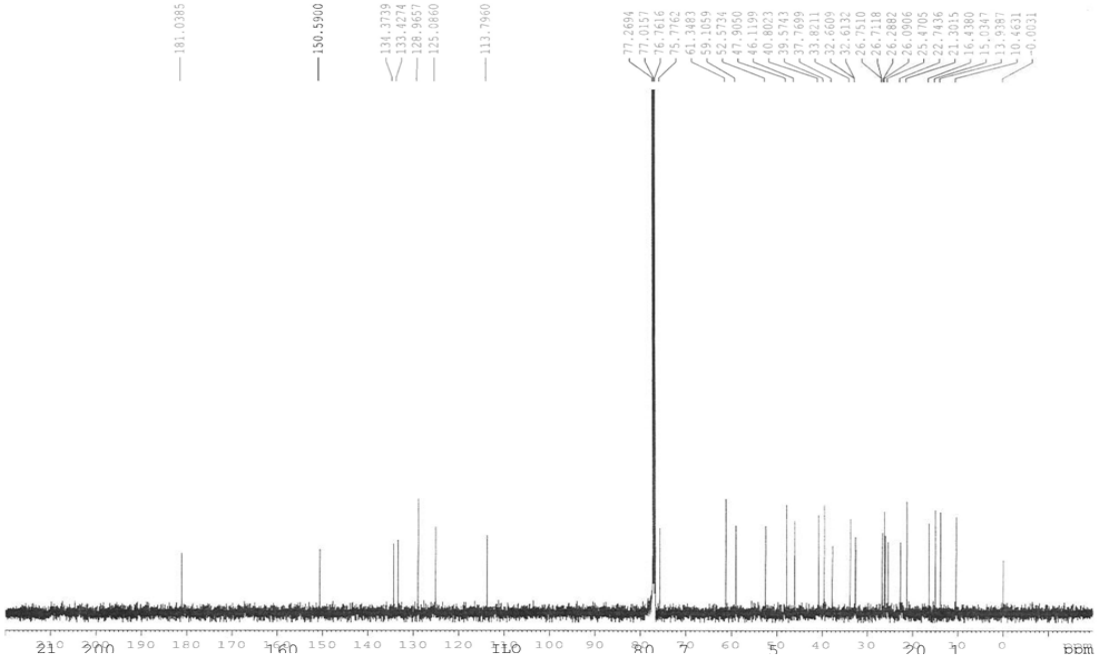

b)

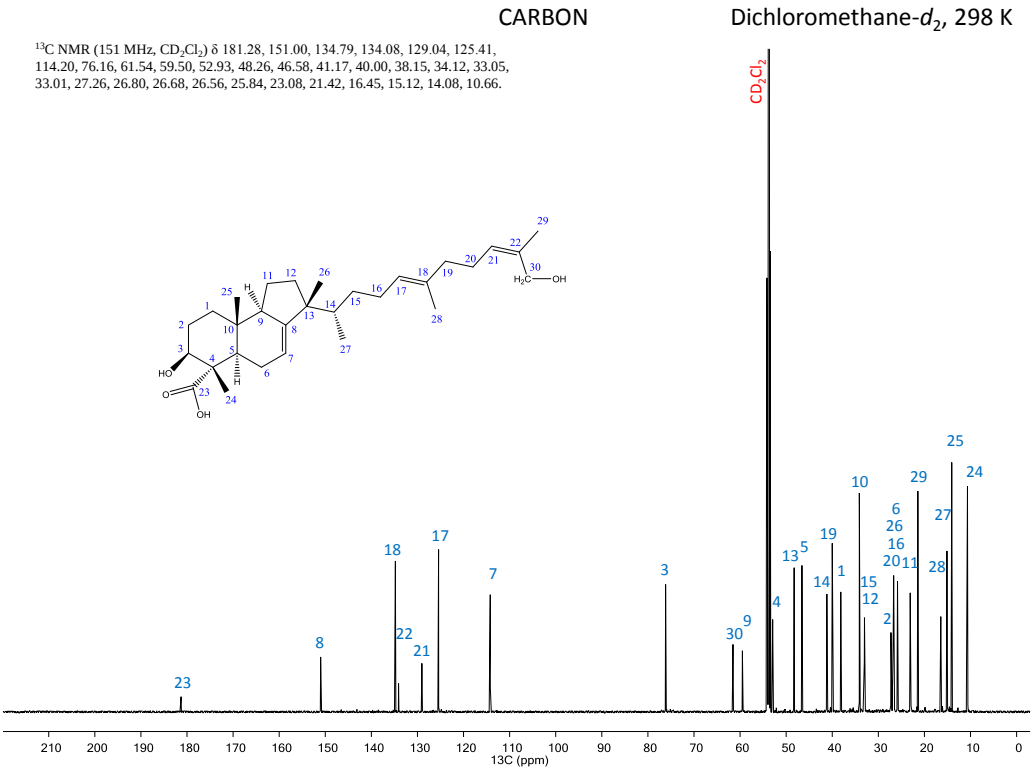

Figure E5: ^{13}C NMR spectrum of compound **113** (commafric A) a) at 125 MHzn in $CDCl_3$, b) 150MHz in CD_2Cl_2.

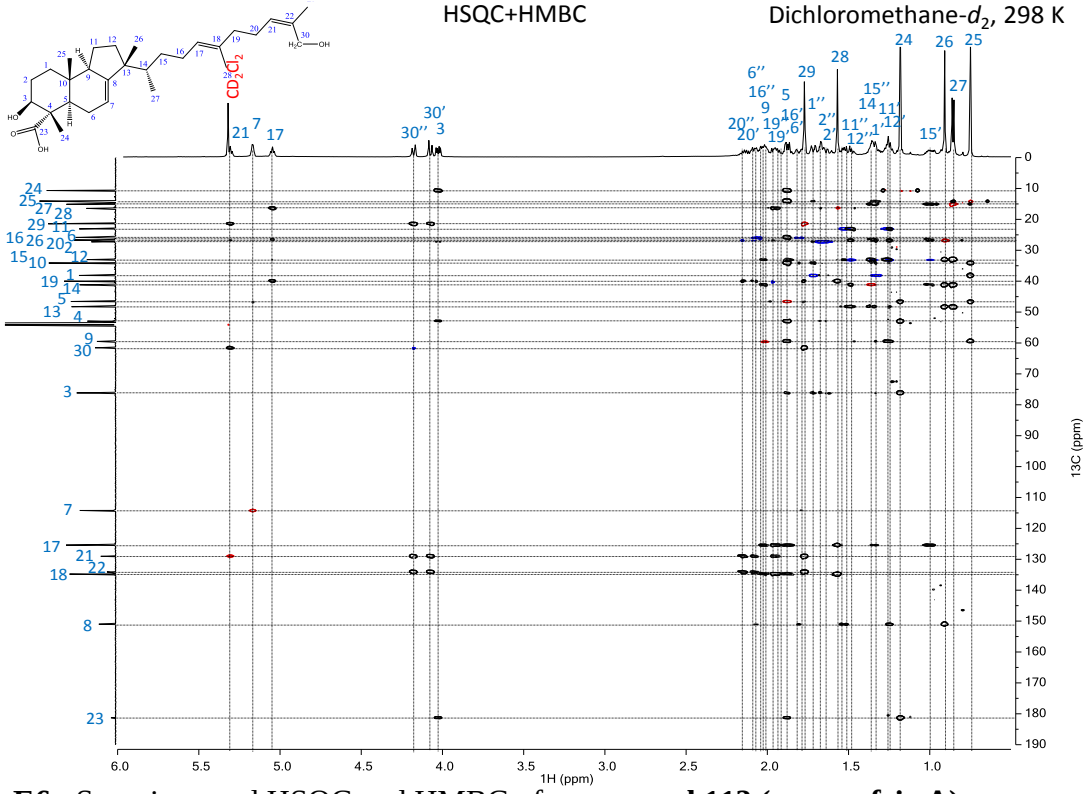

Figure E6: Superimposed HSQC and HMBC of **compound 113 (commafric A)**

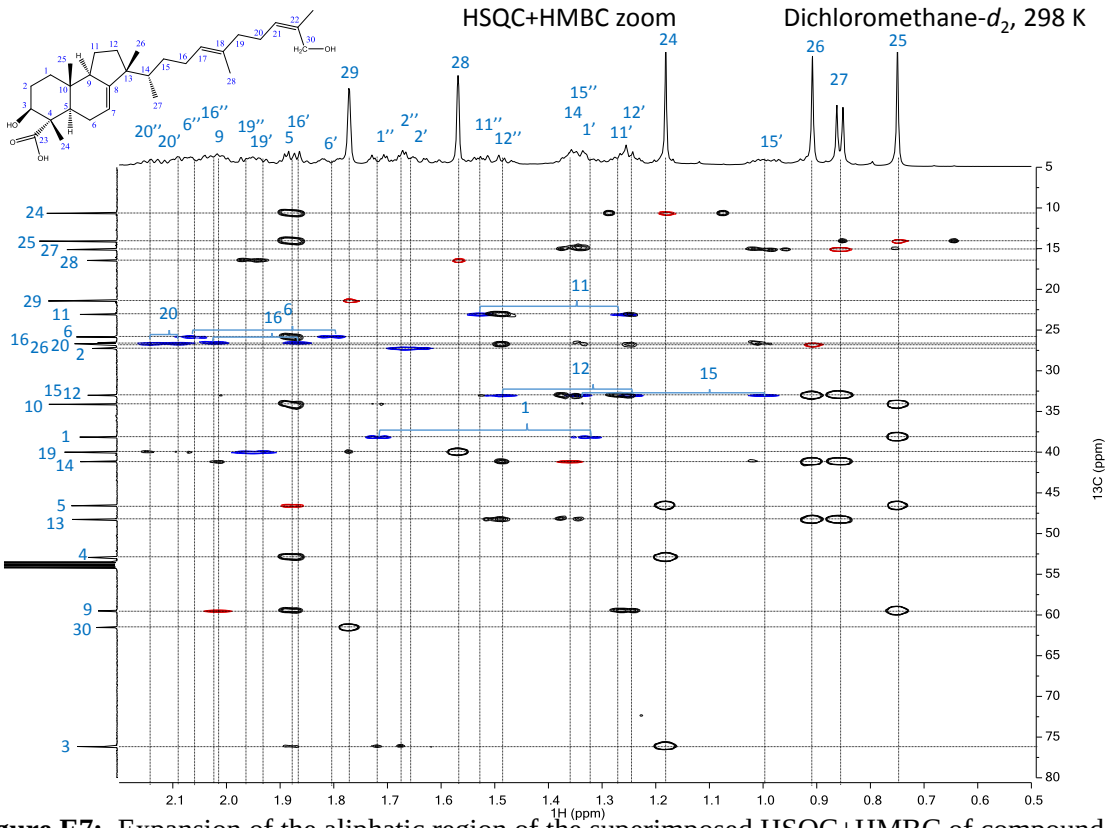

Figure E7: Expansion of the aliphatic region of the superimposed HSQC+HMBC of compound **113**

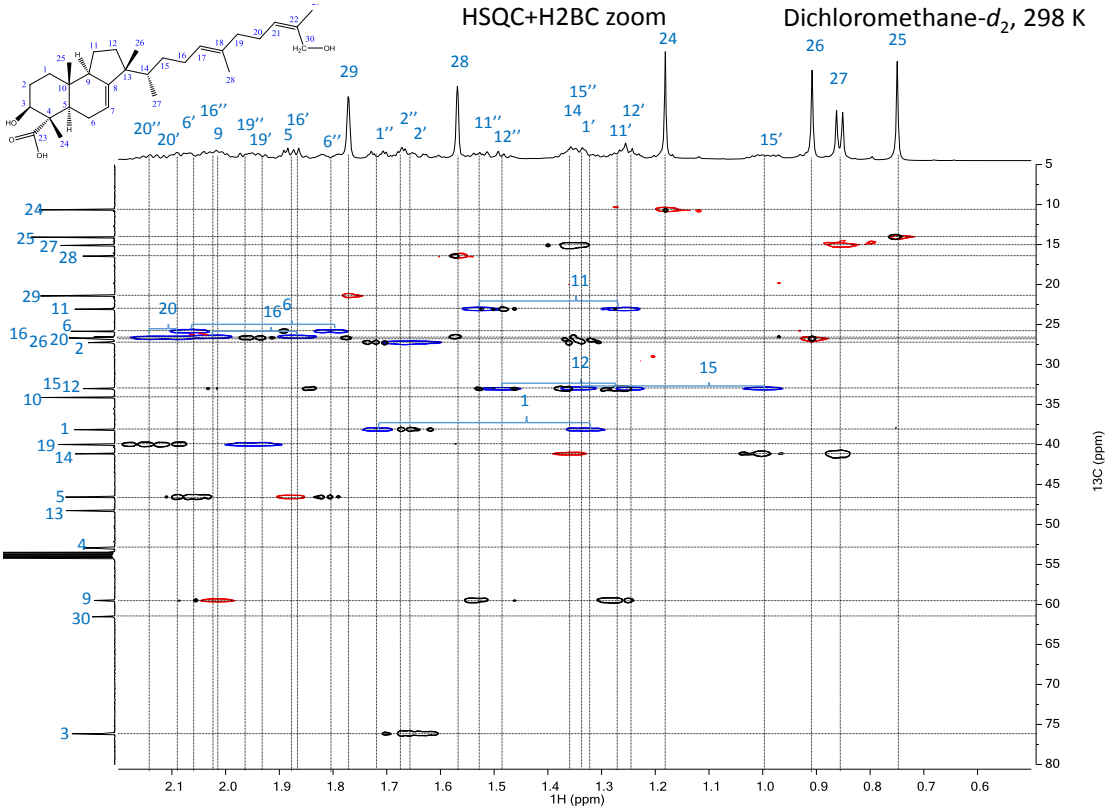

Figure E8: Expansion of the aliphatic region of superimposed HSQC+H2BC of compound **113**

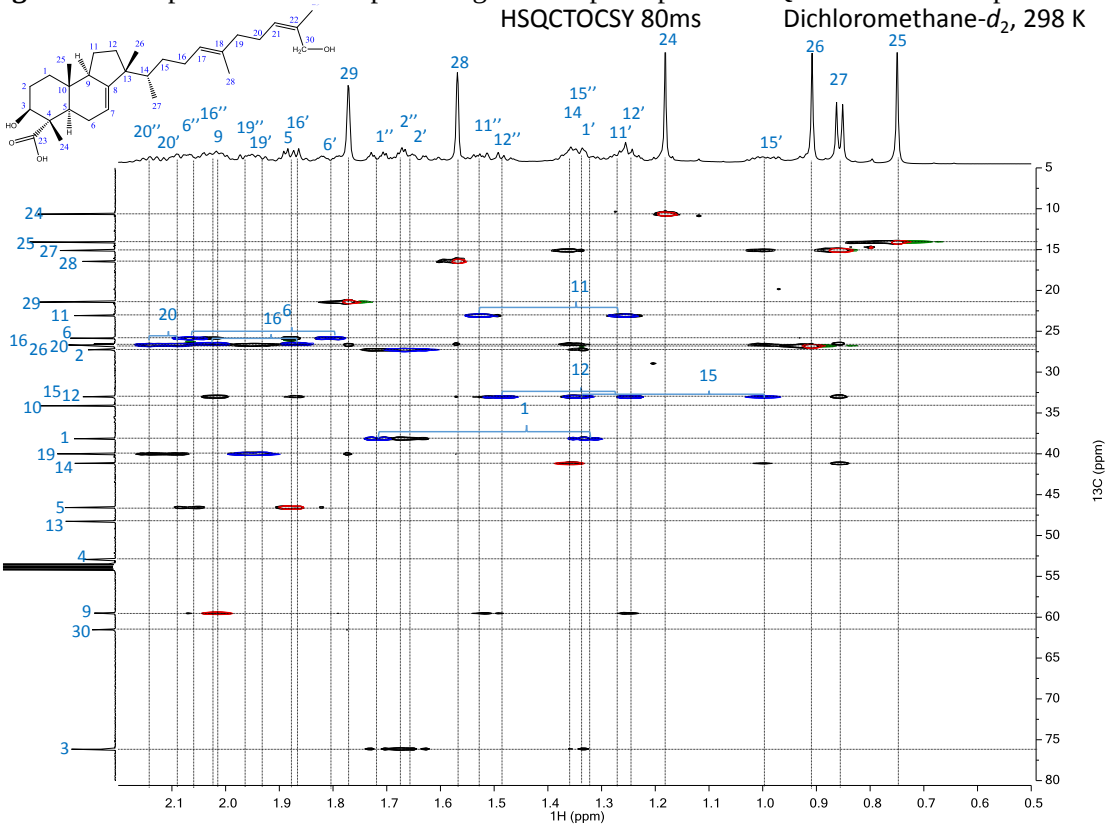

Figure E9: Expansion of the aliphatic region of superimposed HSQC+HSQC-TOCSY of compound **113**

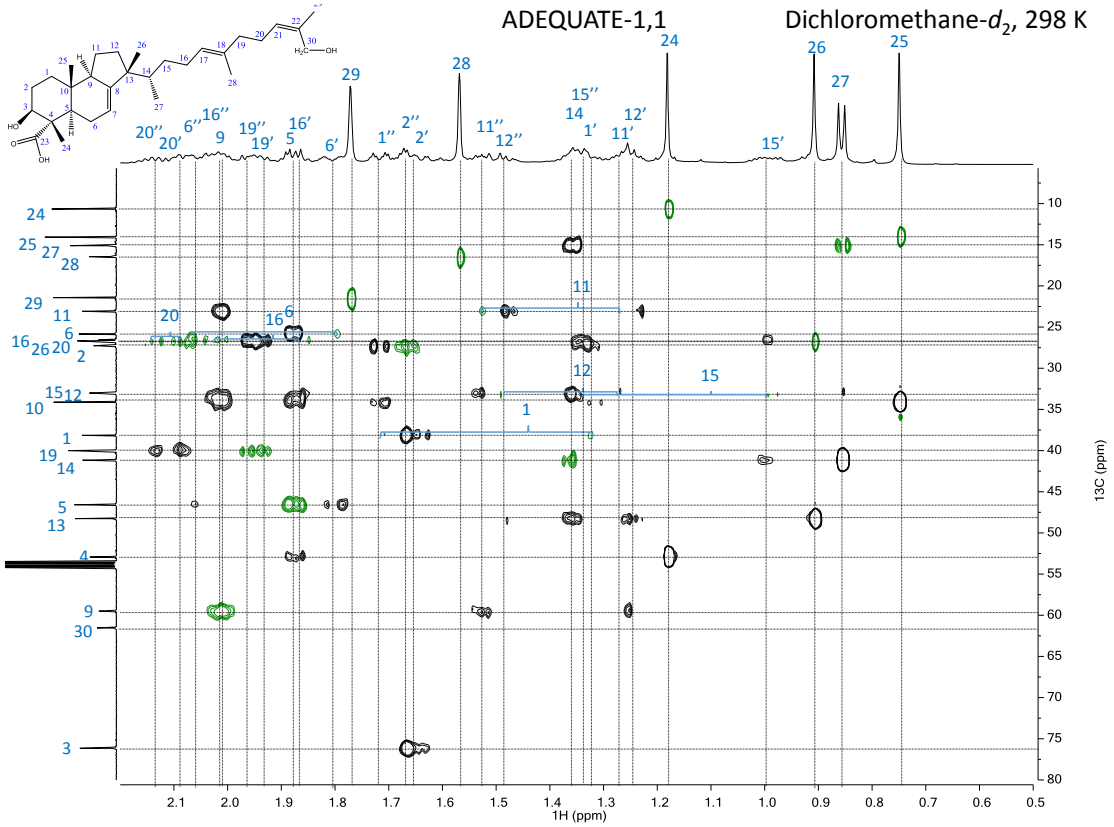

Figure E10: 1,1-ADEQUATE of compound **113** (commafric A)

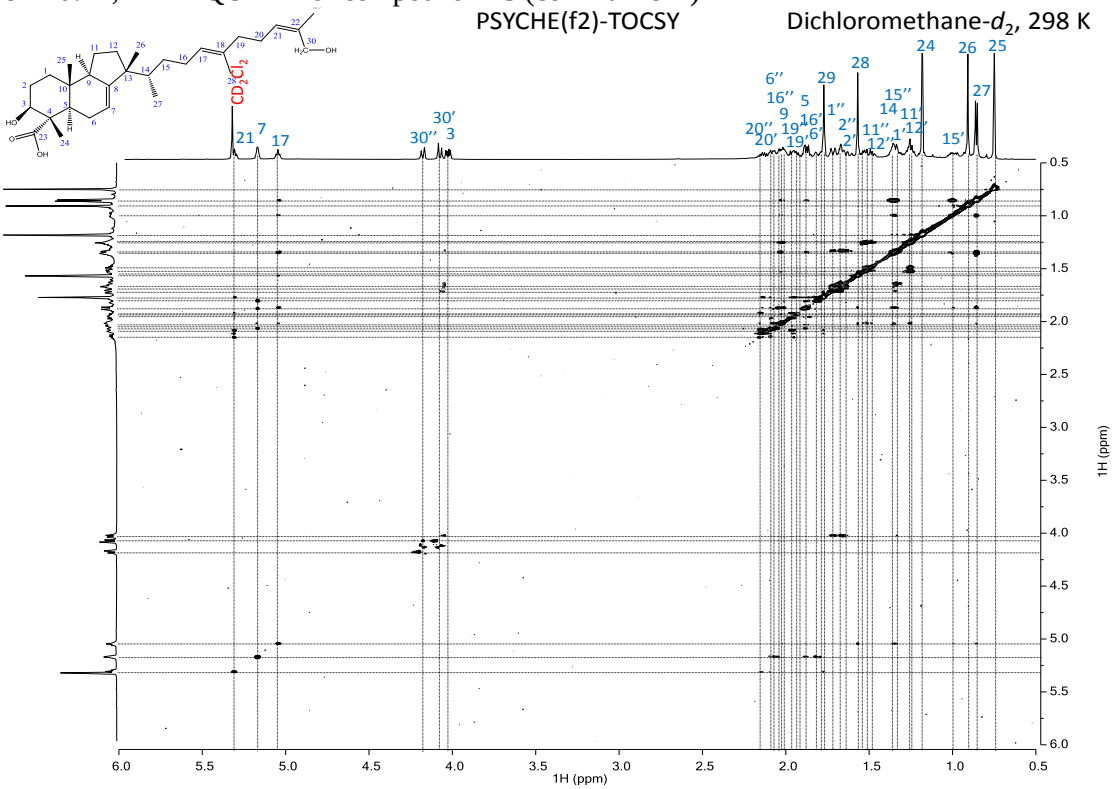

Figure E11: PSYCHE-TOCSY of compound **113** (commafric A)

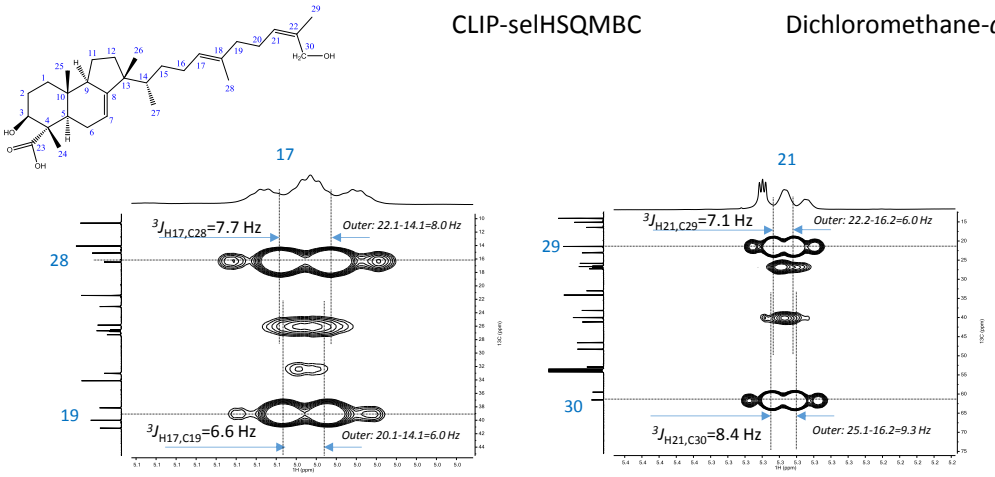

Figure E12: CLIP-selHSQMBC of H17 (left panel) and H21 (right panel) of compound **113** (commafric A)

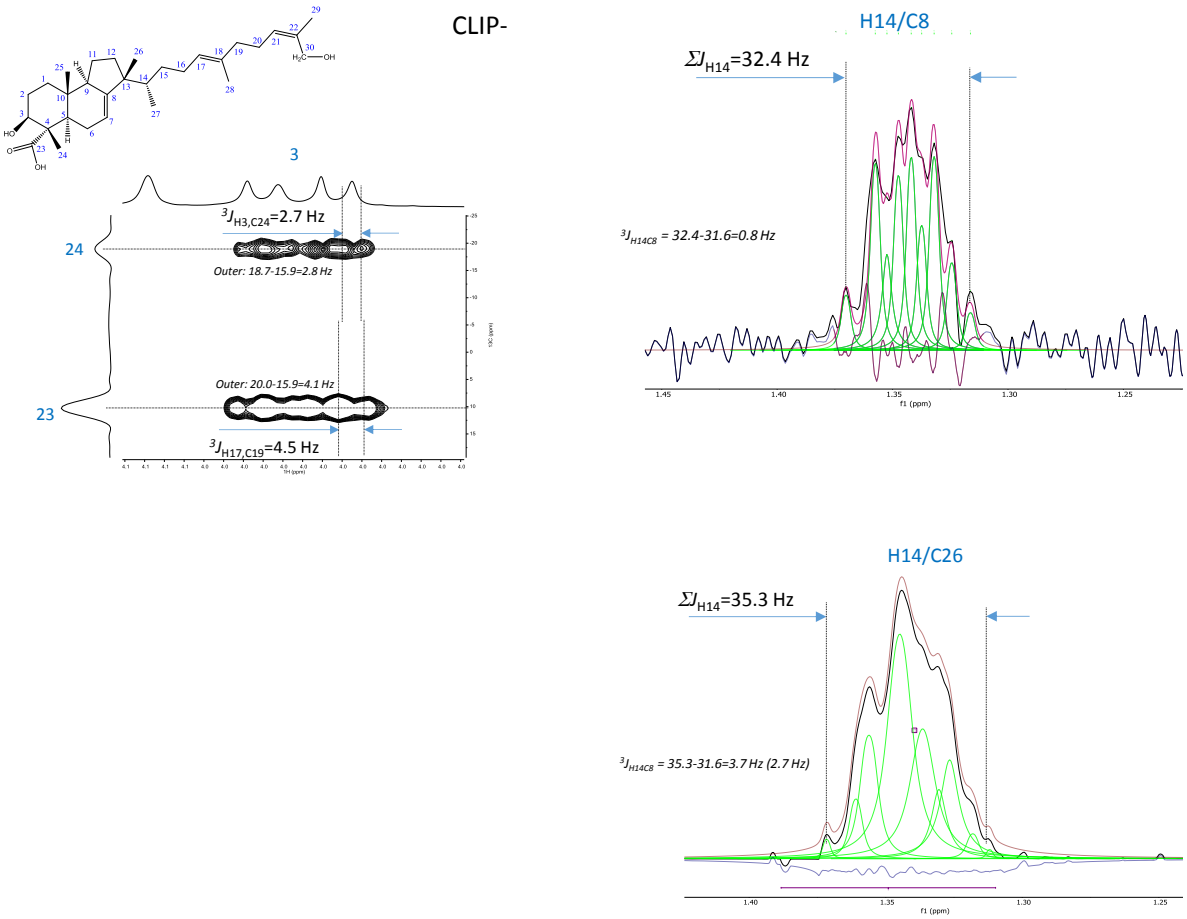

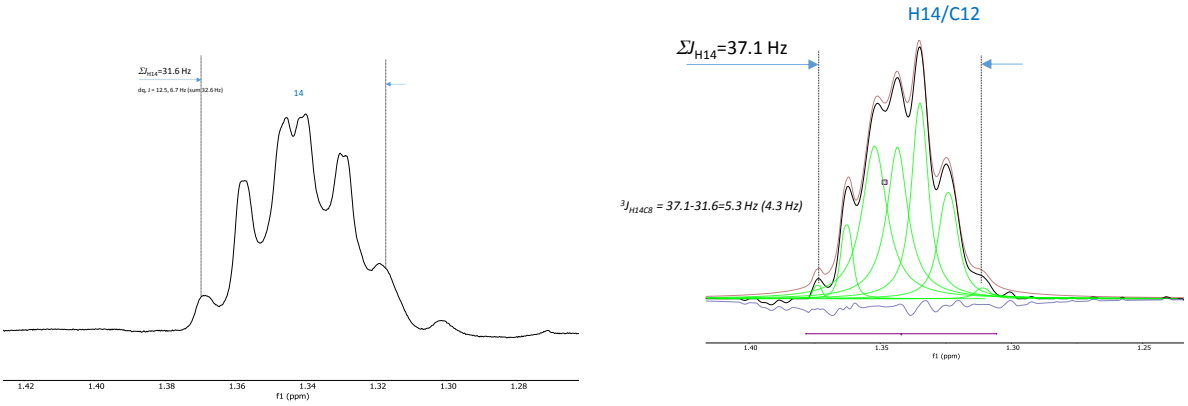

Figure E13: CLIP-selHSQMBC of H3 (upper left panel), CLIP-selHSQMBC projections of H14 (right panels), and CSSF-1D of H-14 (lower left panel) of compound **113 (commafric A)**

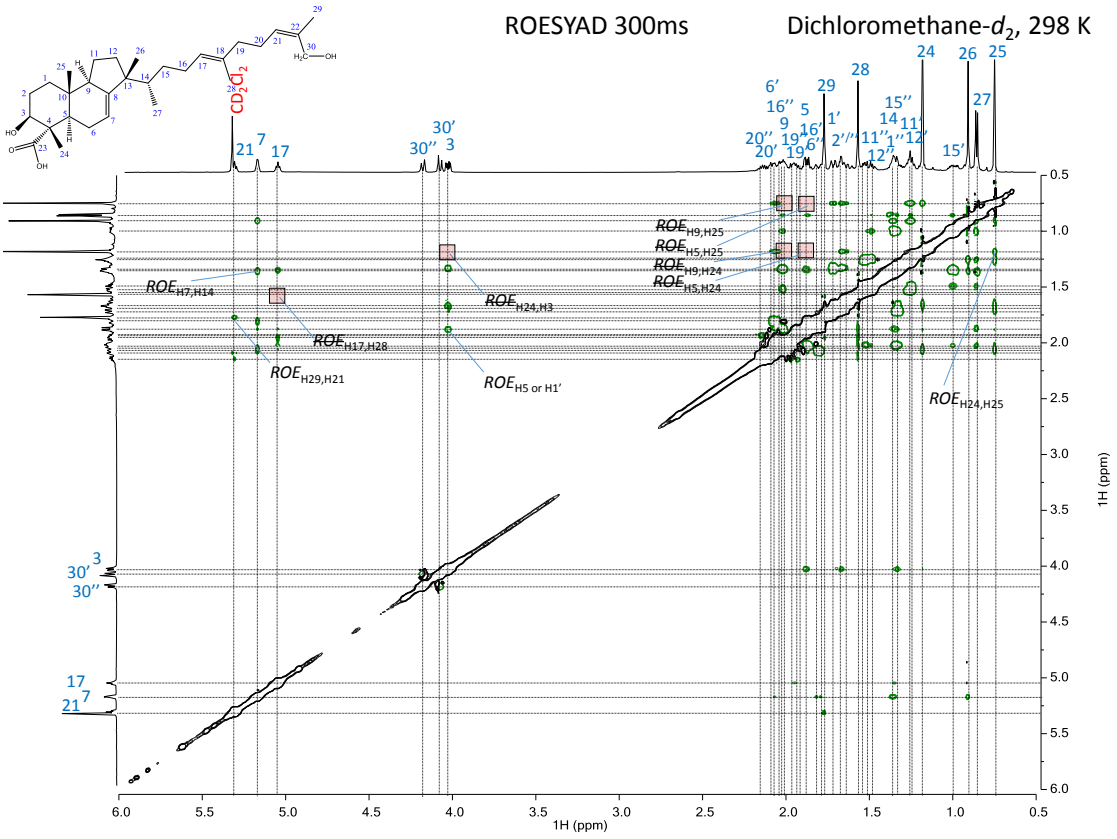

Figure E14: 300ms ROESY of compound **113** (commafric A)

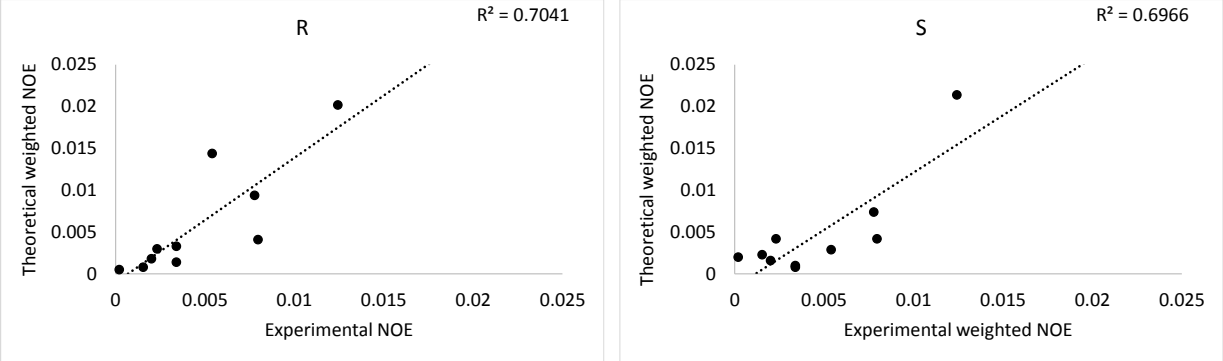

(a) (b)

Figure E15: Selected experimental vs theoretical Boltzmann weighted NOEs calculated from the rotamer ensembles for the (a) R- and (b) S configurations of C-14 of **113**

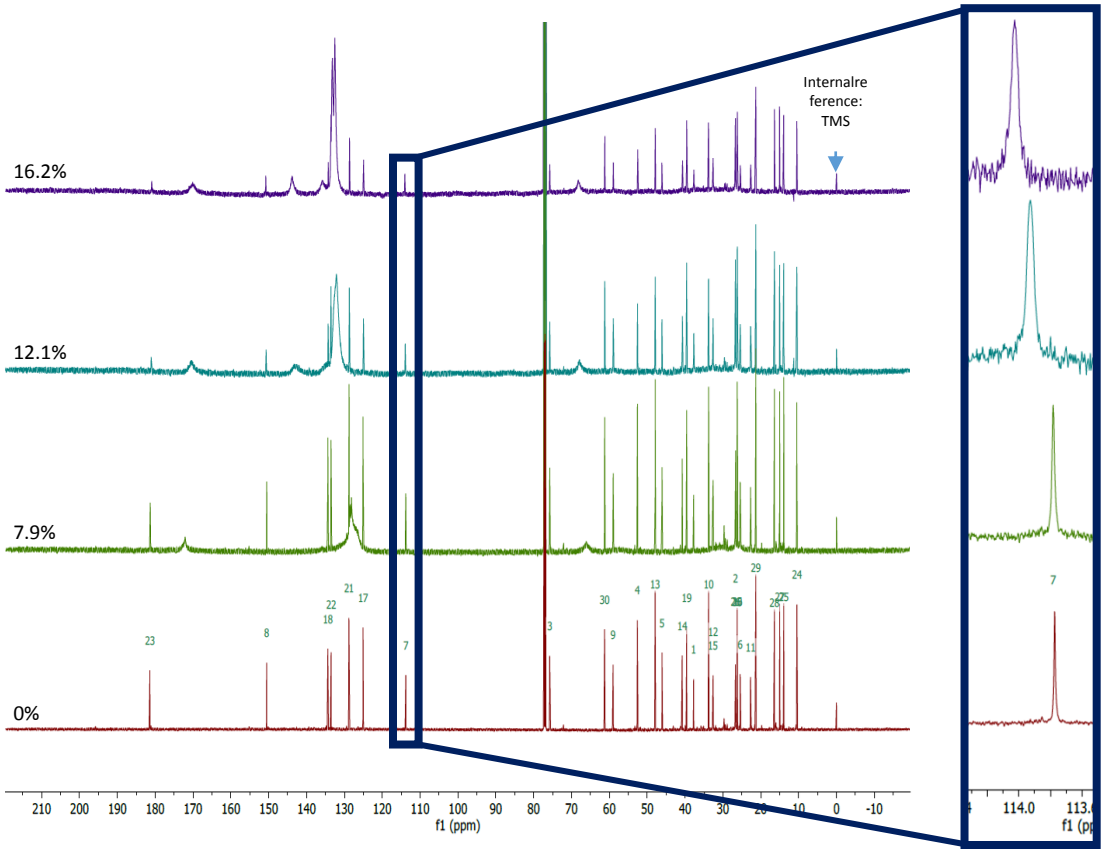

Figure E16: ^{13}C spectra for comound **113** in $CDCl_3$ with 0.03% (v/v) TMS at different PBLG concentrations. Zoomed-in outclip of C-7, showing the change in ppm values, as well as decrease of signal-to –noise ratio.

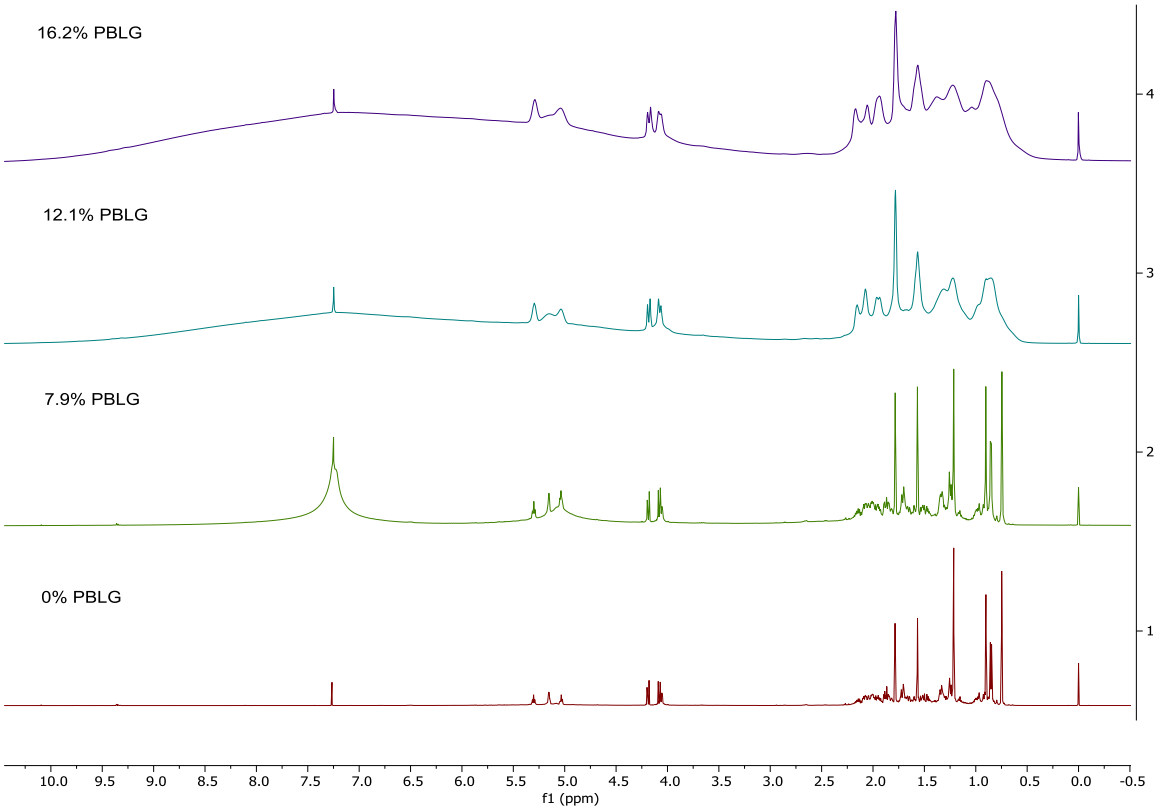

Figure E17: ^{1}H spectra for compound **113** in $CDCl_3$ with 1% (v/v) TMS at different PBLG concentrations.

Appendix F

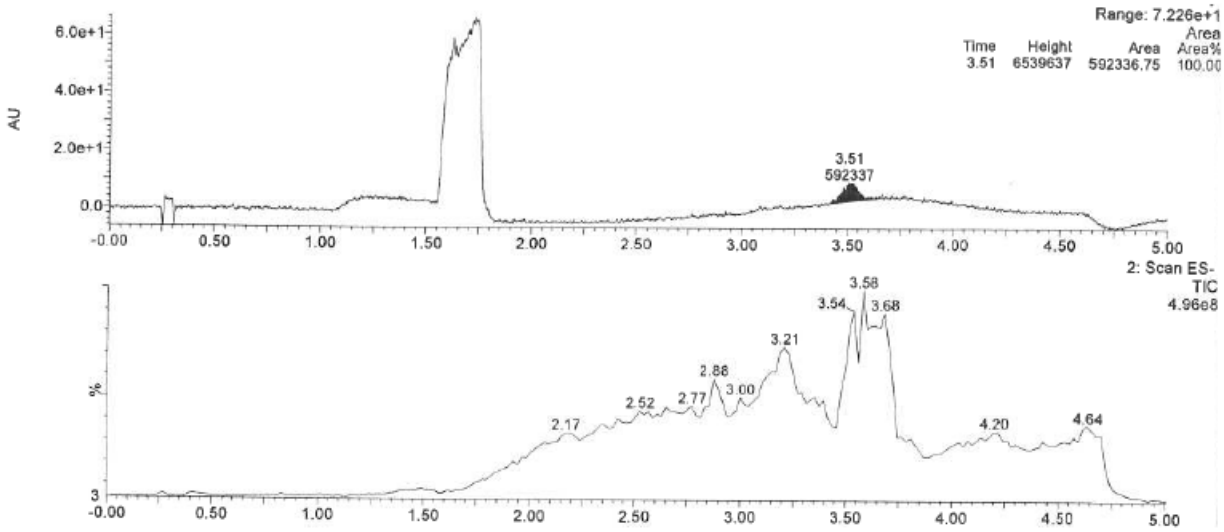

Figure F1: LC-TIC and ESI-MS (in negative mode) of compound **114**

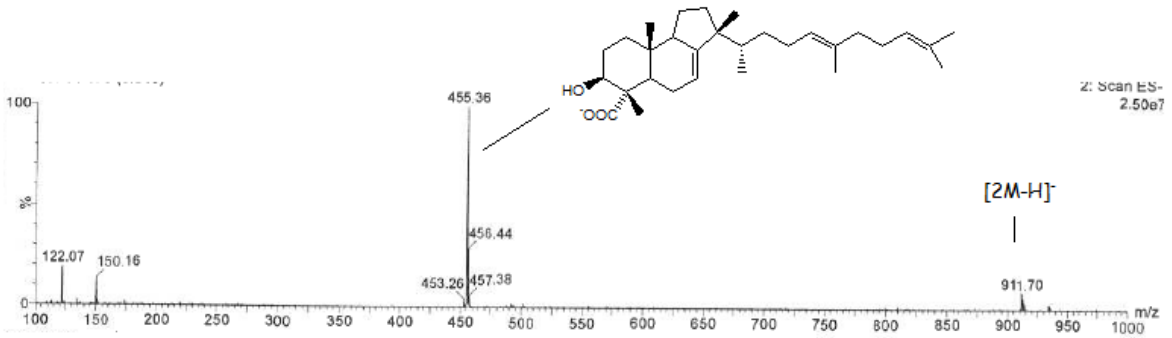

Figure F2: LC-TIC and ESI-MS (in negative mode) of compound **114**

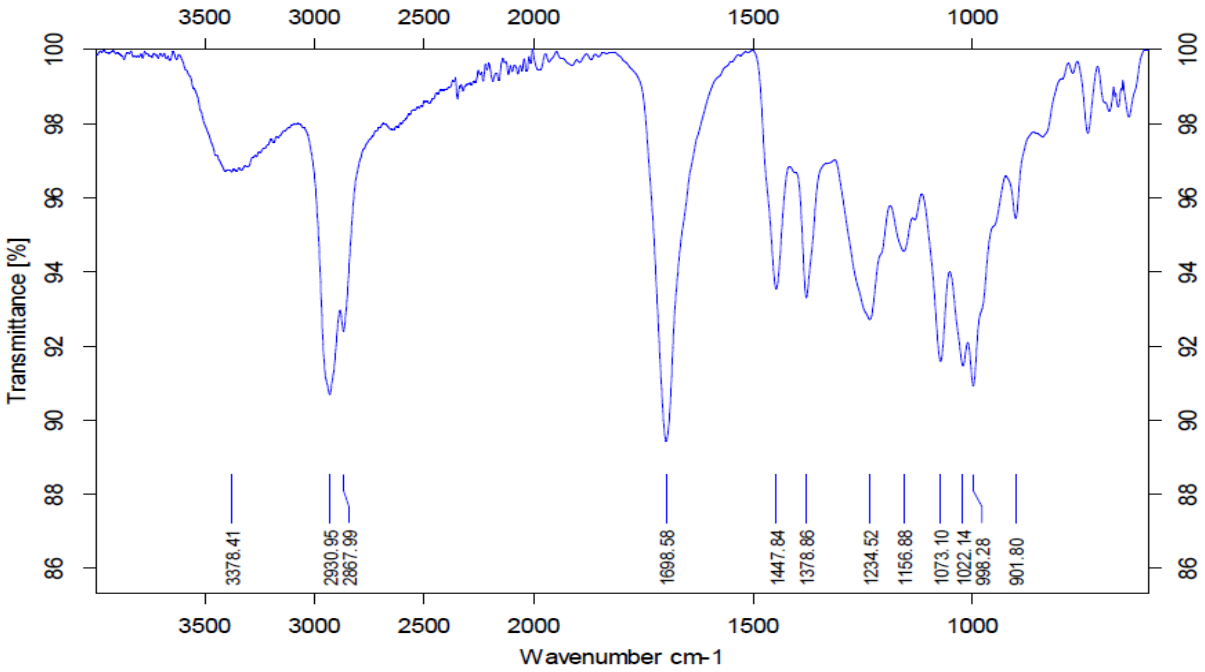

Figure F3: IR of compound **114**

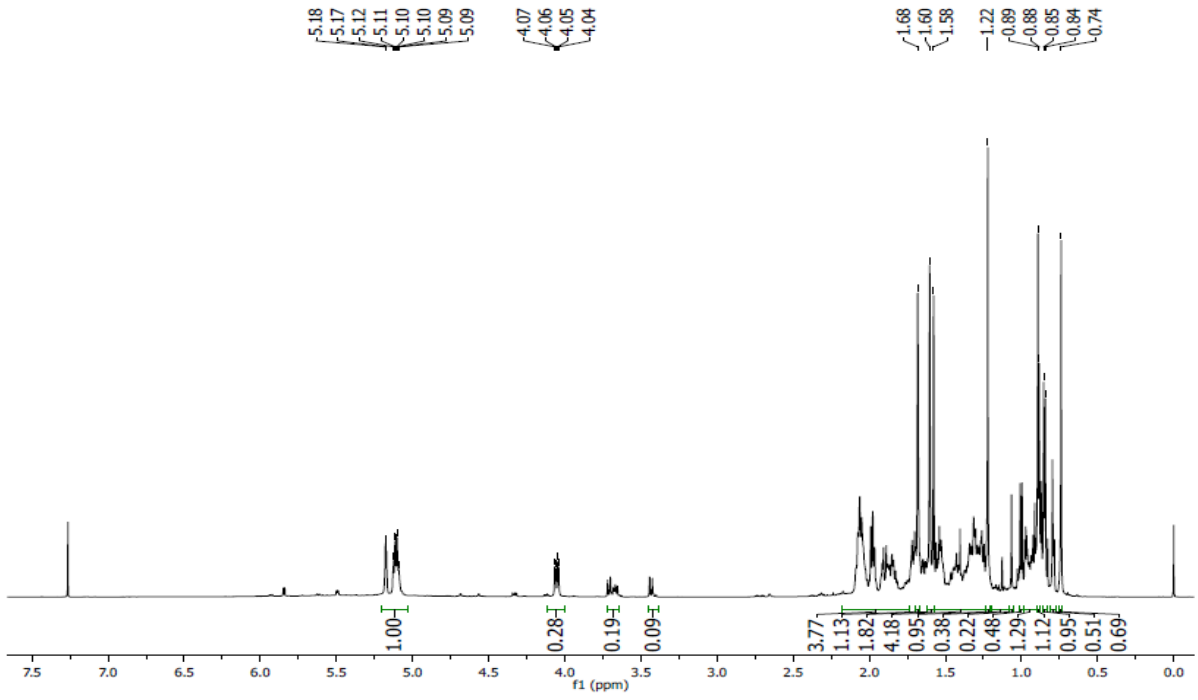

Figure F4: ^{1}H NMR spectrum of compound **114**

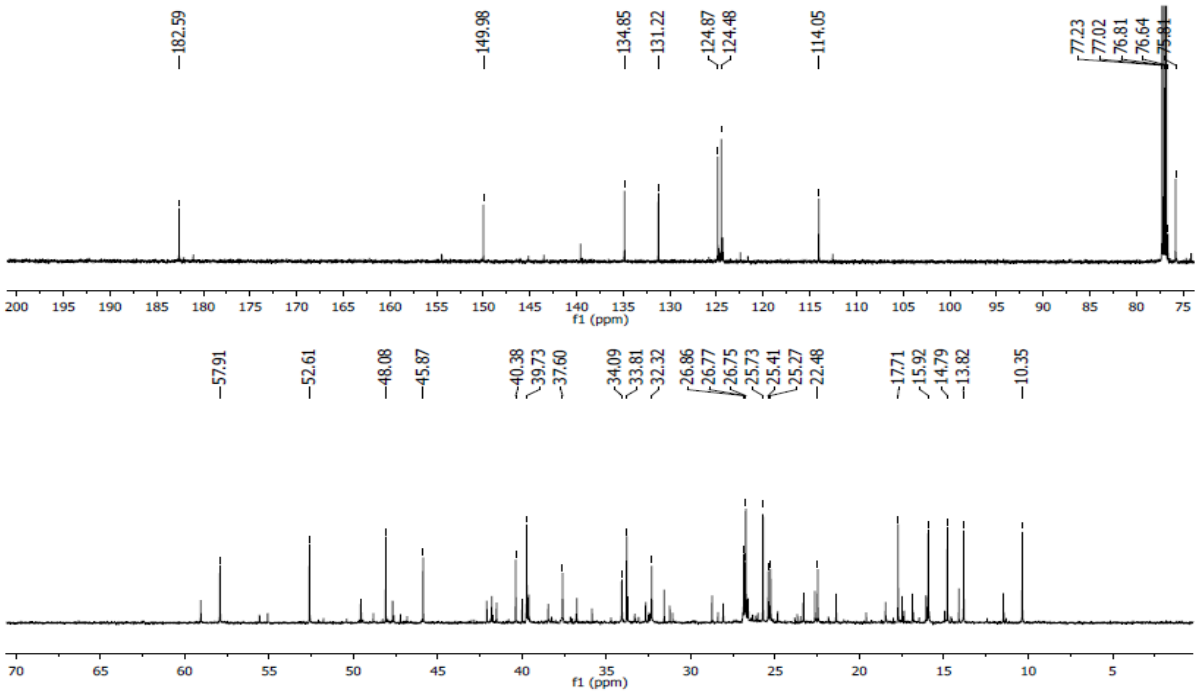

Figure F5: ^{13}C NMR spectrum of compound **114**

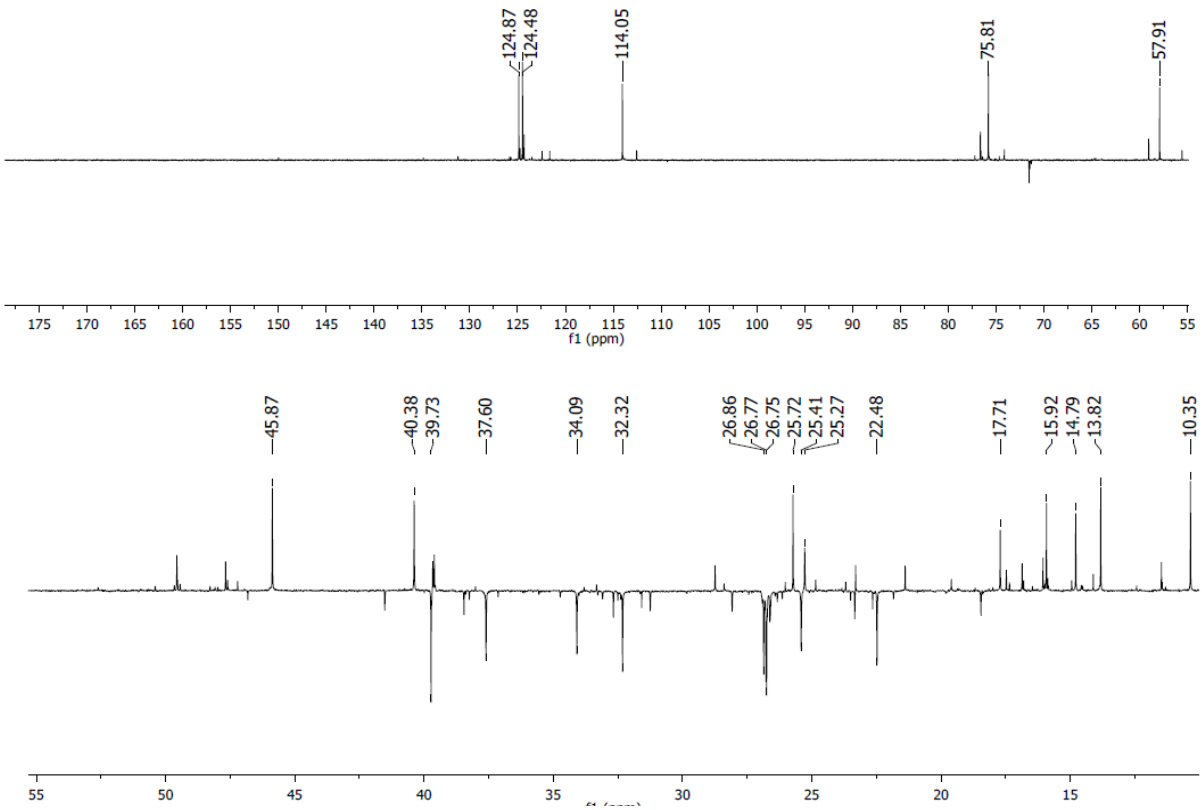

Figure F6: DEPT-135 spectrum of compound **114**